Premature Deterioration of Jointed Plain Concrete Pavements

FINAL REPORT

Date April 2011

By (PI) Dr. J. M. Vandenbossche, P.E.
University of Pittsburgh

COMMONWEALTH OF PENNSYLVANIA
DEPARTMENT OF TRANSPORTATION

CONTRACT # 510601
WORK ORDER # PIT 012

1. Report No.	2.Government Accession No.	3. Recipient's Catalog No.	
4. Title and Subtitle Premature Deterioration of Jointed Plain Concrete Pavements		**5. Report Date** 4/29/2011 **6. Performing Organization Code**	
7. Author(s) L. Ramirez,, M. Geary, J. Vandenbossche, K. Gatti, and F. Mu		**8. Performing Organization Report No.** WO #12	
9. Performing Organization Name and Address University of Pittsburgh Department of Civil and Environmental Engineering 934 Benedum Hall 3700 O'Hara St. Pittsburgh, PA 15213		**10. Work Unit No. (TRAIS)** **11. Contract or Grant No.** 510601 – PIT 012	
12. Sponsoring Agency Name and Address The Pennsylvania Department of Transportation Bureau of Planning and Research Commonwealth Keystone Building 400 North Street, 6th Floor Harrisburg, PA 17120-0064		**13. Type of Report and Period Covered** Final Report: December 1, 2008 – April 29, 2011 **14. Sponsoring Agency Code**	
15. Supplementary Notes			
16. Abstract Six sections of jointed plain concrete pavements (JPCP)s throughout the state were selected as candidates for the evaluation of premature deterioration. The data used in performing the evaluation included manual and historic automated distress survey data, falling weight deflectometer data, and laboratory material characterization data from field samples. For these six sections, a variety of issues including material-related distress, fatigue, and construction deficiencies were determined to be the cause of the premature deterioration. Recommendations for rehabilitating these sections as well as guidelines to deter the reoccurrence of these distresses have been provided.			
17. Key Words Jointed Plain Concrete Pavements, Premature Distress, ASR, Petrographic Analysis, Open Graded Subbase, Material Related Distress, MEPDG, Curing, FWD, Fatigue Cracking, Rehabilitation, MIT Dowel Scanning, Drainage, Finite Element Modeling, Shoulders		**18. Distribution Statement** No restrictions. This document is available from the National Technical Information Service, Springfield, VA 22161	
19. Security Classif. (of this report)	**20. Security Classif. (of this page)**	**21. No. of Pages** 266	**22. Price**

Table of Contents

ACKNOWLEDGEMENTS

The financial and technical support provided by the Pennsylvania Department of Transportation (PennDOT) for this project is gratefully acknowledged. The authors would like to extend their sincere gratitude to Ms. Lisa Tarson as well as the project's technical liaison Mr. Neal Fannin from District 2. The authors would also like to acknowledge Ms. Lydia Peddicord and Mr. Joshua Freeman for their technical input. The completion of this research would not have been possible without the assistance from the following people who helped in identifying the distressed sections, gathering project information, and coordinating the traffic control and coring for each project.

- Mr. William Dipner, District 11
- Mr. Robert Houne, District 12
- Mr. Thomas Boyle, District 12
- Mr. Warner Barate, District 10
- Mr. Adam Mouser, District 6
- Mr. Vincente Morales, District 6
- Mr. George Dunheimer, District 6

The authors would also like to thank American Engineering and Testing for performing the petrographic work.

EXECUTIVE SUMMARY

Six sections of jointed plain concrete pavements (JPCP)s throughout the state were selected as candidates for the evaluation of premature deterioration. These JPCPs include sections of the former SR 60 (re-designated Interstate 376) in Allegheny County, SR 202 in Chester County, US 22 in Westmoreland County, I-79 in Washington County, I-80 in Clinton County, and US 22 in Indiana County. The data used in the evaluation included manually collected distress survey as well as historic automated distress survey data, falling weight deflectometer data and laboratory material characterization data from field samples. Based on this analysis, the following recommendations were derived:

1. OGS: The gradation of the OGS should be modified to a more densely graded material to increase the stability by reducing the permeability to about 750 ft/day. The reduction in the flexural capacity that occurs when an OGS is used in lieu of a stabilized base should be considered when establishing the slab thickness.
2. Placement, Finishing and Curing Recommendations are provided for revising the curing specification as well as on aspects of paving that should be diligently inspected so that a sound concrete pavement is constructed. It is also recommended that the soaked burlap drag no longer be used behind the paver and the concrete temperature and ambient climatic conditions be closely monitored to prevent drying shrinkage cracking.
3. Mixture Design Refinement A refinement of the concrete mixture design specification should be performed. This will help reduce the potential for segregation and make the concrete more durable. The use of a more densely graded aggregate, and a reduction in allowable water to cementitious ratio and paste to aggregate ratio should be considered.
4. Alkali Silica Reaction ASR does not appear to be a problem when the approved mixture design is used during construction.
5. Multi-Lane Paving Guidelines have been developed to reduce the potential for the development of transverse cracks when the mainline the adjacent narrow shoulder are paved during two extremely different temperatures (for example the mainline paved in late fall and the shoulder paved in mid-summer).

Options to Consider

- Reconcile the differences between the observed distress and the distress identified using the automated systems. Identify the cause of the discrepancy, establish new data collection protocol to prevent the collect of erroneous data in the future and establish adjustments factors for adjusting the data currently in the database.
- Calibrate the MEPDG performance prediction models (fatigue cracking, faulting and International Roughness Index) so that the distress observed for pavements in Pennsylvania better matches the predicted distress.
- Develop repair techniques for repairing the distress exhibited on SR-202. This should include evaluating a variety of surface preparation techniques (small jack hammers, hydro demolition, etc.) as well as bonding agents should be considered.
- It is believed that refinements of the concrete mixture design could be made to help reduce the potential for material related distress as well as increasing the ease in which the concrete could be placed, finished and cured. These refinements should be established based on preliminary laboratory mixes and trial field projects.

1 Introduction

This report is the final report of a six-task project with PennDOT to investigate the premature deterioration of jointed plane concrete pavements (JPCPs) within the commonwealth of Pennsylvania. As part of this project, six sections of JPCPs throughout the state were selected as candidates for evaluation. These JPCPs include sections of the former SR 60 (re-designated Interstate 376) in Allegheny County, SR 202 in Chester County, US 22 in Westmoreland County, I-79 in Washington County, I-80 in Clinton County, and US 22 in Indiana County.

For each of the aforementioned projects, potential distressed pavement candidates were provided by the Pennsylvania Department of Transportation (PennDOT) district personnel. From a handful of candidate segments, a representative Distressed Section and representative Control section were selected to evaluate the causes of the distresses based on comparisons. Data used to evaluate the potential reason for the disparity in performance was collected from a variety of sources including PennDOT personnel, field visits consisting of performing distress surveys, coring, FWD testing, and a laboratory study that evaluated various engineering properties of the pavement from the Portland cement concrete (PCC) cores obtained during the field visits.

In Sections 2 through 7 of this report, a summary of the information obtained for each project, the issue(s) believed to be responsible for the observed distress, recommendations for addressing the distress in their current manifestation, and conclusions on how to avoid each distress on future projects similar in scope and nature. In comparing the causes of the distresses observed in three of the six candidate JPCP sections it was noticed that the use of an open graded base layer seemed to play a significant role. In light of this observation, Section 8, which discusses the mechanism through which the OGS contributed to premature deterioration of each of the JPCP pavement sections, is included at the end of this report.

2 SR 60, Allegheny County

2.1 Project Information: SR 60

For SR 60, the selected site is located in Allegheny County. Allegheny County falls under the jurisdiction of PennDOT Engineering District 11. The selected Distressed and Control sections to execute the data collection plan were Segment 303 and Segment 323 in the southbound direction. For each section, a 1000-ft long representative section was chosen based on the pavement condition and the ease of executing traffic control. The orange highlight in Figure 1 presents the location of Segments 303 and 323. In Figure 1, these segments are located between the intersection of SR 60 and Pennsylvania Turnpike 576 and the intersection of SR 60 and McClaren Road. It is also important to note that between the selection of this project and the creation of this report, this portion of SR 60 was re-designated as Interstate 376 and is shown as such in Figure 1.

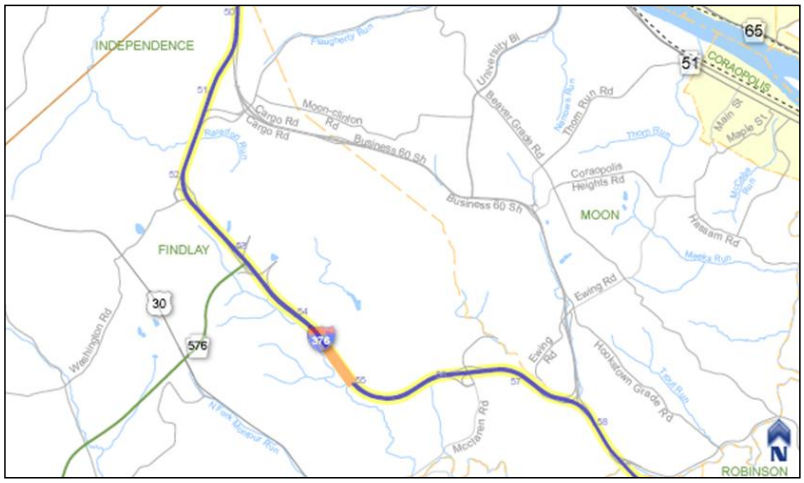

Figure 1: Location of SR 60 Segments 303 and 323 Southbound in District 11.

2.2 Design Information: SR 60

Segments 323 and 303 are JPCP pavements with two lanes per direction. Both segments were constructed in 1992 and at the time of the field data collection were approximately 17 years old. The design features for these segments include 12-ft wide PCC slabs and 1:6

counterclockwise skewed transverse joints. The transverse joint spacing is 20 ft measured along the longitudinal joint with an effective slab diagonal of 25.06 ft. Both longitudinal and transverse joints are sealed with preformed neoprene seals. According to the design information, the pavement structure includes an 11-in thick PCC slab, a 4-in thick open-graded base designated as OGS, and a 4-in 2A subbase. This structure was constructed on top of a compacted subgrade having an American Association of State Highway and Transportation Officials (AASTHO) classification of A-4 soil. The design information also indicates that 1.5-in diameter dowels spaced 12 inches on center, a HMA shoulder and 6-in diameter longitudinal edge drains were also included. Despite the design information, the PCC cores show that the base type for the Control section is a 4-in thick asphalt treated permeable base (ATPB). The pavement thickness also varied between the sections. A cross section of the existing pavement in both the Distressed and Control section are shown in Figure 2 and Figure 3 respectively. The overall existing condition of the pavement as observed when performing the distress survey in November 2009 is presented in Figure 4 and Figure 5.

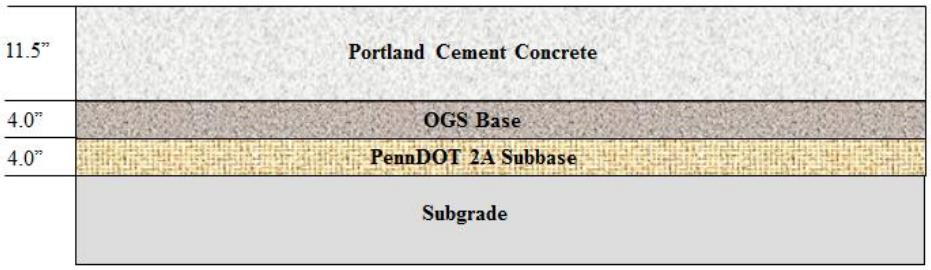

Figure 2: Existing Pavement Cross Section of SR 60 Segment 323 Southbound (Distressed Section)

11.0"	Portland Cement Concrete
4.0"	Asphalt Treated Permeable Base
4.0"	PennDOT 2A Subbase
	Subgrade

Figure 3: Existing Pavement Cross Section of SR 60 Segment 303 Southbound (Control Section)

Figure 4: Overall Condition of SR 60 Segment 323 Southbound (Distressed Section)

Figure 5: Overall Condition of SR 60 Segment 303 Southbound (Control Section).

2.3 Concrete Mixture Design: SR 60

For SR 60, there is no available information regarding the concrete mixture design. Despite this missing information, the visual examination of the retrieved cores indicates that the concrete mixture design used for the Distressed and Control sections might be the same. Observations that led to this conclusion include the following mix properties, which were identified as common for both sections: blast furnace slag coarse aggregate with a maximum size of 1 in, the coarse aggregate gradations appeared similar, and the cement paste color was brown with grey areas around the coarse aggregate particles. Additionally, as will be presented in Section 2.11, the measured concrete properties for these two sections were similar. These properties include the average backcalculated and laboratory determined PCC static elastic modulus as well as compressive strength, Poisson's ratio, coefficient of thermal expansion (CTE), and split tensile strength.

2.4 Climatic Conditions: SR 60

SR 60 is located in a wet freeze climate. To further analyze the climatic conditions, the climatic database provided in the MEDPG was used characterize the project climatic conditions.

The closest climate station to Segments 323 and 303 is the one at the Pittsburgh International Airport (PIA), approximately 13 miles away. The area experiences approximately 150 wet days per year and a mean annual rainfall of 38 in. The freezing index is 323ºF-days and the area is exposed to approximately 55 freeze-thaw cycles per year. The mean annual air temperature is 55 ºF with minimum and maximum average monthly temperatures of 13 ºF and 81 ºF, respectively.

2.5 Traffic Loadings: SR 60

According to information obtained from PennDOT's Internet Traffic Monitoring System (ITMS), as of 2009 the Average Annual Daily Traffic (AADT) of the Distressed section, Segment 323, is approximately 19,000 and the AADT of the Control section, Segment 303, is approximately 23,000. ITMS showed that the percentage of truck traffic for both segments is 7 percent. Based on these values, it can be estimated that from 1992 to 2010 this highway has sustained about 7.5 million 18-kip equivalent single-axle load (ESAL) applications.

2.6 Selection of Distress Survey Section: SR 60

Different information was analyzed to properly select the Distressed and Control sections. Historic automated distress survey data provided by PennDOT, as well as the pavement condition and panoramic images of the roadway obtained from the PennDOT Videolog application were studied in the office to locate road segments exhibiting early-age distress. Based on this preliminary analysis and the observations made during an initial visit to the project, Segments 303 and 323 southbound were selected as the Control and Distressed sections, respectively, due to the observed discrepancy in the distress condition. Although Segment 303 is also exhibiting distress, the quantity and severity is minor when compared to Segment 323.

2.7 Pavement Condition: SR 60

To assess the pavement condition, a distress survey was conducted over 50 slabs in the driving lane of the segments in accordance with the Long Term Pavement Performance (LTPP) Distress Identification Manual [1]. The distress survey included the observation and quantification of transverse joint faulting, transverse joint width, percent spalling of joints and cracks, transverse cracking, and material-related distresses such as staining or map cracking. In addition, lane to shoulder drop off was also measured. A summary of the distress measurements for SR 60 is presented in Table 1. As observed in Table 1, the major distress affecting the pavement is transverse cracking, which is present in 88 percent of the slabs in the Distressed

section and 20 percent in the Control section. According to the historic distress information provided by PennDOT, the transverse cracks started to manifest themselves in the Distressed and Control sections between 7 and 10 years after construction. In the Distressed section, the percentage of slabs containing medium and low severity cracking was 30 percent after 10 years of construction and reached almost 70 percent after 15 years of service.

Table 1: Summary of Performance Data for SR 60

Performance Measurement	Segment 323 (Distressed Section)	Segment 303 (Control Section)
Outside Pavement Edge Faulting, in	0.026	0.024
Outer Wheel Path Faulting, in	0.022	0.039
Transverse Cracks Edge Faulting, in	0.061	0.043
Transverse Cracks Wheel Path Faulting, in	0.06	0.034
Lane-to-Shoulder Drop off, in	0.79	0.29
Transverse Cracking, % Slabs	88	20
Joint Width, in	0.78	0.71
PSR	2.5	3.2

2.7.1 Transverse Joint Faulting

A Georgia-type faultmeter with an accuracy of 4 mils (1 mil = 0.001 in) was used to measure joint faulting at both the edge (1 ft from the lane/shoulder joint) and the wheelpath (2.5-ft from the lane/shoulder joint) of the driving lane. As seen in Table 1, the mean joint faulting for the Distressed and Control sections at both locations is low considering typical values of allowable JPCP mean faulting are between 0.1 in and 0.2 in.

2.7.2 Lane-to-Shoulder Dropoff

The difference in elevation between the driving lane surface and the outside shoulder was also measured using the Georgia-type faultmeter. As presented in Table 1, the average dropoff was 0.81 in for the Distressed section and 0.29 in for the Control section. The minimum and maximum measured values for the Distressed section were 0.39 in and 0.92 in, respectively. For the Control section, 0.047 in and 0.63 in were the minimum and maximum values, respectively.

The larger lane/shoulder dropoff for the Distressed section is indicative of a larger settlement of the HMA shoulder for the section with the OGS base. This granular base has a higher potential for consolidation over time than the ATPB base used in the Control section.

2.7.3 Joint Width

The transverse joint widths were measured for all of the slabs within the sections. Two measurements were made per joint at approximately 1 ft from the lane/shoulder joint and 1 ft from the centerline. The average joint width within the Distressed section was 0.78 in and the average joint width in the Control section was 0.71 in.

2.7.4 Transverse Cracking

As mentioned previously, the major distress observed for both sections was mid-panel transverse cracking. An example is presented in Figure 6. According to the distress identification manual, the transverse cracks were categorized based on their severity level. The severity level is a function of the size of the crack and the size of the spalling around the crack, if any. A breakdown by severity shows that 74 percent of slabs exhibit high severity cracking and 14 percent of slabs exhibit medium severity cracking for the Distressed section. For the Control section, 4 percent of the slabs exhibited low severity cracking, 12 percent of the slabs exhibited medium severity cracking and only 4 percent of the slabs exhibited high severity cracking. Section 2.13 of this report explores the marked difference in the transverse cracking between the Distressed and Control section for SR 60 while Section 8 discusses how the overall performance of the pavement is related to performance of the OGS base layer used in the Distressed section.

Figure 6: Mid-slab Transverse Cracking for SR 60 Segment 323 Southbound, Slab 5 (Distressed section).

2.7.5 Present Serviceability Rating (PSR)

The average PSR of the Distressed and Control sections were 2.5 and 3.2, respectively. Although the faulting of joints and cracks is low, the amount of transverse cracking had a considerable effect on the ride quality.

2.8 FWD Testing: SR 60

Pavement deflection testing was performed using a Falling Wight Deflectometer (FWD) Dynatest model 8002 provided by PennDOT. The measured deflections could be used to backcalculate the elastic modulus of the PCC layer and the modulus of subgrade reaction (k-value), to evaluate the load transfer efficiency (LTE) at joints and cracks, and to assess the potential for the presence of voids under the slab. The FWD testing was conducted in four locations as illustrated in Figure 7. The testing at mid-slab locations provides information to backcalculate the elastic modulus of the PCC layer and the k-value whereas the testing at joints and cracks provide information to assess the joint/crack LTE and the potential for voids beneath the slab.

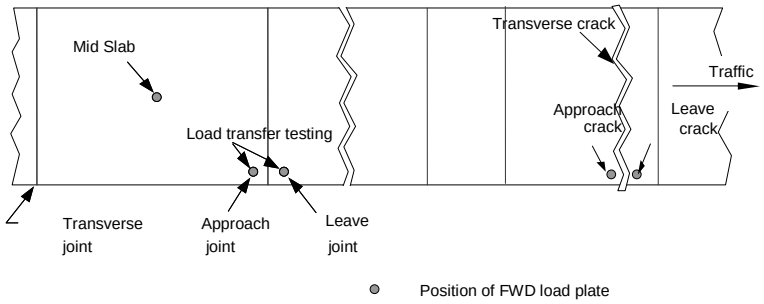

Figure 7: FWD Testing Pattern

The testing for the Distressed section included five mid-slab locations, ten transverse joints and transverse cracks (approach and leave sides), and seven slab edges. The FWD testing for the Control section included seven mid-slab locations, ten transverse joints and transverse cracks (approach and leave sides), and seven slab edges. The average air temperature during testing was 56 ºF. It is recommended to perform FWD testing when the ambient temperature is below 70 ºF to avoid testing when the joints are locked up.

A summary of the results obtained from analysis of the FWD data collected can be found in

Table 2. As observed in the table, the average elastic modulus for the Distressed and Control sections are very similar whereas the modulus of subgrade reaction is higher for the Control section due to the ATPB used in this portion of the road.

Table 2: Summary of Deflection Testing Results for SR 60

Property	Segment 323 (Distressed Section)	Segment 303(Control Section)
	Average	Average
Static Elastic Modulus, psi	5.20E+06	5.00E+06
k-value, psi/in	195	255
Joint Load Transfer, %	46	58
Crack Load Transfer, %	14	40
Average Mid-slab Deflection, mils	2.10	1.89
Corners With Voids, %	45	0

2.8.1 Temperature Gradient

The temperature gradient of the slab during FWD testing is an important variable to consider when using FWD data for void detection. If a positive temperature gradient is present in the slab during testing, then the corners of the slab will curl downward and there is the potential for a false negative in detecting voids. If a negative gradient is present, the slab corners will curl upward and a false positive is possible. In order to reduce the potential for false results, it is recommended that FWD testing be performed when the slabs are flat. This flat condition often occurs when a positive temperature gradient is present in the slab because of the existence of a built-in positive temperature gradient that is established during construction as the slab sets [2].

For this project, only ambient temperature and pavement surface temperature were recorded during FWD testing. An approximation of the temperature gradients in the slab during FWD testing were later predicted using the EICM [3]. Historical climatic data from the Pittsburgh International Airport weather station was used along with the EICM to estimate gradients that would be typically of that time of the year for the ambient temperatures measured. Figure 8 and Figure 9 present the predicted temperature profiles during the time FWD testing was performed for the Distressed and Control sections. The relationship between these profiles and the loss of support will be discussed in Section 2.8.6.

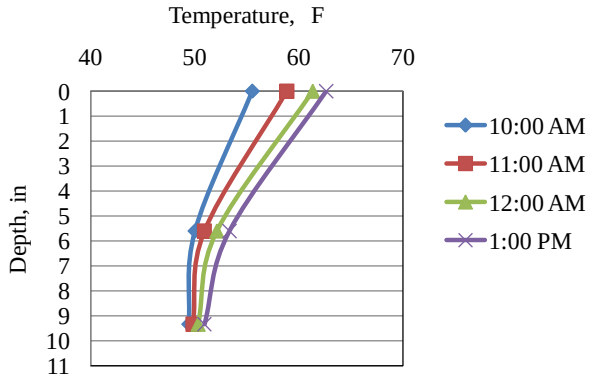

Figure 8: Predicted Slab Temperatures during FWD Testing for SR 60 Segment 323 Southbound (Distressed Section).

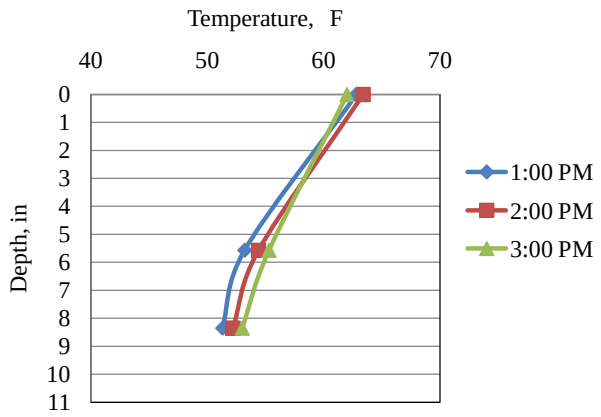

Figure 9: Predicted Slab Temperatures during FWD Testing for SR 60 Segment 303 Southbound (Control Section)

2.8.2 PCC Elastic Modulus

The elastic modulus, E, of the concrete was backcalculated using mid-slab deflection measurements along with the actual thickness of the slab determined from the cores extracted at the same locations. The average backcalculated static elastic modulus obtained for the Distressed and Control sections are in the range of typical values for mature concrete. This value for the Distressed section is 5.20 million psi with a coefficient of variation of 36 percent, whereas for the Control section it is 5 million psi with a standard deviation of 1.4 million psi and a coefficient of variation of 28 percent. Figure 10 presents the backcalculated static PCC elastic modulus along the Distressed section and Figure 11 presents this data for the Control section. The average backcalculated elastic modulus of the Control section is only 4 percent higher than the Distressed section. This small difference is not surprising considering the mix design appears to be the same for both the Distressed and Control sections.

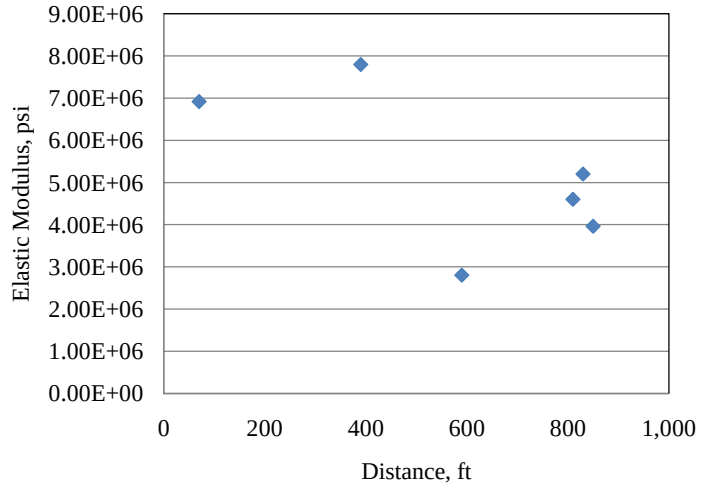

Figure 10: PCC Elastic Modulus for SR 60 Segment 323 Southbound (Distressed Section).

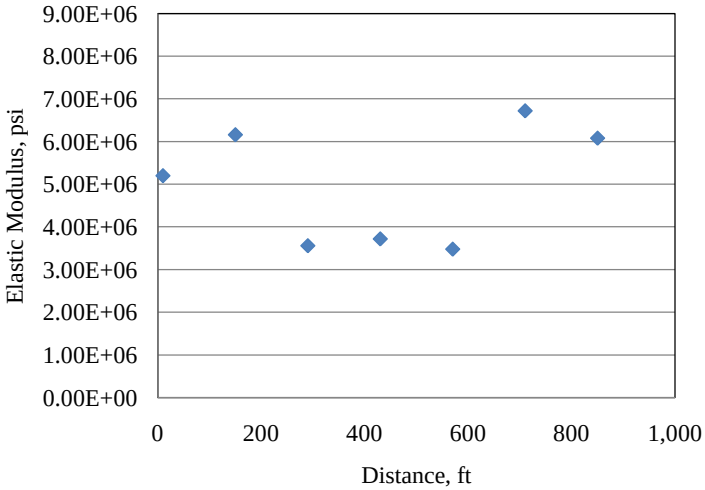

Figure 11: PCC Elastic Modulus for SR 60 Segment 303 Southbound (Control Section).

2.8.3 Modulus of Subgrade Reaction

The modulus of subgrade reaction, k-value, was calculated using mid-slab deflections. The average static k-value for the Distressed section is 195 psi/in with a standard deviation of 88 psi/in and a coefficient of variation of 45 percent. An estimate of the static k-value was achieved by multiplying the dynamic k-value by 0.5. For the Control section, the average static k-value is 255 psi/in with a standard deviation of 95 psi/in and a coefficient of variation of 38 percent. Figure 12 shows the k-value along the Distressed section and Figure 13 presents the k-value along the Control section.

The average modulus of subgrade reaction for the Control section is 30 percent higher than that for the Distressed section. This disparity is due to the higher stiffness of the stabilized base (ATPB) used in the Control section. Based on the pulled cores, debonding typically occurred about 1.5 in below the interface between the slab and the ATPB. There were a couple of cores where the ATPB was bonded to the slab. An example of one of these intact cores is shown in Figure 19. This core was pulled around station 160 ft into the section. It can be seen in Figure 9, that the estimated elastic modulus of the concrete appears to be high at this location. The fact the bond was neglected during the backcalculation process can possibly account for the high elastic modulus predicted in the Control section for the first two and last two FWD tests performed in the Control section. It should be noted that the same high degree of variability in the elastic modulus of the concrete was also observed in the Distressed section even though an unstabilized base was present.

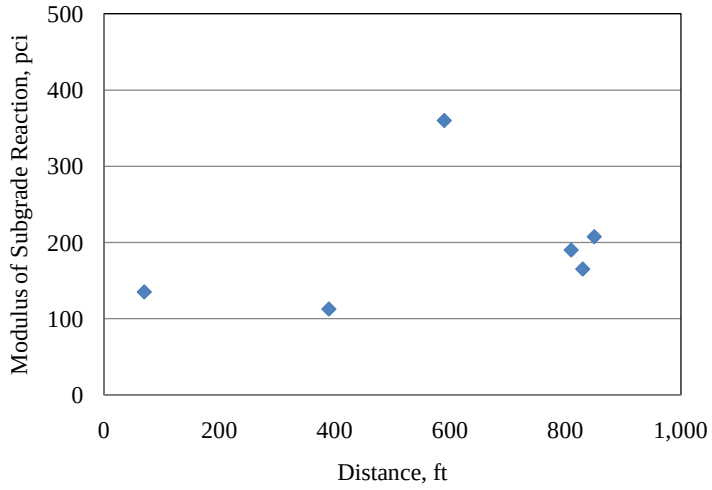

Figure 12: Modulus of Subgrade Reaction for SR 60 Segment 323 Southbound (Distressed Section).

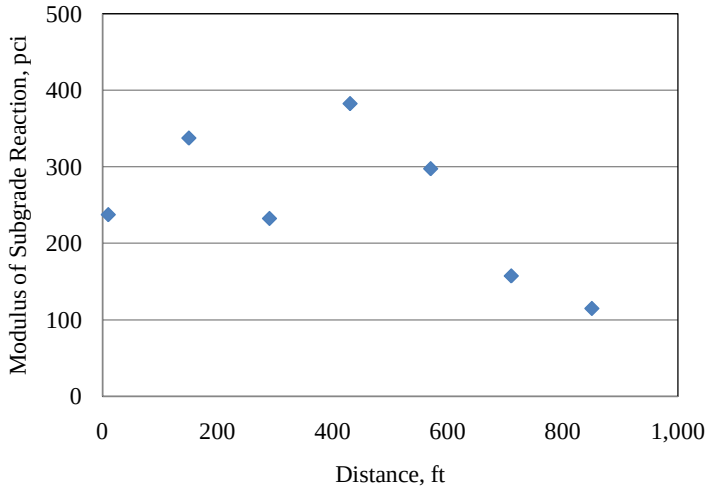

Figure 13: Modulus of Subgrade Reaction for SR 60 Segment 303 Southbound (Control Section).

2.8.4 Joint Load Transfer

The joint load transfer efficiency values for the Distressed and Control sections are presented in Figure 14 and Figure 15, respectively. As observed in these figures, the LTE of the transverse joints for both sections is low considering that a good level of LTE is greater than 70 percent. This low LTE might be due to the incremental damage over time [4], given the age of the pavement. Comparing the two sections, the average LTE for the Distressed section was 46 percent, while the average LTE for the Control section was 58 percent. The higher average value obtained for the Control section is believed to be due to the contribution of the stabilized base to the load transfer. For the Distressed section, the base layer is granular. Comparatively, granular base layers contribute less to the transfer of load the base layer when compared with a stabilized base. Additionally, the differential deflections for the transverse joints are presented in Figure 16 and Figure 17, respectively.

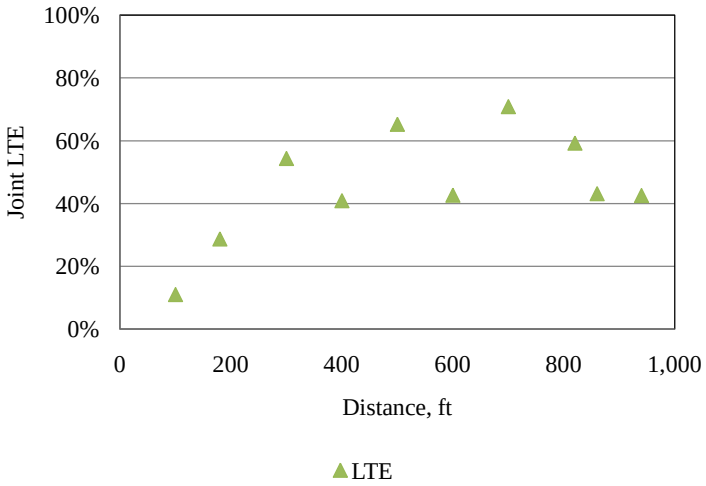

Figure 14: Transverse Joint Load Transfer Efficiencies for SR 60 Segment 323 Southbound (Distressed Section).

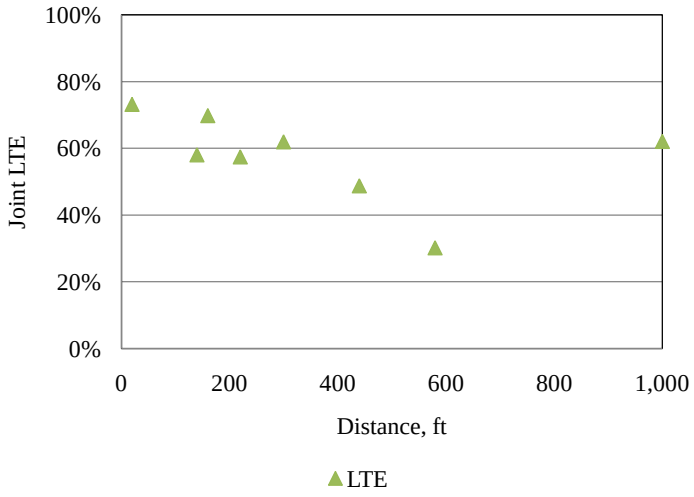

Figure 15: Transverse Joint Load Transfer Efficiencies for SR 60 Segment 303 Southbound (Control Section).

.

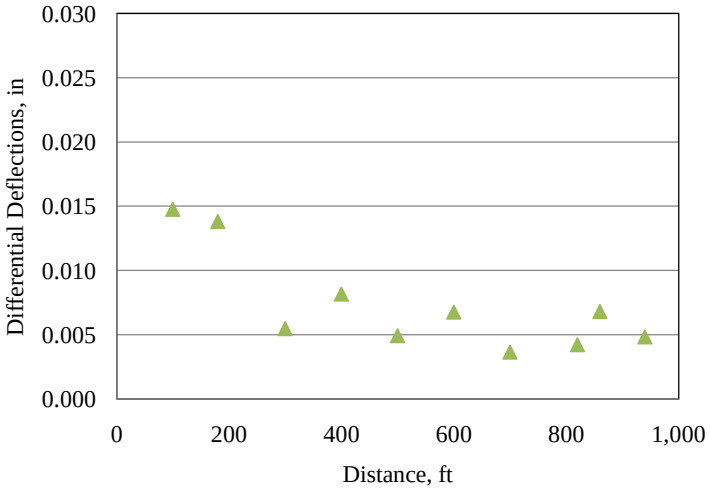

Figure 16: Differential Deflections at Transverse Joints for SR 60 Segment 323 Southbound (Distressed Section).

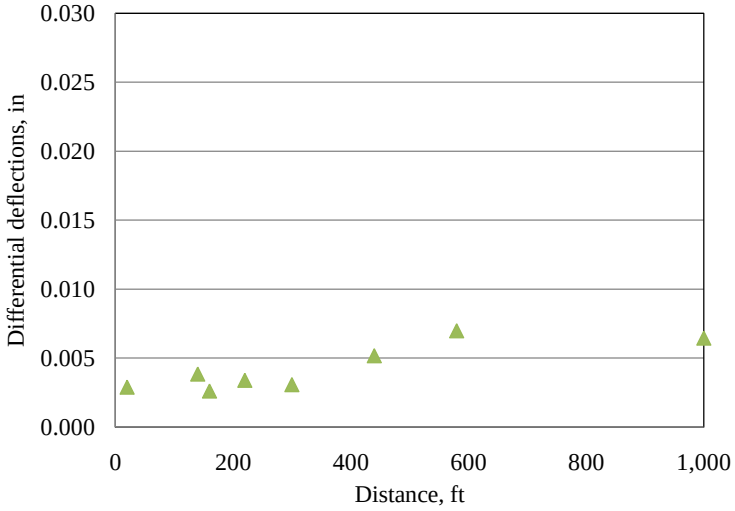

Figure 17: Differential deflections at transverse joints of SR 60 for Segment 303 Southbound (Control Section).

Differential deflections represent the difference between the deflections on the loaded side of the joint to the deflection on the unloaded side of the joint. If differential deflections are greater than 0.01 in, that indicates that there is a problem with load transfer at that location. For the Distressed section, only two of the transverse joints have differential deflections higher than the threshold value. These joints are also having the lowest LTE of the section. In the case of the Control section, none of the transverse joints have differential deflections higher than the threshold value, which agrees with the relatively better performance of the joints in this section.

2.8.5 Crack Load Transfer

The crack load transfer efficiency for the Distressed and Control sections are presented in Figure 18 and Figure 19, respectively. The difference in the average LTE for the cracks in the Distressed and Control sections is quite significant. Crack LTE for the Distressed section is 14 percent while it is 40 percent for the Control section.

The improved performance of the cracks in the Control section is mainly due to the contribution of the stabilized base. The stabilized base restricts movement to a degree and maintains a smaller crack width. This subsequently enhances the aggregate interlock mechanism

between the opposite faces of the crack, as well as its contribution in transferring the load across the crack. A greater portion of the load is also transferred through a stabilized base when compared to that of a granular base. The severity of the cracks were defined based on the crack width and can be correlated with the LTE of the cracks. As observed in Figure 19, the average LTE of the medium severity cracks is 30%, while the average LTE for the low severity cracks is 97%. It can be considered that the crack LTE is essentially a function of the crack width. For example, it can be observed that the LTE for the medium severity crack at 130 ft along the section in Figure 19 is high. It is also found that the width of this crack is much smaller and therefore makes sense that this medium severity crack presents a higher LTE.

A core retrieved at a high severity crack location in the Distressed section is shown in Figure 20. It is observed in this figure that extensive abrasion has taken place at the lower portion of the core. This condition, which implies large differential movements between the crack faces, combined with a large crack width, is likely responsible for the low LTE observed for the cracks in the Distressed section. Figure 21 presents a core retrieved at a low severity crack located in the Control section. As observed in the figure, the PCC layer is completely bonded with the ATPB layer. This condition restrains the opening of the crack and enhances the effectiveness of the aggregate load transfer across the crack.

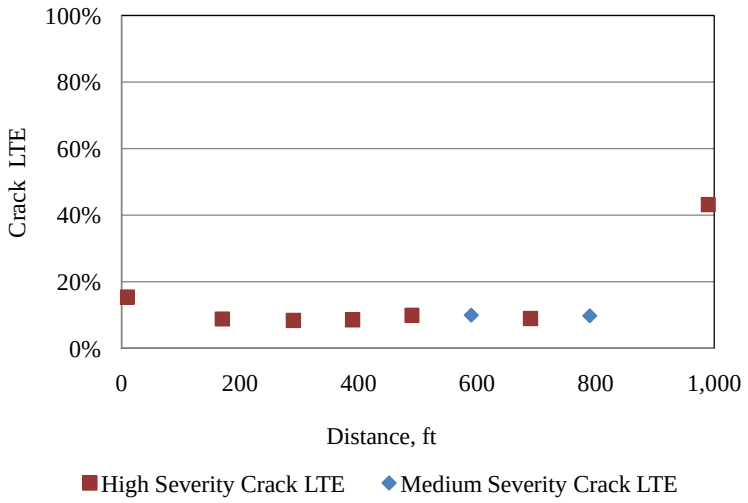

Figure 18: Transverse Crack LTE for SR 60 Segment 323 Southbound (Distressed Section).

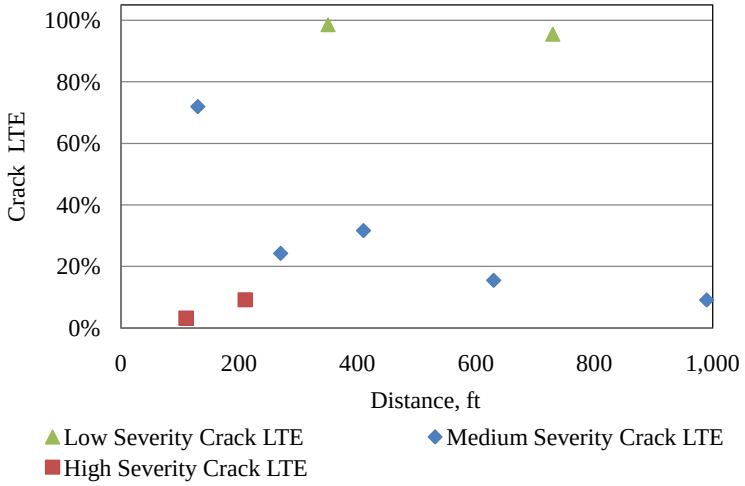

Figure 19: Transverse Crack LTE for SR 60 Segment 303 Southbound (Control Section).

Figure 20: High Severity Transverse Crack Core of SR 60 Segment 323 Southbound Slab 9 (Distressed Section)

Figure 21: Low Severity Transverse Crack Core of SR 60 Segment 303 Southbound Slab 7 (Control Section).

The differential deflections for transverse cracks are presented in Figure 22 and Figure 23 for the Distressed and Control sections, respectively. In the Distressed section, all but two values are above this threshold for differential deflection and only one value is significantly below the threshold. For the Control section, half of the differential deflection values for the Control section are below the threshold value and all of the differential deflections measured for the low severity cracks are well below the threshold values. The overall average differential deflection for the Distressed section is 0.016 in and the average differential deflections for the medium and high severity cracks are 0.015 in and 0.017 in, respectively. For the Control section, the overall average differential deflection is 0.010 in and is 0.001 in and 0.014 in for the low severity and medium severity cracks, respectively. The differential deflections for the Distressed and Control sections agree with the measured crack LTEs.

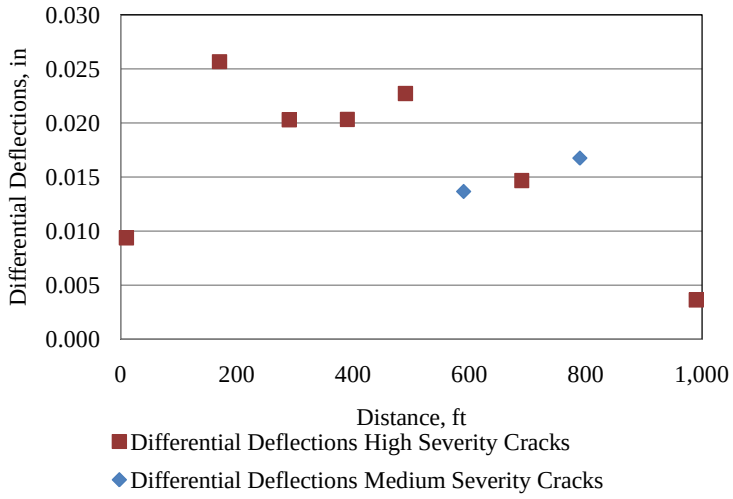

Figure 22: Differential Deflections at Transverse Cracks for SR 60 Segment 323 Southbound (Distressed Section).

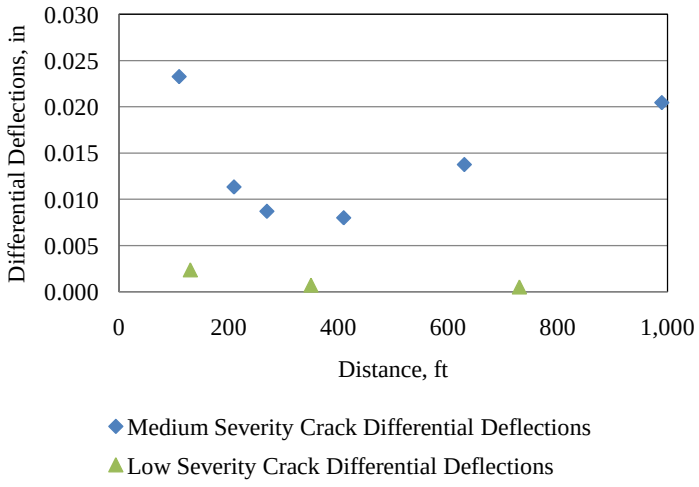

Figure 23: Differential Deflections at Transverse Cracks of SR 60 Segment 303 Southbound (Control Section).

2.8.6 Loss of Support

To determine the presence of voids using FWD data, the load vs. deflection response for each test at the leave side of a joint or crack was determined. This location is tested because it is the most likely location where voids occur. During testing, three different load levels were applied and the deflections were subsequently measured. Using these three load levels and the subsequent deflections, a relationship between deflection and load can be established. The y-intercept of the least-square linear regression equation through the three points is used to indicate whether or not there is the potential for a void. Intercepts greater than 2 mils indicate the possible presence of a void. Figure 24 and Figure 25 present the y-intercept values for the Distressed and Control sections, respectively. As observed in Figure 24, voids appear to be present under the slabs at the transverse joints in the first half of the Distressed section. Additionally, as shown in Figure 24 and Figure 25, voids also appear to be present at many of the transverse cracks in both the Distressed and Control sections.

In the Distressed section, 45 percent of the joint tested have possible voids while 78 percent of the cracks potentially have voids. As observed in Figure 24, the transverse joints and cracks with potential voids tend to be located in the first half of the section. While conducting FWD testing in the Distressed section, the slab surface temperature increased 10 °F and the predicted (assumed linear) gradients increased from 0.65 °F/in to 1.25 °F. It is possible that this led to false negatives in the latter portion of the section since the presence of a large positive gradient causes downward curling of the slab, and hence diminishing the ability to detect a void.

In the Control section, none of the joints or low severity cracks indicates the presence of a void. However, 44 percent of the medium severity cracks show the potential for voids beneath the slab. The identification of voids beneath slab at joints and cracks may be affected by the downward curling of the slab caused by the relatively high positive gradient during the testing (1.26 °F/in). The y-intercept value, which reflects the relative size of the void beneath the slab, could be higher for all of the joints and cracks. This condition suggests the likelihood of the existence of voids at the joints and cracks throughout the whole section.

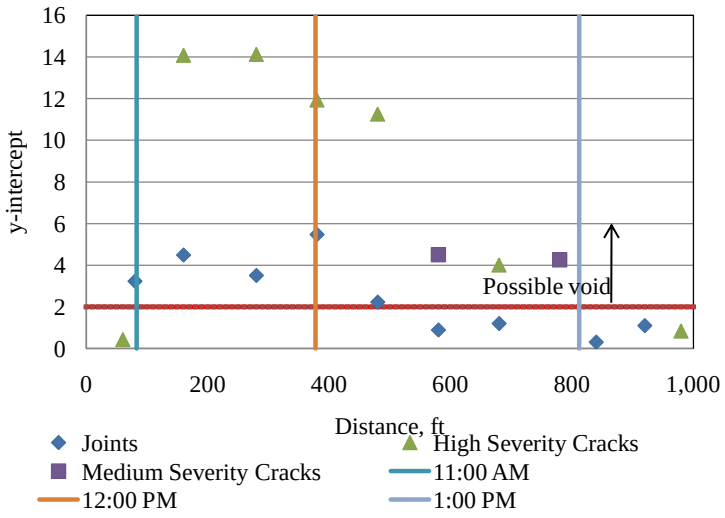

Figure 24: Loss of Support of SR 60 Segment 323 Southbound (Distressed Section).

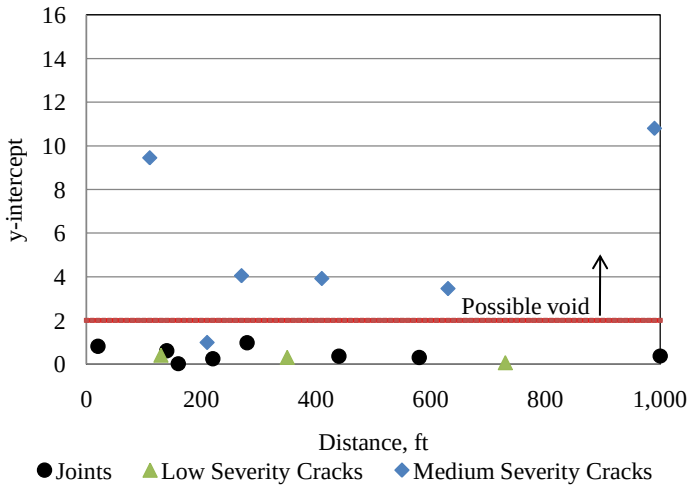

Figure 25: Loss of Support of SR 60 Segment 303 Southbound (Control Section).

2.9 Core Samples: SR 60

A total of nine 6-in diameter cores were retrieved at different slab locations for the Distressed section and nine 6-in diameter cores were retrieved at different slab locations for the Control section. Pertinent information regarding the designation, location, thickness, base type, continuity, and the presence of embedded items can be found in Table 3. From Table 3, the average thickness of the cores for the Distressed section was 11.5 in and 11.0 in for the Control section.

Table 3: Summary of Cores for SR 60 Segment 323 Southbound (Distressed Section)

Core	Location	PCC Thickness (in)	Base Type	No. of Pieces	Embedded Items
C4MS-D-60	Mid-slab	11	Granular	1	No
C9C-D-60	Transverse Crack	11.25	Granular	2	No
C15J-D-60	Joint	11.5	Granular	2	No
C20J-D-60	Joint	11.75	Granular	2	No
C20MS-D-60	Mid-slab	11.5	Granular	1	No
C35C-D-60	Transverse Crack	11.375	Granular	2	No
C42MS-D-60	Mid-slab	11.75	Granular	1	No
C43MS-D-60	Mid-slab	11.5	Granular	1	No
C47MS-D-60	Mid-slab	11.5	Granular	1	No

Table 4: Summary of Cores for SR 60 Segment 303 Southbound (Control Section)

Core	Location	PCC Thickness (in)	Base Type	Base Thickness (in)	No. of Pieces	Embedded Items
C1MS-C-60	Mid-slab	10.5	ATPB	3.5	1	No
C7C-C-60	Transverse Crack	10.5	ATPB	4	1	No
C11C-C-60	Transverse Crack	11	ATPB	3.5	2	No
C15MS-C-60	Mid-slab	11.5	ATPB	4	1	No
C22MS-C-60	Mid-slab	11	ATPB	4	1	No
C29J-C-60	Joint	12	ATPB	3.5	2	No
C36MS-C-60	Mid-slab	11	ATPB		1	No
C43MS-C-60	Mid-slab	11.5	ATPB	3	1	No
C45MS-C-60	Slab	11	ATPB	3.5	1	No

Visual examination of the retrieved concrete specimens revealed that the color of the paste at some areas surrounding the coarse aggregate (slag) was grey rather than brown which is the color of the rest of the paste. This paste discoloration is commonly observed in concretes containing blast furnace slag and is not believed to be detrimental to the concrete.

2.10 Base Samples: SR 60

A total of four granular base samples were obtained from the Distressed section at different locations where PCC cores were retrieved as follows: Slab 4, Slab 9, Slab 15, and Slab 47. A sieve analysis using the portion of each sample passing the No. 4 sieve was performed. Figure 26 through Figure 29 present the gradation curve for each sample represented by a solid line as well as PennDOT's gradation specification for OGS represented by dashed lines. As observed in the figures, the percentage of fines (material finer than 3 mils) is within the range specified by Section 703 of PennDOT Specification 408 which calls for a maximum fines quantity of 5 percent [5] and the entire gradation is in generally in the range of the specification.

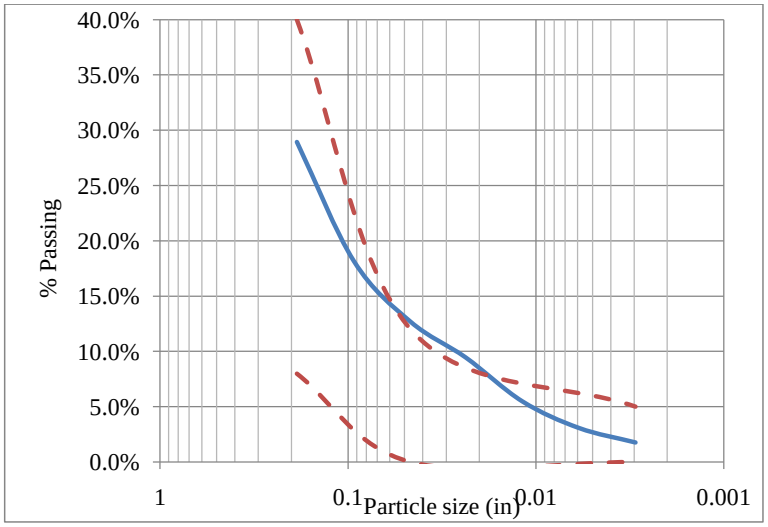

Figure 26: Particle Size Distribution Curve for the Portion Passing the No. 4 Sieve of the OGS Granular Base for SR 60 Segment 323 Southbound Slab 4 (Distressed Section).

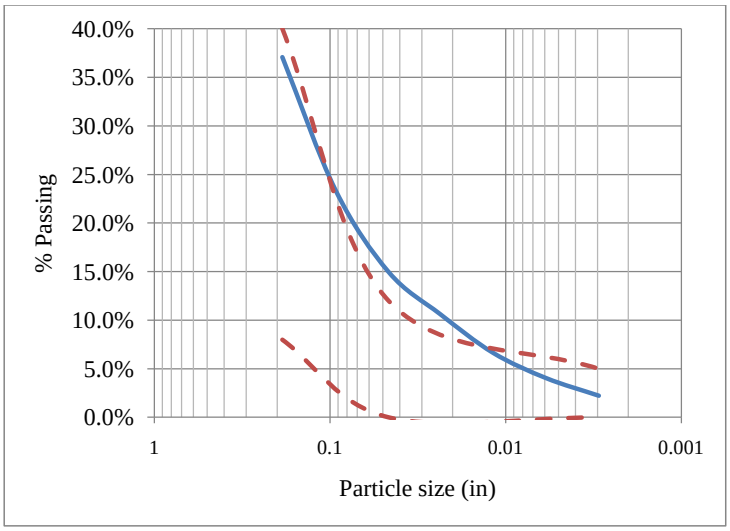

Figure 27: Particle Size Distribution Curve for the Portion Passing the No. 4 Sieve of the OGS Granular Base for SR 60 Segment 323 Southbound Slab 9 (Distressed Section).

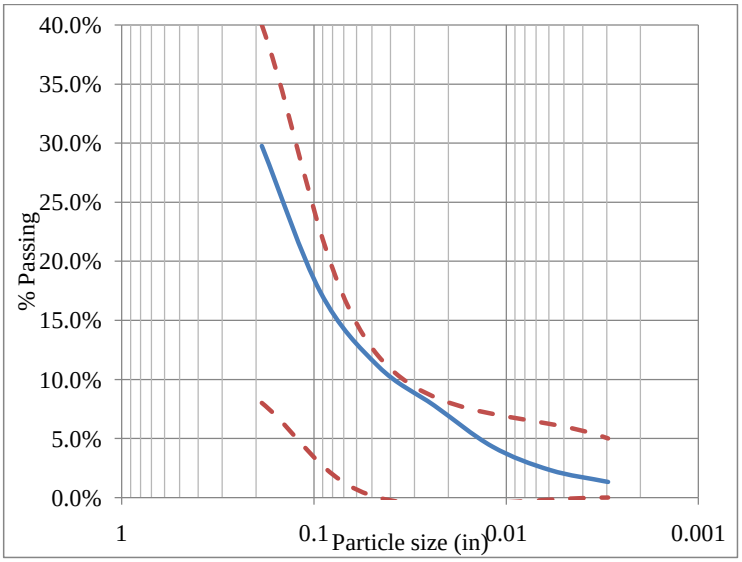

Figure 28: Particle Size Distribution Curve for the Portion Passing the No. 4 Sieve of the OGS Granular Base for SR 60 Segment 323 Southbound Slab 15 (Distressed Section).

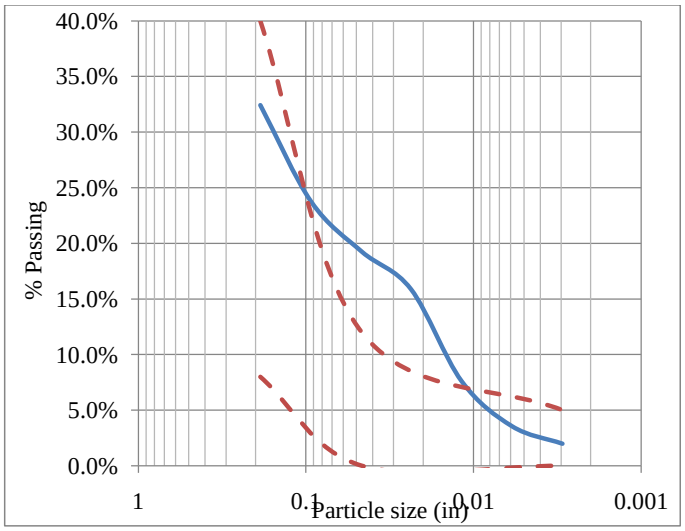

Figure 29: Particle Size Distribution Curve for the Portion Passing the No. 4 Sieve of the OGS Granular Base for SR 60 Segment 323 Southbound Slab 47 (Distressed Section).

2.11 Laboratory Testing Results: SR 60

Several laboratory tests were performed on the retrieved core specimens. The distribution of the testing was performed in accordance to the number of samples, the location, and the observed distress affecting each section. Table 5 presents the results for the following tests: CTE, static modulus of elasticity, Poisson's ratio, compressive strength, and the split tensile strength.

As expected based on the visual similarities observed in the PCC mix, the average results for the aforementioned tests were very similar between the Distressed and Control section specimens. These results support the assumption that the concrete mixture design was the same for both sections. In addition, the results obtained are within typical ranges for mature paving concrete.

Table 5: Summary of Laboratory Test Results for SR 60.

	Distressed			Control		
Laboratory Test	Average	St. Dev	COV	Average	St. Dev	COV
CTE, /°F	5.21E-06	0.62 E-06	12%	5.15E-06	0.37E-06	7%
Static Elastic Modulus, psi	4.55E+06	0.28E+06	6%	4.55E+06	0.51E+06	11%
Poisson's Ratio	0.20	0.01	7%	0.20	0.02	9%
Compressive Strength, psi	5,580	778	14%	6,340	1,087	17%
Split Tensile Strength, psi	480	-	-	492	43	9

2.12 Laboratory and Backcalculated Results Analysis: SR 60

The average backcalculated static elastic modulus values were 14 percent and 10 percent higher than the laboratory-determined values for the Distressed and Control sections, respectively. Despite this difference, it is not considered significant because it is smaller than the variation obtained within specimens for the FWD and laboratory testing. Both the backcalculated and laboratory-determined PCC stiffness are between typical ranges for mature concrete.

2.13 Potential Causes of Distress: SR 60

Comparing the performance of the Distressed and Control sections it can be concluded that the use of a stabilized layer in the Distressed section would have considerably reduced the transverse cracking. Theoretically, the use of a stabilized layer increases the curling and warping stresses in the PCC slab and one would expect to see higher stresses generated in the Control section relative to the Distressed section. While this is true, there are many advantages provided by the use of a stabilized base relative to an unstabilized base. From the retrieved cores, it was observed that the stabilized layer was perfectly bonded to the PCC layer. This condition suggests a monolithic behavior of the PCC slab and the stabilized base. This behavior greatly decreases the load-related stress that contributes to transverse cracking.

In the Distressed section, the use of the OGS may have increased the potential for higher stresses in the slab due to a loss of support that was possibly caused by consolidation of this granular base over time. This conclusion is supported by the FWD data analysis for void detection. Additionally, it is believed that the structural capacity of this section is not sufficient considering the traffic and environmental loads applied.

The MEPDG software was used to analyze the predicted performance of both sections and to validate the assumptions already made regarding the potential causes for the premature transverse cracking of the Distressed section. The analysis of the predicted pavement performance is presented below.

2.14 MEPDG Runs: SR 60

MEPDG files were created for the Distressed and Control sections. When possible, measured or calculated values were used for inputs; otherwise, default values were used. The only difference between the input file used for the Distressed section and the input file used for the Control section was the base layer and the thickness of the PCC layer. Based on the cores pulled from each section, the average thickness was actually 0.5-in lower in the Control section. The following summary discusses the inputs used as well as the results predicted by the MEPDG.

2.14.1 Pavement Structure

The pavement structure for the Distressed section consists of an 11.5-in PCC slab over a 4-in base layer of ATPB and a 4-in layer of PennDOT 2-A subbase. The pavement structure for the Control section consists of an 11-in slab over a 4-in layer of crushed gravel (OGS layer) and a 4-in layer of PennDOT 2-A subbase. The subgrade used for both the Control and Distressed section was an AASHTO A-4 subgrade.

PCC Slab

PCC slab properties are divided into four groups: general properties, thermal properties, PCC strength, and mixture design. The general properties include the unit weight and Poisson's ratio, which were chosen as 150 pcf and 0.20, respectively. The unit weight used was a default value and the Poisson's ratio used was that obtained for each section in the laboratory testing. In the case of the CTE, the laboratory-measured values had to be adjusted in order to match the values used for the calibration of the MEPDG models. The MEPDG models were calibrated using CTE

values form the LTPP database, which were erroneous due to an incorrect value used for the calibration of the test. The CTE of the calibration specimen used in the testing for the development of the LTPP database was found to be improper for the temperature range at which the test is carried out. According to Tanesi et.al [6] the CTE values included in the LTPP database are between 1.0 and 1.5 x 10^{-6} /ºF higher in comparison with CTE values obtained using the correct CTE for the calibration specimen. Consequently, and after some trial runs, 1.5 x 10^{-6} /ºF was added to the laboratory-determined CTE values. The CTE for the Distressed and Control sections to include as input in the MEPDG (ver. 1.1) was 6.7 x 10^{-6} /ºF. For thermal conductivity, 1.25 BTU/hr-ft- ºF was used, and for heat capacity, 0.28 BTU/lb- ºF was used. These are both default values.

The PCC compressive strength properties that were used in the MEPDG runs are based on those obtained in the laboratory. The laboratory-determined values are 5,580 and 6,340 psi for the Distressed and Control sections, respectively. These values were used to backcalculate the compressive strength at 28 days, which is the strength age required by the MEPDG. The percentage of strength gain over time was obtained following the MEPDG. The increase in the PCC modulus of rupture for the period in question (i.e. 18 years) is about 8 percent. The compressive strength were correlated to the Modulus of Rupture using the following equation [7]:

Equation 1

where MR is the PCC modulus of rupture in psi and f'c is the compressive strength expressed in psi.

The 28-day compressive strengths used as inputs in the MEPDG were 4,700 psi and 5,400 psi for the Distressed and Control sections, respectively.

The PCC elastic modulus was also adjusted as the compressive strength using the rate of increase over time predicted by the MEPDG. The adjusted PCC elastic modulus used as input in the MEPDG for the Distressed and Control sections was the same, namely 4.25E+06 psi.

The final portion of PCC slab characterization is mixture design. The values corresponding to mixture design that were used in the MEPDG runs are presented in Table 6.

Table 6: PCC Mixture Design Inputs for SR 60.

Input	Distressed	Control
PCC Strength, psi	4,700	5,400
Cement Type	I	I
Cementitious Material Content, lb/cy	588	588
w/c Ratio	0.42	0.42
Aggregate Type	Dolomite	
Reversible Shrinkage (% of Ultimate Shrinkage)	50	
Curing Method	Curing Compound	

Asphalt Treated Permeable Base

A 4-in asphalt treated permeable base layer was incorporated into the pavement structure as a base beneath the PCC slab for the Control section. The default MEPDG values for the strength properties, gradation and binder properties of this material were used. This includes a Poisson's ratio of 0.35, an effective binder content of 3.5 percent with 8.5 percent air voids. The gradation of this layer is presented in Table 7. The percentage of fines is 5 percent.

Table 7: Asphalt Treated Permeable Base Gradation for SR 60.

Sieve	Cumulative Retained, %
3/4 in	5
3/8 in	20
No. 4	20

Open Graded Subbase (OGS)

A 4-in crushed gravel layer, which represents the OGS, was incorporated into the pavement structure as a base underneath the PCC slab for the Distressed section. The strength properties of this material were calculated based on a known layer coefficient from PennDOT specifications and a correlation between layer coefficient and resilient modulus built in the MEPDG. Based on

this internal correlation, the modulus is approximately 14,500 psi. Other default values provided by the MEPDG software with respect to the OGS are as follows: Poisson's ratio, 0.35; and coefficient of lateral pressure, K_0 of 0.5. The gradation of the OGS was determined based on the PennDOT specifications and it is presented in Table 8.

Table 8: OGS Gradation for SR 60.

Sieve	Minimum % Passing	Maximum % Passing
2 in	100	100
3/4 in	52	100
3/8 in	36	65
No. 4	8	40
No. 16	0	12
No. 200	5	5

2A Subbase Layer

The gradation of the 2A crushed gravel is presented in Table 9. The structural number provided by PennDOT was used with the correlation between structural number and resilient modulus in the MEPDG to calculate the resilient modulus. Based on this correlation the value for resilient modulus used in the MEPDG was approximately 14,500 psi. All other properties for this material were established using the Level 3 default values provided in the MEPDG software. This includes a Poisson's ratio of 0.35 and a 0.5 coefficient of lateral pressure.

Table 9: Summary of Inputs for the 2A Crushed Gravel Layer for SR 60.

Parameter	Value	
Coefficient of Lateral Pressure, K_0	0.5	
Poisson's Ratio	0.35	
Elastic Modulus, psi	25,000	
Aggregate Gradation	Sieve Size	Passing, %
	1 ½ in	100
	1 in	99
	1/2 in	45
	No. 4	16
	No. 16	11
	No. 200	3

Subgrade Soil

An AASHTO A-4 subgrade was used in the MEPDG input file. Poisson's ratio and the coefficient of lateral pressure were assigned utilizing the same default values as were used for the crushed gravel. The gradation of the subgrade soil is shown in Table 10.

Table 10: Subgrade Soil Gradation for SR 60.

Sieve	% Passing
	A-4
4 in	99.8
3 ½ in	99.8
2 in	99.6
1 ½ in	99.4
1 in	98.7
3/4 in	98
1/2 in	96.7
3/8 in	95.6
No. 4	93
No. 10	89.9
No. 40	82.7
No. 80	73.9
No. 200	60.6

2.14.2 Climate

To characterize the climate, the weather station labeled as Pittsburgh International Airport was used for the analysis, and as mentioned previously, this is approximately 13 miles away. A summary of the weather station location can be found in Table 11.

Table 11: Summary of Weather Station Location Information for SR 60.

Climate Station	Latitude, degree	Longitude, degree	Elevation (ft)
Pittsburgh, PA	40.3	-80.14	1175

2.14.3 Pavement Design Features

Additional aspects of the pavement that need to be categorized in the MEPDG include the diameter and spacing of dowel bars, shoulder type, joint spacing and base/slab friction coefficient. A summary of these design features used in the input file for SR 60 can be seen in Table 12.

Table 12: Summary of Pavement Design Feature Inputs for SR 60

Input	Value
Effective Joint Spacing, ft	25.06
Sealant Type	Preformed
Dowel Diameter, in	1.5
Dowel Bar Spacing, in	12
Shoulder Type	Tied PCC Shoulder
Base Type	Granular/Asphalt Treated
Erodibility Index	Very Erodable (5)/ Very Erosion Resistant
PCC-Base Interface	Full Friction Contact
Loss of Full Friction (age in months)	120
Permanent Curl/Warp Effective Temperature Difference, °F	-10

2.14.4 Traffic Inputs

Two-way Annual Average Daily Truck Traffic (AADTT)

The following traffic inputs were used and can be seen in Table 13. This AADTT was calculated for the year 1992 based on historic traffic data obtained from PennDOT, while the rest of the inputs are default values determined considering that this portion of SR 60 has a roadway classification of urban interstate.

Table 13: Summary of Traffic Inputs for SR 60

Input	Value
Initial Two-Way AADTT	2,000
Number of Lanes in Design Direction	2
Percent Trucks in Design Direction, %	50
Percent Trucks in Design Lane, %	90
Operational Speed, mph	65

Traffic Volume Adjustment Factors

The following factors are necessary to determine the AADTT for each truck class, for each month on an hourly basis:

- *Load Monthly Adjustment Factors.*
- *Vehicle Class Distribution Factors.*
- *Hourly Truck Traffic Distribution.*
- *Traffic Growth Factors.*
- *Directional Distribution Factors.*
- *Lane Distribution Factors.*

The load monthly adjustment factors, the vehicle class distribution factors, the hourly truck traffic distribution are default values provided in the MEPDG. These values were used in the absence of actual data. The traffic growth factor was obtained considering a linear growth rate of 3 percent for the traffic. The percent of trucks in the design direction and design lane are typical values based on the road type.

Axle Load Distribution Factors

The axle load distribution factors represent the percentage of the total axle applications within each load interval, for each vehicle class and for each specific axle type. Level 3 default values generated from the LTTP database were assigned for all axle types (single, tandem, tridem, and quad) and all vehicle classes (4 to 13). These values were used in the absence of actual data.

General Traffic Inputs

The following information is contained in this category:

- *Mean Wheel Location, Traffic Wander Standard Deviation, and Design Lane Width.*
- *Number of Axle Types per Truck.*
- *Axle Configuration.*
- *Wheel Base Distribution.*

The values used for these variables are default values given by the MEPDG and were used in the absence of actual data.

2.14.5 Results

A summary of the results from the MEPDG runs compared with the field conditions can be seen in Table 14. The prediction of transverse cracking is quite good for both the Distressed and Control sections. In the case of the predicted faulting, it is over predicted for both sections. A

discussion of the specifics regarding the prediction of these two pavement performance indicators is presented below.

Table 14: Predicted vs. Observed Distress for SR 60.

Distress	SR 60			
	Distressed Section		Control Section	
	Predicted	Observed	Predicted	Observed
Faulting, in	0.118	0.026	0.070	0.024
Cracking, %	91	88	23	18

Figure 30 presents the MEPDG-predicted along with the observed transverse cracking for the Distressed section and Control section. The observed transverse cracking over time (from year 5 to year 16) is based on historic distress data provided by PennDOT, which has been collected using automated distress equipment. The data point for year 17 represents the percentage of transverse cracking of the Distressed section that was manually surveyed as part of the field data collection executed in the present study. Although there are some historic data points missing, it can be observed that transverse cracking began to be visible on the surface of the slabs between years 7 and 10. Additionally, it can be noticed in Figure 30 that, for the Distressed section, from year 11 to year 12, the percentage of cracking increases from 33 percent to 58 percent; and from year 16 to year 17 it increases from 69 to 88 percent.

These significant increases can be associated with the sensitivity of the automated equipment. It is possible that under some conditions the automated equipment does not capture all the transverse cracking, thus, it is being underestimated. Based on this belief, and after observing the predicted cracking in Figure 30, it may be possible that the transverse cracking for the Distressed section initiated its development before the 5^{th} year. Despite the difference in predicted and observed cracking values, it can be observed that the rate of increase in cracking exhibited for both the predicted and observed transverse cracking of the Distressed section over time is similar. This supports the consideration that the structural capacity of this pavement section is lower than it should be for the pavement to reach its intended design life and locates the pavement in the critical zone in terms of the relationship between fatigue damage and transverse cracking. This critical zone is defined as the zone where cracking increases rapidly with relatively smaller increases in damage as shown in Figure 31.

In the case of the Control section, it can be seen in Figure 30 that the prediction of the MEPDG is also considerably accurate. Unlike the Distressed section, the rate of increase for transverse cracking is considerably low. This implies that this pavement section is not located in the critical zone of fatigue damage shown in Figure 31 and suggests that the structural capacity of this pavement section is sufficient to carry the imposed loads over time.

Figure 30: Predicted and Observed Transverse Cracking for SR 60 Segment 323 and 303 Southbound (Distressed and Control Sections)

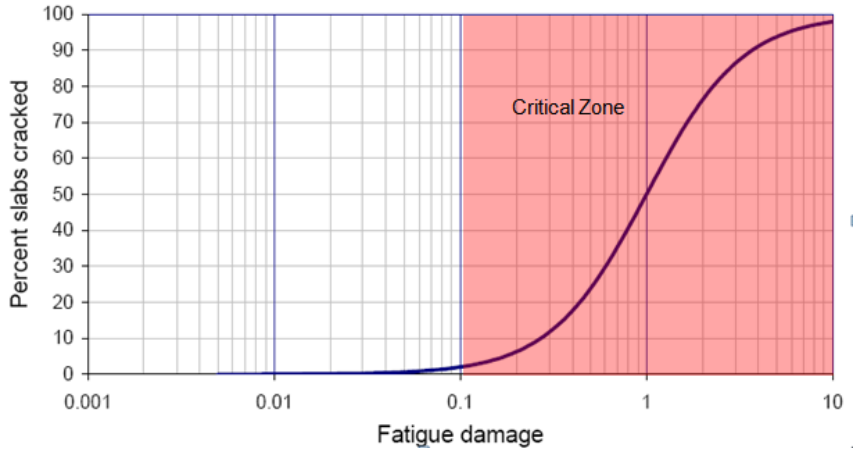

Figure 31: MEPDG Model of the Relationship Between Fatigue Damage and Cracking.

Figure 32 presents the predicted and observed faulting for both the Distressed and Control sections. The observed faulting corresponds to the information obtained as part of the field data collection carried out for the present study. Historic data for faulting was not available. As noticed in the plot, there is a large difference between the predicted and observed faulting. The high predicted faulting is mainly caused by a high upward corner deflection calculated by the MEPDG faulting model, which is function of the CTE of the slab. This upward corner deflection has a considerable effect on the initial maximum mean transverse joint faulting. It is believed that the MEPDG faulting model requires a recalibration considering the required adjustment of the CTE values already discussed.

Figure 32: Predicted vs. Observed Joint Faulting for SR 60 Segments 323 and 303 Southbound (Distressed and Control Sections).

By comparing the performance of both sections, it can be concluded that the structural contribution of the stabilized base played an important role in the acceptable performance of the Control section. Although the main purpose of a stabilized base is to provide uniform support and resist erosion, it can be concluded that the bonding between PCC slab and the stabilized base contributes greatly in reducing the critical load-related bending stress as well.

2.15 Rehabilitation Recommendations: SR 60

2.15.1 Distresses and Deficiencies

As mentioned previously, the primary distress in both the Distressed and Control sections for SR 60 is mid-slab transverse cracking. In addition to transverse cracking, the joints and cracks are exhibiting low load transfer efficiencies and a loss of support under the slab near the cracks. While these issues are present in both the Distressed and Control sections, the extent is different between the sections with the extent of these issues being much greater in the Distressed section. In the case of SR 60 the extent of the deficiencies has a considerable influence on the recommendations for each section and therefore the recommended rehabilitation options will be discussed in two separate sections.

2.15.2 Recommendations for Segment 323 (Distressed Section)

A substantial amount of cracking (90 percent of the slabs have cracks of medium or high severity) along with poor load transfer at the joints and cracks and voids beneath the slab near the cracks.

There appears to be distress that could be related to/or exacerbated by inadequate drainage. The existing drainage system should be inspected with a video camera to ensure it is working properly. Any damaged sections should be removed and replaced and any debris restricting flow should be flushed from the system.

Due to the extensive amount of distress observed, an overlay is recommended. If an unbonded PCC overlay is constructed, it is suggested that slab stabilization be performed. This will require an extensive amount of urethane for the stabilization since the base consist of OGS. Slab stabilization will be beneficial in helping to stabilize the OGS and reduce further breakdown/consolidation of the layer. Stabilization of a pavement with an open graded base can be costly but other districts have shown that this can be performed successfully on pavements having an OGS base in Pennsylvania. Stabilization of the OGS base could also lead to a decrease in the effectiveness of drainage beneath the pavement but based on the experience of other districts is appears that this reduction does not significantly affect the performance.

It is not necessary to perform load transfer restoration at the joints or cracks or full-depth repairs for the deteriorated cracks if an unbonded overlay is constructed since the rigidity of the overlay will help in bridging over the distress. The use of a thick geotextile material as is

currently being used by the Missouri Department of Transportation, as well as many other states, should be considered to help reduce the potential for the distress reflecting up into the overlay.

Another option would be the construction of an HMA overlay. Pre-overlay repairs required for this rehabilitation option would be much more extensive and should include slab stabilization, load transfer restoration at the joints and full-depth repairs of the deteriorated cracks, as suggested in the AASHTO 1993 Guide for Design of Pavement Structures [8].

Crack and seat is another rehabilitation alternative to consider. The success of a crack and seat project is largely a function of the stiffness of the subgrade. If the subgrade is not sufficiently stiff, the energy imposed to fracture the slab will be absorbed by the soft subgrade. This makes it difficult to break the slab into sufficiently small fragments that they are able to expand and contract independently and therefore reduced the performance of the HMA overlay placed above this layer. According to Sebesta and Scullion (2007), the CBR for the subgrade of an 11-in slab should be above 6 for low risk, between 2 and 6 for moderate risk and below 2 would be high risk. The subgrade is classified as A-4. This soil classification exhibits a broad range of CBR values that can fall under either moderate risk or low risk. It is suggested that if break and seat is an alternative being considered, the CBR of the subgrade be measured. It is believed that the OGS in its present condition could also contribute to the absorption of energy by the layers beneath the slab. For this reason, difficulties in fracturing the slab could be encountered even if the CBR of the subgrade is above 6.

2.15.3 Recommendations for Segment 303 (Control Section)

For the Control section of SR 60, the transverse cracking is significantly less than in the Distressed section but the performance history graph shows an upward trend in the development of cracking. Therefore, even though the PSR is slightly above 3, it will most likely begin to decline relatively quickly. Therefore, if sufficient funding an overlay could be placed on this section while work is being performed on the adjacent section to prevent having to come back and address these deficiencies in a few years. As stated with the Distressed section, an HMA overly would require pre-overlay repairs consisting of slab stabilization full depth repairs for the cracks and dowel bar retrofits to restore load transfer at the joints. If an unbonded PCC overlay is placed then just slab stabilization, and possibly the placement of a geotextile material as suggested for the distressed section, would be sufficient. Since much life is still remaining in this section of roadway, a break and seat is not suggested as a possible rehabilitation alternative.

2.16 Future Projects: SR 60

SR 60 illustrates the relatively lower structural capacity of OGS and the tendency to create loss of support conditions. The loss of support conditions subsequently lead to increased stresses being generated in the pavement and an earlier decline in the performance of the pavement. It should be noted that the design life for this pavement was 20 years and it is now 18 years old. Therefore, this design is close to meeting its expected design life. The performance would have been extended if it was not for the combination of the longer panel lengths (20-ft skewed joints) in combination with an OGS base. As seen by the performance of the Control section, reducing the load related stress by using a stabilized base was sufficient in extending the performance. It is possible that the use of an OGS along with the current standard joint spacing of 15 ft would also result in increasing the performance life. Currently, both a 15-ft joint spacing and a stabilized base are specified and both will contribute to decreasing fatigue cracking and reduce the number of areas with a loss of support beneath the slab.

3 SR 202, Chester County

3.1 Project Information: SR 202

For SR 202, the selected site is a section located in Chester County constructed between 2000 and 2002. Chester County falls under the jurisdiction of PennDOT Engineering District 6. The selected segment to execute the data collection plan for SR 202 was Segment 440 northbound located in the municipality of Tredyffrin, PA. A 1000-ft long representative section within the segment was chosen based on the pavement condition and the ease with which traffic control could be executed. Since the selected representative section contains considerable portions of both distressed and non-distressed or low severity distressed slabs, the selection of an additional Control section was not necessary. The green highlight in Figure 33 shows the location of Segment 440 between the junction with SR 422 and SR 252.

Figure 33: Location of Segment 440 Northbound of SR 202 in District 6.

3.2 Design Information: SR 202

Segment 440 is a JPCP pavement with four lanes per direction. According to the design information, the pavement structure for Segment 440 includes a 13-in thick PCC slab, over a 4-in thick ATPB, an 8-in 2A subbase, and an AASHTO A-4 subgrade. The slabs are 12 ft wide with a 15 ft transverse joint spacing. All joints are sealed with an asphalt sealant. The diameter of the dowels is 1.5 in. The shoulder consists of a tied PCC shoulder. Six-in diameter longitudinal

edge drains are present underneath the pavement. A cross section of the existing pavement representing the average layer thickness can be seen in Figure 34 and the overall condition of the pavement can be seen in Figure 35.

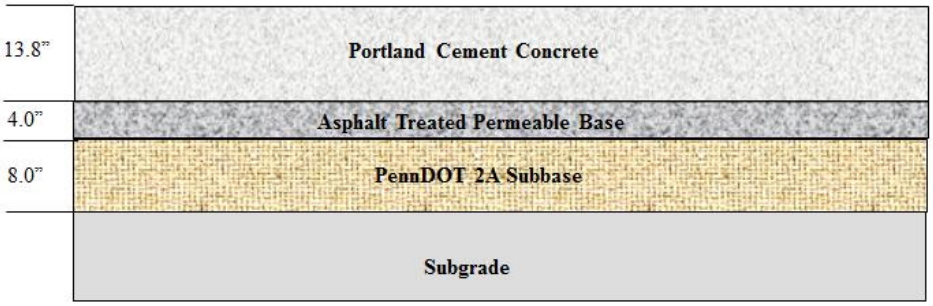

Figure 34: Existing Pavement Cross Section of SR 202 Segment 440 Northbound

Figure 35: Overall Condition of SR 202 Segment 440 Northbound.

3.3 Concrete Mixture Design: SR 202

The concrete mixture design information for SR 202 segment 400 provided by PennDOT is presented in Table 15. The mixture design had a w/c ratio ranging between 0.38 and 0.44.

Table 15: Concrete Mixture Design for SR 202 Segment 440 Northbound

Material	Specific Gravity	Absorption	Batch Weight (lbs per yd^3)
Type I Cement (Keystone Cement)	3.15	n/a	611
Coarse Aggregate (Devault Quarry ICM 15A14) No. 57	2.8	unknown	1852
Fine Aggregate (Hanson/Mays Landing Sand & Gravel MAI NJA)	2.63	unknown	1212-1308

3.4 Climatic Conditions: SR 202

SR 202 is located in a wet freeze climate with a relatively high number of wet days per year. The closest climate station to this section of SR 202 is located in Pottstown, PA, which is 6.3 miles away. Based on the data from this weather station, the area experiences approximately 143 wet days per year and a mean annual rainfall of 42 in. The freezing index is 447 ºF-days and the area is exposed to an average of 86 freeze-thaw cycles per year. The mean annual air temperature is 52 ºF with minimum and maximum average monthly temperatures of 32 ºF and 87 ºF, respectively.

3.5 Traffic Loadings: SR 202

According to the information obtained from the PennDOT ITMS, the AADT of Segment 440 is approximately 41,000 with 7 percent trucks. Based on historic traffic information provided by PennDOT, the pavement has experienced nearly 6.5 million ESALs between 2002 to the beginning of 2009.

3.6 Selection of Distress Survey Section: SR 202

Historic automated distress survey data provided by PennDOT, as well as panoramic images of the roadway obtained from the PennDOT Videolog application were reviewed in the office to locate road segments exhibiting early-age distress. Combining the results of the Videolog assessment with an initial visit to the project, however, only Segment 440 was selected for the field study since it contains areas exhibiting both a high amount of distress and areas exhibiting no distress at all. A 1000-ft representative section was selected within Segment 440 to carry out the testing and data collection.

3.7 Pavement Condition: SR 202

As part of assessing the premature deterioration of SR 202, a pavement condition survey was conducted over the driving lane of the Segment 440 with the segment consisting of 67 slabs. The distress survey was performed according to the Distress Identification Manual for the LTPP [1], and included the observation and quantification of transverse joint faulting, transverse joint width, percent spalling of joints and cracks, transverse cracking, and material-related distresses such as staining or map cracking. In addition, the lane to shoulder drop off was also measured. A summary of the distress for SR 202 is presented in Table 16. As observed in the table, the major distress affecting the section is joint spalling. Joint spalling was observed in 94 percent of the slabs. For the slabs exhibiting joint spalling, the primary location of this distress is at the intersection of the longitudinal and transverse joints and along the lane/shoulder joint. Examples of the joint spalling at the intersection of the longitudinal and transverse joint are shown in Figure 36 and Figure 37. Although the severity and extent of the spalling are significant, the location in this instance does not significantly affect the ride quality of the road. This observation is reflected in the last IRI measurement made by PennDOT and the estimated PSR of the section determined during the site visit. The most recent measured IRI at the time the distress survey was conducted was 81 in/mile and the PSR was determined to be 3.5.

Table 16: Summary of Performance Data for SR 202 Segment 440 Northbound

Performance Measurement	Value
Outside Pavement Edge Faulting, in	0.017
Outer Wheel Path Faulting, in	0.018
Lane-to-Shoulder Dropoff, in	0.20
Percent of Slabs with Joint Spalling %	94
Percent of Slabs with Map-cracking %	55
Joint Width, in	0.41
PSR	3.5
IRI (in/mile)	81

3.7.1 Transverse Joint Faulting

As seen in Table 16, the mean joint faulting for Segment 440 at both the wheelpath and

outside edge are low considering that typical values of allowable JPCP mean faulting are between 0.1-in and 0.2-in.

3.7.2 Lane-to-Shoulder Dropoff

As presented in Table 16, the average measured value for lane-to-shoulder dropoff using the Georgia type faultmeter for the entire section was 0.20-in. The minimum and maximum measured values were 0.016 and 0.70-in, respectively. These dropoffs are too minimal to affect the serviceability of the pavement.

3.7.3 Joint Width

The transverse joint widths were measured for all of the slabs within the section. Two measurements per joint were performed at approximately 1 ft from either edge of the slab. The total average joint width for the project was 0.41 in. The joint width was fairly constant along the surveyed section, as suggested by a coefficient of variation of less than 12 percent.

3.7.4 Spalling at Slab Corners

The major distress observed in the section was spalling at the intersection of the longitudinal and transverse joints. A typical manifestation of this distress can be seen in Figure 36 and Figure 37. This type of distress is present in 94 percent of the slabs. A further breakdown of the data reveals that the severity of the spalling is high in 44 percent of the slabs, moderate in 35 percent, and low in 15 percent of the slabs.

Figure 36: Joint Intersection between Adjacent Lanes of SR 202 Segment 440 Northbound Slabs 31 and 32.

Figure 37: Joint Intersection between Adjacent Lanes of SR 202 Segment 440 Northbound Slabs 47 and 48.

3.7.5 Map Cracking

Map cracking was the other major distress observed in Segment 440. Map cracking over the entire surface of the slab was observed in 55 percent of the slabs. The microcracks within the map cracked areas are mainly oriented in the longitudinal direction of the slabs and are interconnected by finer cracks randomly distributed as shown in Figure 38 and Figure 39.

Figure 38: Close-up of Fine Microcracking of SR 202 Segment 440 Northbound, Slab 10.

Figure 39: Close-up of Microcracking of SR 202 Segment 440 Northbound, Slab 27.

3.8 FWD Testing: SR 202

FWD testing for Segment 440 of SR 202 was performed using an FWD Dynatest model 8002 provided by PennDOT. The testing regime included six mid-slab locations, eleven transverse joints (approach and leave sides), and six slab edges with the purpose of testing at each location being expounded upon in Section 2.8. The average air temperature during testing was 38 ºF. This is well below the maximum recommended FWD testing temperature of 70 ºF and subsequently it is not believed that the slab expansion would raise concern with respect to the validity of LTE measurements.

3.8.1 Temperature Gradient

In addition to recording the air temperature, slab temperatures were also monitored throughout the FWD testing to evaluate their effects on joint lockup and slab curling conditions. Following the Strategic Highway Research Program (SHRP) LTPP protocol [9], 0.5-in diameter holes were drilled 8-in apart to obtain temperatures at the top, middle and bottom of the PCC slabs as presented in Figure 40. The basic procedure for taking these measurement consists of drilling three holes into the slab and filling each hole with approximately 1-in of mineral oil.

Using a thermocouple, the temperature of the oil is measured at half hour intervals during the execution of the FWD testing. Due to inconsistencies in the measured slab temperature values, it was deemed necessary to also predict the temperature profile in the slabs using the EICM. Figure 41 presents the predicted slab temperatures during FWD testing. Based on Figure 41, a predicted average gradient of 1.07 ºF/in (assumed linear) was present during the execution of the FWD test.

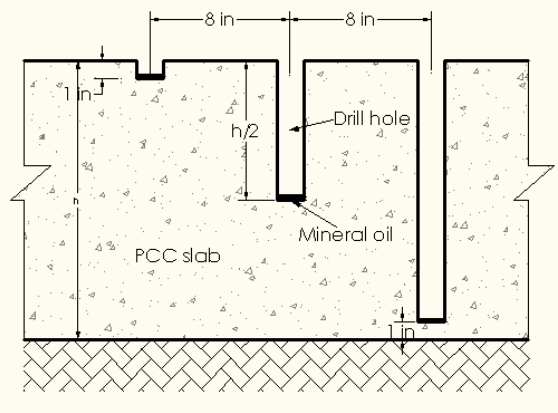

Figure 40: Borehole Layout for Determining the Temperature Gradient During FWD Testing.

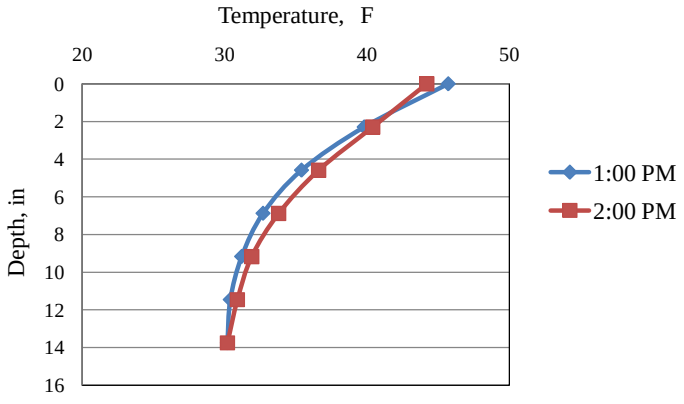

Figure 41: Predicted Slab Temperatures During FWD Testing for SR 202 Segment 440 northbound.

3.8.2 PCC Elastic Modulus

The FWD test data was analyzed to backcalculate the static elastic modulus of the PCC and the k-value for the underlying layers. A 'two-layer' method developed by Ioannides and Khazanovich [10] was used to adjust the estimated elastic modulus of the PCC layer from the AREA method for the existence of bonded ATPB base.

The following formula, Equation 2, was developed for two bonded plates:

Equation 2

Where,

Equation 3

In Equation 2, E_e equals the backcalculated E of the slab from the AREA method and h_e is equal to h_1. Since the moduli for both the PCC and the ATPB are unknown, a parameter called β is defined to represent the ratio in stiffness between the two layers.

Equation 4

This β value is a function of the base layer and is recommended to be .067 for an ATPB [11].

The FWD data was also used to determine the potential for loss of support underneath the slabs, and to determine the joint load transfer efficiency. A summary of the results can be found in Table 17.

Table 17: Summary of Deflection Testing Results for SR 202 Segment 440 Northbound

Property	Value
Static Elastic Modulus, psi	6.35E+06
k-value, psi/in	145
Joint Load Transfer, %	83
Average Mid-slab Deflection, mils	1.5
Corners With Voids, %	0

The static elastic modulus, E, of the PCC slab was backcalculated using mid-slab deflection

measurements along with the slab and asphalt thickness determined from the cores extracted at the FWD locations. Figure 42 presents the backcalculated static PCC elastic modulus along the segment. As shown in Figure 42, the average backcalculated static elastic modulus for the entire section is 6.35 million psi with a coefficient of variation of 18 percent.

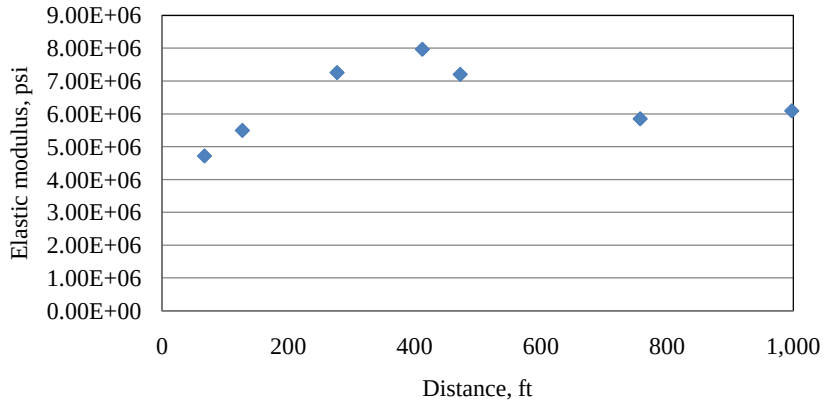

Figure 42: PCC Elastic Modulus for SR 202 Segment 440 Northbound.

.

3.8.3 Modulus of Subgrade Reaction

The modulus of subgrade reaction, k-value, was calculated using mid-slab deflections. Figure 43 shows the k-value along the section. The average static k-value for the section is 145 psi/in with a standard deviation of 20 psi/in and a coefficient of variation of 14 percent.

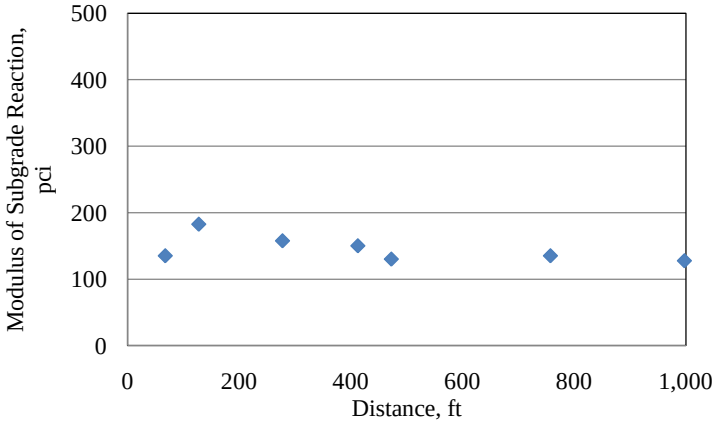

Figure 43: Modulus of Subgrade Reaction for SR 202 Segment 440 Northbound.

3.8.4 Joint Load Transfer

The joint load transfer efficiency values for the entire section are presented in Figure 44. As observed in the figure, the LTE is good (higher than 70 percent) for the majority of the transverse joints. This superior load transfer efficiency was expected considering the 1.5-in dowels used, the 13-in slab thickness, and the pavement is only 8-years old. As mentioned before, the effect of the temperature in the measured LTE values is negligible for this specific section due to the relatively low ambient temperature of 38 ºF present when the FWD testing was performed.

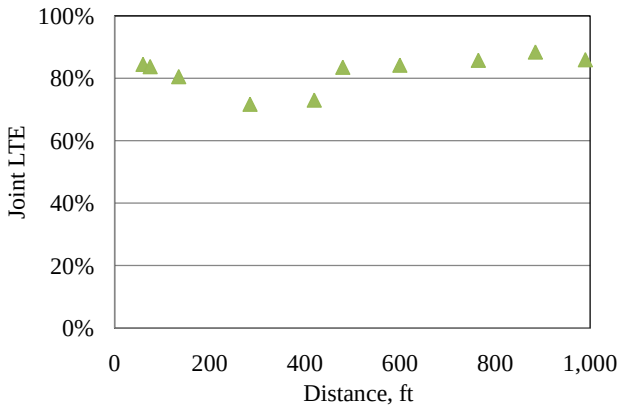

Figure 44: Joint Load Transfer Efficiencies for SR 202 Segment 440 Northbound.

The differential deflections for transverse joints are presented in Figure 45. As seen in Figure 45, the difference between the deflection on the loaded side and the unloaded side of the joints is consistently almost zero along the section. This condition agrees with the good performance of the joints with respect to no faulting and high load transfer efficiencies observed in Segment 440.

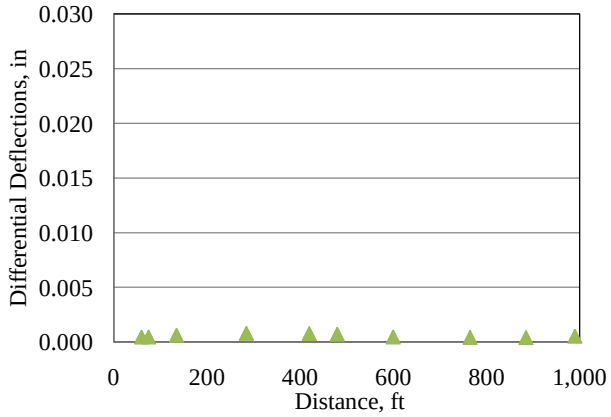

Figure 45: Differential Deflections at Transverse Joints for SR 202 Segment 440 Northbound.

3.8.5 Loss of Support

To determine the potential for the presence of voids beneath the slab, the load vs. deflection response for each station was determined. Figure 46 presents the positive y-intercept values, which are relative to the voids size. Values of the y-intercept are higher than 2 mils, indicating a void might be present. The significance of temperature gradients in the slab during the analysis for loss of support is discussed in the Section 2.8.6. However, the temperature gradients predicted at the time of FWD testing for SR 202 likely did not influence the FWD void detection analysis, as is indicated by the consistency between the measurements at different time of the day. Figure 46 presents the void detection analysis results for Segment 440 and shows that the potential of voids being present throughout the entire section is low.

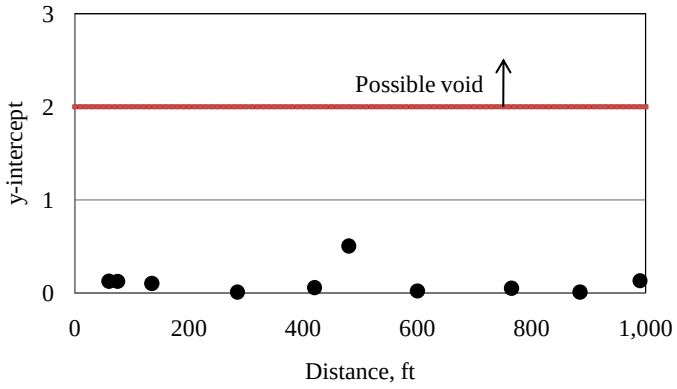

Figure 46: Loss of Support Results for SR 202 Segment 440 Northbound.

3.9 Core Samples: SR 202

A total of sixteen 6-in diameter cores were retrieved at different slab locations of the driving lane and the adjacent lane. From the driving lane, seven cores were pulled from mid-slab locations, two from transverse joints, and three from longitudinal joints. From the adjacent lane four cores were obtained from mid-panel locations. The average thickness of the cores for the driving lane was 13.8-in whereas this value for the adjacent lane was 13.4-in. Table 18 presents a summary containing the general information of the obtained specimens.

The visual examination of the retrieved cores revealed deficiencies that can be associated with the construction stage of the pavement. Along with excessive amounts of entrapped air voids, the majority of the cores showed segregation of the coarse aggregate as well as areas that could visually be identified as having remarkably low entrained air. This was especially prevalent in the upper portion of the cores. Together, these conditions suggest over-consolidation of the concrete mixture during placement.

Table 18: Summary of the Cores for SR 202 Segment 440 Northbound

Core	Location	PCC Thickness (in)	Base Type	No. of Pieces	Embedded Items
C4J-202	Joint	14.25	ATPB	3	Dowel Bar Slice
C5MS-202	Mid-slab	13.5	ATPB	1	
C5MS-A-202	Mid-slab Adjacent Lane	12.75	ATPB	1	
C5/5A LJ-202	Longitudinal Joint	14	ATPB	3	
C9MS-202	Mid-slab	13.5	ATPB	1	
C9MS-A-202	Mid-slab Adjacent Lane	13	ATPB	1	
C19MS-202	Mid-slab	13.75	ATPB	1	
C28MS-202	Mid-slab	14	ATPB	1	
C28MS-202-A	Mid-slab Adjacent Lane	14	ATPB	1	
C29J-202	Joint	14	ATPB	3	
C32/32A LJ-202	Longitudinal Joint	13.5	ATPB	6	Tie bar
C40LJ-202	Longitudinal Joint	14	ATPB	2	
C51MS-202	Mid-slab	14	ATPB	1	
C51MS-202-A	Mid-slab Adjacent Lane	14	ATPB	1	
C52MS-202	Mid-slab	13.5	ATPB	1	
C67MS-202	Mid-slab	13.75	ATPB	1	

3.10 Laboratory Testing Results: SR 202

Several laboratory tests were performed on the retrieved specimens from the driving and adjacent lane. Table 19 presents the results of the following tests: CTE, modulus of elasticity, Poisson's ratio, compressive strength and split tensile strength.

The results for all the tests carried out on the cores are very consistent throughout the section and are within typical ranges for paving concrete.

Table 19: Summary of Laboratory Test Results for SR 202

	Driving Lane			Adjacent Lane		
Laboratory Test	Average	St. Dev	COV	Average	St. Dev	COV
CTE, /°F	6.00E-06	0.29E-06	5%	6.00E-06	0.23E-06	4%
Elastic Modulus, psi	3.50E+06	0.18E+06	5%	3.50E+06	0.16E+06	5%
Poisson's Ratio	0.23	-	-	0.20	0.03	13%
Compressive Strength, psi	5,680	268	5%	5,760	510	9%
Split Tensile Strength, psi	458	25	5%	370	-	-

The laboratory and backcalculated values for strength and stiffness were fairly constant along the section, however, a significant difference between the laboratory-determined and the backcalculated static elastic modulus was observed. The average of the backcalculated stiffness values is 88 percent higher than the average of the laboratory values. Despite accounting for the bonded asphalt treated permeable base, the high PCC elastic could be caused be the result of the influence of the β parameter. The recommended β parameter by Khazanovich, Tayabji, and Darter suggests that the concrete is 15 times stiffer than the asphalt, however, considering the relatively low elastic modulus values obtained from the laboratory testing and the cold temperature during the FWD testing, the β parameter is likely higher than what was recommended to use

3.11 Petrographic Analysis: SR 202

Two cores from SR 202 were examined according to ASTM specification C856 "Petrographic Examination of Hardened Concrete" and ASTM specification C457 "Microscopical Determination of Air Void Content and Parameters of the Air Void System in Hardened Concrete." These cores were from the mid-slab locations of Slab 5 and Slab 9. Slab 5 exhibited significant spalling along the centerline longitudinal joint between the driving lane and the adjacent lane as well as spalling along both transverse joints. The spalling along the transverse joints was closer to the longitudinal joint between the driving lane and the adjacent lane than it was to the lane/shoulder longitudinal joint. Typical locations of the spalled areas are

shown in Figure 47. Slab 9, the other slab from which a core was taken for petrographic analysis, did not exhibit any spalling.

Figure 47: Overall View of Slab 5 SR 202 Segment 440 Northbound

Table 20 presents the results from the petrographic and hardened air void analysis relevant to the determination of the cause of the distresses for SR 202.

Table 20: Summary of Petrographic Analysis of Cores from SR 202 Segment 440 Northbound

	C5-MS202	C9-MS202
Nominal Maximum Aggregate Size, in	3/4	3/4
Water/Cement Ratio	0.38-0.43 Estimate	0.38-0.43 Estimate
Air Void Content, %	4.9	3.6
Entrapped Air, %	3.6	0.7
Entrained Air, %	1.3	2.9
Specific Surface in^2/in^3	560	780
Spacing Factor, in	0.009	0.007
Conformance	Air voids are not consistent with current technology for freeze thaw resistance	Air voids are consistent with current technology for freeze thaw resistance
Distribution of Aggregate	Fair (Coarse Aggregate), Uniform (Fine Aggregate)	Fair (Coarse Aggregate), Uniform (Fine Aggregate)
Depth of Carbonation	Negligible to 1/4-in	Negligible*

* Measured From Sawcut Surface

The entrained air is relatively low for both specimens and the air void distribution is fair to poor. An acceptable air void distribution to protect against durability (or D-) cracking for

moderate to severe freeze/thaw conditions is defined by the American Concrete Institute (ACI) as the specific surface area being greater than 600 in^2/in^3 and the spacing factor being smaller than 0.008 in. Comparing the results in Table 20 to these criteria, it can be seen that the air system for Core C5-MS202 is inadequate. Furthermore, the depth of carbonation and the frequent occurrence of drying shrinkage microcracks indicate that the curing of the pavement was somewhat inadequate.

3.12 Analysis of Potential Distress Causes: SR 202

3.12.1 Joint Spalling

The major distress affecting the performance of this section is joint spalling, which is present in 94 percent of the slabs and is mainly concentrated at the slab corners. According to the gathered information, it was originally believed that this distress was a consequence of freeze-thaw expansion of the pore water in the concrete, along with the inability of the poor air void system to dissipate such stresses. The petrographic analysis revealed that in the two cores tested, both the volume and the distribution of the entrained air voids did not satisfy the recommendation set by ACI considering the moderate to severe freeze thaw exposure conditions.

Based on these conclusions, it seems apparent that the joint spalling can indeed be attributed an insufficient air void system. The influence of the traffic loads on spalling can be noticed particularly keenly in the wheelpath shown in Figure 47, as the spalled concrete tends to be dislodged in this area. It was also noted that this distress was observed at the pavement surface but none of the cores pulled exhibited deterioration at the bottom of the core. Generally, D-cracking is more extensive at the bottom since the bottom of the slab is typically saturated. This indicates that the entrained air void system might be better at the bottom of the slab than the top.

3.12.2 Map Cracking

In addition to the spalling, it was also observed that more than 50 percent of the slabs have areas with mapcracking. The approximate depth based on an unaided visual examination of this mapcracking is 0.1 in. This cracking was observed to develop over the entire panel. The microcracks are mainly oriented in the longitudinal direction of the slabs and are interconnected by finer cracks randomly distributed. This is an indication of inadequate curing. Additional information obtained from the petrographic analysis revealed that carbonation has taken place in the concrete to a depth between 0 and 0.2 in. This was most likely the reason for the traffic wear

on the surface.

3.13 Rehabilitation Recommendations: SR 202

3.13.1 Distresses and Deficiencies

The major distresses observed in SR 202 is spalling and map cracking. The map cracking is not contributing to any structural or functional deficiencies. The spalling, on the other hand, is problematic. The manifestation of these distresses can be attributed the concrete mixture design and the paving, curing and finishing practices that resulted in a high water/cementicious ratio at the surface, a poor entrained air system and segregation throughout the depth of the pavement. Although the observation of the various distresses and deficiencies are based on data obtained from Segment 440 alone, other segments that were part of the original analysis section and that exhibit similar distress patterns should also be considered for these rehabilitation measures.

3.13.2 Recommendations for Segment 440

Typical repairs made to address spalling are a full-depth repair if the depth of spalling exceeds more than 1/3 the depth of the slab or a partial depth repair if the depth of the spalling is less than 1/3 the depth of the slab. For SR 202, the spalling developed as a result of D-cracking associated with the poor entrained air system. Since the bottom of the slab is always saturated, D-cracking tends to be more prevalent at the bottom of the slab when compared to that observed on the surface. Therefore, full-depth repairs are typically necessary. For SR 202, the distress does not generally develop at depths greater than 1/3 the depth of the slab since the entrained air void system at the bottom of the slab is better than at the top of the slab. It would be beneficial to pull a few more cores to verify this throughout the distress section. With the depth of the spalling being restricted to the upper portion of the slab, partial depth repairs might be effective. If regions are found where the deterioration runs throughout the depth of the slab then full depth repairs would be necessary. These repairs would help to extend the life of the pavement but it can be expected that the deterioration would eventually develop along the newly created joints in the original concrete adjacent to the repair area. It might be possible to further deter the continued deterioration by applying a sealant on the exposed portion of the existing slab prior to placing the repair material. Before this is attempted, one must insure that the sealant does not deter the bond between the existing slab and the repair material.

3.14 Future Projects: SR 202

Much of the observed distress can be related to construction issues and the quality of the concrete. Carbonation occurs when the carbon dioxide from the atmosphere reacts with the solid calcium hydroxide in the cement paste. Even the carbonation of C-S-H is possible if the calcium hydroxide is depleted. The permeability of the concrete has a substantial influence on the diffusion of carbon dioxide and hence the water-to-cement ratio and proper curing are two of the most influential factors influencing the rate of carbonation. These are also the primary factors contributing to the drying shrinkage cracking observed. Proper curing should include avoiding adding water to the pavement surface to aid in finishing as well as a uniform application of curing compound at an appropriate application rate. It is also critical that the curing compound used have sufficient water retention characteristics. The Minnesota Department of Transportation has found that the use of 100% poly-alpha-methystyrene resin is effective in retaining water in the concrete. It is also important that a sufficient amount of resin be present and therefore it is suggested that the curing compound consist of a minimum of 42 percent solids. It is suggested that the following curing compound requirements considered for adoption:

Properties	Minimum	Maximum
Total Solids, % by weight of compound	42	
% reflectance in 72 hours (ASTM E1347)	65	
Loss of Water, kg/m^2 in 24 hours (ASTM C156)		0.15
Loss of Water, kg/m^2 in 24 hours (ASTM C156)		0.40
Settling Test, ml/100 ml in 72 hours		2
V.O.C. Content, g/L		350
Infrared Spectrum Vehicle		100% alpha methylstyrene

These recommended values are based on those provided by the Minnesota Department of Transportation Specifications. Additional information regarding the study that led to the development of these specifications can be found at the following webpage, http://www.mrr.dot.state.mn.us/research/pdf/200106p.pdf.

Over consolidation can be a possible cause of the reduction in entrained air between the time the fresh concrete was tested and the entrained air was measured in the hardened concrete. Over

consolidation would also account for the segregation observed. The recommendation for future projects is therefore to be more vigilant with respect to adhering to construction specifications. Special attention should be paid to insuring proper workability of the concrete and also preventing over consolidation by ensuring the vibration settings on the paver are correct.

Refinement of the concrete mixture design would also be beneficial in reducing the potential for segregation. Using a more uniformly graded coarse aggregate along with using a lower water/cementicious ratio will help reduce the potential for segregation as well as drying shrinkage cracking at the pavement surface.

4 US 22, Westmoreland County

4.1 Project Information: US 22 Westmoreland County

This section of US-22, which was constructed in 2003, is part of a reconstruction effort in Westmoreland County. This portion of US-22 is under the jurisdiction of PennDOT District 12. The selected segment to execute the data collection plan was Segment 50 eastbound and is located in a commercial area in the municipality of Murrysville, PA. Its location relative to other roads in the municipality of Murrysville is represented by the green highlight shown in Figure 48. A 1000-ft long representative section within the segment was chosen based on the pavement condition and the ease with which traffic control could be executed. Since the representative section presents considerable portions of distressed as well as non-distressed slabs, the selection of an additional control section was not necessary.

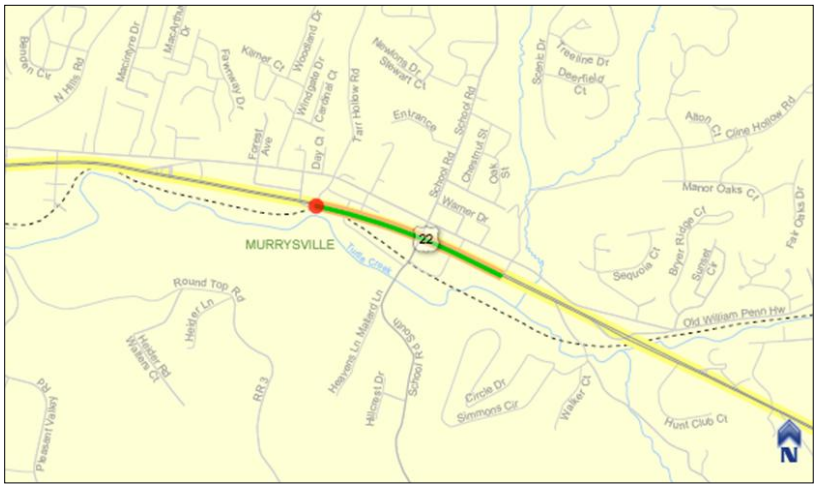

Figure 48: Location of Segment 50 Eastbound of US-22 Murrysville in District 12

4.2 Design Information: US-22 Westmoreland County

This JPCP section of US-22 in Westmoreland County consists of a 12-in PCC slab with a 4-in thick asphalt treated permeable base and a 5-in 2A subbase over an AASHTO A-4 subgrade. For this project there are two lanes per direction with each lane being 12-ft wide and having a transverse joint spacing of 15 ft. The transverse and longitudinal joints are sealed with asphalt.

The diameter of the dowels is 1.5 in with the dowels being placed 12-in on center beginning 6 in from the edge of the slab. The shoulder in this section of US-22 consisted of a tied PCC curb and gutter shoulder. For subsurface drainage, a longitudinal edge drain system is present beneath each shoulder that consists of 6- in diameter pipes.

During the site visit, it was found that full-depth repairs were performed within the section and that the stabilized base was removed in the area of the repairs and replaced with a granular base material. Based on the retrieved cores, full-depth repairs were performed on at least Slab 8 through Slab 12, since a granular base was found below the slab and not the ATPB present in the other portion of the roadway. According to information provided by PennDOT, these slab replacements were performed to repair corner breaks that developed prematurely in the pavement. The existing pavement cross section representing the average pavement layer thicknesses is shown in Figure 49 and overall condition of the pavement is presented in Figure 50.

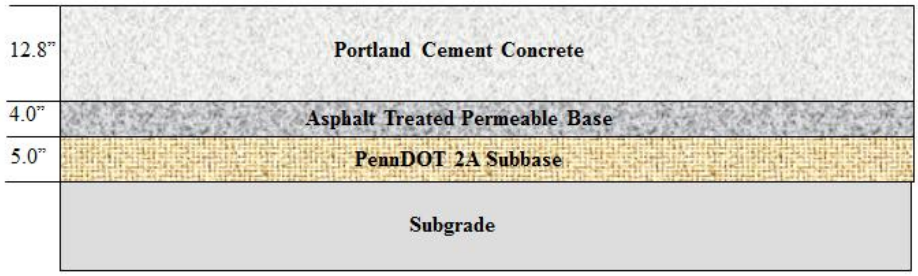

Figure 49: Existing Pavement Cross Section of US-22 Murrysville Segment 50 Eastbound

Figure 50: Overall Condition of US-22 Murrysville Segment 50 Eastbound.

4.3 Concrete Mixture Design: US-22 Murrysville

The concrete mixture design information for US-22 Murrysville Segment 50 eastbound provided by PennDOT is presented in Table 21.

Table 21: Concrete Mixture Design for US-22 Murrysville Segment 50 Eastbound

Material	Specific Gravity	Absorption	Batch weight (lb per yd^3)
Type 1 Cement (St. Lawrence)	3.15	n/a	382
Coarse Aggregate (Hanson No. 57)	2.57	Unknown	1881
Fine Aggregate (Hanson Type A)	2.61	Unknown	1284
Ground Granulated Blast Furnace Slag (Holcim)	Unknown	n/a	206
Water Reducer (Catexol 100N), oz	Unknown	n/a	17
Air Entrainer (Catexol 360), oz	Unknown	n/a	5.7
Water	1	n/a	138

4.4 Climatic Conditions: US-22 Murrysville

The closest weather station to the project site is 13 miles away in Pittsburgh, PA at the Allegheny County Airport. Based on the data from this weather station, the area experiences

approximately 160 wet days per year and a mean annual rainfall of 40 in. The freezing index is 328 ºF-days and the area is exposed to approximately 39 freeze-thaw cycles per year. The mean annual air temperature is 56ºF with minimum and maximum average monthly temperatures of 33ºF and 81ºF, respectively.

4.5 Traffic Loadings: US-22 Murrysville

According to the information obtained from the PennDOT ITMS, the AADT of Segment 50 of US-22 in 2009 was approximately 3,000 with 6 percent trucks. This traffic results in the accumulation of 6 million ESALS between 2003 and 2009.

4.6 Selection of Distress Survey Section: US-22 Murrysville

Different sources of information were analyzed to properly select the representative section within the project. Historic automated distress survey data provided by PennDOT, as well as the pavement condition and panoramic images of the roadway from PennDOT's Videolog application were studied in the office to locate road segments presenting early-age distress.

Due to the nature of the existing distress for this project, the use of the mentioned tools and data did not provide sufficient information for the selection of the representative section prior to the site visit. Therefore, the selection of the section was accomplished during an initial visit to the project. During this visit, it was also determined that the selection of a separate Control and Distressed section was not necessary due to the existence of distressed as well as non-distressed areas within the same 1000-ft representative section.

4.7 Pavement Condition: US-22 Murrysville

To assess the pavement condition, a distress survey was conducted in the driving lane of Segment 50 eastbound and consisted of 67 slabs. The distress survey was performed according to the Distress Identification Manual for the LTPP Program [1], and included the quantification of transverse joint faulting, transverse joint widths, spalling, and transverse cracking. Additionally, material-related distresses, such map cracking were identified. The distressed slabs in the surveyed section were located in clusters. The slabs located between 120 and 270 ft, 675 and 735 ft and 855 and 915 ft from the beginning of the section exhibited distress while the remainder of the sections were relatively distress free.

A summary of the average results for the measurements taken during the survey is presented in Table 22. In addition to the observed distresses, it was also noticed that pavement

rehabilitation activities, such as diamond grinding and full-depth repairs, were performed on Segment 50. Diamond grinding was performed on an extensive area of the selected section and full depth repairs were performed to repair corner cracks.

Table 22: Summary of Performance Data for US-22 Murrysville Segment 50 Eastbound

Performance Measurement	Value
Outside Pavement Edge Faulting, in	0.028
Outer Wheel Path Faulting, in	0.024
Lane-to-Shoulder Dropoff, in	0.21
Percent of Slabs with Map Cracking, %	28
Join Width, in	0.45
PSR	3.9

Although the passing lane was not part of the distress survey, it was noted that in addition to the driving lane, the adjacent passing lane also exhibited several full-depth repairs as well as extensive diamond grinding. Unlike the driving lane, the areas in which full depth repairs were performed to repair corner breaks for the passing lane were distinguishable based on visual observation and not based on observed base type. This can be seen in Figure 51

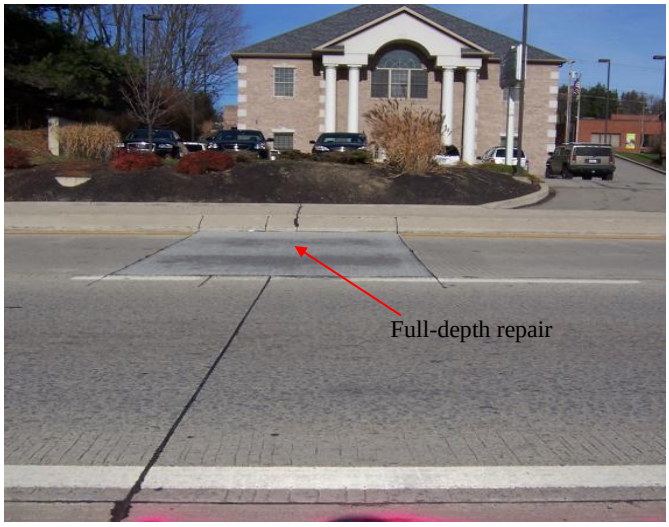

Figure 51: Full Depth Repair in the Passing Lane of US-22 Murrysville Segment 50 Eastbound.

4.7.1 Transverse Joint Faulting

The mean joint faulting values for Segment 50 at both locations presented in Table 22 are low considering that typical allowable values for the mean faulting of a JPCP are between 0.1 in and 0.2 in. Taking into account the age of the pavement and its structural and drainage characteristics, the low faulting measurements that were taken were expected.

4.7.2 Lane-to-Shoulder Dropoff

As with the other projects, the difference in elevation between the driving lane surface and the outside shoulder was measured using the faultmeter. As presented in Table 22, the average measured value for the entire section was 0.21 in. The minimum and maximum measured values were 0.08 in and 0.58 in respectively.

4.7.3 Joint Width

The transverse joint widths were also measured for all of the slabs within the section. Two measurements per joint were performed at approximately 1-ft from each edge of the slabs. The overall average joint width for the section was 0.45 in. The variation of the joint width along the section and its potential relationship with joint lockup will be presented in Section 4.13.

4.7.4 Material-Related Distresses

A common distress observed in the section was fine map cracking. At midslab, the cracking is oriented parallel to the longitudinal joints. The fine cracks concentrated near the transverse joints with the concentration of cracking being heavier at the intersection of the transverse and longitudinal joints. Typical examples can be seen in Figure 52 and Figure 53. In addition, white deposits were observed in the vicinity of the fine cracks in the corners. These deposits can be seen in Figure 52. Based on the cracking pattern and the presence of the white precipitate, it appears that alkali-silica reaction (ASR) might be present. A variation in the color of the cement paste between different slabs and in some cases within the same slab was observed during the visual observation of the cores. Some of this variation in the color of the cement paste can be attributed to the use of a ground granulated blast furnace slag while in other cases it is apparent that different concrete mixtures were used in constructing various sections of the roadway.

Figure 52: Joint Close-up of US-22 Murrysville Segment 50 Eastbound Slabs 48 and 49.

Figure 53: Slab Close up of Midslab Longitudinal Cracking from US-22 Murrysville Segment 50 Eastbound, Slab 8.

4.7.5 Transverse Joint Spalling and Corner Cracks

Although joint spalling was not present in the section, it was observed during the distress survey that some slabs exhibited a clearly defined crack parallel to the transverse joint, as shown in Figure 54. This crack, which appears to be a consequence of a structural problem, could eventually cause spalling at the transverse joint. To further investigate this particular problem, several cores were retrieved from the transverse joints at the dowel bar locations and a Magnetic Imaging Tool (MIT Scan-2) was used to evaluate the alignment and location of the dowels. The cores retrieved at dowel bar locations revealed the existence of joint lockup determined by the fact that the retrieved dowel was immovable within the core as seen in Figure 55. It can also be seen in Figure 55 that the crack at the bottom of the joint is very tight indicating that this is not a working joint. A summary of the results from the MIT Scan-2 is presented in Section 4.13.1.

Corner cracks were not present of the time the survey was performed because they had been repair prior to this time. Corner cracks can develop as a result of pumping that result in the development of voids beneath the slab. The FWD results will show that voids are not present. Another cause of the development of corner cracks could be joint lockup.

Figure 54: Joint Close-up of US-22Murrysville Segment 50 Eastbound, Slabs 61 and 62.

Figure 55: PCC Core Retrieved at the Transverse Joint of Slab 8 of US-22 Murrysville Segment 50 Eastbound.

4.7.6 Present Serviceability Rating (PSR)

Even though the percentage of distressed slabs within the section is significant, the nature and severity of the problems at the time of data collection has not affected the serviceability of the pavement. This is reflected by the average PSR of the section which was 3.9.

4.8 FWD Testing: US-22 Murrysville

The testing for this section included seven mid-slab locations, twenty transverse joints (approach and leave side of the joint), and seven slab edges. The average air temperature during testing was 51.5ºF. In addition to the air temperature, slab temperatures were monitored throughout the FWD testing to evaluate joint lockup and slab curling conditions, following the SHRP LTPP protocol [9], as discussed in Section 3.8.1. Figure 56 shows the slab temperatures measured during the FWD testing. As observed in Figure 56, a negative gradient, where the bottom of the slab is warmer than the top, was present for FWD testing performed before 10:00 AM. After 10:00 AM, positive gradients were present. Since the magnitude of the largest gradient measured during FWD testing was only 0.25 ºF/in, it can be concluded that the temperature gradients in the slabs during testing did not significantly influence the test results.

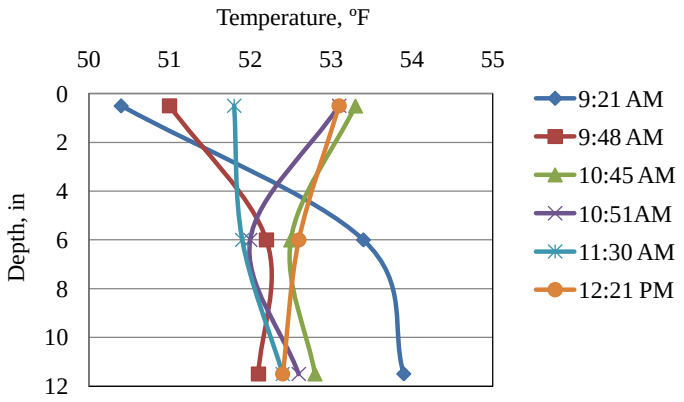

Figure 56: Slab Temperature During FWD Testing for US-22 Murrysville Segment 50 Eastbound

The FWD data was used to backcalculate the elastic modulus of the PCC and the modulus of subgrade reaction, to determine the potential for loss of support beneath slab corners, and to determine the joint load transfer efficiency. A summary of the FWD data analysis can be found in Table 23.

Table 23: Summary of Deflection Testing Results for US-22 Murrysville Segment 50 Eastbound

Property	Value
Static Elastic Modulus (Distressed), psi	3.65E+06
Static Elastic Modulus (No Distress), psi	7.00E+06
Static k-value, psi/in	215
Joint Load Transfer, %	85
Average Mid-slab Deflection, mils	1.6
Corners With Voids, %	0

4.8.1 PCC Elastic Modulus

The elastic modulus of the PCC was backcalculated using mid-slab deflection measurements, with the actual thickness of the slab determined from the cores extracted at the FWD locations, and accounting for the bonded ATPB, as was discussed in Section 3.8. Figure 57 presents the

backcalculated static PCC elastic modulus along the section. As observed in the figure, there is a significant variation in the stiffness of the PCC layer along the section with a coefficient of variation of 38 percent. As mentioned previously, it appears that at least two separate concrete mixture designs were used in the construction of this section of roadway. This might be the result of paving the blockouts in front of the business access driveways with a separate mixture than the other throughway sections. One indicator of this is that the color of the paste in some of the cores was greyish, as is commonly found with concrete containing ground granulated blast furnace slag (GGBFS). The paste of the other cores was dark beige in color. The FWD locations in regions where the cores were beige are circled in red in Figure 57. Of the slabs for which coring was performed, the only slabs replaced, as evidenced by the granular base found to be present, were Slabs 8 through 12, beginning at a distance along the project of 178-ft. The average static elastic modulus for the cores taken in the sections without distress was 7.00 million psi with a COV of 16 percent. The average elastic modulus for the distressed slabs was 3.65 million psi with a COV of 16 percent.

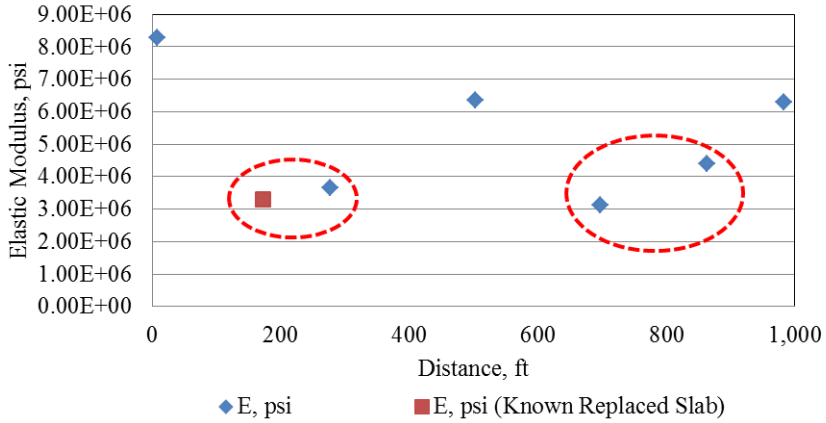

Figure 57: PCC Elastic Modulus for US-22 Murrysville Segment 50 Eastbound.

4.8.2 Modulus of Subgrade Reaction

The static modulus of subgrade reaction, k-value, was calculated using mid-slab deflections. Figure 58 shows the k-value along the section. The static k-value for the area of the replaced slab is 215 psi/in with a standard deviation of 38 psi/in. As observed in Figure 58, the k-value is relatively constant indicating uniform support conditions throughout this project.

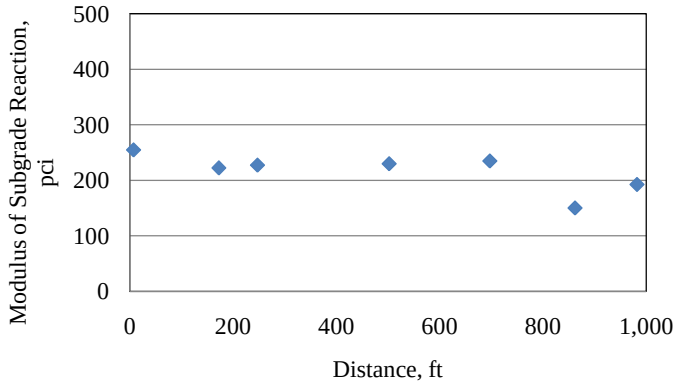

Figure 58: Modulus of Subgrade Reaction for US-22 Murrysville Segment 50 Eastbound.

4.8.3 Joint Load Transfer

The joint load transfer efficiency along this section of roadway is shown in Figure 59. The average value is 81 percent and as observed in Figure 59, the LTE is good (higher than 70%) for the majority of the joints. Although, several of the joints have a LTE below 70%, considering the relatively young age of the pavement combined with the fact that 1.5-in dowels were used in constructing this section of roadway, it would be anticipated that the LTEs should not be below 80 percent.

The dashed circles in Figure 59 indicate joints in regions where the slabs are exhibiting the pattern of fine interconnected cracking. It should be noted that the joints in the distressed regions, as well as the joints directly adjacent to the distressed regions, tend to have higher levels of load transfer. The expansion resulting from ASR could result in narrower cracks widths and higher load transfer efficiencies.

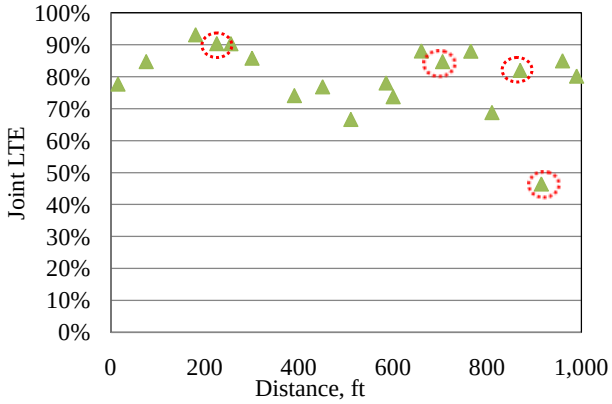

Figure 59: Joint Load Transfer Efficiencies for US 22 Murrysville Segment 50 Eastbound.

The differential deflections for the representative section are presented in Figure 60. As observed in Figure 60, the values are significantly below the threshold for poor joint performance, which is 0.01 in.

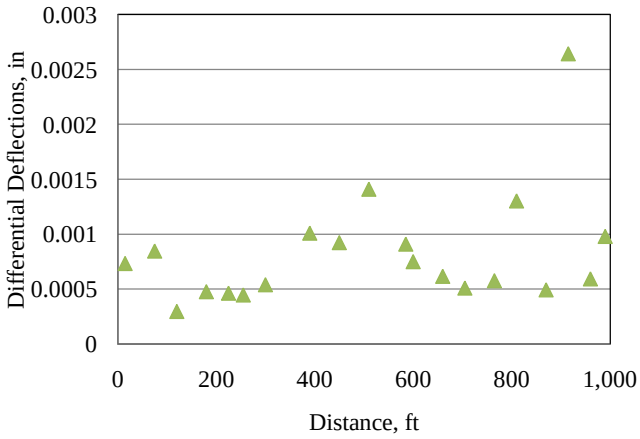

Figure 60: Differential Deflections at Transverse Joints for US-22 Murrysville Segment 50 Eastbound.

4.8.4 Loss of Support

Figure 61 presents the y-intercept values of the load vs. deflection relationship for the FWD

data collected at the corner of the slab. As observed in Figure 61, there appears to be no voids present throughout the entire section. The consistency of the y-intercept values along the section help to emphasize the minimal influence of the measured temperature gradients on the FWD testing since these values were obtained when both small positive and small negative temperature gradients were present.

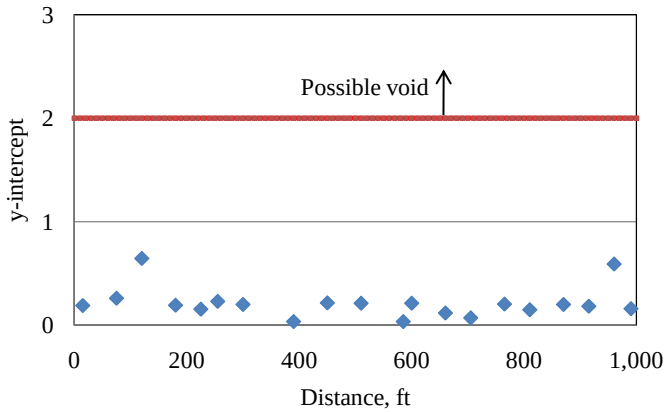

Figure 61: Loss of support for US-22 Murrysville Segment 50 Eastbound.

4.9 Core Samples: US-22 Murrysville

Thirteen, 6-in diameter, cores were retrieved at different slab locations throughout the representative section of US-22 in Murrysville. Seven cores were pulled from mid-slab locations, five were pulled from transverse joints, and one was pulled from a panel that exhibited significant micro cracking. Table 24 presents a summary containing some general information about the cores. The average thickness of the cores is 12.8-in.

Table 24 shows that there was an asphalt treated base for each core location except for the location of three of the cores where a granular base was present. This might indicate that this is an area where a repair was made since when replacing the slab, the bonded ATPB would most likely adhere to the bottom of the slab as it was lifted out. Replacing the ATPB would be difficult due to the limited space available for proper compaction. Therefore, a granular material may have been used to reconstruct the base layer. Another indicator that this might be a repair area is that the dowel depth measured for the cores pulled at the joints indicate that the dowels

are at about 6 to 6.5 in above the base. This would be a reasonable depth since the design thickness was 12 in. The thickness of the pavement actually ended up ranging between 12.5 and 14 in in thickness. The depth of the dowel in the section assumed to be a repair area is located about 7 in up from the base, indicating that the dowel height was established based on the as-built thickness and not the designed thickness. Wear was exhibited on the surface of all the cores.

Table 24: Summary of Cores for US-22 Murrysville

Core	Location	PCC Thickness, in	Base type	Base Thickness, in	No. of Pieces	Embedded Items
C1MS-22	Mid-slab	13	ATPB	3.5	1	
C8J-22 [D]	Joint	12.5	Granular		4	Dowel Bar
C12MS-22 [D]	Mid-slab	11.2	Granular		1	
C12J-22 [D]	Joint	13	Granular		2	Dowel Bar
C17MS-22 [D]	Mid-slab	12.5	ATPB	3.5	1	
C17J-22 [D]	Joint	12.75	ATPB	3.0	3	
C26J-22	Joint	14	ATPB		4	
c	Mid-slab	14	ATPB	3.5	1	
C46MC-22 [D]	Slab	12.5	ATPB	3.5	1	
C47MS-22 [D]	Mid-slab	12.5	ATPB	3.5	1	
C58MS-22 [D]	Mid-slab	12	ATPB	3.5	1	
C58J-22 [D]	Joint	13	ATPB	2.5	5	Dowel and Dowel Basket
C66MS-22	Mid-slab	13	ATPB	3.5	1	

[D] Cores pulled from slabs exhibiting distress.

As mentioned previously, the color of the paste in the cores taken throughout the section also varied. The color of the paste for the cores pulled from areas not exhibiting distress was grey, especially in the lower portion of the core. This indicates that GGBFS was used. The color of the cores in the distressed sections were predominately dark beige, indicating that the proportion of GGBFS in this concrete might be lower than in the areas not exhibiting distress. This can be seen in Figure 62. Based on the cores pulled, the type of coarse aggregate used appears to be consistent throughout the section surveyed.

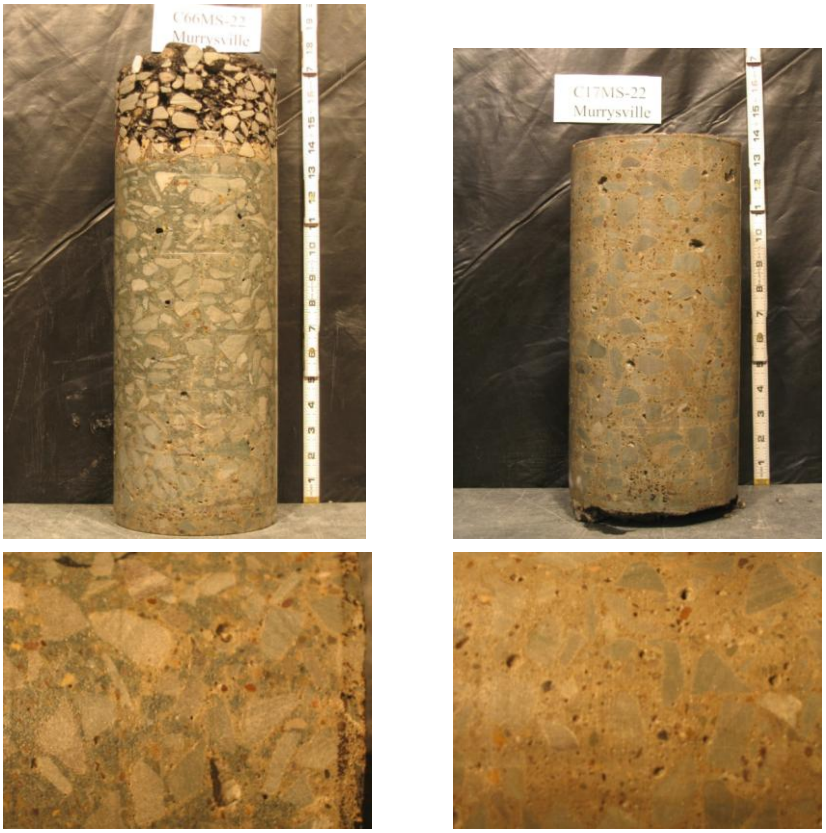

a.) Core from Slab without Distress b.) Core from Distressed Slab

Figure 62 Variations Observed in the Color of the Paste of a Core Pulled from a.) A Distressed Slab and b.) A Slab without Distress.

Each core pulled at the transverse joints contained horizontal cracks running parallel to the plane of the slab surface, as shown in Figure 55. These horizontal cracks were observed not only in the four cores pulled from the joints of slabs in the distressed regions, but also the core (core C26J-22 in Table 24) pulled from a joint located approximately 400 feet into the section, a substantial distance away from the distressed areas. These horizontal cracks typically develop from internal stresses created when the joints lock-up. The expansion created as a result of ASR could be the cause of some of this cracking. The fact that the horizontal cracking is also present

in regions not exhibiting distress indicates that there could also be dowel bar misalignment or inadequate lubrication of the dowels during construction contributing to joint lock-up. Further investigation of these causes is provided in subsequent sections.

4.10 Laboratory Testing: US-22 Murrysville

Several laboratory tests were performed on the retrieved specimens. The distribution of the testing was performed in accordance to the number of samples, the location of the core, and the observed distresses. Table 25 presents the results of the laboratory testing on the cores from US-22 Murrysville. These results include coefficient of thermal expansion (CTE), modulus of elasticity, Poisson's ratio, and compressive strength. As can be observed in Table 25, there is a high variation in both the compressive strength and elastic modulus obtained from the lab testing. This variability will be discussed in Section 4.11.

Table 25: Summary of Laboratory Test Results for US-22 Murrysville

Laboratory Test	Average	St. Dev	COV
CTE, /°F	5.81E-06	3.40E-07	6%
Elastic Modulus, psi	3.85E+06	1.04E+06	27%
Poisson's Ratio	0.23	0.01	6%
Compressive Strength, psi	6,430	1,270	20%

4.11 Petrographic Analysis: US-22 Murrysville

Two cores from SR 202 were examined according to ASTM specification C856 "Petrographic Examination of Hardened Concrete" and ASTM specification C457 "Microscopical Determination of Air Void Content and Parameters of the Air Void System in Hardened Concrete". These cores were from the mid-slab of Slab 17 and Slab 34. Slab 17 exhibited significant cracking. Slab 34, exhibited no distress. Figure 63 shows visible ASR cracking where the joints intersect at Slab 17. Figure 64 depicts the condition of the slab surface for Slab 34.

Figure 63: Map Cracking Observed on Slab 17 US 22, Westmoreland County Segment 50 Eastbound

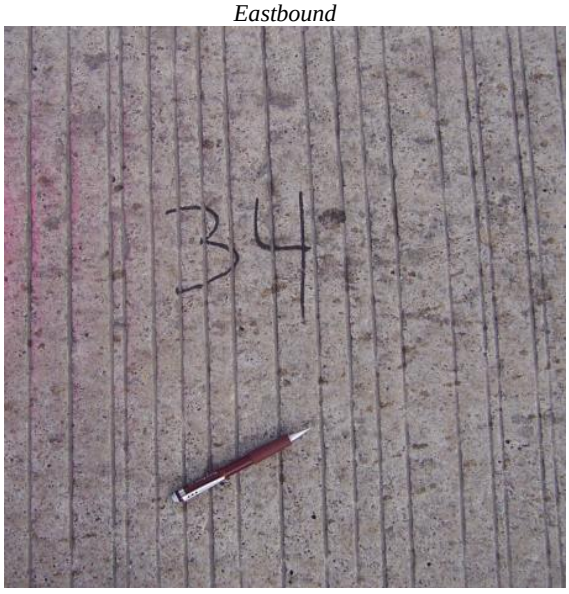

Figure 64: Overall View of Slab 34 US-22, Westmoreland County Segment 50 Eastbound

Drying shrinkage cracking and carbonation was identified at the surface. There was also erosion/wear at the surface throughout the section indicating a non-abrasion resistant paste. This can be seen in Figure 65. This can be the result of inadequate finishing/curing practices or a concrete mixture with a high water to cement ratio.

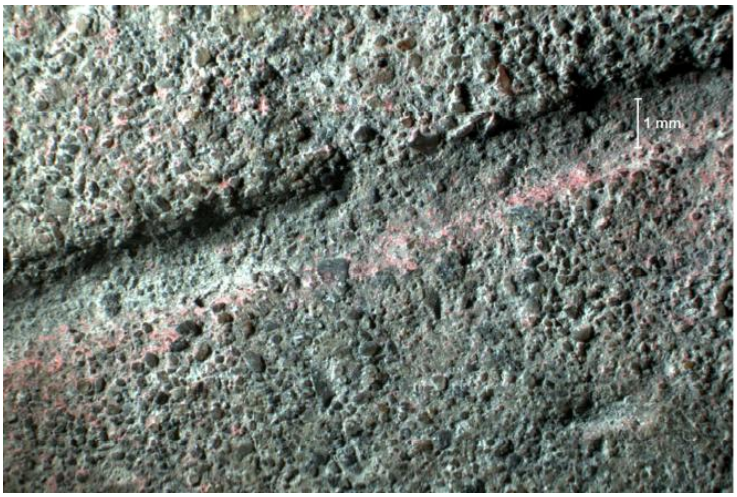

Figure 65: Wear/Erosion of the Pavement Surface as Seen on the Surface of Core C34-MS22.

Table 26 presents the results from the hardened air void analysis for US 22, Westmoreland County. As can be seen from Table 26, the freeze-thaw durability of the concrete for both cores is adequate.

Table 26: Summary of Petrographic Analysis of Cores from US 22, Westmoreland County Segment 50 Eastbound

	C17-MS22	C34-MS22
Nominal Maximum Aggregate Size, in	3/4	3/4
Coarse Aggregate Type	Crushed Limestone	Crushed Limestone
Water/Cement	0.38-0.43 Estimate	0.38-0.43 Estimate
Air Void Content, %	6.3	6.8
Entrapped Air, %	0.9	0.7
Entrained Air, %	5.4	6.1
Specific Surface in^2/in^3	1050	1160
Spacing Factor, in	0.004	0.003
Conformance	Air voids are consistent with current technology for freeze thaw resistance	Air voids are consistent with current technology for freeze thaw resistance
Distribution of Aggregate	Good (Coarse Aggregate), Good (Fine Aggregate)	Good (Coarse Aggregate), Good(Fine Aggregate)
Depth of Carbonation	Negligible to .32 in	Negligible to .36 in

C17-MS22 exhibited fair to poor overall condition but C34-MS22 exhibited a good overall condition. The fair to poor overall condition of C17-MS22 is the result of the fact that ASR is developing within the coarse aggregate resulting in the cracking observed on the surface of the core.

The ASR found in Core C17-MS22 can be seen in Figure 66. The pink area at the top of the core in Figure 66 was the result of the application of phenolphthalein to observe the depth of carbonation and is not related to ASR. The ASR associated microcracking in Figure 66 is indicated by the red lines drawn throughout the depth of the core. The ASR developed within the coarse aggregate and the fine chert aggregate particles. The chert represents only a small portion of the fine aggregate. Figure 67 shows Core C34-MS22 where no microcracking is present. The influence of the ASR in the core from Slab 17 is highlighted in Figure 68. This figure shows a crack that has formed through two coarse aggregate particles and a fine chert aggregate particle. The microcrack through the coarse aggregate is filled with ASR gel. This effect on the microstructure, when extrapolated to the bulk properties of the concrete, can significantly decrease the strength of the concrete.

Figure 66: Development of ASR Gel in Carbonate (Coarse) Aggregate at Depth in Core C17-MS22 of US-22 Murrysville, Westmoreland County Segment 50 Eastbound.

Figure 67: Overall Condition of Core C34-MS22 of US-22 Murrysville Westmoreland County Segment 50 Eastbound

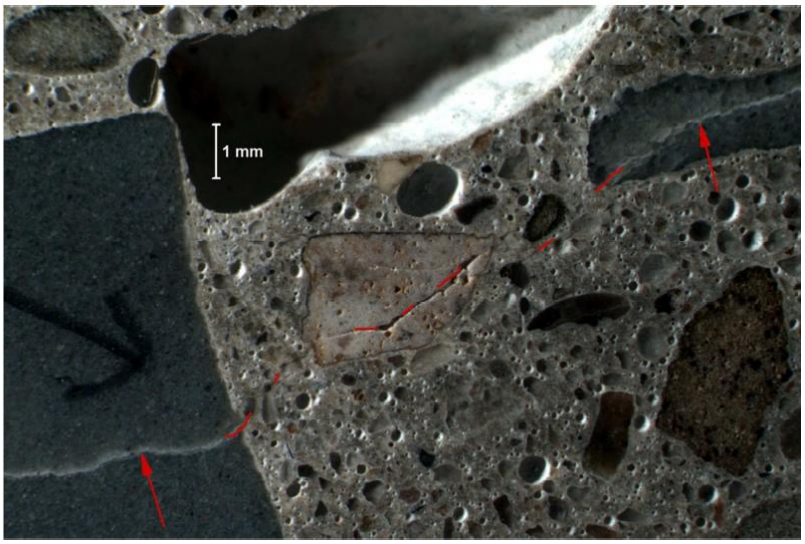

Figure 68: Influence of ASR on Microstructure of Concrete in Core C17-MS22 of US-22 Murrysville Segment 50 Eastbound. Magnification 10x

As was commented on in Section 4.7.4, and can be observed in Figure 66 and Figure 67, there is a significant difference in the coloration of the cement paste between the two cores examined by petrographic analysis. The blue coloration of the cement paste in the bottom portion of Figure 67 is the result of hydrated ground granulated blast furnace slag incorporated in the mix design as a supplementary cementitious material. The residual Portland cement in C17-MS22 is between 9 to 10 percent, while the residual slag is estimated to be between less than 1 percent. This level of GGBFS incorporated in the mix is representative of a level typical of a processing addition in the manufacturing of Portland cement. The residual Portland cement in C34-MS22 is between 5 to 7 percent while the residual slag is estimated to be between with 4 and 6 percent. This would represent a purposeful addition, represented by the mix design information summarized in Section 4.3. The incorporation of GGBFS mitigated the development of ASR Core C34-MS22 by reducing the effective alkali content of the cementitious material.

4.12 Laboratory and Backcalculated Results Analysis: US-22 Murrysville

As mentioned in Section 4.11, the microcracking that developed in some of the slabs can result in a significant reduction in the strength and stiffness of the concrete. Like the backcalculated values, the laboratory measured stiffness and strength showed significant variation along the section. Although there is a difference between the backcalculated and laboratory values, the variation along the section follows a similar trend. This is illustrated in Figure 69 where the dashed red circles highlight the distressed areas.

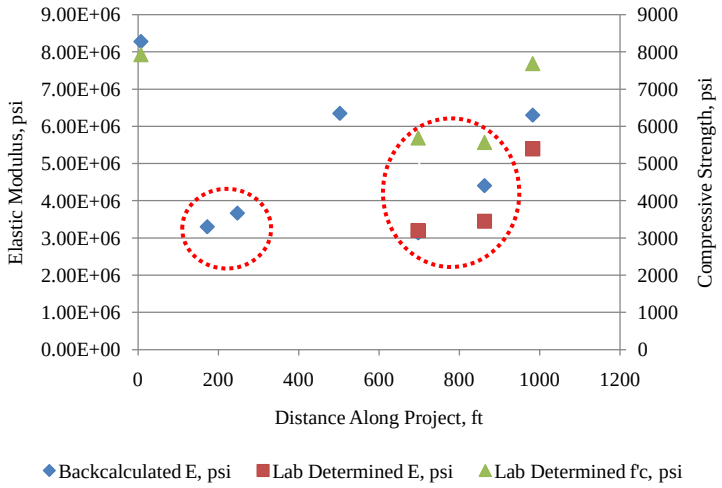

Figure 69: Backcalculated Elastic Modulus, Laboratory-Determined Elastic Modulus, and Compressive Strength along US-22 Murrysville Segment 50 Eastbound.

By incorporating the results of the petrographic analysis into the interpretation of the laboratory determined data it is clear that as stated in Section 4.11 the ASR is negatively influencing the structural properties of the concrete. Figure 70 shows the lab determined compressive strength and elastic modulus along the section with different series differentiating between data from map cracked and non-map cracked areas. Table 27 summarizes the statistics assuming that map cracked and non-map cracked areas are inherently different. From the results presented in Table 27 it can be seen that considering the map cracked and non-map cracked areas separately results in a decrease in the variation within each area. When comparing the differences in the statistics between the two areas it can be seen that there is a 29 percent

reduction in the compressive strength and a 40 percent reduction in the elastic modulus of the concrete due to the effects of ASR.

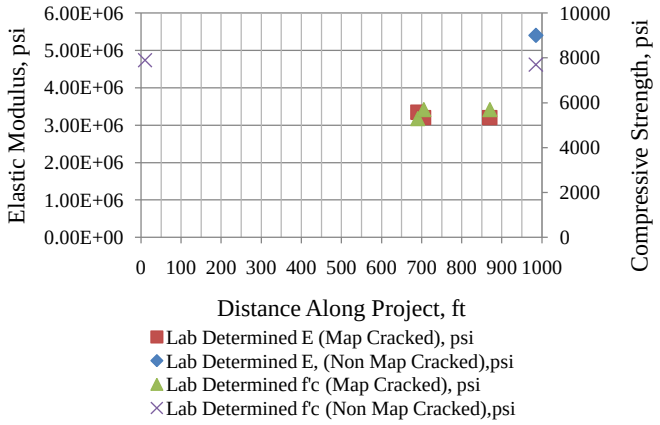

Figure 70: Influence of ASR on Concrete Structural Properties for US-22 Murrysville Segment 50 Eastbound

Table 27: Summary of Laboratory Test Results for US-22 Murrysville Segment 50 Eastbound Comparing Map Cracked and Non-Map Cracked Areas

	Map Cracked Slabs	**Non Map Cracked Slabs**
Average Compressive Strength, psi	7800	5570
Standard Deviation, psi	140	230
COV	2%	4%
Average Elastic Modulus, psi	3.25E+06	5.40E+06
Standard Deviation, psi	8.7E+04	N/A
Coefficient of Variation, %	3%	N/A

4.13 Scanning of Dowel Bars Using Magnetic Imaging Tomography: US-22 Murrysville

As mentioned in Section 4.7, the transverse joints for this pavement section were examined using a MIT Scan-2. The MIT Scan-2 was specifically developed by MIT GmbH of Dresden,

Germany for measuring dowel and tie bar alignments in PCC pavements. A total of 46 transverse joints were evaluated.

The MIT Scan-2 device used to assess the joints at US-22 Murrysville is property of the Federal Highway Administration (FHWA) and was used in this project as part of a demonstration of the capabilities of this tool to PennDOT personnel through the Concrete Pavement Technology Transfer program. The device consists of a scan unit, onboard computer, and a rail system as shown in Figure 71. The theory of operation of the MIT Scan-2 is that it emits an electromagnetic pulse and detects the subsequently induced magnetic field. Because of the use of electromagnetism, any metallic objects in the proximity of the scan unit influence the measurements. The MIT Scan-2 measures dowel placement within 0.2 in. per 18 in. dowel length and with 95 percent reliability for assessing the rotational alignment of a dowel.

Figure 71: Dowel Scanning Using the MIT Scan-2 at US-22 Murrysville Segment 50 eastbound.

Once the MIT Scan-2 data was collected, two tools were used to process the data. One was the MIT Scan Data Analyzer, a spreadsheet developed by Fugro Consultants. Another useful tool was the MagnoProof software that accompanies the MIT Scan-2. This software produces color gradient images representing the strength of the induced magnetic field created when the

dowel bars are exposed to electromagnetic pulses generated by the scanner. These magnetic field strength images give the user a visual representation of the alignment of the dowels for a particular joint. An example image for Joint 4 of this project is shown in Figure 72.

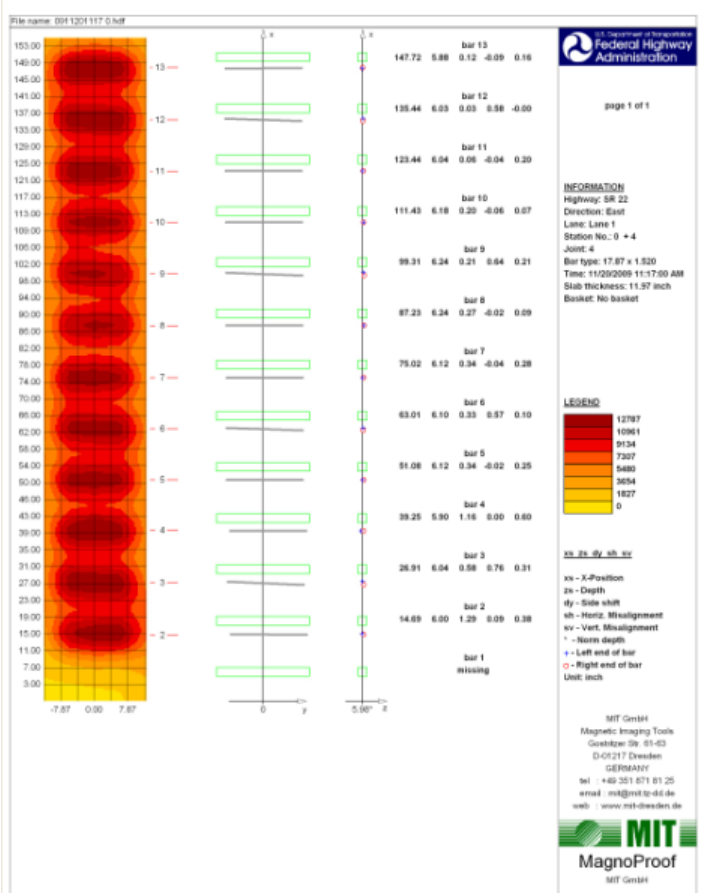

Figure 72: Visual Representation of the Dowel Locations at Joint 4 for US-22 Murrysville Segment 50 Eastbound.

4.13.1 Analysis of MIT Scan-2 Data

With the use of the aforementioned tools, data collected from the MIT Scan-2 was used to

determine if the distress observed in Segment 50, as shown in Figure 54, can be attributed to misaligned dowels. Multiple comparisons and observations were made using this data, including:

- Comparison of Joint Score and Distress
- Comparison of LTE and Distress
- Comparison of Joint Width and Distress
- Visual Inspection of MagnoProof Outputs
- Examination of Joint Cores Containing Dowels

Despite the available information, no definitive conclusions could be drawn with respect to whether or not the observed distress could be related to dowel misalignment.

Joint Score and Distress

The joint score concept was developed by Yu and Khazanovich [12] and is a weighting system used to rate the potential of a given joint to lockup. According to Yu and Khazanovich, a joint score greater than ten indicates at least a moderate risk for joint lockup. Figure 73 shows the joint scores for the joints of this project. As can be seen in Figure 73, there is no clear relationship between the areas exhibiting the clearly defined crack parallel to the transverse joint and the joint score. In addition, some of the joints are missing scores. During the execution of the scans, these joints were skipped because they were located at entrances to businesses along Segment 50 and were not accessible for testing. It should also be noted that the last six joints in the section were also not evaluated.

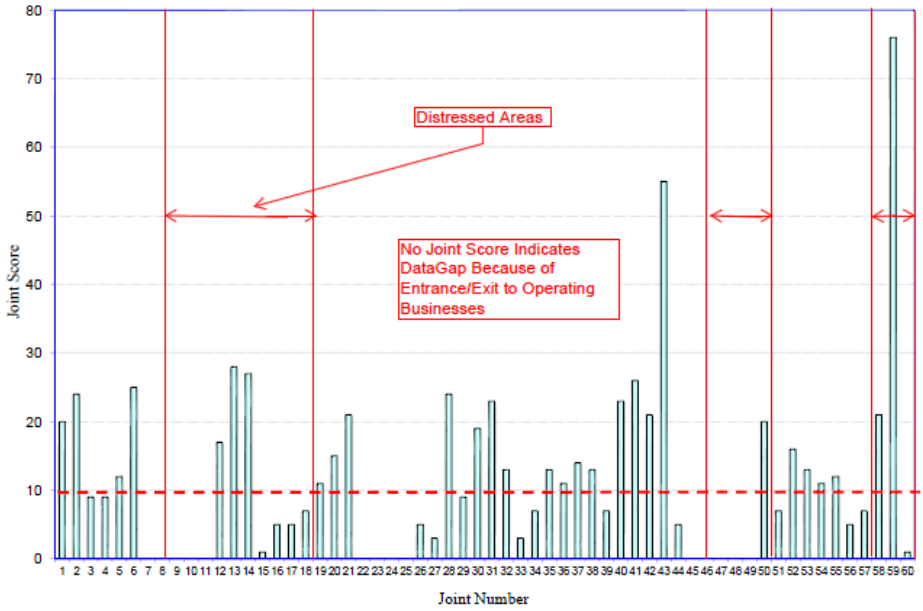

Figure 73: Joint Scores along US-22 Murrysville for Segment 50 Eastbound.

LTE and Distress

Load transfer efficiency data obtained from FWD testing was compared to the areas of the segment where ASR cracking was observed in attempt to correlate the LTE with this distress. The expansive nature of ASR should result in locked joints. Any high LTE outside of these areas could be the result of locked joints from dowel bar misalignment of inadequate lubrication of the dowel bars at the time of construction. Figure 74 shows that the LTE increases as joints become closer to the distressed areas with the LTE being quite high within the distressed areas. It should be pointed out that a core was pulled in a non-distressed area from joint 26 and the LTE at this joint is only 73%, indicating that the joint is not locked. The core did reveal a horizontal crack running parallel to the surface of the slab along mid-depth of the dowel. This joint is circled in Figure 74. This type of cracking could help explain the relatively low LTEs exhibited in the non-distressed sections. The cracking might be attributed to stress generated by the ASR in the distressed regions, insufficient lubrication of the dowel and/or dowel misalignment.

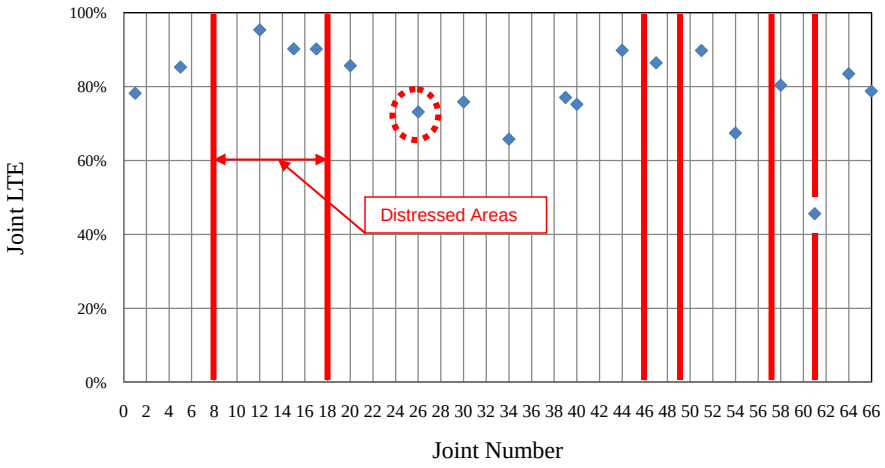

Figure 74: Comparison of Joint LTE with Known Distressed Areas of US-22 Murrysville for Segment 50 Eastbound

Joint Width and Distress

The measured joint widths at each joint, as well as the locations of the distressed areas, are shown in Figure 75. The purpose of this comparison was to determine if the distressed areas had smaller joint widths relative to the rest of the segment. If so, this could also indicate potential joint lockup. In order to draw some conclusions from this data, the magnitude of the joint width at known locations with locked joints was compared to other locations. Both Joints 12 and 58 were known to be locked since they contained embedded dowels that were immobile. The joint widths at Joints 12 and 58 are 0.42 and 0.48 in respectively. The average joint width for all the joints measured is 0.45 in and the standard deviation is 0.05 in. Therefore, it is concluded that the joint widths at Joints 12 and 58 are not significantly different from the other joints. As observed in Figure 75 the joint width exhibits a downward trend along the section, however, the cause for this is unknown.

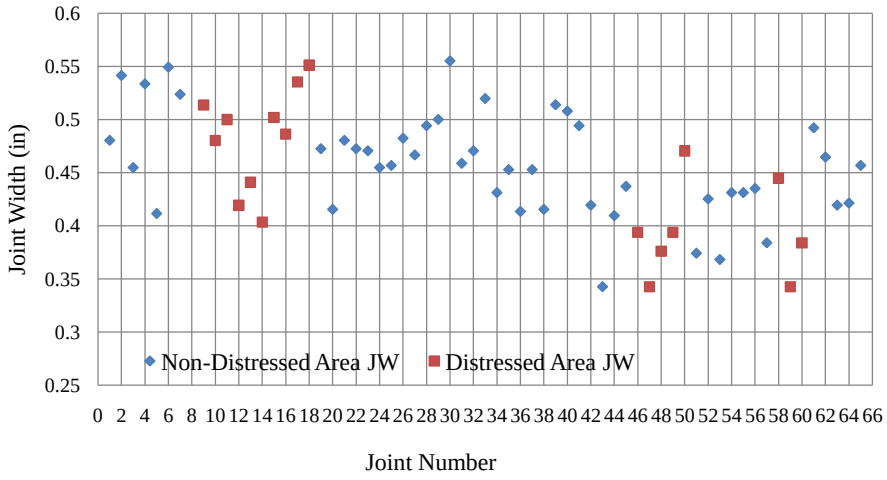

Figure 75: Transverse Joint Width along US-22 Murrysville Segment 50 Eastbound.

Visual Inspection of MagnoProof Outputs

For all joints scanned by MIT Scan-2, the visual outputs from the MagnoProof software were inspected. An example can be seen in Figure 76. Figure 76 shows a dowel bar that was most likely knocked out of its support as the paver passed. While Figure 70 shows a misaligned dowel bar, most of the MagnoProof outputs that were available did not exhibit such misalignments.

In looking at the MagnoProof outputs for the areas exhibiting the clearly defined crack parallel to the transverse joint and comparing them to outputs for the areas in which there was no such cracking, there was no trend present that suggested a potential cause of this cracking.

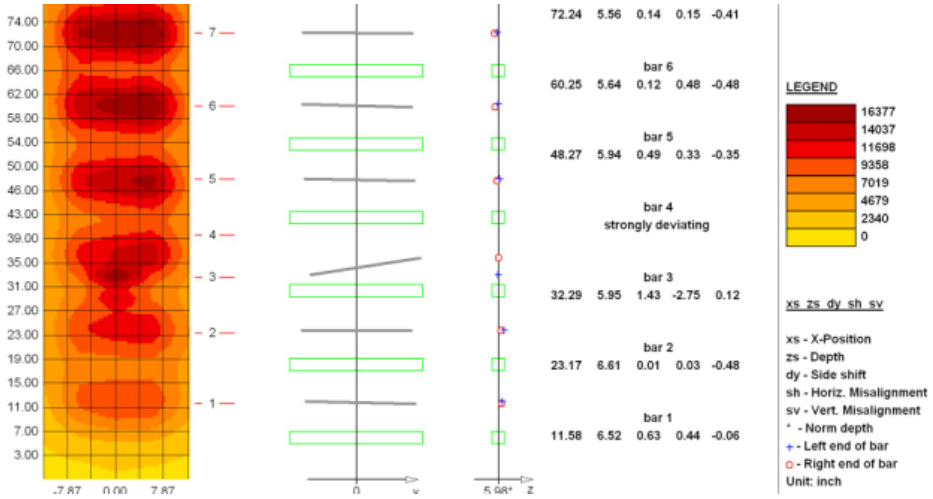

Figure 76: MagnoProof Output Illustrating Misaligned Dowel at Joint 14 of US-22 Murrysville for Segment 50 Eastbound

Doweled Cores

As shown in Table 24, there were two cores pulled from joints that contained dowel elements. These cores are from Joints 12 and 58, respectively. The cores with the embedded dowels could not be pulled apart even though the joint propagated directly through the middle of the core. This observation supports the fact that joint lockup is occurring within the section. Both joints exhibit transverse cracks within the vicinity of approximately 6 in from the joints and both joints had joint scores above ten with at least one neighboring joint with a score above ten. The examination of the MagnoProof outputs showed that the primary misalignment of both joints was horizontal misalignment but that in both cases the misalignment was less than 2 in. Khazanovich and Snyder [13], have documented that 2 in of misalignment in either vertical tilt or horizontal skew has negligible effect on pullout and shear performance measures. However, this criterion assumes that the dowel bars were properly lubricated and provided no restriction in joint movement.

4.14 Potential Causes of Distresses: US-22 Murrysville

4.14.1 Material-related Distress

For Segment 50 of US-22 Murrysville, the major distress affecting this section is ASR-cracking, which is present in almost 30 percent of the slabs. This cracking is oriented parallel to transverse and longitudinal joints and generally extended over the entire slab. Section 4.11 presents evidence determining that the cause of this distress is due to ASR. It is apparent, based on visual observation of the coloration of the cement paste in the cores, that the concrete is not uniform throughout the section. In particular, as discussed in Section 4.11, it can be concluded that the variation in coloration is due to the amount of GGBFS included in the concrete mixture. The use of GGBFS tends to give the concrete a blue/greyish color. The larger quantities of GGBFS found in the concrete used to construct the non-distressed sections seems to have mitigated the ASR.

Drying shrinkage cracks were also observed. These typically develop with the water to cement ratio is too high or inadequate finishing or curing techniques were used.

4.14.2 Transverse Joint Spalling

Developed joint spalling was not present in the representative section; however, it was observed that some slabs exhibited a clearly defined crack parallel to the transverse joint. This cracking, which appears to be a consequence of joint lockup, could eventually cause spalling at the transverse joint.

4.14.3 Repaired Corner Breaks

It was noticed during the retrieval of cores and during the conducting of the distress survey that for this Segment 50 full-depth repairs were executed at some areas of the driving and passing lane. It was later determined that these repairs occurred in areas for which the original slabs exhibited corner breaks. In the driving lane, these repairs included entire slab replacements while in the passing lane the repairs were executed only at areas adjacent to the existing transverse joints and over lengths shorter than an entire slab length. This repair was illustrated in Figure 51. It appears that the corner cracks were the result of joint-lock up issues. The joint lock-up could be the result of the expansive forces produced by the ASR in adjacent sections in combination with misaligned dowels and inadequate lubrication of the dowel at the time of construction.

4.15 Rehabilitation Recommendations: US-22 Murrysville

4.15.1 Distresses and Deficiencies

As mentioned throughout this section of the report, the major distresses and deficiencies for US-22 in Murrysville are drying shrinkage cracking, ASR related cracking, a unique transverse crack a short distance from some of the transverse joints, corner cracks that were previously repaired and relatively low LTE outside of the distressed areas. From the cores pulled at the locations of the dowels, it is also apparent that the joints were locked. Although the observation of the various distresses and deficiencies are based on data obtained from Segment 50 alone, other segments that were part of the original analysis section and that exhibit similar distress patterns should also be considered for these rehabilitation measures.

4.15.2 Recommendations for Segment 50

Fortunately, the ASR is only exhibited in localized areas having concrete with low amounts of GGBS. These sections will eventually have to be removed and replaced. The transverse cracks running adjacent to the transverse joints only developed in the sections with the ASR distress since it was caused by the joint lock-up pressures resulting from the ASR related expansion. Therefore, replacing these slabs will also address the transverse cracks. The other material related distress observed was drying shrinkage cracking. These cracks are not a sufficient depth to prevent further deterioration and do not need to be addressed.

The low load transfer efficiencies seem to be the result of horizontal cracks running parallel to the slab surface. This cracking most likely developed due to stress generated by joint lock-up. These joints should be closely monitored and full depth repairs will most likely need to be performed when the LTE drop below 70. At this time, additional coring is suggested to confirm that the LTE is the result of this horizontal cracking. If some of the joints with low LTEs are not exhibiting the horizontal cracking that dowel retrofits can be performed in lieu of full depth repairs to restore the load transfer.

4.16 Future Projects: US-22 Murrysville

Based on the results of the petrographic analysis, it is recommended that the material acceptance results for this project be reviewed. PennDOT, in publication 408 [5] section 704.1(g), allows the use of potentially expansive aggregate provided the deleterious expansion can be shown to be limited through the use of a pozzolan such as GGBFS. It appears that the use

of the reactive aggregate was approved by PennDOT based on the accepted mix design but that the mix delivered to the site was not always the same as the one approved by PennDOT considering the reactive nature of the project aggregates. For future projects, methods should be implemented to ensure this type of issue does not re-occur.

It is suggested that the curing specifications be changed, as previously described, to help address the drying shrinkage that was observed. It has been noticed that many of the pavers in the state drag wet burlap hung behind the paver along the surface of the pavement. This burlap is continually soaked, which results in an increase in the water to cement ratio on the pavement surface. This is then worked into the surface by about six to eight finishers following behind the paver. Figure 77 and Figure 78 below show the wet burlap drag and the resulting slurry

Figure 77: Wet Burlap Drag and Finishing Behind the Paver

Figure 78: Slurry Produced by the Wet Burlap Drag behind the Paver

Regarding joint lock-up, PennDOT Publication 408 Section 705.3 specifies that a bond breaker be provided to dowel bars such that the pull out resistance of the dowel as measured by AASHTO M254 is not exceeded. It has been noticed on other projects throughout the region that although dowels are originally coated with a bond breaker material, this material can become dirty while being stored on-site and that some of these dirty bars were installed at the time of paving. This could contribute to dowel lockup as well and should be avoided on future projects.

5 I 79, Washington County

5.1 Project Information: I 79

The selected site for this project is a section of I79 in Washington County. Washington County falls under the jurisdiction of PennDOT Engineering District 12. Segment 470 and Segment 480 northbound were selected as the Distressed and Control section, respectively. A 1000-ft long representative section within each segment was chosen based on the pavement condition and the ease of executing traffic control. The green highlight in Figure 79 and Figure 80 show the location of the Distressed and Control section, respectively.

Figure 79: Location of I 79 Segment 470 Northbound (Distressed Section) in District 12.

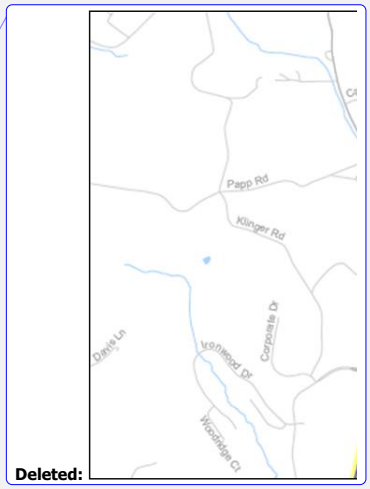

Figure 80: *Location of I 79 Segment 480 Northbound (Control Section) in District 12.*

5.2 Design Information: I 79

Segment 470 and Segment 480 northbound are JPCP pavements with two lanes per direction. Segment 470 and Segment 480 were constructed in the construction seasons of 1994 and 1997 respectively. The design features for these segments include 12-ft wide PCC slabs and 1:6 counterclockwise skewed transverse joints. The joint spacing is 20 ft measured along the lane/shoulder joint with an effective slab diagonal of 25.06 ft. 1.5 in dowel bars were installed at

12 in off center at the transverse joints and the transverse joints are sealed with preformed neoprene. According to the design information, the pavement structure consists of a 12-in PCC slab, a 4-in open graded base (OGS) and a 4-in 2A subbase. However, it was found during the field testing that the PCC slab for the Control section was on average 1-in thicker than that of the Distressed section.

According to soils data from the Natural Resources Conservation Service [14] the subgrade soil has an AASHTO classification of A-4 and A-6. For the Distressed section, the subgrade is mainly A-4 with a small area with A-6 soil. In the case of the Control section, the subgrade in the majority of the section is A-6 soil with a small portion of A-4 soil. The pavement has longitudinal edge drains that were included as part of the original construction. The inside and outside shoulders consist of tied PCC and are 5-ft and 10-ft wide, respectively. Cross sections of the existing pavement in both the Distressed and Control section can be seen in Figure 81 and Figure 82 while an overall view of the Distressed and Control sections can be seen in Figure 83 and Figure 84, respectively.

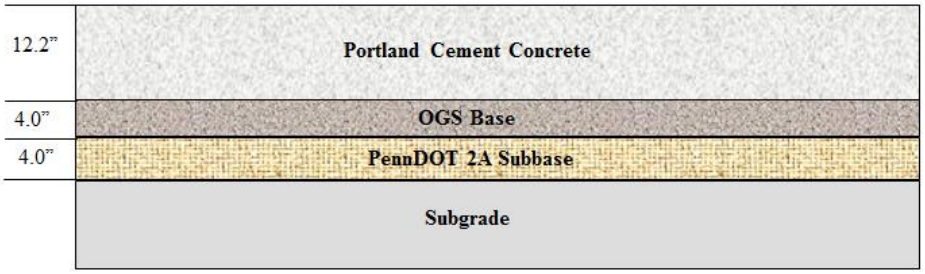

Figure 81: Existing Pavement Cross Section of I-79 Segment 470 Northbound (Distressed Section)

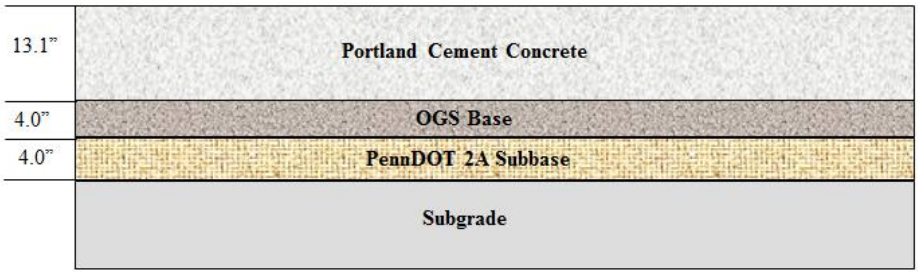

Figure 82: Existing Pavement Cross Section of I-79 Segment 480 Northbound (Control Section)

Figure 83: *Overall Condition of I 79 Segment 470 Northbound (Distressed Section)*

Figure 84: Overall Condition of I 79 Segment 480 Northbound (Control Section)

5.3 Concrete Mixture Design: I 79

For I79 there is no available information regarding the concrete mixture design. Despite this missing information, based on the visual examination of the retrieved cores, it can be concluded that the concrete mixture designs used for the Distressed and Control sections are different. As observed in Figure 85, the coarse aggregate for the Distressed section is blast furnace slag whereas it is limestone for the Control section. The coarse aggregate gradation for the Control section also appears to be more uniform than that for the Distressed section. Additionally, the paste color for the specimens in the Control section was constant from top to bottom (brown). In the case of the Distressed section, a color variation from brown to grey was observed in the paste. The grey color was present around some coarse aggregate particles. This discoloration is a normal process in concrete containing blast furnace slag and it is not a detrimental characteristic.

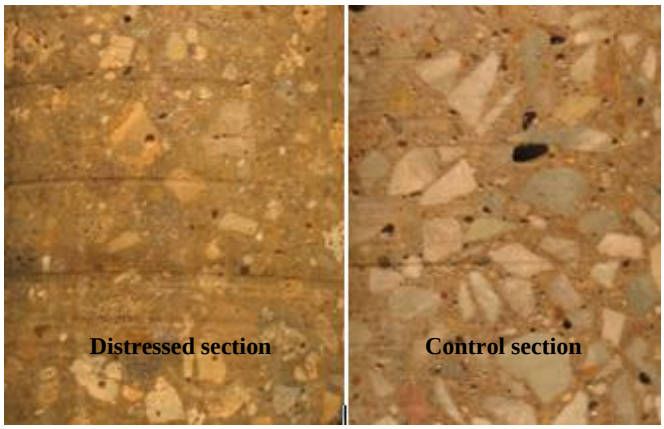

Figure 85: Concrete Core Surface Detail of I 79 Segments 470 and 480 Northbound (Distressed and Control Sections).

5.4 Climatic Conditions: I 79

I 79 is located in a wet freeze climate with a relatively high number of wet days per year. To further analyze the climatic conditions, a virtual weather station created by the EICM [3], was also used to characterize the project climatic conditions. The representative coordinates of the two segments analyzed for I 79 are 40.29° latitude and -80.16° longitude. The two closest climate stations are the one labeled in EICM database as Pittsburgh International Airport, which is 2.2 miles away, and the Allegheny County Airport, which is 21.3 miles away. According to

the weather stations, the area experiences approximately 148 wet days per year and a mean annual rainfall of 37-in. The freezing index is 706 ºF-days and the area is exposed to approximately 76 freeze-thaw cycles per year. The mean annual air temperature is 49.0 ºF with minimum and maximum average monthly temperatures of 29.9 ºF and 79.3 ºF, respectively.

5.5 Traffic Loadings: I 79

Like many of the other projects, traffic data for this site was found using PennDOT's ITMS. As of 2008, the one-way AADT for the Distressed and Control sections is approximately 18,000 with 17 percent trucks. From 1993 to 2009 this highways has sustained about 12.5 million ESAL applications.

5.6 Selection of Distress Survey Section: I 79

As was done with the other projects, candidate segments were selected in the office based on distress data provided by PennDOT, and a PennDOT Videolog analysis. In addition to these resources, once on site, the final selection of the segments depended on the ease with which traffic control could be executed. For this project, the Distressed and Control sections were selected to be Segment 470 and Segment 480 respectively.

5.7 Pavement Condition: I 79

To assess the pavement condition, a distress survey was conducted over a 1,000-ft representative section in the driving lane of both the Distressed and Control sections. The distress survey was performed according to the Distress Identification Manual for the LTPP [1], and included the observation and quantification of transverse joint faulting, transverse joint width, percent spalling of joints and cracks, transverse cracking, and material-related distresses such as staining or map cracking. In addition, lane to shoulder drop off was also measured. A summary of the distress measurements for I 79 is presented in Table 28.

As can be observed in the table, very little distress is observed in the Control section. This is also reflected by the high PSR for the section. For the Distressed section on the other hand, the primary distress types were transverse cracking and subsequent spalling of the transverse cracks. Spalling of the transverse joints was also observed. As can be seen from the PSR of the Distressed section, these distresses have a significant impact on the quality of the ride in this section.

Table 28: Summary of Performance Data for I 79

Performance Measurement	Segment 470 (Distressed Section)	Segment 480 (Control Section)
Outside Pavement Edge Faulting, in	0.03	0.04
Outer Wheel Path Faulting, in	0.02	0.03
Transverse Cracks Edge Faulting, in	0.06	n/a
Transverse Cracks Wheel Path Faulting, in	0.06	n/a
Lane-to-shoulder Dropoff, in	0.32	0.13
Percent of Slabs with Transverse Cracking, %	48	0
Percent of Slabs with Transverse Joint Spalling, %	10	4
Percent of Slabs with Longitudinal Joint Spalling, %	24	0
Percent of Slabs with Cracked PCC Shoulder, %	40	0
Joint Width, in	0.70	0.69
PSR	2.5	3.9

5.7.1 *Transverse Joint Faulting*

Faulting was measured at every joint and crack in the Distressed and Control sections. At each joint and crack, faulting measurements were made at both the outside pavement edge (1-ft from the lane/shoulder joint) and at the outer wheelpath of the outside lane (2.5-ft from the lane/shoulder joint). The average faulting for the joints in the Distressed section is 0.03-in and 0.06-in for the cracks. The average faulting for the joints in the Control section is 0.04-in. Therefore, the faulting for each section was insignificant.

5.7.2 *Lane-to-Shoulder Dropoff*

As observed in Table 28, the shoulder dropoff is higher in the Distressed section than the Control section. However, both values are not considered high in terms of severity. The maximum and minimum values for the Distressed section are 0.78-in and 0.07-in. The corresponding values for the Control section are 0.35-in and 0.02-in. Figure 86 shows a section

of the longitudinal joint between the lane and the shoulder in the Distressed section. An interesting observation in this figure is that, in addition to the difference in elevation between slab and shoulder, there is a horizontal separation between the driving lane and the shoulder. This separation suggests failure of the tie bars connecting these two elements.

Figure 86: *Lane-to-Shoulder Joint of I 79 Segment 470 Northbound (Distressed Section)*

5.7.3 Joint Width

As observed in Table 28, the average crack width for both the Distressed and Control sections is the same. This condition was not surprising considering the similarities between both sections regarding the variables that affect joint width (i.e. joint spacing, base type, and PCC coefficient of thermal expansion).

5.7.4 *Transverse Cracking*

In the Distressed section, 48 percent of the slabs exhibited mid-panel transverse cracking compared with no slabs exhibiting this distress in the Control section. A breakdown by severity

reveals that in the Distressed section, 12 percent of the cracks are of low severity, 30 percent are of medium severity, and 6 percent are of high severity. It was found that Panels 25, 26, and 27, which are located in the middle of the Distressed section, have very poor support conditions. This is evidenced by the fact that the panels can be seen moving when traffic passes. Figure 87 shows one such panel. The crack in Figure 87 is a high severity crack that has significant faulting and spalling and even extends through the concrete shoulder.

Figure 87: *High Severity Transverse Crack of I 79 Segment 470 Northbound (Distressed Section)*

Figure 88 shows a low severity crack with an asphalt patch. Fourteen percent of the slabs in the Distressed section have an asphalt patch. The patches can be found at cracks, transverse joints, and longitudinal joints. The crack in this picture has been traced over with a marker to enhance its visibility.

Figure 88: *Digitally Enhanced Low Severity Transverse Crack and an Asphalt Patch of I 79 Segment 470 Northbound (Distressed Section)*

5.7.5 Topographic Characteristics and Drainage

The Distressed and Control sections are located in cut areas as seen in Figure 89 and Figure 90 respectively. As observed in the figures, both sections are situated next to steep side slopes for which runoff water drains towards the pavement structure and is collected by a grass lined channel. The direction of the transverse slope of the pavement is different between the sections. The transverse slope in the Distressed section is directed such that all the water on the pavement surface drains towards the outside shoulder, while the transverse slope in the Control section is such that half the water drains towards the inner shoulder and half drains towards the outside shoulder. As a result, the ditch at the outside shoulder of the Distressed section collects more runoff water from the pavement than the ditch at the outside shoulder of the Control section. The side slope next to the Distressed section is also much larger and contributes a larger volume of water draining to the ditch than the corresponding side slope in the Control section. Another important difference in the overall drainage condition between the sections is that the longitudinal slope of the pavement for the Control section is considerably larger than that for the Distressed section.

It was also noticed that several areas in the Distressed section exhibited drainage deficiencies. These areas were characterized by the absence of grass and dry natural soil with desiccation cracks on the surface as observed in Figure 91. The dimensions and severity of these areas varied along the section but were most pronounced in the areas adjacent to Panels 20 through 30. It is believed that the drainage deficiency is created by a combination of both poor grading of the ditch and lack of proper maintenance to guarantee positive flow towards a

drainage collector. Because of these deficiencies, ponding of water seems to have occurred resulting in a weakened structural capacity of the pavement. In the case of the Control section, no potential areas were ponded water gathered were observed.

Figure 89: *Side Slope of I 79 Segment 470 Northbound (Distressed Section) (photo taken after overlay placement)*

Figure 90: *Side Slope of I 79 Segment 480 Northbound (Control Section)*

Figure 91: Typical Ponding Area of I 79 Segment 470 Northbound (Distressed Section) (photo taken after overlay placement)

5.7.6 *Present Serviceability Rating*

The average PSR of the Distressed section was approximately 2.5, which is considerably lower than the 3.9 PSR of the Control section. This discrepancy underscores the importance of determining the source of the difference in performance between the Distressed and Control sections.

5.8 FWD Testing: I 79

In both the Distressed and Control sections, the FWD testing included seven mid-slab locations and ten transverse joints (approach and leave sides). Eight transverse cracks were also tested on both the approach and leave sides in the Distressed section. FWD testing at mid-slab locations was used to determine PCC elastic modulus and modulus of subgrade reaction. FWD testing at joints and cracks was used to determine their load transfer efficiencies, differential deflections, and whether or not there was the potential for a loss of support. A summary of the results obtained by analyzing the FWD test data can be found in Table 29.

Table 29: Summary of Deflection Testing Results for I 79.

Property	Segment 470 (Distressed section)	Segment 480 (Control section)
	Average	Average
Static Elastic Modulus, psi	4.70E+06	5.35E+06
k-value, psi/in	230	280
Joint Load Transfer, %	50	96
Crack Load Transfer, %	15	N/A
Mid-slab Deflection, mils	1.73	1.44
Corners with Voids, %	100	100
Maximum Air Temperature During Testing, °F	52	46

5.8.1 *Temperature Gradient*

In accordance with the LTPP guidelines [9], temperature gradient measurements were made in the field during FWD testing at depths shown in Figure 40 of Section 3.8.1. Section 2.8.1 explains the importance of these measurements with respect to the interpretation of FWD results. The measured temperature gradient for the Distressed and Control sections can be seen in Figure 92 and Figure 93, respectively.

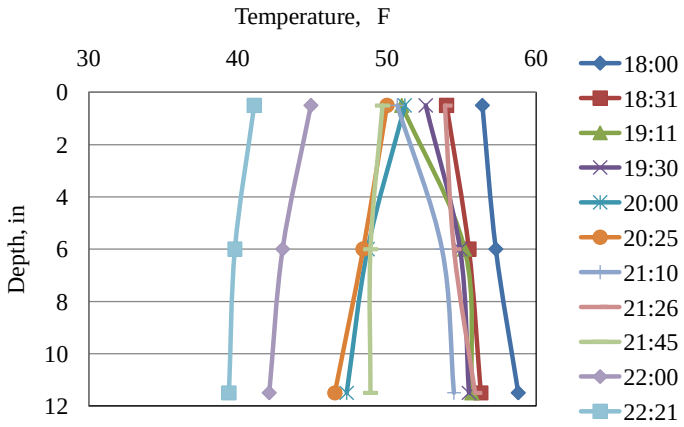

Figure 92: Temperature Gradients during FWD Testing for I 79 Segment 470 Northbound (Distressed Section)

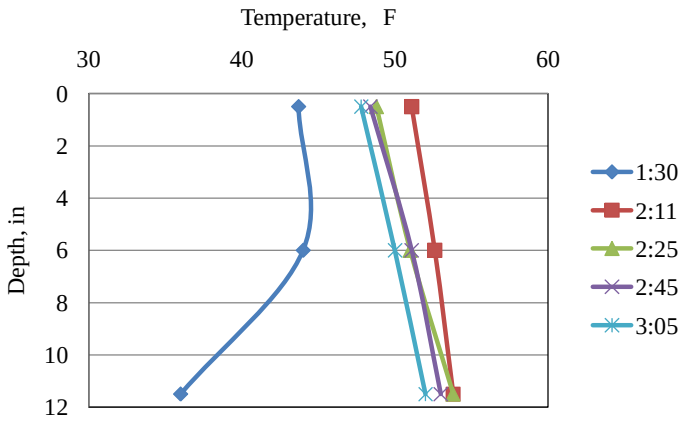

Figure 93: Temperature Gradients during FWD Testing for I 79 Segment 480 Northbound (Control Section)

5.8.2 PCC Elastic Modulus

The elastic modulus, E, of the concrete slab was backcalculated using mid-slab deflection measurements along with the actual thickness of the slab determined from the cores extracted at the FWD locations. Figure 94 and Figure 95 show the PCC elastic modulus for the Distressed and Control sections, respectively.

The average backcalculated static elastic modulus for the Distressed section is 4.70 million psi with a coefficient of variation of 23 percent. The average backcalculated static elastic modulus for the Control section is 5.35 million psi with a standard deviation of 1.98 million psi and a coefficient of variation of 37 percent. These average values are between typical ranges for mature concrete in highways. In both the Control and Distressed sections there is high variability with the variability being even more pronounced in the Control section. Taking this variability into account, the difference between the average values for both sections is not considered significant. Although the results of the laboratory testing for I 79 will be presented later, the relatively higher static elastic modulus for the Control section shown here agrees with the laboratory-determined values.

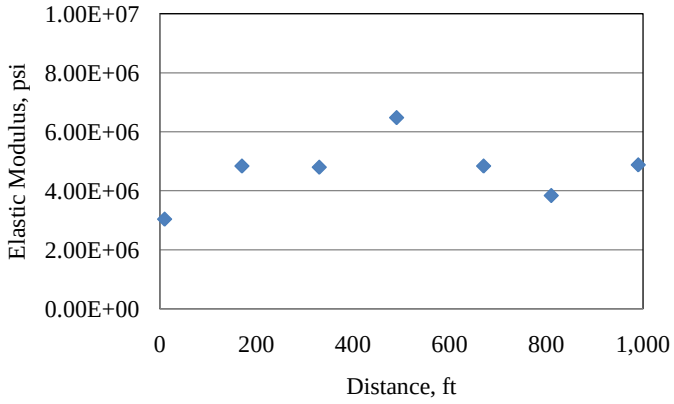

Figure 94: *PCC Elastic Modulus for I 79 Segment 470 Northbound (Distressed Section)*

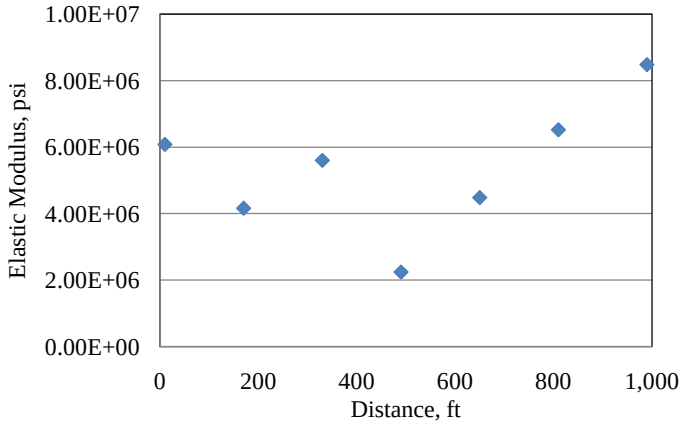

Figure 95: *PCC Elastic Modulus for I 79 Segment 480 Northbound (Control Section)*

5.8.3 *Modulus of Subgrade Reaction*

The modulus of subgrade reaction, k-value, was calculated using mid-slab deflections. Figure 96 and Figure 97 show the k-value along the Distressed and Control sections, respectively. The average static k-value for the Distressed section is 230 psi/in with a standard deviation of 55 psi/in and coefficient of variation of 24 percent. The average static k-value for the Control section is 280 psi/in with a standard deviation of 95 psi/in. The coefficient of variation is 34 percent. While the variability is considerably high for both sections, the average

k-values obtained are still typical for an unstabilized base. A higher average k-value was expected for the Distressed section considering that, as mentioned before, the subgrade in the Distressed section is mainly A-4 soil, whereas it is mainly A-6 soil in the Control section. During the field data collection, three panels (Slabs 27 to 29) were visually observed to be moving whenever traffic passed by suggesting significant support problems.

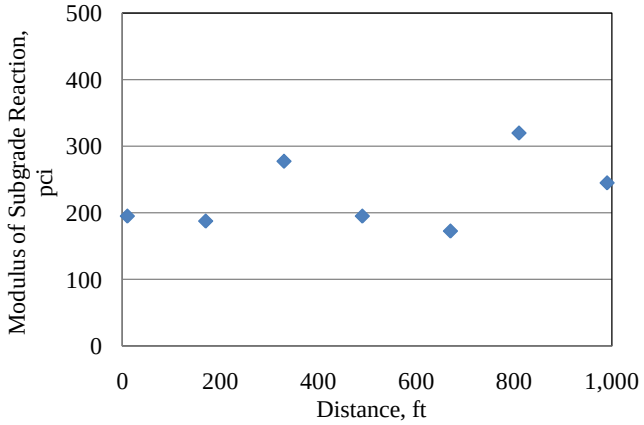

Figure 96: *Modulus of Subgrade Reaction for I 79 Segment 470 Northbound (Distressed Section)*

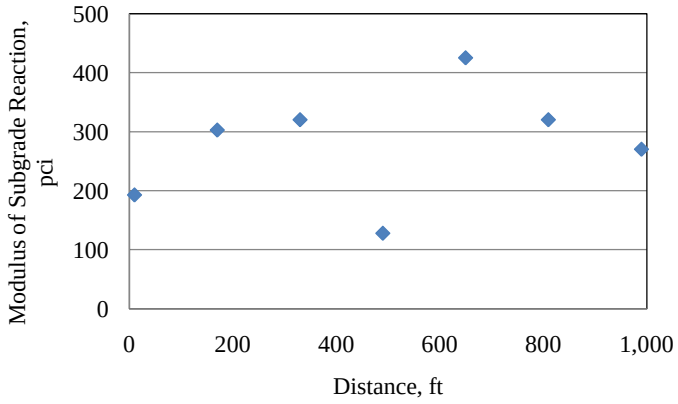

Figure 97: Modulus of Subgrade Reaction for I 79 Segment 480 Northbound (Control Section)

5.8.4 Joint Load Transfer

The joint load transfer for the Distressed and Control sections of I 79 are presented in Figure 98 and Figure 99. The relative performance between the Distressed and Control sections with respect to transverse joint load transfer was quite varied. The average LTE for the Distressed section was 42 percent and there was only one location for which the load transfer was above the recommended acceptable value of 70 percent. As one can surmise from the average value of 42 percent, many values were significantly lower than 70 percent indicating poor load transfer. The transverse joints in the Control section on the other hand had an average LTE of 93 percent. These high LTEs are indicative of consistently good load transfer performance in this segment. In the Distressed section, approximately half of the joints with poor load transfer have spalling.

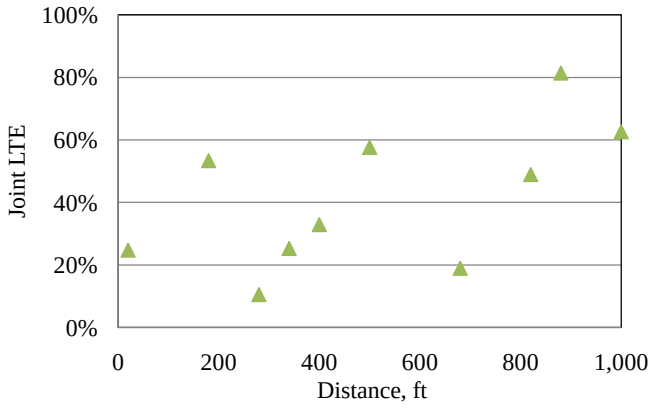

Figure 98: Transverse Joint Load Transfer Efficiencies of I 79 Segment 470 Northbound (Distressed Section)

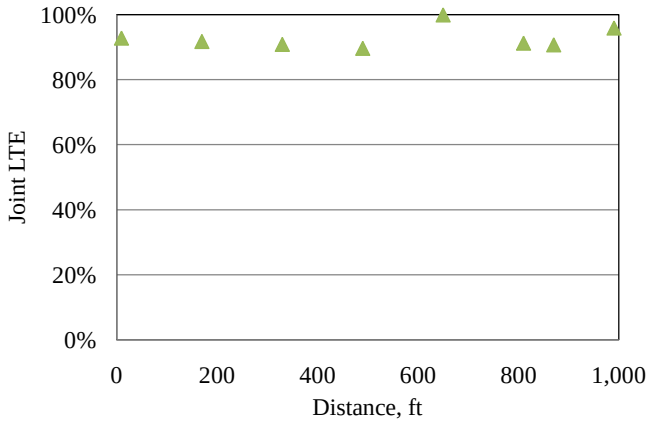

Figure 99: Transverse Joint Load Transfer Efficiencies of I 79 Segment 480 Northbound (Control Section)

The differential deflections at joints for the Distressed and Control sections can be seen in Figure 100 and Figure 101, respectively. In the Distressed section, the differential deflections range from 2 to 23 mils. Low differential deflections correspond to high LTE and vice versa. A possible explanation for this is that there could be variability in the OGS base. While there are voids underneath all of the joints, some are larger than others. In general, the largest voids correspond to the locations where the LTE is the lowest.

In the Control section, the LTE along the section is excellent and all of the differential deflections are less than 2 mils. However, analyzing the measured peak deflections revealed that these values are considerably high with an average value of 15 mils. This condition suggests a potential loss of support beneath the slabs.

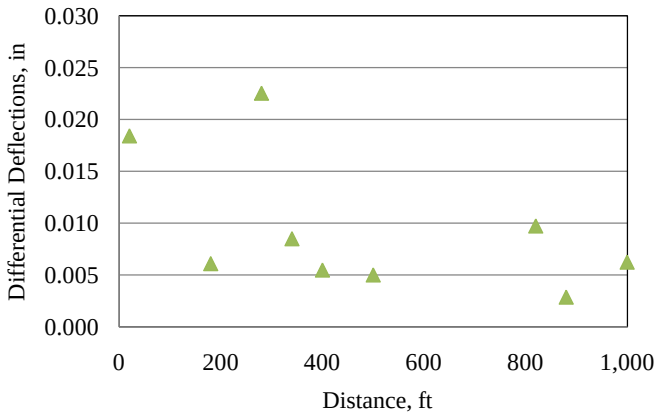

Figure 100: Differential Deflections at Transverse Joints for I 79 Segment 470 northbound (Distressed section)

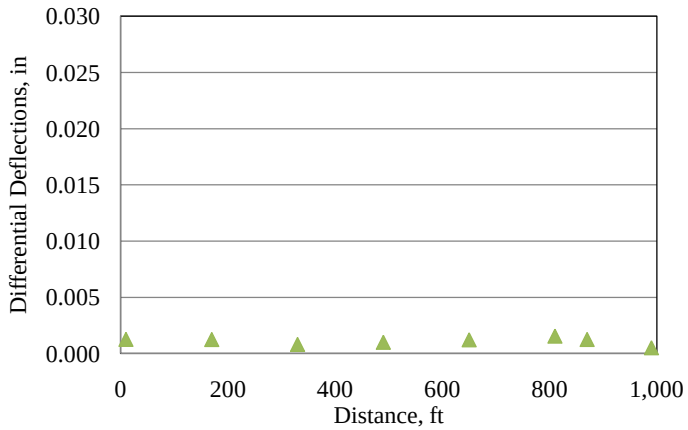

Figure 101: Differential Deflections at Transverse Joints for I 79 Segment 480 northbound (Control section)

5.8.5 *Crack Load Transfer*

The crack load transfer efficiencies for the Distressed section of I 79 is shown in Figure 102. These crack load transfer efficiencies are considerably low throughout the section. The average crack load transfer efficiency is 10 percent. For a granular base, the base typically contributes approximately 30 percent in the load transfer. The very low crack LTEs for the Distressed

section is an indication of dowel looseness and a weakened base beneath the slab that is not providing complete support. The differential deflections, shown in Figure 103 are relatively high. The value is greater than 5 mils for every location with some locations exhibiting differential deflections more than 15 mils. The majority of the locations tested had medium severity cracks and at some locations, as previously mentioned, could be seen moving under traffic loads. This observation suggests serious support issues beneath the slab.

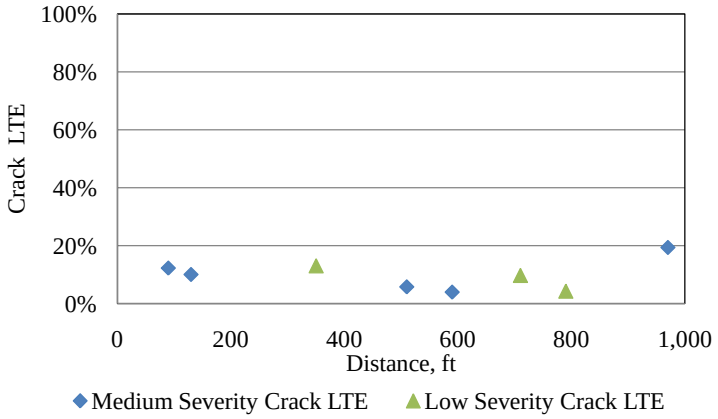

Figure 102: Transverse Crack Load Transfer Efficiencies for I 79 Segment 470 Northbound (Distressed Section)

The differential deflections measured for the cracks in the Distressed section are presented in Figure 103. As stated previously, if differential deflections are greater than 10 mils, then there is a problem with load transfer. Almost all of the locations tested had differential deflections greater than 10 mils and the locations that did not exceed this threshold were close to 10 mils differential deflection. The values with larger differential deflections all have poorer load transfer efficiencies.

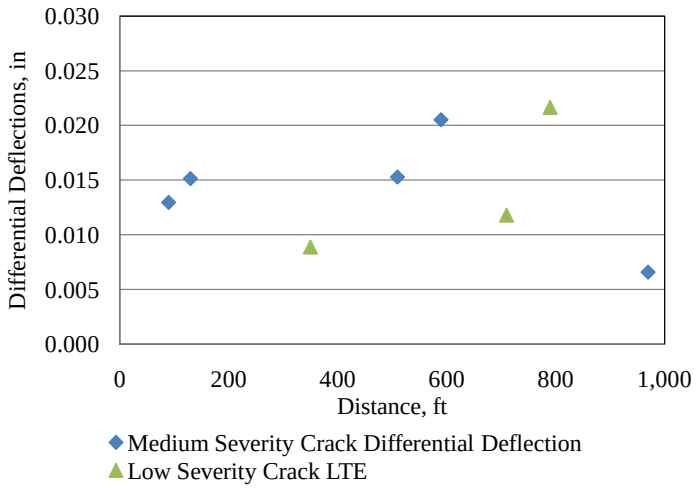

Figure 103: Differential Deflections at Transverse Cracks for I 79 Segment 470 Northbound (Distressed Section)

5.8.6 Loss of Support

To determine the presence of voids, the load vs. deflection response for each station was determined. Figure 104 and Figure 105 present the y-intercept of the load vs. deflection relationship obtained from the FWD data at each station for which void analysis was desired. Values of the y-intercept higher than 2 mils imply the presence of a void. As mentioned in Section 2.8.1, temperature gradients in the slab can influence void detection results. For I 79, the magnitude of the temperature gradients measured at the time of the FWD testing for both sections (0.3°F/in Distressed section and 0.4°F/in Control section) is not considered influential in regards to the void detection results.

The Distressed section shows the potential for voids at every joint and crack. This agrees with the load transfer efficiencies and differential deflections calculated at these locations. It is suspected that the base beneath the slab has been eroded or experienced significant settlement.

As mentioned previously, the load transfer efficiencies in the Control section are extraordinarily good with virtually no faulting, however, the section shows the potential for voids at every joint. This implies that even with a limited contribution of the base layer in load transfer, the dowels and aggregate interlock are working efficiently and are able to maintain a high level of load transfer. While no pumping or staining of fines near the longitudinal or

transverse joints was observed out in the field; there is a potential for a reduction in support through consolidation or aggregate degradation since an OGS was used.

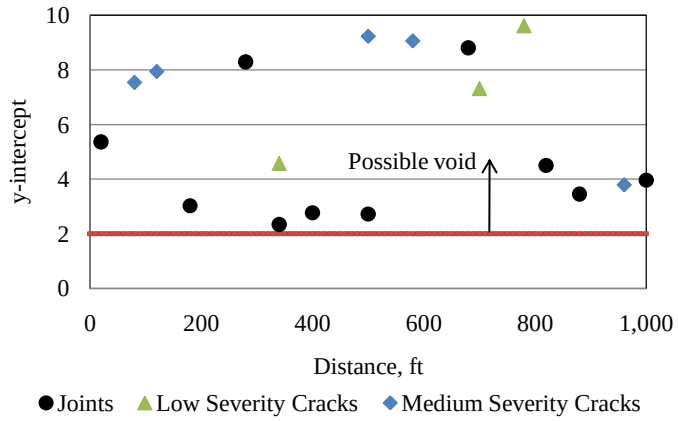

Figure 104: *Loss of Support for I 79 Segment 470 Northbound (Distressed Section)*

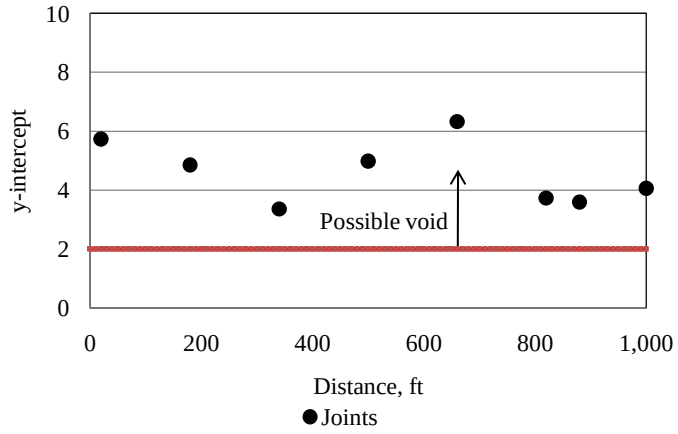

Figure 105: *Loss of Support for I 79 Segment 480 Northbound (Control Section)*

5.9 Core Samples: I 79

A total of eleven 6-in diameter cores were retrieved from the Distressed section and nine 6-in diameter cores were retrieved from the Control section. Table 30 and Table 31 present a summary of the cores pulled from the Distressed and Control sections respectively. In the Distressed section, seven cores were pulled from mid-slab locations, two from transverse cracks, and two from transverse joints. In the Control section, seven cores were pulled from mid-slab locations and two were pulled from transverse joints. Although the design slab thickness was 12-in, the average length of the cores from the Distressed section was 12.2-in and the average length of the cores from the Control section was 13.1-in. The implications of this variability in thickness between the Distressed and Control sections will be discussed in later sections.

Table 30: *Summary of Cores for I 79 Segment 470 Northbound (Distressed Section)*

Core	Location	PCC Thickness (in)	Base Type	No. of Pieces	Embedded Items
C1MS-D	Mid-slab	12.5	Granular	1	No
C5C-D	Transverse Crack	13	Granular	1	No
C9MS-D	Mid-slab	12.5	Granular	1	No
C14J-D	Joint	12	Granular	2	Yes
C17MS-D	Mid-slab	12	Granular	1	No
C25MS-D	Mid-slab	12	Granular	1	No
C33MS-D	Mid-slab	12.25	Granular	1	No
C41MS-D	Mid-slab	12	Granular	1	No
C44J-D	Joint	12	Granular	2	No
C49C-D	Transverse Crack	11.75	Granular	2	No
C51MS-D	Mid-slab	12.5	Granular	1	No

Table 31: Summary of Cores for I 79 Segment 480 Northbound (Control Section)

Core	Location	PCC Thickness, in	Base Type	No. of Pieces	Embedded Items
C1MS-C	Mid-slab	13	Granular	1	No
C9MS-C	Mid-slab	13	Granular	1	No
C13J-C	Joint	13	Granular	2	Yes
C17MS-C	Mid-slab	13	Granular	1	No
C25MS-C	Mid-slab	13.5	Granular	1	No
C33MS-C	Mid-slab	13	Granular	1	No
C41MS-C	Mid-slab	13.5	Granular	1	No
C44J-C	Joint	13	Granular	3	No
C50MS-C	Mid-slab	13.25	Granular	1	No

5.10 Base Samples: I 79

A total of three granular base samples were obtained from the Distressed section at different locations where PCC cores were retrieved. These locations include Slabs 1, 5, and 51. For the Control section, four granular base samples were obtained from Slabs 9, 17, 33, and 50. A sieve analysis using the portion of each sample passing the No. 4 sieve was performed. Figure 106 through Figure 112 present the gradation curve for each sample with the dashed lines representing PennDOT's specification band for this material. As observed in the figures, the percentage of fines (material finer than 3 mils) is within the range specified by Section 703 of PennDOT Specification 408, which calls for a maximum fines quantity of 5 percent. The samples are in fair agreement with the specification in general.

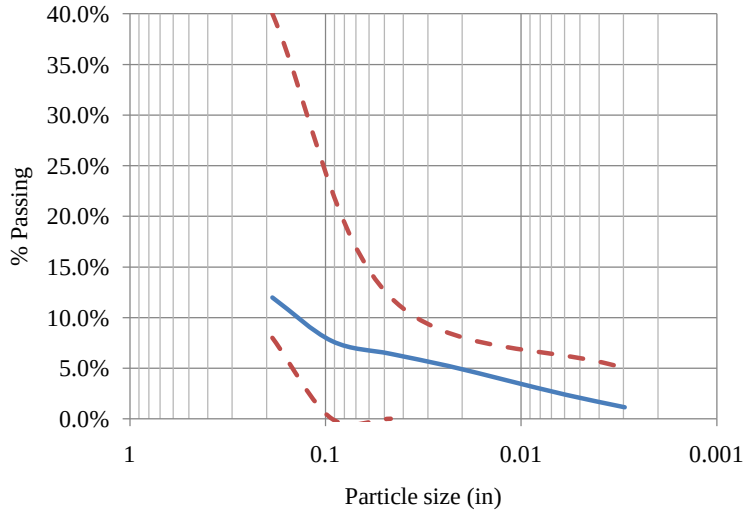

Figure 106: Particle Size Distribution Curve for the Portion Passing the No. 4 Sieve of the OGS Granular Base for I 79 Segment 470 Northbound Slab 1 (Distressed Section).

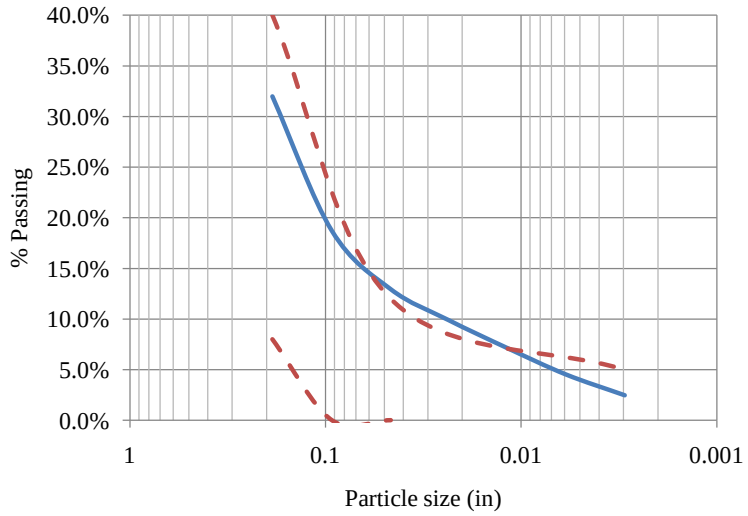

Figure 107: Particle Size Distribution Curve for the Portion Passing the No. 4 Sieve of the OGS Granular Base for I 79 Segment 470 Northbound Slab 5 (Distressed Section).

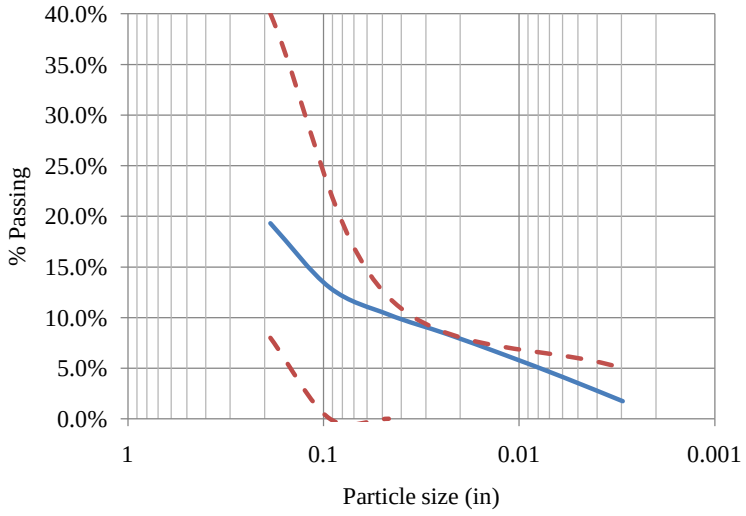

Figure 108: Particle Size Distribution Curve for the Portion Passing the No. 4 Sieve of the OGS Granular Base for I 79 Segment 470 Northbound Slab 51 (Distressed Section).

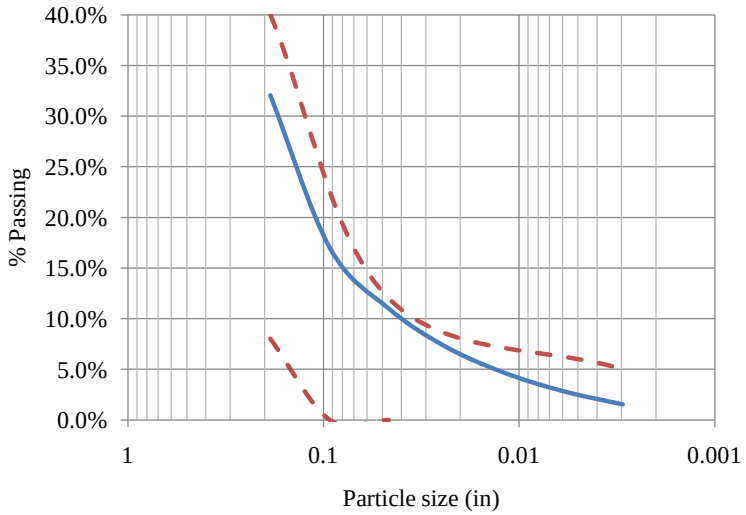

Figure 109: Particle Size Distribution Curve for the Portion Passing the No. 4 Sieve of the OGS Granular Base for I 79 Segment 480 Northbound Slab 9 (Control Section).

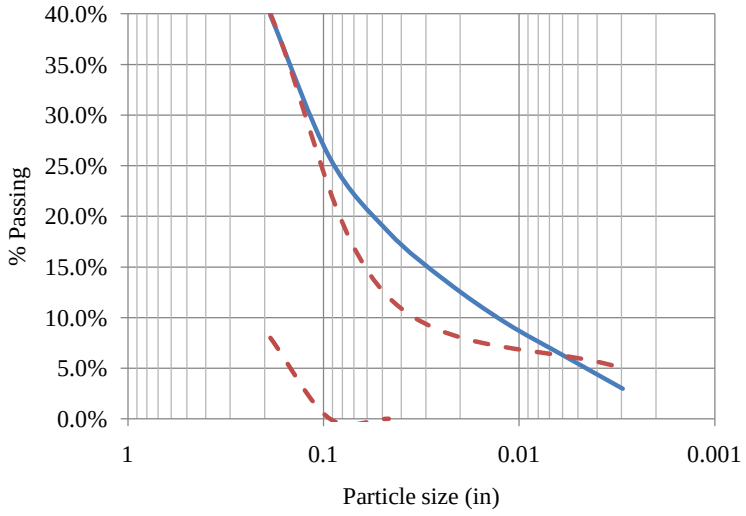

Figure *110*: Particle Size Distribution Curve for the Portion Passing the No. 4 Sieve of the OGS Granular Base for I 79 Segment 4*8*0 Northbound Slab *17* (Control Section).

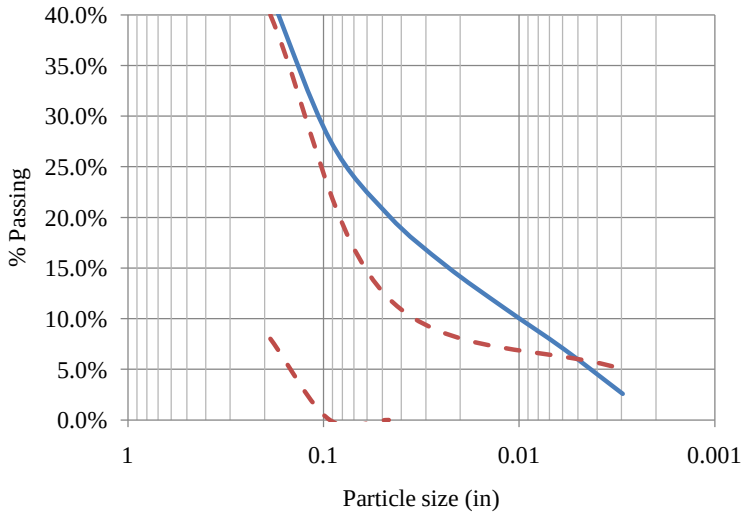

Figure 111: Particle Size Distribution Curve for the Portion Passing the No. 4 Sieve of the OGS Granular Base for I 79 Segment 480 Northbound Slab 33 *(Control Section).*

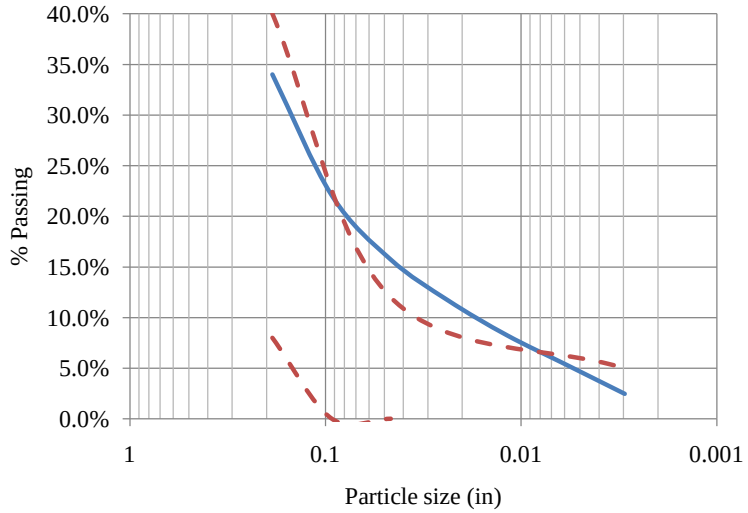

Figure 112: Particle Size Distribution Curve for the Portion Passing the No. 4 Sieve of the OGS Granular Base for I 79 Segment 480 Northbound Slab 50 (Control Section).

5.11 Laboratory Testing Results: I 79

Table 32 presents a summary of the laboratory testing results for I 79. The average values for the Distressed and Control sections are fairly similar, which implies that the influence of the concrete properties on performance could be limited. Considering that the concrete mixture designs were different for both sections although similar material properties were measured for the concrete used in paving the two sections.

Table 32: Summary of Laboratory Test Results for I 79

	Distressed			Control		
	Average	St. Dev	COV	Average	St. Dev	COV
CTE, /°F	5.5E-06	0.4E-06	8%	5.7E-06	0.1E-06	1%
Elastic Modulus, psi	5.20E+06	1.50E+06	3%	5.55E+06	0.2E+06	4%
Poisson's ratio	0.24	0.01	3%	0.22	0.01	6%
Compressive Strength, psi	8000	710	9%	8800	380	4%
Split Tensile Strength, psi	585	75	13%	550	-	-

5.12 Laboratory and Backcalculated Results Analysis: I 79

The average backcalculated static elastic modulus values were smaller than the laboratory-determined values for both the Distressed and Control sections. The FWD backcalculated static elastic modulus values were 10 percent and 4 percent smaller than the laboratory-determined static elastic modulus for the Distressed and Control sections, respectively. This difference is not considered significant because it is smaller than the variation obtained within specimens for the FWD and laboratory testing. Both the backcalculated and laboratory-determined PCC elastic moduli are between typical ranges for mature concrete.

5.13 Potential Causes of Distress: I 79

Considering the pavement performance and the pavement structure and drainage conditions of both the Distressed and Control sections, it is believed that the lack in structural capacity and the poor drainage of the Distressed section are the primary contributors to the premature transverse cracking affecting this section. In order to validate this hypothesis several runs of the MEPDG software were executed using the information previously presented. The analysis of the pavement performance prediction is presented below.

5.14 MEPDG Runs: I 79

MEPDG files representing the actual field conditions were created for both the Distressed and Control sections. In the absence of measured or calculated values, default inputs were used. For I 79, the only differences between the input file used for the Distressed section and the input

file used for the Control section were the measured material properties from the lab, the thicknesses of the PCC layer obtained from the cores, and the subgrade type. All other inputs are the same between the two sections. The following summary discusses the inputs used as well as the results obtained.

5.14.1 *Pavement Structure*

The pavement structure used for the MEPDG runs includes a 12-in PCC slab for the Distressed section and a 13-in slab for the Control section. These thicknesses are based on average core thicknesses obtained in the field. In both the Distressed and Control sections are on top of a 4-in layer of crushed gravel (OGS layer) and a 4-in layer of PennDOT 2-A subbase. The subgrade was characterized as an AASHTO A-4 subgrade for the Distressed section and an A-6 subgrade for the Control section.

PCC Slab

In the MEPDG, PCC slab properties are divided into four groups: general properties, thermal properties, PCC strength, and mixture design. The general properties include the unit weight and Poisson's ratio, which were chosen as 150 pcf and 0.20, respectively. The CTE was adjusted in accordance with the explanation given in Section 2.14.1. The adjusted CTE values to be used as inputs in the MEPDG were 7.0 and 7.2 x 10^{-6} /ºF for the Distressed and Control sections, respectively. For thermal conductivity, 1.25 BTU/hr-ft- ºF was used, and for heat capacity, 0.28 BTU/lb- ºF was used. These are default values.

Another PCC input that was different between the two sections was the 28-day compressive strength. As explained in Section 2.14.1, this property was determined based on the laboratory-determined compressive strengths of cores. The strength of the cores are 8,000 psi and 8,800 psi for the Distressed and Control sections, respectively and the 28-day values adjusted for the use in the MEPDG were 6,500 and 7,700 psi for the Distressed and Control sections, correspondingly. The PCC elastic modulus was also adjusted as explained in Section 2.14.1. The adjusted PCC elastic moduli used as input in the MEPDG were 4.8 and 5.2 x 10^{-6} psi for the Distressed and Control sections, respectively.

The rest of the values used in the mix design were default values or average values based on PennDOT specifications. A complete list of mixture design information can be seen in Table 33.

Table 33: PCC Mixture Design Inputs for I 79.

Input	Distressed	Control
PCC Strength, psi	6,500	7,700
Cement Type	I	I
Cementitious Material Content, lb/cy	588	588
w/c Ratio	0.42	0.42
Aggregate Type	Limestone	
Reversible Shrinkage (% of Ultimate Shrinkage)	50	
Curing Method	Curing Compound	

OGS

A 4-in crushed gravel layer, which represents the OGS, was incorporated into the pavement structure as a base layer. The strength properties of this material were calculated based on a correlation between the layer coefficient of a material and the resilient modulus. The known layer coefficient from PennDOT specifications that was input in to the MEPDG was 0.11. MEPDG, default values provided by the MEPDG software were used for the other required inputs for the OGS layer for both the Distressed and Control sections. Using default values resulted in the use of a Poisson's ratio of 0.35 and a coefficient of lateral pressure, $K_{0,}$ of 0.5. The gradation of the OGS is presented in Table 34 and is based on PennDOT specifications.

Table 34: OGS Gradation for I 79.

Sieve	Minimum %	Maximum %
2 in	100	100
3/4 in	52	100
3/8 in	36	65
No. 4	8	40
No. 16	0	12
No. 200	5	5

2A Subbase Layer

The gradation of the 2A crushed gravel is presented in Table 35. The structural number provided by PennDOT was used with the correlation between structural number and resilient

modulus in the MEPDG to calculate the resilient modulus. Based on this correlation, the value for resilient modulus in the MEPDG was approximately 14,500 psi. All other properties for this material were established using the Level 3 default values provided in the MEPDG software. As with the OGS layer, this includes a Poisson's ratio of .35 and a K_o of 0.5.

Table 35: Summary of Inputs for the 2A Crushed Gravel Layer of I 79

Parameter	Value	
Coefficient of Lateral Pressure, K_0	0.5	
Poisson's Ratio	0.35	
Elastic Modulus, psi	25,000	
Aggregate Gradation	Sieve Size	Passing, %
	1 ½ in	100
	1 in	99
	1/2 in	45
	No. 4	16
	No. 16	11
	No. 200	3

Subgrade Soil

An AASHTO A-4 and A-6 subgrade was used in the input file for the Distressed and Control section, respectively. The Poisson's ratio and the coefficient of lateral pressure were assigned using the same default values as were used for the crushed gravel. The gradation of the subgrade soil is shown in Table 36.

Table 36: Subgrade Soil Gradation for I 79

Sieve	% Passing	
	A-4	A-6
4 in	99.8	
3 ½ in	99.8	100
2 in	99.6	99.8
1 ½ in	99.4	99.5
1 in	98.7	99
3/4 in	98	98.4
1/2 in	96.7	97.4
3/8 in	95.6	96.4
No. 4	93	93.5
No. 10	89.9	90.2
No. 40	82.7	82.4
No. 80	73.9	73.5
No. 200	60.6	63.2

5.14.2 *Climate*

The Pittsburgh weather station, which is located just a few miles away, was used to obtain the climate input file for the MEPDG. A summary of the weather station location can be found in Table 37.

Table 37: Summary of Weather Station Location Information for I 79

Climate Station	Latitude, degree	Longitude, degree	Elevation ft
Pittsburgh, PA	40.3	-80.14	1175

5.14.3 *Pavement Design Features*

Additional aspects of the pavement that need to be categorized in the MEPDG include the diameter and spacing of dowel bars, shoulder type, joint spacing and base/slab friction coefficient. A summary of these design features used in the input file for I 79 can be seen in Table 38.

Table 38: Summary of Pavement Design Feature Inputs for I 79

Input	Value
Effective Joint Spacing, ft	25.06
Sealant Type	Neoprene
Dowel Diameter, in	1.5
Dowel Bar Spacing, in	12
Shoulder Type	Tied PCC Shoulder
Base Type	Granular
Erodibility Index	Very Erodable (5)
PCC-Base Interface	Full Friction Contact
Loss of Full Friction (age in months)	245
Permanent Curl/Warp Effective Temperature Difference, °F	-10

5.14.4 *Traffic Inputs*

Two-way Annual Average Daily Truck Traffic (AADTT)

The following traffic inputs were used and can be seen in Table 39. This AADTT was based on historic traffic data obtained from PennDOT while the rest of the inputs are default values determined considering that this portion of I 79 has a roadway classification of urban interstate.

Table 39: Summary of Traffic Inputs for I 79

Input	Value
Initial Two-Way AADTT	3,500
Number of Lanes in Design Direction	2
Percent Trucks in Design Direction, %	50
Percent Trucks in Design Lane, %	90
Operational Speed, mph	65

Traffic Volume Adjustment Factors

The following factors are necessary to determine the AADTT for each truck class, for each month, on an hourly basis.

- *Load Monthly Adjustment Factors.*

- *Vehicle Class Distribution Factors.*
- *Hourly Truck Traffic Distribution.*
- *Traffic Growth Factors.*
- *Directional Distribution Factors.*
- *Lane Distribution Factors.*

The load monthly adjustment factors, the vehicle class distribution factors, and the hourly truck traffic distribution that were used in this analysis are the default values provided in the MEPDG. These values were used because of the absence of actual data for this project. The traffic growth factor was obtained assuming a 3 percent linear growth rate in the traffic. The percent of trucks in the design direction and design lane are typical values based on the road type.

Axle Load Distribution Factors

The axle load distribution factors represent the percentage of the total axle applications within each load interval, for each vehicle class, and for each specific axle type. Level 3 default values generated from the LTTP database were assigned for all axle types (single, tandem, tridem, and quad) and all vehicle classes (4 to 13). These values were used in the absence of actual data.

General Traffic Inputs

The following information is contained in this category:

- *Mean Wheel Location, Traffic Wander Standard Deviation, and Design Lane Width.*
- *Number of Axle Types Per Truck.*
- *Axle Configuration.*
- *Wheel Base Distribution.*

The values used for these variables are the default values embedded within the MEPDG and were used in the absence of actual data.

5.14.5 *Results*

A summary of the results from the MEPDG runs compared with the field conditions can be seen in Table 40. The prediction of cracking is fairly accurate for both sections, especially for the Control section. On the other hand, the predicted faulting by the MEPDG exhibits a remarkable variation from the measured faulting.

Table 40: Predicted vs. Observed Distress for I 79.

Distress	I 79			
	Distressed Section		Control Section	
	Predicted	Observed	Predicted	Observed
Faulting, in	0.171	0.03	0.157	0.04
Transverse Cracking, %	25	48	1.6	0

Figure 113 presents the MEPDG predicted against the observed transverse cracking. The observed transverse cracking over time (from year 5 to year 14) is based on historic distress data provided by PennDOT, which was collected using automated distress detection equipment. The data point from the pavement management system for year 15 represents the percentage of transverse cracking in the Distressed section that was manually surveyed as part of the field data collection effort for this study. As observed in Figure 113, the historic distress data exhibits some anomalies. Despite the anomalies, it can be concluded that in the Distressed section, transverse cracking began to become visible on the surface of the slabs between years 7 and 10. Additionally, it can be noticed in Figure 113 that from year 14 to year 15, the percentage of cracking varies from 18 to 48 percent. As mentioned previously, this variation can likely be attributed to the inability of the automated equipment to identify cracks. Consequently, and as mentioned in Section 2.14.5, it is possible that the transverse cracking quantified using the automated equipment is being underestimated.

The slope of the predicted transverse cracking trend presented in Figure 113 implies that the fatigue damage the Distressed section is significant. For the Control section, the predicted and observed transverse cracking shown in Table 40 suggest that the Control section has not yet reached the critical zone of fatigue damage. The increase in slab thickness for the Control section was effective in decreasing the fatigue cracking, as predicted using the MEPDG.

The fatigue transverse cracking is function of different factors that affect the magnitude of the bending stress, such as slab thickness, PCC modulus of elasticity, strength and CTE and shrinkage, joint spacing, and subgrade support. However, certain conditions can accelerate the development of this load-related distress. One of these conditions is the prolonged exposure of the pavement unbound layers to excess moisture. This exposure can lead to softening of the pavement layers and subgrade as they become saturated and remain saturated for extended

periods of time. Exposure to moisture can also degrade the quality of the material. As mentioned in Section 5.7.5, several areas exhibiting drainage deficiencies were observed in the Distressed section. This condition explains the difference between the predicted and observed transverse cracking for year 15. Additionally, it is noteworthy that the MEPDG software does not consider such drainage deficiencies in its analysis and this consideration can also explain the difference between predicted and observed performance.

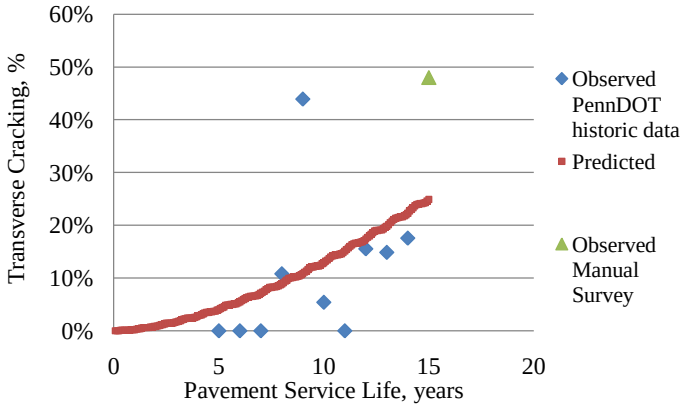

Figure 113: Predicted and Observed Transverse Cracking for I 79 Segment 470 (Distressed section)

Figure 114 presents the predicted and observed faulting for both the Distressed and Control sections of I 79. The observed faulting corresponds to the data measured as part of the field data collection for the present study. Historic data for faulting was not available from PennDOT. As is evident in Figure 114, there is a large difference between the predicted and observed faulting in both the Distressed and Control sections. As discussed in Section 2.14.5, the high predicted faulting is principally caused by a high upward corner deflection calculated by the MEPDG.

Figure 114: Predicted vs. Observed Joint Faulting for I 79 Segments 470 and 480 (Distressed and Control Sections)

By comparing the predicted and observed performance of both the Distressed and Control sections, it can be concluded that the relatively lower structural capacity of the pavement resulting from the decrease in slab thickness by an inch and the poor drainage conditions of the Distressed section are the major contributors to the premature distresses exhibited by the pavement.

5.15 Rehabilitation Recommendations: I 79

Between conducting the pavement distress survey and the release of this report, there have been some rehabilitation activities on I-79. It was noticed during a subsequent visit to the project location in August 2010 that an asphalt overlay was in the process of being placed over the Distressed section. It also appeared that there was some pre-overlay repair performed prior to constructing the overlay.

5.15.1 *Distresses and Deficiencies*

As mentioned previously, the major distress in the Distressed sections for I-79 is transverse cracking. In addition to transverse cracking, there are also load transfer deficiencies and subbase support issues. While the support issues are present in both the Distressed and Control sections, the extent of the distress is greater in the Distressed section. In the case of I-79, the extent of the deficiencies has a considerable influence on the recommendations for each section and therefore the recommended rehabilitation options will be discussed in two separate sections. Although the

observation of the various distresses and deficiencies are based on data obtained from Segment 470 (Distressed) and Segment 480 (Control), other segments that were part of the original analysis section and that exhibit similar distress patterns should also be considered for these rehabilitation measures.

Recommendations for Segment 470 (Distressed Section)

In the case of the Distressed section, it appears that the drainage issues might have been localized to this segment because of the role that the unique topographical conditions in this area played preventing the water from draining away from the pavement. It is suggested that a video inspection be performed on the drainage systems and that all damaged sections be removed and replaced. It is also suggested that all clogged regions identified during the inspection be flushed clean. Although a distress survey was not performed for any of the adjacent segments in the originally considered section, the fact that only Segment 470 was overlaid with asphalt seems to anecdotally suggest that this segment was in relatively poor condition when compared to the adjacent segments.

Prior to the placement of the overlay, full-depth repairs should be performed on all medium and high severity transverse cracks. Load transfer restoration should also be performed at the joints exhibiting low load transfer. Full-depth repairs could be performed in lieu of load transfer restoration and slab stabilization at the joints indicating the presence of a void. It is also recommended that the drainage of the ditch between the hillside and the pavement for Segment 470 be improved. Care should be taken to ensure positive drainage in the longitudinal direction and subsequent proper maintenance of the ditch should be performed. In addition, a camera inspection of the existing drainage system should be performed to ensure that it is functioning properly. Ensuring proper drainage away from the Distressed area without ensuring proper subsurface drainage will likely not ameliorate the existing problem significantly.

Recommendations for Segment 480 (Control Section)

As mentioned in the FWD analysis section, the only deficiency noticed in the Control section was the presence of voids beneath the slabs. As discussed previously, these voids could be the result of settlement or migration of the subbase or subgrade into the OGS layer. The LTE at the joints is still quite high so pumping is not providing a substantial contribution to the loss of support. Although the voids have not yet resulted in increased fatigue damage to the point where mid-slab cracking has developed, there exists the potential for these issues to arise. Slab

stabilization could be performed to prevent problems from developing in the future. This should be accompanied by video camera inspection of the drainage system before and after execution to ensure that existing drainage is functional and that it is still functioning after the slabs are stabilized. At this point, the pavement section is performing well and will exceed its expected design life.

5.16 Future Projects: I 79

The drainage conditions of the Distressed section seem to have significantly influenced the manifestation of distress in Segment 470 and therefore highlights the need to ensure positive drainage in the design process and to insure proper maintenance of the drainage system. The use of a stabilized base would help to mitigate some of the drainage issues encountered. Current design policy will help to reduce the potential of this occurring in the future. The Control section does show that an OGS base can be used successfully if drainage is properly accounted for and sufficient slab thickness is provided.

6 I 80, Clinton County

6.1 Project Information: I 80

For I 80, the selected site is a section located in Clinton County. Clinton County falls under the jurisdiction of PennDOT District No. 2. Portions of Segment 1914 and Segment 1920 were selected to represent the Distressed section and Segment 1930 was chosen to represent the Control section. Once these segments were chosen as the Distressed and Control sections, a 1000-ft long representative section within each segment was chosen based on the pavement condition and the ease of executing traffic control. The location of these Segments with respect to the surrounding area can be seen as the green highlight in Figure 115 and Figure 116.

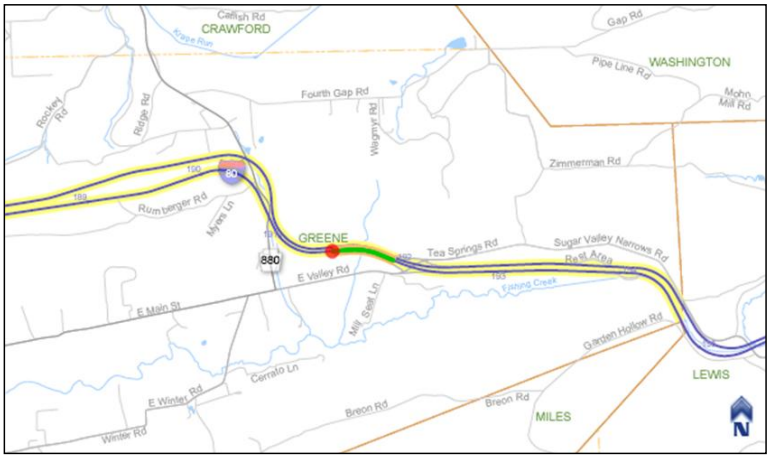

Figure 115: Location of I 80 Segments 1914 and 1920 Eastbound in District 2.

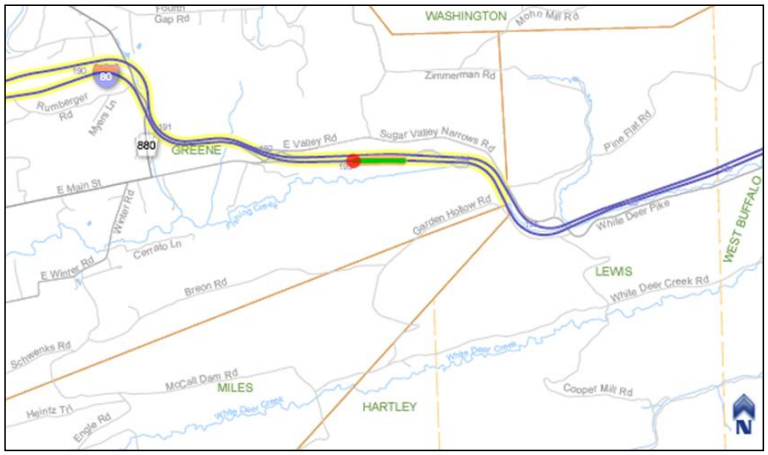

Figure 116: Location of I 80 Segment 1930 Eastbound in District 2.

6.2 Design Information: I 80

The selected segments, Segments 1914, 1920, and 1930 are all in the eastbound direction. All of these segments were originally constructed in 1992. The design information provided by the District shows that the 12-in JPCP was constructed over an existing 10-in PCC pavement that was on top of a 6-in OGS base. Prior to the construction of the 12-in pavement, the 10-in pavement was rubblized and a 6-in OGS layer was placed on top of the rubblized pavement. Therefore, the existing structure consists of a 12-in JPCP pavement over a 10-in rubblized base with a 6-in OGS layer below both the existing pavement and the rubblized pavement. Each lane of the existing pavement is 12-ft wide. The transverse joints are skewed 1:6 counterclockwise and spaced at 20-ft intervals. The design information also indicates 1-in diameter dowels are present at 12-in on center. The sealant type for the joints is preformed neoprene. Longitudinal edge drains are also present. The inside and outside shoulders are 4-ft and 10-ft wide tied PCC shoulders, respectively. A cross section of the existing Distressed and Control sections can be seen in Figure 117 and Figure 118 while an overall view of these sections are shown in Figure 119 and Figure 120 respectively.

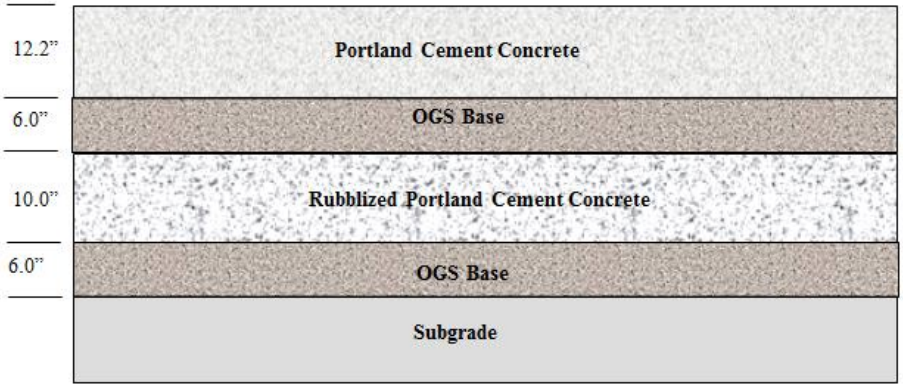

Figure 117: Existing Pavement Cross Section of I-80 Segment 1914 and 1920 Eastbound (Distressed Section)

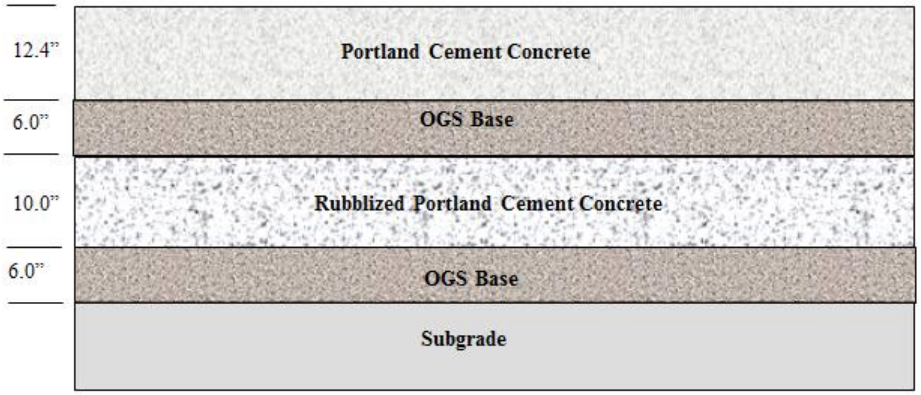

Figure 118: Existing Pavement Cross Section of I-80 Segment 1930 Eastbound (Control Section)

Figure 119: Overall Condition of I 80 Segment 1914 (Portion of Distressed Section)

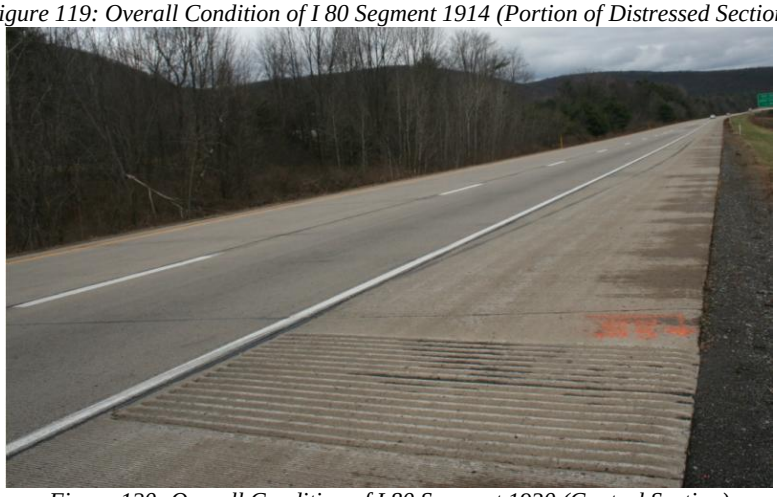

Figure 120: Overall Condition of I 80 Segment 1930 (Control Section)

6.3 Concrete Mixture Design: I 80

For I 80, there is no available information regarding the concrete mixture design for the existing pavement. Despite this limitation, some conclusions can still be drawn based on the visual examination of the retrieved cores. It seems that the concrete mixture design used for both the Distressed and Control sections was the same. Observations that led to this conclusion include the common coarse aggregate type and size, aggregate distribution, and the cement paste

color between the Distressed and Control section. Figure 121 presents mid-slab cores retrieved from both the Distressed and Control sections. Additionally, as will be presented in Section 6.11 and Section 6.8, the difference in the measured concrete properties was relatively low. These properties include the average backcalculated and laboratory determined static elastic modulus as well as the laboratory determined compressive strength, Poisson's ratio, coefficient of thermal expansion (CTE), and split tensile strength.

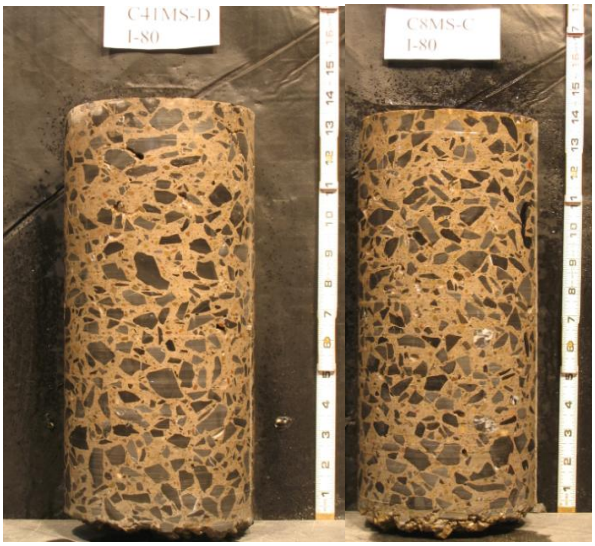

Figure 121: Mid-slab Cores from Distressed and Control Sections of I 80.

6.4 Climatic Conditions: I 80

I-80 is located in a wet freeze climate with a relatively high number of wet days per year. The representative GPS coordinates of the section are 41.04° latitude and 77.31° longitude. The three closest climate stations are: Williamsport, which is 33.2 miles away; Selinsgrove, which is 38 miles away; and Clearfield, which is 46.9 miles away. These three weather stations were all used to create the virtual weather station for the desired location based on interpolation. According to the created weather station, the area experiences approximately 170 wet days per year and a mean annual rainfall of 41 in. The freezing index is 494 ºF days and the area is exposed to approximately 79 freeze-thaw cycles per year. The mean annual air temperature is 51 ºF with minimum and maximum average monthly temperatures of 32 ºF and 86 ºF, respectively.

6.5 Traffic Loadings: I 80

Traffic data for this site was found using PennDOT's ITMS and it was found that each segment has the same traffic volume and truck percentage. As of 2009, the one-way AADT is approximately 12,000. The percentage of trucks is 35 percent. Based on these numbers, the pavement has approximately seen 12 million ESALs over its life thus far.

6.6 Selection of Distress Survey Section: I 80

Candidate segments were selected in the office based on historic distress data provided by PennDOT, a PennDOT video log analysis and the ease with which traffic control could be executed at the Segment. Based on these criteria, Segments 1914 and 1920 were selected to represent the Distressed section and Segment 1930 was chosen to represent the Control section. The Distressed section was split between two segments because the beginning of Segment 1914 contained an exit ramp and the whole segment could not be used.

6.7 Pavement Condition: I 80

To assess the pavement condition, a distress survey was conducted over a 50-slab section in the driving lane. The distress survey was performed according to the Distress Identification Manual for the LTPP [1]. A summary of the distress measurements is presented in Table 41. Both the Distressed and Control sections exhibit transverse cracking and transverse joint spalling with the difference between the sections being the prevalence of these distresses. The Distressed section exhibits some type of transverse cracking in 98 percent of the slabs, longitudinal cracking and transverse joint spalling. Despite these distresses, both sections have high PSR values with the PSR for the Distressed section being only lightly lower. This observational paradox is due to the fact that the majority of the transverse cracking and spalling was of low severity and had not resulted in faulting. The joint faulting was also low for both sections.

Table 41: Summary of Performance Data for I 80.

Performance Measurement	Segment 1914 & 1920 (Distressed Section)	Segment 1930 (Control Section)
Joint Edge Faulting, in	0.02	0.02
Joint Wheelpath Faulting, in	0.02	0.02
Crack Edge Faulting, in	0.02	0.03
Crack Wheelpath Faulting, in	0.03	0.03
Transverse Cracking (Medium Severity), % Slabs	20	6
Transverse Cracking (Low Severity), % Slabs	78	46
Longitudinal Cracking (Low Severity), % Slabs	42	0
Transverse Joint Spalling, % Joints	20	6
Cracked PCC Shoulder, % Slabs	10	24
Microcracking, % Slabs	96	88
Lane-to-Shoulder Drop-off, in	0.17	0.18
Joint Width, in	0.7	0.7
PSR	3.3	3.7

6.7.1 Transverse Joint Faulting

Both the Distressed and Control sections contain 1-in diameter dowel bars. Coincidentally, the average faulting in the Distressed and Control sections are the same, with 0.02-in for joints and 0.03-in for cracks. This is low considering that typical values of allowable JPCP mean faulting are between 0.1-in and 0.2-in.

6.7.2 Lane-to-Shoulder Dropoff

As observed in Table 41, the shoulder drop-off is slightly higher in the Control section compared to the Distressed section. The maximum and minimum values for the Distressed section are 0.34-in and 0.02-in. These values for the Control section are 0.45-in and 0-in. These values are not considered high in terms of severity.

6.7.3 Joint Width

The joint width, as seen in Table 41, is the same for both the Distressed and Control sections. This was not surprising considering that the factors affecting the joint width (i.e. joint spacing, CTE, and base type) are the same for both sections.

6.7.4 Transverse Cracking

Based on the manual distress survey executed as part of this study, 98 percent of the slabs in the Distressed section and 52 percent in the Control section have transverse cracks. However, based on the retrieved cores at crack locations, there are both full-depth transverse cracks as well as cracks with an average depth of less than 1-in. This condition possibly suggests a symbiosis of fatigue-related and material-related distresses in both sections. Upon further inspection, it was determined that only 20 percent of the slabs in the Distressed section exhibited medium severity cracks whereas 78 percent exhibited low severity cracks. According to the retrieved cores, the medium severity cracks are full-depth whereas the low severity cracks have developed only in the upper portion of the slabs. While the full depth crack was ultimately caused by fatigue, it is likely that the prolific low severity cracks extending only slightly into the core are due to material or construction deficiencies.

A re-examination of the cores from the Control section in the same manner revealed that only 6 percent of the slabs in the Control section have cracks that extend through the depth of the pavement and 46 percent of the slabs exhibit low severity transverse cracks. Although the cracks with shallow depth in both sections could be the start of purely fatigue related cracks, carbonation depth analysis presented in Section 6.13 suggests that these cracks have existed for quite some time. It is also unlikely that 78 percent of the slabs in the Distressed section and 26 percent of the slabs in the Control section would simultaneously be exhibiting an early stage fatigue crack. The unlikeliness of the low severity cracks being purely the result of fatigue is based on the assumption that the fatigue cracks do not take a significant time period to develop through the depth of the slab. Additionally, almost half of these low severity transverse cracks (i.e. 22% of the total slabs) do not traverse the slab from joint to joint. They cross only a portion of the slab which in most of the cases is from the longitudinal joint between the driving and passing lane to about the mid-section of the slab.

According to historic distress data provided by PennDOT, the transverse cracking began to be visible on the surface between the 11^{th} and 12^{th} years of the pavement's service life for both

the Distressed and Control sections. Figure 122 shows a slab with a low severity transverse crack and Figure 123 shows a medium severity transverse crack.

Figure 122: Low Severity Transverse Crack of I 80 Segment 1914 Eastbound (Distressed Section)

Figure 123: Medium Severity Transverse Crack of I 80 Segment 1914 Eastbound (Distressed Section)

6.7.5 Longitudinal Cracking

Low severity longitudinal cracking is present in 42 percent of the slabs in the Distressed section. There is no longitudinal cracking in the Control section Figure 124 shows a longitudinal crack in the Distressed section.

Figure 124: Longitudinal Crack of I 80 Segment 1914 Eastbound (Distressed Section)

6.7.6 Material-Related Cracking

Two different types of material-related cracks were encountered along the Distressed and Control sections. The most common type, present in 96 percent of the slabs in the Distressed section and in 88 percent in the Control section, is map-cracking located in an area between the outer longitudinal joint and the wheel path as seen in Figure 125. The other type of material-related cracking is the low severity transverse and longitudinal cracks, which were found in both sections but more extensively in the Distressed section. In the Distressed section, 78 percent of the slabs contain this type of cracking while it can be found that only 46 percent of the slabs in the Control section contain this cracking.

Figure 125: Digitally Enhanced Map-cracking of I 80 Segment 1914 Eastbound (Distressed Section)

6.7.7 Present Serviceability Rating (PSR)

The average PSR of the Distressed section was 3.3, which is slightly lower than the 3.7 PSR of the Control section. The reason the PSRs are relatively similar and relatively high is because both sections exhibit minimal faulting and the majority of the transverse cracks are low severity.

6.8 FWD Testing: I 80

The FWD testing pattern used for the Distressed segments of I 80 included five mid-slab locations, nine transverse joints (approach and leave sides), seven transverse cracks (approach and leave sides), and seven edges. For the Control section, five mid-slab locations, ten transverse joints (approach and leave sides), nine transverse cracks (approach and leave sides)), and seven edges were tested. FWD testing was used to determine the PCC static elastic modulus, modulus of subgrade reaction (k-value), differential deflections, load transfer efficiencies across joints and cracks and loss of support. A summary of these results can be found in Table 42.

Table 42: Summary of Deflection Testing Results for I 80

Property	Segment 1914 and 1920 (Distressed Section)	Segment 1930 (Control Section)
Static Elastic Modulus, psi	4.45E+06	6.15E+06
Static k-value, psi/in	330	380
Joint Load Transfer, %	86	80
Crack Load Transfer, %	74	66
Average Mid-slab Deflection, mils	1.39	1.15
Corners with Voids, %	89	70
Maximum Air Temperature During Testing, °F	37	40

6.8.1 Temperature Gradients

As with the other projects, temperature gradients during FWD testing were made in accordance with LTPP guidelines [9]. For I 80, the temperature gradients were only measured in one section, the Distressed section, during FWD testing. However, surface temperature measurements were made throughout the FWD testing regime. The maximum surface temperature measurement taken during FWD testing in the Control section was 43 ^{o}F. This is close to the surface temperatures encountered during FWD testing in the Distressed section as shown in Figure 126. Based on the proximity of the surface temperatures during FWD testing in the Control section to that in the Distressed section, it can be concluded that the temperature gradients also did not vary significantly between sections. The maximum temperature gradient shown in Figure 126 is 0.25^{o}F/in which is not significant with respect to the interpretation of FWD results.

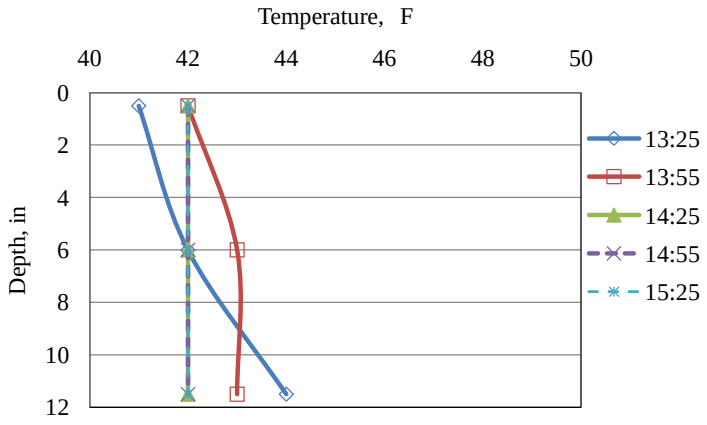

Figure 126: Temperature Gradients during FWD Testing for I 80 Segment 1914 and 1920 Eastbound (Distressed Section)

6.8.2 PCC Elastic Modulus

The static elastic modulus of the PCC slab was backcalculated using mid-slab deflection measurements along with the actual thickness of the slab determined from the cores extracted at FWD locations. In using FWD data to determine the static elastic modulus and modulus of subgrade reaction, only data from the mid-slab location of non-cracked slabs is supposed to be used. This requirement presented an issue in the Distressed section because 100 percent of the slabs in the Distressed section were cracked. Despite this problem, mid-slab testing was performed on slabs towards the end of the segment that exhibited cracks that were extremely tight (no measurable crack width) under the assumption that they did not extend throughout the depth of the slab. This was later confirmed through the visual examination of cores from these locations. Figure 127 and Figure 128 show the PCC elastic modulus for the Distressed and Control sections, respectively.

The average static elastic modulus for the Distressed section is 4.45 million psi with a coefficient of variation of 13 percent. Even though there is some variability among the backcalculated values, these values only represent conditions within 180 ft due to the aforementioned limitation. The average static elastic modulus for the Control section is 6.15 million psi with a coefficient of variation of 17 percent. In the Control section, the values of the static elastic modulus increase along the section. It is also interesting to note that the average backcalculated elastic modulus of the Control section is 38 percent higher than the Distressed

section. Despite the observation from the FWD data of a higher elastic modulus in the Control section, this is not supported by the laboratory-determined values. It is believed that the variation of the structure along the Control section creates the differences in FWD deflections. This variation might not be properly explained by the backcalculation method due to the complexity of the pavement structure for this particular project.

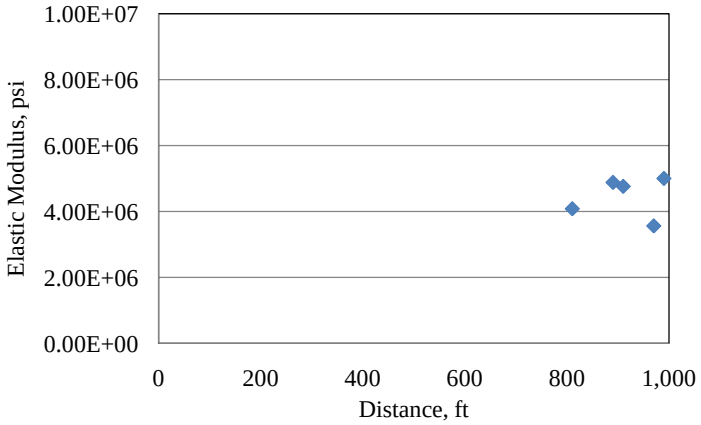

Figure 127: PCC Elastic Modulus for I 80 Segment 1920 Eastbound (Distressed Section)

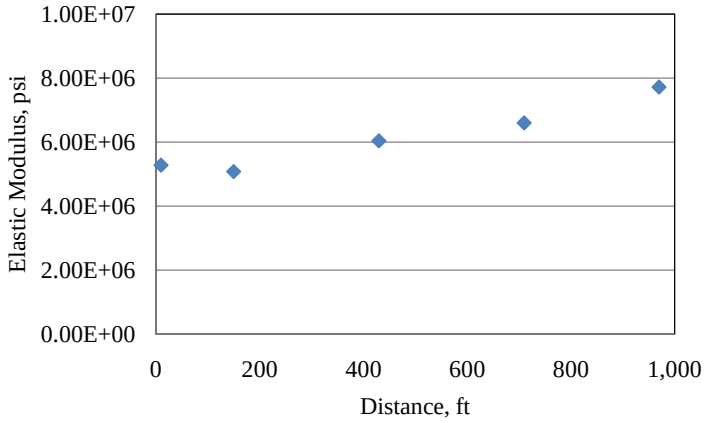

Figure 128: PCC Elastic Modulus for I 80 Segment 1930 Eastbound (Control Section)

6.8.3 Modulus of Subgrade Reaction

Deflections at mid-slab were used to determine the modulus of subgrade reaction. As with measuring the static elastic modulus of the PCC in the Distressed section, the k-value was only measured at the end of the section due to the amount and severity of the cracking in the rest of the section. Figure 129 and Figure 130 show the k-value along the Distressed and Control sections, respectively.

The average static k-value for the Distressed section is 330 psi/in with a coefficient of variation of 9 percent. These values only represent conditions within 180 ft and in Segment 1920, the k-value of the rest of the section is unknown. The average static k-value for the Control section is 380 psi/in with a coefficient of variation of 38 percent. Additionally, as seen in Figure 130, the k-values for the Control section decrease considerably in the second half. As mentioned before, it is believed that the structure of the pavement, specifically the support conditions, varies along the Control section. This condition can be responsible for the remarkably difference in the k-values between the halves of the section.

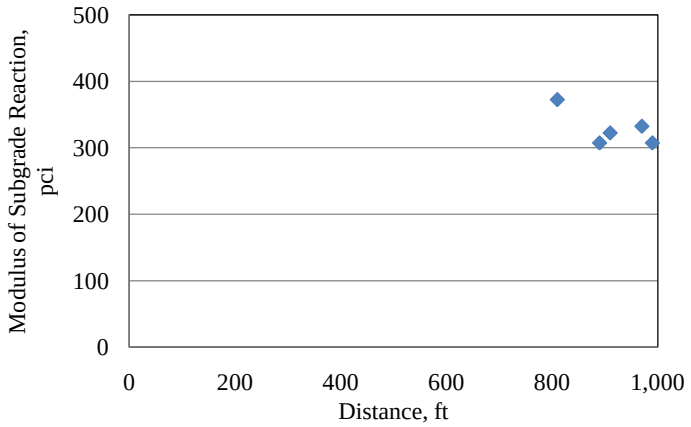

Figure 129: Modulus of Subgrade Reaction for I 80 Segment 1920 Eastbound (Distressed Section)

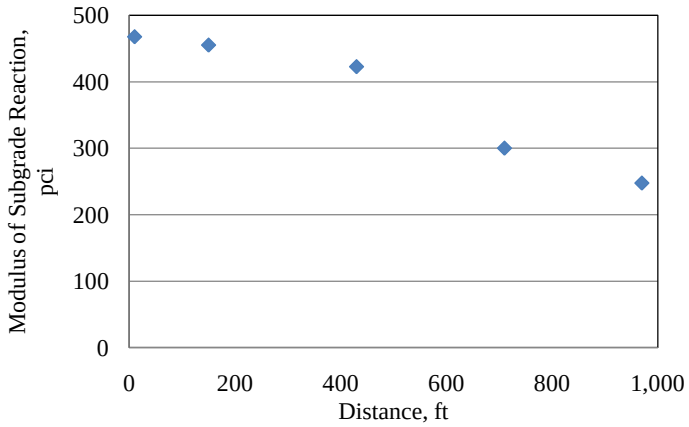

Figure 130: Modulus of Subgrade Reaction for I 80 Segment 1930 Eastbound (Control Section)

6.8.4 Joint Load Transfer

The joint load transfer efficiency for the Distressed and Control sections of I80 are presented in Figure 131 and Figure 132 respectively. The average joint load transfer efficiencies for the Distressed and Control sections are 79 and 71 percent, respectively. In the case of the Control section it can be observed in the existence of two different levels of LTE. The first 200 ft of the section exhibits LTE values greater or equal than 80 percent, whereas in the rest of the section, the LTE is close to 70 percent and even lower at some locations. This condition may be caused by the possible variation of pavement structure along the section as mentioned above. These values are quite high for an interstate roadway approaching 20 years old with only 1-in diameter dowels.

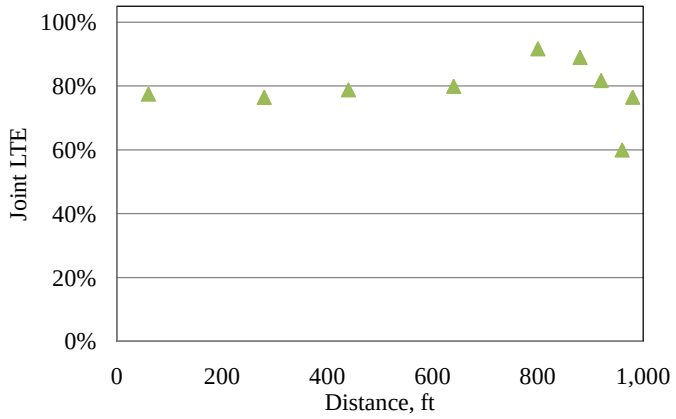

Figure 131: Transverse Joint Load Transfer Efficiencies for I 80 Segments 1914 and 1920 Eastbound (Distressed Section)

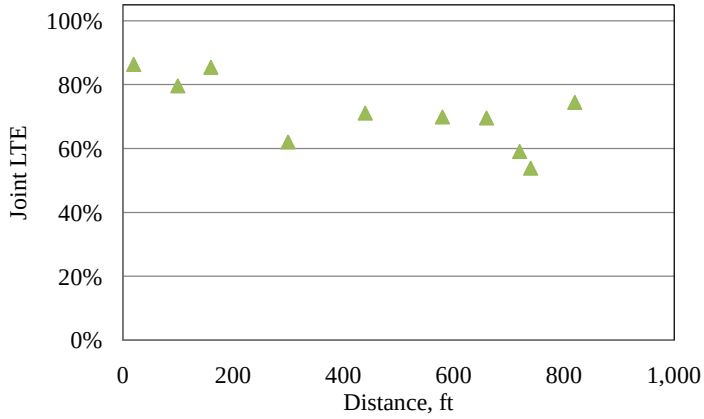

Figure 132: Transverse Joint Load Transfer Efficiencies for I 80 Segment 1930 Eastbound (Control Section)

Differential deflections are the difference between the deflections on the loaded side of the joint to the deflection on the unloaded side of the joint. Differential deflections that are greater than 0.01 in indicate that there is a problem with load transfer at that location. None of the locations tested in any of the segments had differential deflections greater than this threshold value. This agrees with the good LTE values measured for both sections. The differential deflections for joints are presented in Figure 133 and Figure 134 for the Distressed and Control

sections respectively.

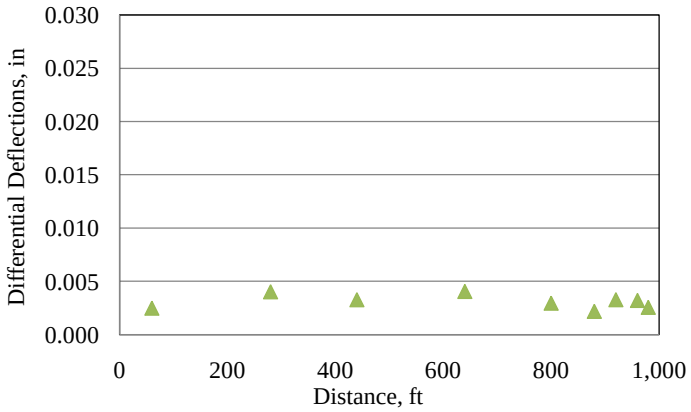

Figure 133: Differential Deflections at Transverse Joints for I 80 Segments 1914 and 1920 Eastbound (Distressed Section)

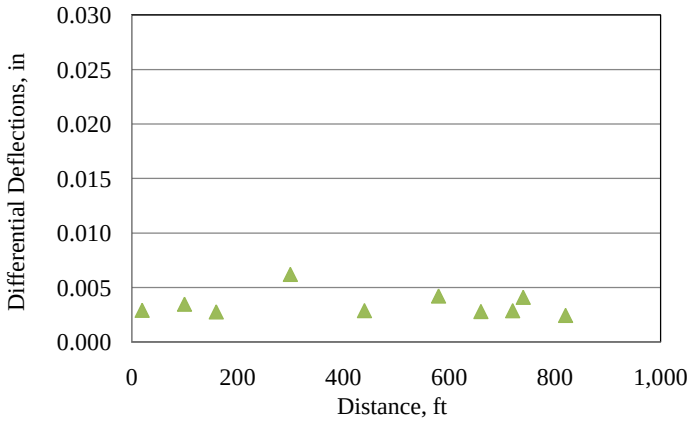

Figure 134: Differential Deflections at Transverse Joints for I 80 Segment 1930 Eastbound (Control Section)

6.8.5 Crack Load Transfer

The crack load transfer efficiencies for the Distressed and Control sections of I 80 are shown in Figure 135 and Figure 136, respectively. The average crack load transfer efficiencies at the approach and leave sides of the cracks for the Distressed and section are 75 and 74 percent, respectively. As can be observed in Figure 135, there are three locations along the Distressed section for which the load transfer efficiency is significantly lower than the rest of the section.

The average LTE for only these three locations is only 11 percent while the average crack LTE for the other cracks is 100 percent. All three of the underperforming test locations are at cracks of medium-severity. Additionally, all three of those panels have longitudinal cracks. The rest of the locations have very high load transfer efficiencies with cracks that are of low-severity and crack widths that are too small to be measured.

In the Control section, the same trend can be observed considering the performance of low and medium severity cracks. Much like the Distressed section, the average LTE of the medium severity cracks in the Control section, 21 percent, is much lower than the average LTE for the low severity cracks, 94 percent.

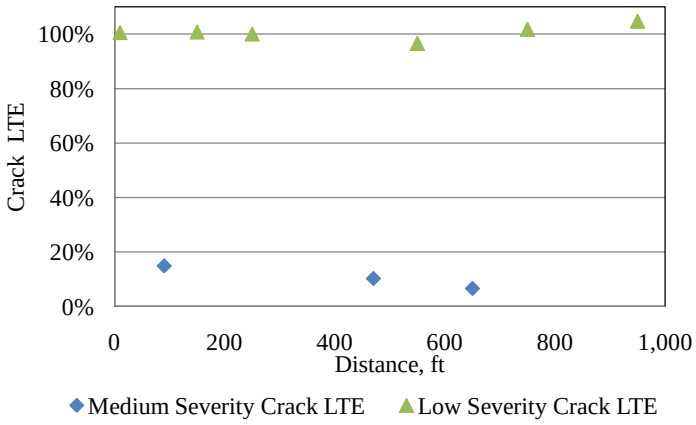

Figure 135: Transverse Crack Load Transfer Efficiencies of I 80 Segments 1914 and 1920 Eastbound (Distressed Section)

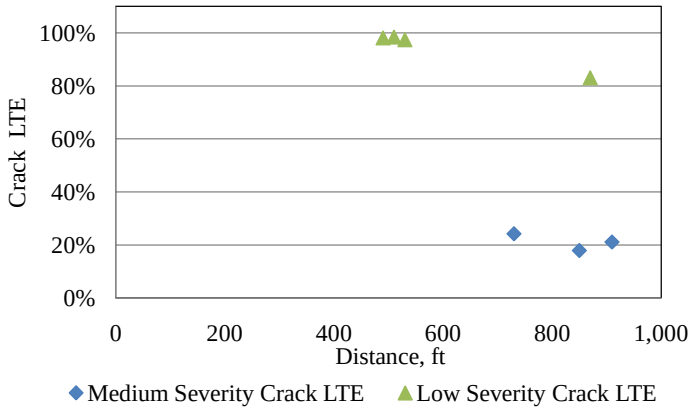

Figure 136: Transverse Crack Load Transfer Efficiencies of I 80 Segment 1930 eastbound (Control Section)

The differential deflections for transverse cracks are presented in Figure 137 and Figure 138 for the Distressed and Control sections respectively. In the Distressed section, the locations where the differential deflections are greater than 0.01-in are the same locations that have poor load transfer efficiency and medium severity cracks. The same is true for the Control section. These results agree with the load transfer efficiency values.

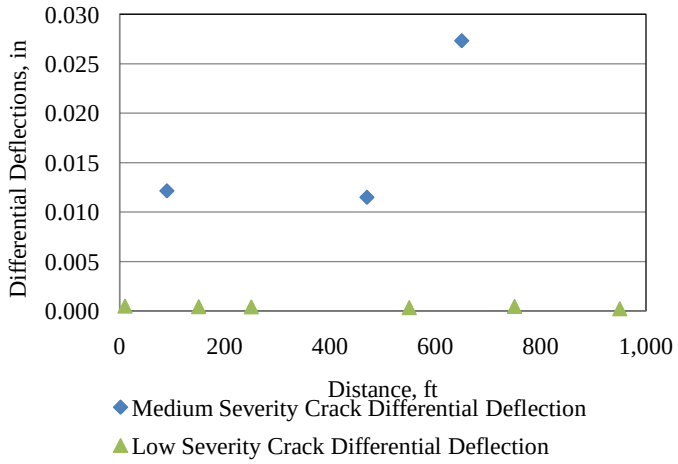

Figure 137: Differential Deflections at Cracks for I 80 Segments 1914 and 1920 Eastbound

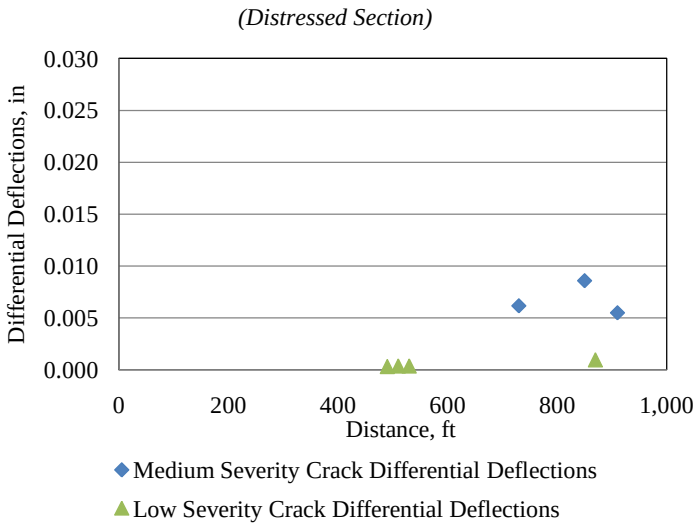

Figure 138: Differential Deflections at Cracks for I 80 Segment 1930 Eastbound (Control Section)

6.8.6 Loss of Support

To determine the presence of voids, the load vs. deflection response for each station was determined. As mentioned previously and explained in detail in Section 2.8.6, when the load vs. deflection relationship is plotted for the standard load levels and the deflection intercept value is greater than two mils, then the potential exists for the presence of voids beneath the slab. The load vs. deflection graphs for I 80 is presented in Figure 139 and Figure 140. These figures are for the Distressed and Control sections respectively. The Distressed section, shown in Figure 139, shows the potential for voids at eight joints and three medium severity cracks. The Control section, shown in Figure 140, shows the potential for voids at eight joints and two medium severity cracks. One contradiction to the generally observed trend for the Control section is that there is one crack of medium severity that does not show the potential for voids. Concerning this particular crack, the potential for voids, although not above the threshold value, is still higher than all of the low severity cracks. The loss of support for the cracks in both sections agrees with the load transfer efficiencies calculated above. Considering that the base is unstabilized, there is a potential for pumping. Despite the unstabilized base and the measured voids underneath the slab determined through FWD testing, no evidence of pumping was observed in the field. The

presence of voids at joints and crack locations is believed to be caused by consolidation of the OGS over time.

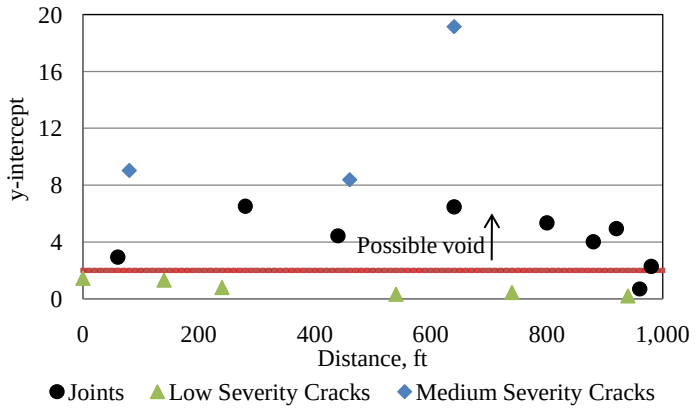

Figure 139: Loss of Support Results for I 80 Segments 1914 and 1920 Eastbound (Distressed Section)

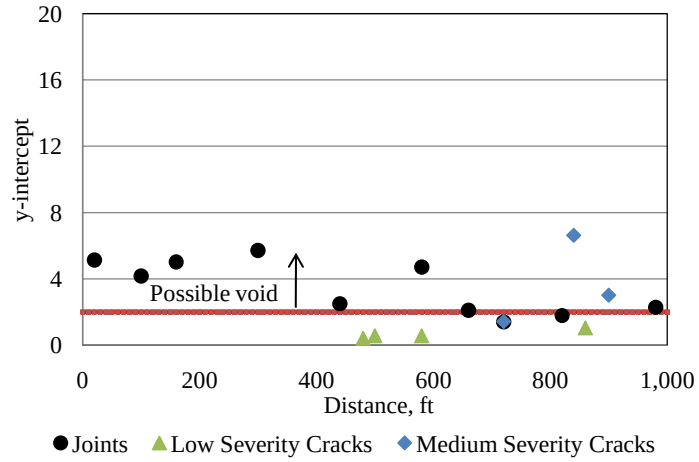

Figure 140: Loss of Support Results for I 80 Segment 1930 Eastbound (Control Section)

6.9 Core Samples: I 80

For I 80, ten cores were pulled from the Distressed section and eight were pulled from the Control section. Table 43 presents a summary of the cores pulled from each section. In the

Distressed section, five cores were pulled from mid-slab locations, two from transverse cracks, two from transverse joints, and one from a panel that exhibited a large amount of micro-cracking. In the Control section, six cores were pulled from mid-slab locations and two were pulled from transverse joints. The average length of the cores from the Distressed section was 12.2-in and the average length of the cores from the Control section was 12.4-in.

Table 43: Summary of Cores for I 80 Segments 1914 and 1920 Eastbound (Distressed Section)

Core	Location	PCC Thickness (in)	Base Type	No. of Pieces	Embedded Items
C5C-D	Transverse Crack	12	Granular	3	No
C13C-D	Transverse Crack	11.75	Granular	1	No
C22J-D	Joint	12	Granular	4	No
C25MC-D	Microcrack	12	Granular	1	No
C33J-D	Joint	12.5	Granular	3	No
C41MS-D	Mid-slab	12.25	Granular	1	No
C45MS-D	Mid-slab	12.5	Granular	1	No
C46MS-D	Mid-slab	12.25	Granular	1	No
C49MS-D	Mid-slab	12.5	Granular	1	No
C50MS-D	Mid-slab	12.5	Granular	1	No

Table 44: Summary of Cores for I 80 Segment 1930 Eastbound (Control Section)

Core	Location	PCC Thickness (in)	Base Type	No. of Pieces	Embedded Items
C1MS-C	Mid-slab	12.5	Granular	1	No
C8MS-C	Mid-slab	12.5	Granular	1	No
C22MS-C	Mid-slab	12	Granular	1	No
C25MS-C	Mid-slab	12.5	Granular	1	No
C33J-C	Joint	12.5	Granular	4	Dowel Bar Cavity
C36MS-C	Mid-slab	12	Granular	1	No
C41J-C	Joint	12.75	Granular	2	No
C49MS-C	Mid-slab	12.5	Granular	1	No

From the visual observation of the retrieved cores, it is important to highlight the following:

- Excessive entrapped air, as well as honeycombing, was found in the majority of the specimens for the Distressed and Control sections.
- The entrained air system for all of the cores, in both sections, appears to be well distributed throughout the depth of the specimens.
- Microcracks were observed on the surface of most of the specimens for both the Distressed and Control sections. One remarkable difference between the two sections concerning the cracks however is that there is a significant difference in the depth of the microcracks between the sections. The average depth of the microcracks in the Distressed section was 0.8-in ranging from 0.4-in to 1.5-in; while the cracks in the Control section are only visible on the pavement surface but not visible on the sides of the cores.
- The observed microcrack path was through the paste as well as through the interfacial transition zone (ITZ) between cement paste and aggregate. Only a few of microcracks went through coarse aggregate particles.
- The color of the paste for both sections was found to be constant throughout the depth of all of the specimens.
- No segregation was observed in any of the specimens and the aggregate appears to be well graded for all of the cores.

6.10 Base Samples: I 80

A granular base sample was obtained for the Distressed section from Slab 33. For the Control section a granular base sample was obtained from Slab 8. A sieve analysis using the portion of each sample passing the No. 4 sieve was performed. Figure 141 and Figure 142 present the gradation curve for each sample. As observed in the figures, the gradation of the samples agrees well with the specification and the percentage of fines (material finer than 3 mils) is within the range specified by Section 703 of PennDOT Specification 408 which calls for a maximum fines quantity of 5 percent

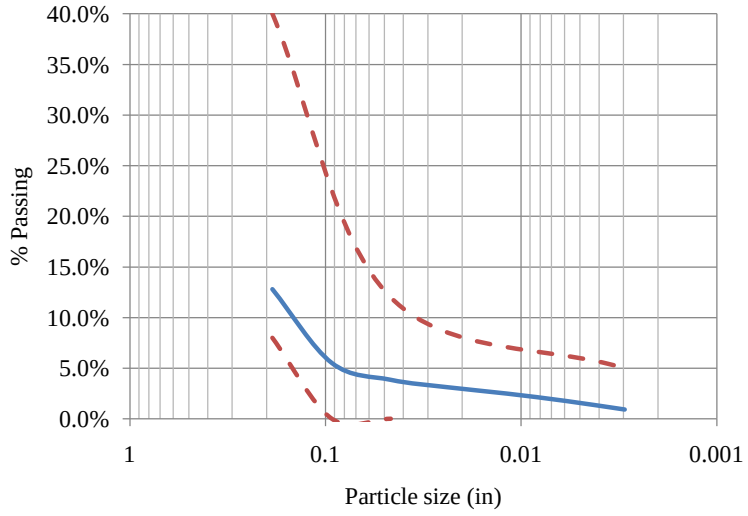

Figure 141: Particle Size Distribution Curve for the Portion Passing the No. 4 Sieve of the OGS Granular Base for I 80 Segment 1914 Eastbound Slab 33 (Distressed Section)

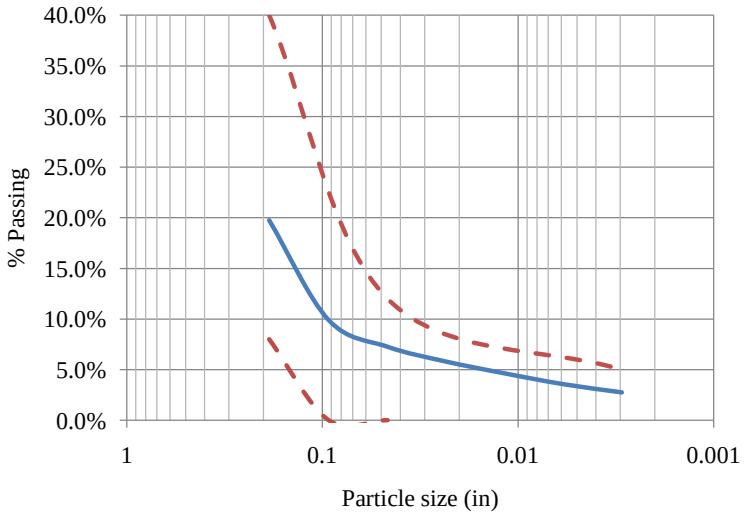

Figure 142: Particle Size Distribution Curve for the Portion Passing the No. 4 Sieve of the OGS Granular Base for I 80 Segment 1930 Eastbound Slab 8 (Control Section)

6.11 Laboratory Testing Results: I 80

Table 45 presents a summary of the laboratory testing results for I 80. It is noteworthy that the average values for all properties measured in the laboratory are fairly similar for both the Distressed and Control section. This result supports the hypothesis made in the mixture design section, Section 6.3, that the mixture design for both sections was the same.

Table 45: Summary of Laboratory Test Results for I 80.

	Distressed			Control		
Laboratory Test	Value	St. Dev	COV	Value	St. Dev	COV
CTE, /°F	4.9E-06	0.3E-06	5%	5.0E-06	0.2E-06	3%
Elastic Modulus, psi	3.80E+06	0.6E+06	16%	3.95E+06	0.4E+06	10%
Poisson's Ratio	0.21	0.02	7%	0.22	0.03	11%
Compressive Strength, psi	5400	420	8%	5200	660	13%
Split Tensile Strength, psi	575	30	6%	415	21	5%

6.12 Laboratory and Backcalculated Results Analysis: I 80

The static elastic moduli measured in the lab from cores were generally much lower than the backcalculated static elastic moduli especially for the Control section. For the Distressed section, the average measured elastic modulus was 3.80 million psi and 4.00 million psi for the Control section. These values seem like they might be a little low for concrete of this age but not sufficiently low that it was have a substantial impact on the performance.

The average backcalculated static elastic moduli for the Distressed and Control sections were 4.45 million psi and 6.15 million psi, respectively. The backcalculated values for the Control section exhibited more variability (i.e. 17 percent) and are considered relatively high, taking into account the properties measured in the laboratory. As mentioned before, it is suspected that due to variations in the support conditions and the complexity of the pavement structure, the backcalculated values are not accurately representing the stiffness of the pavement layers in the Control section.

6.13 Petrographic Analysis: I 80

One core from I 80 was examined according to ASTM specification C856 “Petrographic Examination of Hardened Concrete” and ASTM specification C457 “Microscopical

Determination of Air Void Content and Parameters of the Air Void System in Hardened Concrete". The core was from a microcracked region of Slab 25 as shown in Figure 125. Slab 25, other than the microcracked region, exhibited cracks in the transverse direction as shown in Figure 143. These cracks, as highlighted in Figure 143, did not extend across the entire slab, but did happen to occur roughly at mid-slab.

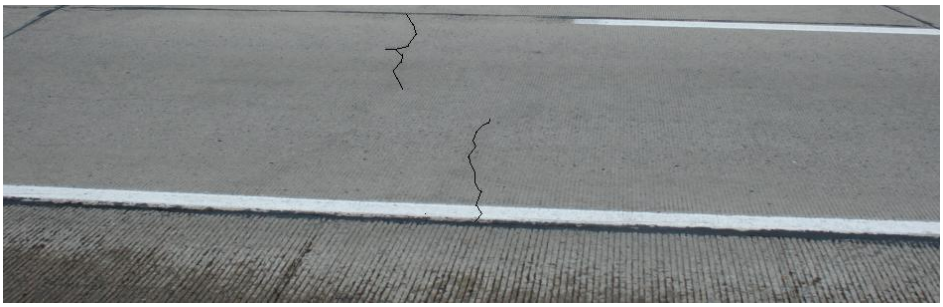

Figure 143: Digitally Enhanced View of Slab 25 I 80 Segment 1914 Eastbound (Distressed Section)

Table 46 presents the results from the petrographic and hardened air void analysis relevant to the determination of the cause of the distresses for I 80. the air void system in its present state is substandard for this pavement's freeze thaw exposure conditions because it does not meet the requirements for spacing factor or specific surface area recommended by ACI to achieve good freeze thaw resistance. The recommended requirements set forth by ACI are a spacing factor <.008-in and a specific surface area >600in^2/in^3. Despite the current state of the air void system, it was also noted that secondary ettringite has partly or completely filled much of the finer air voids throughout the upper half of the core reducing the air void system in that region. This is illustrated in Figure 144. Despite these observations, the pavement has still functioned fairly well for almost 20 years without significant amounts of spalling or d-cracking near the joints.

Table 46: Results Summary of Petrographic Analysis of Core from I 80 Segment 1914 Eastbound (Distressed Section)

	C25-MC80
Nominal Maximum Aggregate Size	¾
w/cm	.40-.45 Estimate
Air Void Content, %	5.3
Entrapped Air, %	2.5
Entrained Air, %	2.8
Specific Surface in^2/in^3	530
Spacing Factor (in)	0.009
Conformance	Air voids are not consistent with current technology for freeze thaw resistance
Distribution of Aggregate	Good (Coarse Aggregate), Good (Fine Aggregate)
Depth of Carbonation	Negligible to 0.3 in*

* Measured From Sawcut Surface

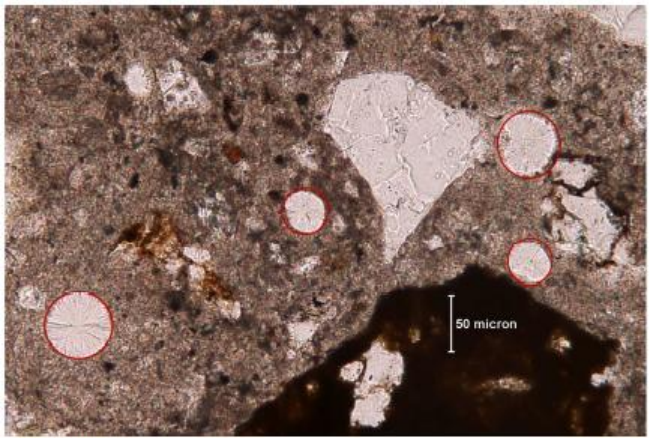

Figure 144: Illustration of Ettringite Filled Air Voids (Circled in Red) in I 80 Core MC25-D. Magnification 200x

The petrographic analysis also revealed that the core is exhibiting signs of ASR, with the coarse aggregate being the source of the reactive silica. This is shown in Figure 145. The blue

line in Figure 145 indicates the boundary between the coarse aggregate and the paste with the aggregate being to the right of the blue line. The arrows in the figure point out the ASR gel and its migration through a microcrack in the aggregate and into a microcrack within the paste.

On a larger scale, the developing ASR is contributing to expansion throughout the depth of the core and causing internal cracking, it is noteworthy however that the microcracking caused by the ASR is only visible with magnification or the aid of a dye. This cracking takes the form of sub-horizontal microcracks at depth within the core as illustrated in Figure 146 by the red lines throughout the depth of the core and manifests itself as sub-vertical microcracks within the top 13-mm (.5-in) of the pavement, as shown in Figure 147. The large colored rectangular area in Figure 146 and Figure 147 represents the area tested for carbonation, while the slightly darker red lines represent ASR. Figure 147 was included to illustrate the sub-vertical microcracks in the region that were also tested for carbonation. Although it appears that minor amounts of ASR has developed, it does not appear that is has significantly affected the performance of the pavement to date.

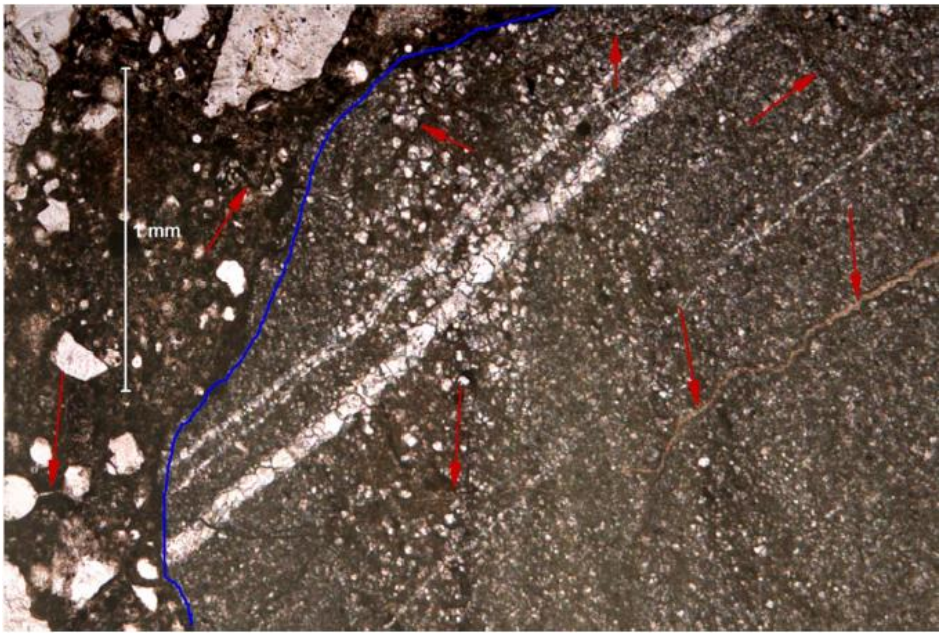

Figure 145: Development of ASR gel in Carbonate (Coarse) Aggregate of I 80. Magnification

40x.

Figure 146: Illustration of the Extent of Microcracking Due to ASR within Core C25MC-D of I80.(ASR Illustrated by Red Lines)

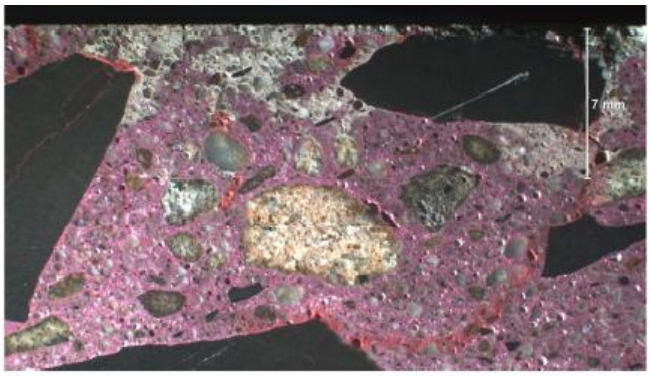

Figure 147: Illustration of Sub-Vertical Microcracking due to ASR near C25MC-D Core Surface. Magnification 5x

6.14 Potential Causes of Distress: I 80

I 80 is exhibiting two main types of distress, fatigue transverse cracking and material-related cracking. In order to assess the fatigue cracking, the MEPDG software was used to analyze the predicted pavement performance. The results of this analysis are presented in section 6.14.1.

The map-cracking was found in a common and localized area adjacent to the outer lane-shoulder joint. Available moisture is required for ASR to occur. This can explain why the map cracking is primarily prevalent around the joints since these locations are a source of moisture infiltration into the pavement structure and are also prone to retaining moisture. The orientation and spacing of the cracks do not follow a noticeable trend; they are randomly oriented and distributed as seen in Figure 148. The depth of the microcracks shown in Figure 148 is approximately 0.7-in and the visual observation of the core revealed that at some points the crack goes through the coarse aggregate.

Figure 148: Top View of PCC Core Retrieved at a Microcracked Location of I 80 Segment 1914 Eastbound, Slab 25,(Distressed Section)

The low-severity transverse cracks are mainly located at mid slab and extend across the entire width of the slab; however, there were several slabs with multiple parallel low-severity transverse cracks that did not cross the entire slab width. It is then believed that the cracks seem to initiate at the outside edge of the pavement and propagate towards the center of the pavement. The fact that these cracks occur roughly at mid-slab also suggests that there is a load component associated with them, since the critical loading scenario of axle loads would result in the highest tensile stresses being generated at the outside edge of mid slab. The low-severity longitudinal cracks that did traverse the entire length of the slab were remarkably tight. The average depth of these cracks, as measured from the retrieved cores, was 0.8 in and in some of the specimens, the crack traveled through coarse aggregate particles. Considering these observations and the results of the petrographic analysis, it is believed that both the micro-cracking observed along the joints, as well as the transverse and longitudinal low-severity cracking could be exacerbated by the drying shrinkage cracks. It seems the cracks initiated at the top of the slab as a result of material related problems as well as traffic and environmental loads. This is because, with a positive built-in temperature gradient, slabs that have close-to-zero temperature gradients tend to curl upward resulting in critical stresses at the top of the slabs.

The tight transverse cracking is present in both the Distressed and Control sections. However, a noticeably higher percentage of slabs in the Distressed section present tight cracks

than the Control section. Since it has generally been established that these sections are quite similar in terms of structure and materials, it is paradoxical that the performances are so different. This variation points to construction related factors being a potential source of the variation in performance between the Distressed and Control sections. Evidence for this consideration was presented in Section 6.9 where it was discussed that the depth of the cracking measured from cores pulled at mid-slab locations with low severity transverse cracks was significantly different between the Distressed and Control sections. The average depth of the crack was .8-in for the Distressed section and not measureable for the Control section. This significant variation in response does not imply, like the measured material and structural related properties, that the sections are indeed the same.

An explanation of the discrepancy in the cracking depth between the two sections might be that these cracks are a combination of plastic and long term drying shrinkage. While the amount of long term drying shrinkage should be about the same for the two pavements since they are exposed to the same environment, the amount of plastic shrinkage could be different considering the superior protection against the wind provided by trees on both sides of the Control section. High winds influence the rate of evaporation of water from the surface. This is especially critical during the curing period which is the key time in terms of controlling plastic shrinkage cracking. In addition to the prevailing wind condition, the variation between the sections could also be attributed to differing temperature and solar radiation conditions during paving of the different sections. The combination of the three aforementioned factors could have dominated the evaporation from the surface that occurred during the construction of the Distressed section and led to the discrepancy in the performance.

Based on the results of the Petrographic analysis and the discussion in Section 6.13, the ASR present in the core tested from I 80 seems to be due to reactive silica in the coarse aggregate. While the ASR is might be a concern for the extended life performance of I 80, it should be noted that the microcracking that has already occurred due to ASR has not adversely affected the material properties of the concrete as indicated by the laboratory determined strength properties. Furthermore, although ASR was visible through dying techniques, the microcracks created by the ASR, unlike those created by the drying shrinkage, were not visible on the core through visual inspection.

6.14.1 MEPDG Runs

In assisting with assessing the performance of both the Distressed and Control sections, MEPDG was used for each section to predict their expected performance. In establishing the inputs into the MEPDG, measured or calculated values were used when possible, otherwise, default values were used. Based on the evidence presented thus far for I 80, the only differences between the input file used for the Distressed section and the input file used for the Control section are the different average thicknesses and average laboratory determined properties that were actually measured for the different sections. The following sections are a summary of the inputs used in the MEPDG files.

6.14.2 Pavement Structure

The pavement structure for the Distressed section is a 12.2-in PCC slab over a 6-in layer of crushed gravel (OGS layer), a 10-in existing rubblized JPCP layer, another 6-in layer of crushed gravel (OGS) and an AASHTO A-4 subgrade. The only difference with the pavement structure in the Control section is that a 12.4-in PCC slab was used instead of the 12.2-in slab. The difference between these two thicknesses is not significant.

PCC Slab

PCC slab properties are divided into four groups: general properties, thermal properties, PCC strength, and mixture design. The general properties include the unit weight and Poisson's ratio, which were chosen as 150 pcf and 0.20, respectively. The CTE was adjusted in accordance with the explanation given in Section 2.14.1. The adjusted CTE values to be used as an input in the MEPDG were 6.4 x 10^{-6} /ºF for both the Distressed and Control sections. For thermal conductivity, 1.25 BTU/hr-ft- ºF was used, and for heat capacity, 0.28 BTU/lb- ºF was used. These are default values.

Another PCC input that was different between the two sections was the 28-day compressive strength. As explained in Section 2.14.1, this property was backcalculated based on the laboratory-determined strengths of 5,400 psi and 5,200 psi for the Distressed and Control sections, respectively. The adjusted 28-day values used as input in the MEPDG were 4,600 and 4,400 psi for the Distressed and Control sections, correspondingly. The PCC elastic modulus was also adjusted as explained in Section 2.14.1. The adjusted PCC elastic moduli to be used as input in the MEPDG were 3.5 and 3.7 million psi for the Distressed and Control sections, respectively.

The rest of the values used in the mix design were default values or average values based on PennDOT specification. A complete list of mixture design information can be seen in Table 47.

Table 47: PCC Mixture Design Inputs for I 80

Input	Distressed	Control
PCC Strength, psi	4,600	4,400
Cement Type	I	I
Cementitious Material	588	588
w/c Ratio	0.42	0.42
Aggregate Type	Limestone	
Reversible Shrinkage (% of Ultimate Shrinkage)	50	
Curing Method	Curing Compound	

OGS

A 6-in crushed gravel layer, which represents the OGS, was incorporated into the pavement structure as a base underneath of the PCC slab and also underneath the rubblized PCC layer. Both layers were given the same properties. The strength properties of this material were calculated based on a known layer coefficient from PennDOT specifications and a correlation between the layer coefficient and resilient modulus built into the MEPDG. Based on this internal correlation, the returned modulus value is approximately 14,500 psi. Other default values provided by the MEPDG software with respect to the OGS are as follows: Poisson's ratio, 0.35; and coefficient of lateral pressure, K_0 of 0.5. The gradation of the OGS was determined based on the PennDOT specifications and it is presented in Table 48.

Table 48: Crushed Gravel Gradation for I 80.

Sieve	Minimum % Passing	Maximum % Passing
2 in	100	100
3/4 in	52	100
3/8 in	36	65
No. 4	8	40
No. 16	0	12
No. 200	5	5

Rubblized PCC Layer

The 10-in JPCP layer that had been rubblized prior to the construction of the existing JPCP was given all default values for a rubblized pavement in the MEPDG. The layer properties are in Table 49.

Table 49: Rubblized PCC Layer Inputs for I 80

Input	Value
Unit Weight, pcf	150
Poisson's Ratio	0.2
Elastic/Resilient Modulus, psi	150,000
Thermal Conductivity, BTU/hr-ft-F°	1.25
Heat Capacity, BTU/lb-F°	0.28

Subgrade Soil

An AASHTO A-4 subgrade was used in the MEPDG input file. Poisson's ratio and the coefficient of lateral pressure were assigned using the same default values as were used for the crushed gravel. The gradation of the subgrade soil is shown in Table 50.

Table 50: Subgrade Soil Gradation for I 80.

Sieve	% Passing
	A-4
4 in	99.8
3 ½ in	99.8
2 in	99.6
1 ½ in	99.4
1 in	98.7
3/4 in	98
1/2 in	96.7
3/8 in	95.6
No. 4	93
No. 10	89.9
No. 40	82.7
No. 80	73.9
No. 200	60.6

6.14.3 Climate

To characterize the climate at the location of the Distressed and Control sections, a virtual weather station was created based on climatic data in the three closet weather stations. The three closest weather stations to the locations of the study sections are located in Williamsport, PA which is 33.2 miles away, Selinsgrove, PA which is 38.0 miles away, and Clearfield, PA which is 46.9 miles away. The latitude and longitude of the virtual weather station created are in Table 21. The depth of the water table used in the sensitivity analysis for the two climatic regions was 10-ft. A summary of the virtual weather station location information can be seen in Table 51.

Table 51: Summary of Weather Station Location Information for I 80.

Climate Station	Latitude, degree	Longitude, degree	Elevation, ft
Loganton, PA	41.04	-77.31	1398

6.14.4 Pavement Design Features

Additional aspects of the pavement that need to be categorized in the MEPDG include the diameter and spacing of dowel bars, shoulder type, joint spacing, and base/slab friction coefficient. A summary of these design features used in the inputs files for I 80 can be seen in Table 52.

Table 52: Summary of Pavement Design Feature Inputs for I 80

Input	Value
Effective Joint Spacing, ft	25.06
Sealant Type	Neoprene
Dowel Diameter, in	1.0
Dowel Bar Spacing, in	12
Shoulder Type	Tied PCC Shoulder
Base Type	Granular
Erodibility Index	Fairly Erodable (4)
PCC-Base Interface	Zero Friction Contact
Loss of Full Friction (age in months)	n/a
Permanent Curl/Warp Effective Temperature Difference, °F	-10

6.14.5 Traffic Inputs

Two-way Annual Average Daily Truck Traffic (AADTT)

The following traffic inputs were used in the input files for I 80 and can be seen in Table 53. The initial two-way AADTT was calculated for the year 1992 based on historic information obtained from PennDOT.

Table 53: Summary of Traffic Inputs for I 80

Input	Value
Initial Two-Way AADTT	5280
Number of Lanes in Design Direction	2
Percent Trucks in Design Direction, %	50
Percent Trucks in Design Lane, %	90
Operational Speed, mph	60

Traffic Volume Adjustment Factors

The following factors are necessary to determine the AADTT for each truck class, for each month, on an hourly basis:

- *Load Monthly Adjustment Factors.*
- *Vehicle Class Distribution Factors.*
- *Hourly Truck Traffic Distribution.*
- *Traffic Growth Factors.*
- *Directional Distribution Factors.*
- *Lane Distribution Factors.*

The load monthly adjustment factors, the vehicle class distribution factors, and the hourly truck traffic distribution are default values provided in the MEPDG. These values were used in the absence of actual data. The traffic growth was estimated to be 3 percent per year with linear growth.

Axle Load Distribution Factors

The axle load distribution factors represent the percentage of the total axle applications within each load interval, for each vehicle class, and for each specific axle type. Level 3 default values generated from the LTTP database were assigned for all axle types (single, tandem, tridem, and quad) and all vehicle classes (4 to 13). These values were used in the absence of actual data.

General Traffic Inputs

The following information is contained in this category:

- *Mean Wheel Location, Traffic Wander Standard Deviation, and Design Lane Width*
- *Number of Axle Types per Truck*
- *Axle Configuration*
- *Wheel Base Distribution*

The values used for these variables are default values given by the MEPDG and were used in the absence of actual data.

6.14.6 Results

A summary of the results from the MEPDG runs compared with the field observations can be seen in Table 54. As seen in the table, the prediction of the MEPDG for cracking and faulting are considerably different from the observed values.

Table 54: Predicted vs. Observed Distresses for I 80

Distress	Interstate 80			
	Distressed		Control	
	Predicted	Observed	Predicted	Observed
Faulting, in	0.26	0.03	0.27	0.03
Cracking, %	72	20[1]	94	6[1]

[1]These values only represent the working cracks that propagate throughout the depth of the slab.

Figure 149 presents the predicted and observed transverse cracking for both the Distressed and Control sections. The observed transverse cracking over time (from year 5 to year 17) is based on historic distress data provided by PennDOT. This data has been collected using automated distress equipment. The data points for year 18 represent the percentage of transverse cracking in the Distressed and Control sections that were manually surveyed as part of the present study. As observed in the plot, the historic distress data exhibited some anomalies that, according to PennDOT personnel, are typical for automated surveys. As observed in Figure 149, for the Distressed section, there is a remarkable difference between the percentage of cracking from the historic distress data and the percentage of cracking observed as a result of the manual distress survey carried out in this study. This difference might also be caused by deficiencies associated with the automated distress equipment. Comparing the observed and predicted cracking for year 18, it can be seen that the MEPDG is greatly over predicting the fatigue cracking for this pavement. This result is not surprising considering the complexity of the pavement structure for this specific project.

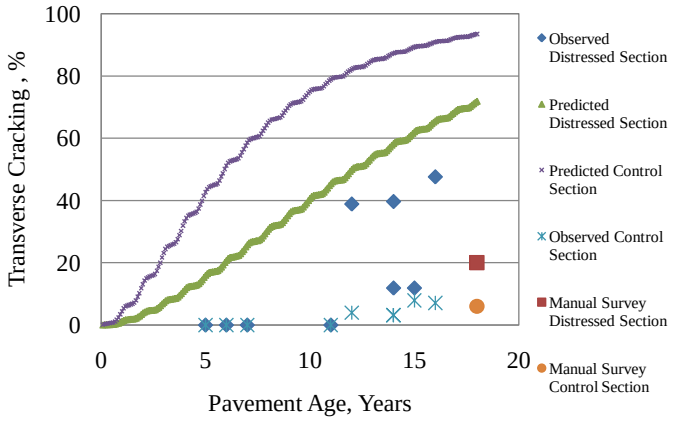

Figure 149: Predicted and Observed Transverse Cracking for I 80 Segments 1914 and 1920 and Segment 1930 Eastbound (Distressed and Control Sections Respectively)

Figure 150 presents the predicted and observed faulting for both the Distressed and Control sections. The observed faulting corresponds to the data measured as part of the field data collection for the present study. Historic data for faulting was not available. As noticed in the plot there is a large difference between the predicted and observed faulting. The high predicted faulting is most likely the result of the dowels being only 1-in in diameter.

Figure 150: Predicted and Observed Faulting for I 80 Segments 1914 and 1920 and Segment 1930 Eastbound (Distressed and Control Sections Respectively)

6.15 Rehabilitation Recommendations: I 80

6.15.1 Distresses and Deficiencies

The major distress in both the Distressed and Control sections for I-80 is mid-slab transverse cracking of varying severity. Some material related cracking was also identified. The other issues include poor load transfer at the medium severity cracks for both sections and some of the joints in the control section. Voids are beginning to develop beneath the slab but should not be a major issue it the load transfer can be restored relatively quickly. As seen in the MEPDG predictions, this pavement with long joint spacing and small diameter dowels has greatly exceeded its design expectations.

6.15.2 Recommendations for Segments 1914 and 1920 (Distressed Section) and Segment 1930 (Control Section)

Although these recommendations are based on data obtained from Segments 1914 and 1920 (Distressed Section) and Segment 1930 (Control Section), other segments that exhibit similar distress patterns should also be considered for any elected rehabilitation measures. While there were difficulties in modeling the field performance of I-80 using the MEPDG, it is still believed that medium severity transverse cracks are due in part to fatigue. Although, only 6 percent of the slabs have medium severity cracks with the remainder of the cracks being of low severity. Based on the historical performance, data it appears that the rate of deterioration is beginning to increase. This should be considered in comparing rehabilitation options that extend the life of the existing pavement and rehabilitation options that add additional structural capacity.

To address medium severity transverse cracking full-depth repairs are suggested. For I 80, there are many low severity cracks that do not extend through the entire depth of the pavement. These types of cracks, shown in Figure 151, can result in secondary cracks that deviate from what can be considered a primary crack extending across the slab. As mentioned in the previous section, these cracks are believed to be the result of drying shrinkage of the concrete. While they do not extend through the depth of the pavement, in many cases they do create a location with a reduced effective thickness and increased likelihood of being the location of the initiation of a fatigue crack. It appears that the initiation of a fatigue crack from a drying shrinkage crack is indeed happening in this section as evidenced by Figure 151**.** This figure shows a working crack with drying shrinkage crack branching off of it. The boundary area for the full depth repairs

should extend beyond this low severity crack as well.

Figure 151: Medium Severity Transverse Crack with Digitally Enhanced Branching Drying Shrinkage Crack on I 80 Segment 1914 (Distressed Section)

Because of the tightness of the drying shrinkage cracks and the uncertainty surrounding their future development into full depth transverse cracks, it is recommended to do nothing to address these cracks at this point in time. This recommendation is also valid for the longitudinal cracks as they also appear to be due to drying shrinkage. The extent of the medium severity transverse cracks within the section, 20 percent in the Distressed section and 6 percent in the Control section, suggests that this is an economically viable option for this pavement as the extent is not such that reconstruction or an unbonded overlay is yet needed. This concrete pavement restoration technique will only serve to enhance the existing remaining life of the current pavement.

Another issue to address is that FWD testing revealed that voids are present at the corners of many of the slabs in both the Distressed and Control section. As mentioned previously, no pumping or staining of fines was observed in the field. In fact, because of the pavement structure including a rubblized pavement and an additional granular subbase, it is unlikely that migration of fines from the subgrade could be an issue for this pavement. However, voids could be possible do the consolidation or breakdown of the OGS material or pumping due to fines in the OGS placed on top of the rubblized pavement after the rubblization process.

It is believed that since the pavement is 18 years old and the base type is granular that these

voids are due to settlement of the OGS layer from the many load applications over the years. However, because of the pavement age, it is doubtful that the voids will increase in size as most of the possible settlement has been realized already. In addition, there appears to have been no adverse effects to the pavement structure from the voids as load transfer efficiency is good at most of the joints in both the Distressed and Control section. A further breakdown of the LTEs at the transverse joints revealed that while some joints had LTEs less than the recommended value of 70 percent, these joints did not exhibit exceedingly poor load transfer. The lowest load transfer efficiency at the joints of I 80 was 54 percent at one of the joints in the Control section. This value, while not great, does not suggest complete failure of the dowels either. Therefore, performing slab stabilization as a means of addressing the voids underneath the slab might not be a rehabilitation procedure that provides good economic value for this section of I 80.

Finally, in addressing all of the repairs in the previous paragraphs, it is important to also consider the durability issues associated with the pavement, particularly the deficient air void system in the Distressed section and the potential for future damage due to the further development of the ASR. Assessing the future impact of these issues, while beyond the scope of this project, should play a role in the general rehabilitation strategy for this project since the future impact of these distresses could decide whether a functional or structural rehabilitation measure is more appropriate.

At this point in time a good opportunity exists to perform this work on the distress section since the structural distresses have not deteriorated to the point where they are significantly affecting the functionality of the pavement. In some instances, rehabilitation measures such as a relatively thin asphalt overlay can exacerbate ASR by raising temperatures at the pavement surface and trapping moisture in the PCC layer. Both heat and moisture exacerbate ASR. If additional deterioration does develop as a result of the asphalt overlay, a second unbonded overlay can be placed using the asphalt overlay as a bond breaker as long as vertical clearance is not a major issue. The same approach would be appropriate for the control section although the low amount of fatigue cracking (6 percent) indicates the immediate need to increase the structural capacity (placement of the overlay) is unnecessary.

6.16 Future Projects: I 80

The drying shrinkage cracks present on I 80 highlight the need for adequate curing and finishing of the concrete pavement. In this case, the drying shrinkage cracks effectively reduced

the cross sectional area of the pavement. When these cracks occurred in the middle third of the pavement, they most likely resulted in the development of transverse fatigue cracks and a subsequent reduction of the fatigue life of the concrete. In addition, drying shrinkage cracks enhance the ability of moisture to infiltrate the pavement and induce more and deeper ASR cracking in the concrete.

With respect to finishing, over finishing should be avoided as it creates an area on the top of the slab with an increased w/c ratio and makes it more susceptible to drying shrinkage. With respect to curing in adverse conditions such as curing on hot and sunny days or days with a brisk prevailing wind, it is imperative to immediately follow the finishing and tining of the pavement with the application of an adequate amount of curing compound as per PennDOT Publication 408 [5]. Consideration should be made in revising the curing specification as previously mentioned.

Although ASR and freeze-thaw damage was observed, the extent of the damage was not detrimental in meeting the intended design life of the pavement so these material related distresses were not considered to be detrimental.

7 US 22, Indiana County

7.1 Project Information: US 22, Indiana County

This section of US-22, for which construction was finished in 2009, is part of a reconstruction effort in Indiana County. This project is a new JPCP construction just outside of Blairsville, PA on US-22. It consists of sections of new pavement in both the eastbound and westbound directions of US-22. Each direction has two 12-ft lanes with a 10-ft outside tied PCC shoulder and an inside tied shoulder of which the width is either 2-ft where a turning lane is required or 8-ft where no turning lane is required. The location of the project is shown in Figure 152.

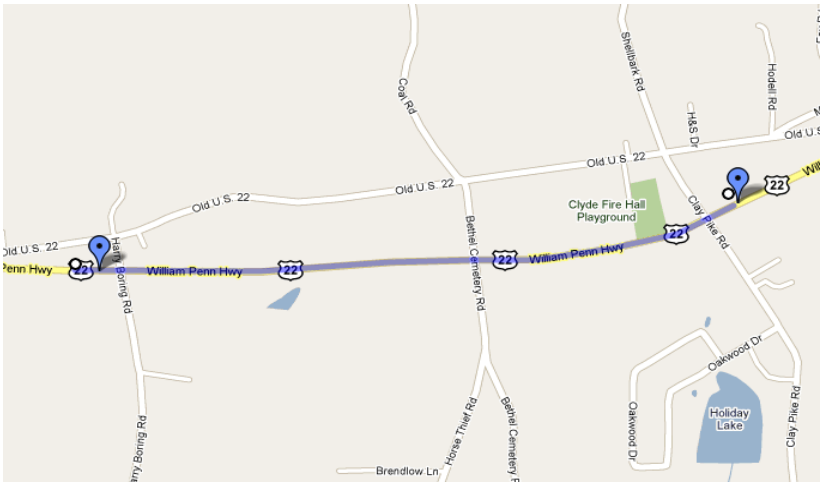

Figure 152: Location of the Segments of US-22, Indiana County in District 10

While the pavement mainline was constructed in October 2008, the 2-ft shoulders were constructed in July 2009. One week after the 2-ft shoulders were paved, mid-panel cracks were noticed on the shoulders. In response to this cracking, the contractor went back and sawed and sealed mid-panel joints in some of the shoulders that had not cracked until requested by PennDOT to stop doing this. The purpose for investigating this project was to determine the cause of this cracking. As part of achieving this objective, various sections were selected to investigate the differences between the shoulders that cracked, those that were sawed at mid-panel and cracked, those that were sawed at mid-panel and did not crack, and those that were not

sawed and did not crack. The sections exhibiting these behaviors are given in Table 55.

Table 55: Stations with 2-ft shoulders along US-22, Indiana County

Section	Station Beginning	Station End	Direction
1	464+50	472+00	Westbound
2	473+38	481+00	Eastbound
3	508+70	514+20	Eastbound
4	522+15	531+00	Westbound
5	532+30	541+10	Eastbound
6	555+50	561+35	Westbound
7	562+65	566+00	Eastbound

7.2 Design Information: US 22, Indiana County

The mainline and shoulders for US 22 Indiana County consists of a 10-in thick doweled JPCP pavement. The base is a 4-in cement treated permeable base course with a 2-in 2A subbase. Beneath the 2A subbase is an 18-in backfill of rock embankment and a geotextile separator layer above an A-4 subgrade. Longitudinal edge drains were provided at the bottom of the rock fill layer. The diameter of the dowels is 1.5-in. These dowels were placed 12-in apart beginning at 6 in from the slab edge. There were also 30-in tie bars were also installed 30 in off center along the length of the lane shoulder joint and at the longitudinal joint between the lanes.

A cross section of the existing pavement and an overall condition of the section of US 22, Indiana County that was investigated is shown in Figure 153 and Figure 154 respectively. Where a turning lane was required along the roadway in either direction, the location of the median was shifted to accommodate the turning lane. This resulted in the need to shorten the width of the inside shoulder opposite direction to 2-ft, as shown in Figure 154. A plan view of the shift from the 8-ft inside shoulder in both directions when a turning lane is required is shown in Figure 155.

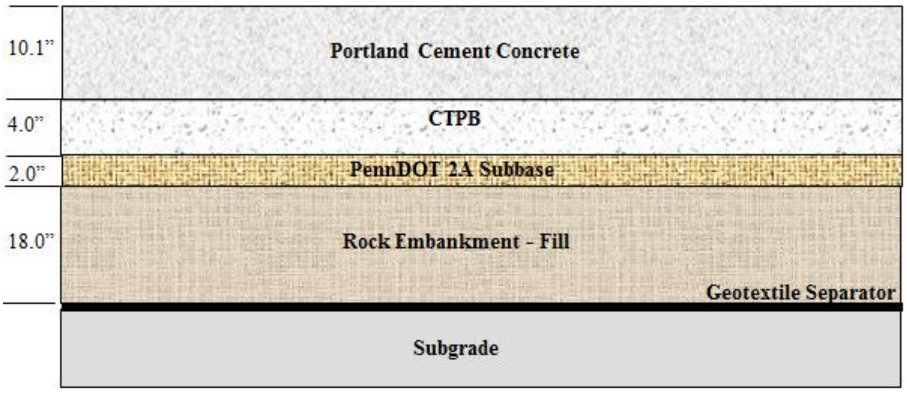

Figure 153: Existing Pavement Cross Section of US-22, Indiana County

Figure 154: Overall View of US 22, Indiana County, Showing 2-ft Shoulder

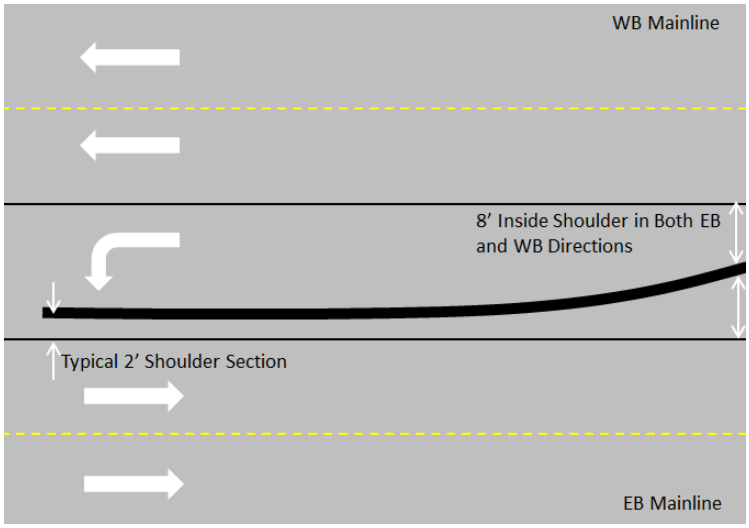

Figure 155: Plan View of 2-ft Shoulder Section with Turning Lane at US 22, Indiana County

7.2.1 Concrete Mixture Design: US 22, Indiana County

The concrete mixture designs used for the mainline and the 2-ft shoulders can be seen in Table 56 and Table 57 respectively. These mixtures are essentially the same with the only exception being a slightly lower w/c ratio in the two mixes used for the 2-ft shoulders. The w/c ratios for the mainline and mixture I and mixture II for the shoulders are 0.45, 0.43, and 0.41 respectively.

Table 56: Concrete Mixture Design for the Mainline of US 22, Indiana County

Material	Specific Gravity	Absorption	Batch Weight lb/yd^3
Type 1 Cement (Cemex Cement-Louisville, KY)	3.15	n/a	500 lbs.
Coarse Aggregate (Hanson-Torrance Quarry)	2.67	0.59	1833 lbs.
Fine Aggregate (New Enterprise- Ishman)	2.59	1.24	1130 lbs.
Class F Fly Ash (Headwaters Co.- Hatfield Power Station)	2.40	n/a	88 lbs.
Air Entrainment (BASF- Cleveland, OH MBVR)	n/a	n/a	13 oz.
Water Reducer (BASF- Cleveland, OH 200-N)	n/a	n/a	18 oz.
Water (Blairsville City)	1	n/a	266 lbs.

Table 57: Concrete Mixture Designs for the Shoulders of US 22, Indiana County

Material	Specific Gravity	Absorption	Mixture I (Sections 1, 3, 4 and 6)	Mixture II (Sections 2, 5 and 7)
			Batch weight, / yd^3	Batch weight /yd^3
Type 1 Cement (Cemex Cement-Louisville, KY)	3.15	n/a	500 lbs.	500 lbs.
Coarse Aggregate (Hanson-Torrance Quarry)	2.68	0.52	1840 lbs.	1840 lbs.
Fine Aggregate (New Enterprise- Ishman)	2.59	1.24	1157 lbs.	1187 lbs.
Class F Fly Ash (Headwaters Co.- Hatfield Power Station)	2.40	n/a	88 lbs.	88 lbs.
Air Entrainment (BASF- Cleveland, OH MBVR)	n/a	n/a	13 oz.	13 oz.
Water Reducer (BASF- Cleveland, OH 200-N)	n/a	n/a	18 oz.	18 oz.
Water (Blairsville City)	1	n/a	255 lbs.	243 lbs.

7.3 Quality Control Information: US 22, Indiana County

7.3.1 Fresh Concrete Properties: US 22, Indiana County

Both the slump and air content of the fresh concrete used for quality control purposes were obtained and are presented in Table 58.

Table 58: Fresh Concrete Properties of US 22, Indiana County as Determined by PennDOT Quality Control

	Mainline	Shoulder
Slump, in	1.3	1.5
Air, %	5.7	5.3

7.3.2 Hardened Concrete Properties: US 22, Indiana County

The 7 and 28-day compressive strengths of the concrete obtained as part of the quality control protocol were also obtained and are presented in Table 59.

Table 59: Compressive Strength of Concrete for US 22, Indiana County as Determined by PennDOT Quality Control

Age	Strength, psi	
	Mainline	Shoulder
7-day	3220	3330
28-day	4805	4600

7.4 Climatic Conditions: US 22, Indiana County

The three closest climate stations to US 22, Indiana County are Johnstown, which is 26.6 miles away Du Bois, which is 39.8 miles away, and Pittsburgh, which is 46 miles away. Based on these three stations, it was possible to interpolate a virtual weather station for the project site. The weather station shows that the project area experiences about 202 wet days per year and a mean annual rainfall of 41 in. The freezing index is 869 ºF-days and the area is exposed to approximately 54 freeze-thaw cycles per year. The mean annual air temperature is about 48 ºF with minimum and maximum average monthly temperatures being 28 ºF and 78 ºF, respectively. Table 60 summarizes the climatic conditions for the first week after the 2-ft shoulders were paved.

Table 60: Climatic Conditions in the First Week after the Construction of the 2-ft Shoulder for US 22, Indiana County

Date	High, °F	Low, °F	Precipitation, in	Sunshine
7/13/2009	71	57	0.14	Yes
7/14/2009	72	52	0.07	Yes
7/15/2009	80	54	0.09	Yes
7/16/2009	82	66	0.08	No
7/17/2009	71	57	0.13	No

7.5 Traffic Loadings: US 22, Indiana County

Since this project is newly constructed, traffic was not allowed on the road at the time of this study. At the time of writing this report, PennDOT did not have this project updated in the iTMS database and therefore, traffic data for the exact project site was not available. The AADT of the closest segment of US 22 is 8714 with 19 percent trucks.

7.6 Selection of Distress Survey Sections: US 22, Indiana County

As mentioned previously, the mechanism responsible for the development of the premature transverse cracks of the shoulders is investigated for this project. The situations investigated as part of this study include sections where the shoulders cracked, sections where the shoulders were sawed at mid-slab and still cracked, sections where the shoulders were sawed and sealed at mid-slab and did not crack, and sections that were not sawed and sealed and did not crack. Because of the disparity between this project and the other five, the selection of a Control and Distressed sections was not appropriate for US 22, Indiana County. Instead, the variability in the performance of the shoulders between the scenarios just mentioned was assessed. Of the 7 sections listed in Table 55, Section 1 was selected as the section to be manually surveyed since it was the section with the most cracking in the shoulders. This is also the section from which cores in both the mainline and shoulder were taken.

7.7 Pavement Condition: US 22, Indiana County

The mainline for US 22, Indiana County was constructed in October 2008 and the 2-ft shoulders were constructed in July 2009. The concrete was placed by the contractor, New Enterprise, in accordance with the specifications set forth by PennDOT. After placing the concrete, the shoulder surface was tined in the transverse direction and a curing compound was applied. During the week of paving the 2-ft shoulders, several of the days were extremely hot followed by colder nights. One week after the 2-ft shoulders were paved, mid-panel cracks were noticed by PennDOT engineers.

The mid-panel cracking in the shoulders was the only distress that the pavement exhibited. A typical crack can be seen in Figure 156 while a breakdown of the number of shoulder slabs cracked per section can be found in Table 61. The majority of the cracks propagated across the full width of the shoulder (full-length cracks); however, there were a few cracks that only partially traversed the width of the slab (partial-length cracks). The cracks were more open along the free edge and tight at the edge adjacent to the mainline. All of the cracks were wider at the top than at the bottom. This could be an indication of top-down cracking or just the result of the restraint provide by the base restricting further crack opening near the bottom of the slab. Based on these two observations, it seems possible that the cracks initiated at the upper outside edge away from the junction of the shoulder and the mainline.

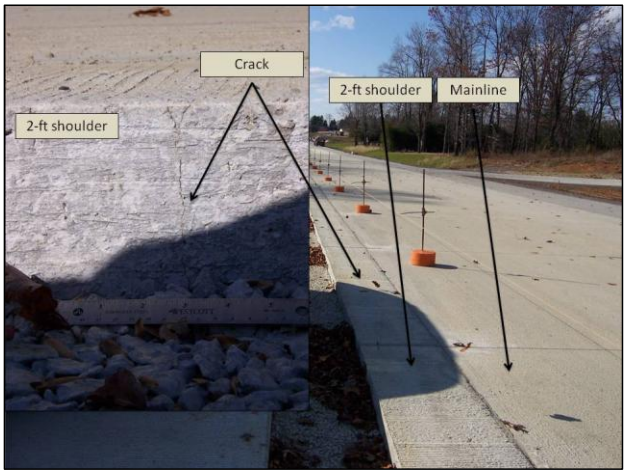

Figure 156: Typical Crack Found in the 2-ft Shoulder of US 22, Indiana County

Table 61: Summary of Cracking in the 2-ft Shoulders of US 22, Indiana County

Section	Percentage Cracked	Remarks
1	84%	No midbay sawing
2	25%	No midbay sawing
3	11%	No midbay sawing
4	57%	All panels sawed and sealed midbay
5	0%	All panels sawed and sealed midbay
6	0%	All panels sawed and sealed midbay
7	0%	No midbay sawing

7.8 Core Samples: US 22, Indiana County

As part of this project, a total of nineteen 4-in diameter cores were pulled at various locations. Nine of the cores were pulled from mid-panel along the mainline, five were pulled from a non-cracked shoulder, two were pulled from a non-cracked area of a cracked shoulder, two were pulled from cracks that propagate all the way across the shoulder (full-length cracks), and one was pulled from a crack that propagated only partially across the shoulder. A summary of the pulled cores can be found in Table 62.

Table 62: Summary of Cores Pulled from US-22, Indiana County

Core	Location	PCC Thickness, in	Base Type	No. of Pieces
1-S15C-NCA	Non-cracked area of a cracked shoulder	10.2	CTPB	1
1-M15	Mainline mid-slab	10.25	CTPB	1
1-S29NC	Non-cracked shoulder	10.25	CTPB	1
1-M29	Mainline mid-slab	10.5	CTPB	1
1-S38C-FL	Full length crack from a cracked shoulder	10.5	CTPB	1
1-M38	Mainline mid-slab	10.5	CTPB	1
1-S50C-PL	Partial length crack from a cracked shoulder	10.375	CTPB	1
4-S4NC	Non-cracked shoulder	10.5	CTPB	1
4-M4	Mainline mid-slab	10.25	CTPB	1
4-S17C-FL	Full length crack from a cracked shoulder	9.75	CTPB	1
4-M17	Mainline mid-slab	9.5	CTPB	1
4-S33C-NCA	Non-cracked area of a cracked shoulder	9.5	CTPB	1
4-M33	Mainline mid-slab	9.5	CTPB	1
6-S3NC	Non-cracked shoulder	10.5	CTPB	1
6-M3	Mainline mid-slab	10	CTPB	1
6-S6NC	Non-cracked shoulder	10.75	CTPB	1
6-M6	Mainline mid-slab	10	CTPB	1
6-S9NC	Non-cracked shoulder	*	CTPB	1
6-M9	Mainline mid-slab	10.25	CTPB	1

* Not Obtained

7.9 Laboratory Testing Results: US 22, Indiana County

In total, sixteen cores were obtained that were not cracked and upon which it was feasible to perform a variety of destructive and non-destructive testing. The testing performed included CTE, elastic modulus, Poisson's ratio, compressive strength, and split tensile strength. Before testing, every core needed to be cut in order to achieve the 2:1 length to diameter ratio conforming to ASTM C 42. The results from the various tests performed along with the standard deviation are presented in Table 63.

7.9.1 Commentary on the Laboratory Results: US 22, Indiana County

A difference of less than 5 percent was observed between the concrete for paving the mainline in comparison with the concrete for paving the shoulder in terms of their CTE, elastic modulus and the Poisson's ratio. A statistical t-test with 90 percent confidence level was performed to see if there was actually a statistical difference between the two mixes with regards to CTE, elastic modulus, and Poisson's ratio. Results from these tests indicated that there was no significant difference between the two mixes with respect to CTE and Poisson's ratio. There was however a statistically significant difference between the two mixes with respect to elastic modulus. Despite this finding, this difference is not practically significant since the compressive strength of the mainline was only five percent higher.

While the CTE, elastic modulus, and Poisson's ratio were relatively similar, the shoulder has a measured compressive strength 10 percent lower and a measured split tensile strength 20 percent lower than the mainline. Statistical t-tests were also performed for these values revealing that on a statistical basis, the difference in compressive strength between the two sections was only significant at an 85 percent confidence level while the difference in split tensile strength was significant at a 90 percent confidence level. Again, the difference between practical and statistical significance needs to be assessed. Based on the results in the laboratory, it can only be concluded with 40 percent confidence that the compressive strength for the mainline is at least 500 psi greater than that for the shoulder. This further highlights the similarities in the mixes used for the mainline and the shoulder.

Table 63: Summary of Laboratory Test Results for US 22, Indiana County

Laboratory Test	Mainline			Shoulder		
	Mean	SD	COV	Mean	SD	COV
CTE, microstrain/°F	6.00	0.41	7%	5.8	0.2	3%
Elastic Modulus, 10^6 psi	4.80	0.24	5%	4.55	0.19	4%
Poisson's Ratio	0.17	0.03	15%	0.18	0.01	8%
Compressive Strength, psi	7,330	750	10%	6,590	660	10%
Split Tensile Strength, psi	670	78.2	12%	555	31.8	6%

7.10 Potential Causes of Distress: US 22, Indiana County

Because the transverse cracks in the shoulder were observed before any traffic was allowed on the pavement or shoulder, it is logical to conclude that the distress was solely caused by environmental stresses. The environmental stress mainly develops when a change in temperature or moisture tends to deform (elongate, shorten, or curve) the PCC slabs and this deformation is restrained. Cracking, therefore, can be expected when the developed environmental stress exceeds the strength of the concrete. Factors that might contribute to the deformation of the PCC slabs (both mainline and shoulder) and generate a sufficiently large stress to crack the concrete are discussed in the following sections.

7.10.1 Structure

Geometry

The dimension of a concrete slab (for both mainline and shoulder) are important when determining the effects of thermal expansion and contraction caused by daily and seasonal variations in temperature. If the slab is restrained, stresses build up in the longitudinal and transverse directions. When large slab dimensions are combined with high CTE values, high internal stress develops.

In this project, the shoulder was paved after a long period when the adjacent mainline had already gained adequate stiffness. Shortly after the shoulder was paved, it became subjected to the movement of the adjacent mainline. Because the mainline would want to move and subsequently subject the young shoulder to stress, one possible cause of the transverse cracking

observed at US 22, Indiana County is that the width of the 2-ft shoulder was not sufficient to resist the stresses generated in the shoulder by contraction of the adjacent mainline. It is also possible that the shoulder failed in flexure. This could be the case since the dimensions of the shoulder slabs are relatively small compared to a typical slab.

Shoulder Type

Concrete shoulders, which are tied to the mainline, provide structural support and can reduce edge deflections. They can also prevent moisture and debris from penetrating into the pavement structure. Despite these advantages, shoulders and mainline slabs also provide restraints to each other through the tie bars. When the thermal deformation between the shoulder and the mainline is incompatible, this favors the development of internal tensile stresses.

Tie Bar Layout

The size and spacing of tie bars dictate the level of restraint between the mainline slabs and the shoulder slabs. The thicker the diameter of the tie bar and the smaller the spacing between tie bars, the more restraint provided. Typically, all agencies use the same tie bar layout, 30-in long tie bars at 30-in on center spacing, when constructing projects such as US 22, Indiana County. This means that the tie bars were embedded into the 24-in shoulder approximately 15 in deep resulting in more than half of the width of the shoulder containing a tie bar. Therefore, the shoulder was essentially completely attached to the mainline and had very little freedom to move.

Base Type

The importance of the base type is that it dictates the amount of friction generated between the slab and the base. Friction at the slab/base interface causes restraint when the slab tries to expand and contract due to changes in temperature. This restraint causes stresses to develop at the interface and throughout the depth of the slab. The tensile stress that develops in the concrete due to the restraint at the slab/base interface is proportional to the slab length, the unit weight of the concrete and the coefficient of friction [15]. The coefficient of friction for the CTPB used at US 22, Indiana County is relatively high compared to a granular base. For the transverse cracking that occurred at US 22, Indiana County, the CTPB provided resistance to movement and caused internal stresses to build up when the shoulder was being dragged by the mainline.

7.10.2 Materials

CTE

The CTE of concrete, which describes how the concrete changes in size when subjected to a change in temperature, is an extremely important parameter when characterizing stress development in pavements. This is because large CTE values indicate large deformations. When those deformations are restrained by the base and adjacent slabs through tie bars, large stresses develop.

Stiffness

The stiffness of the concrete determines the magnitude of induced stresses and deflections. In mechanistic pavement response analysis, the PCC elastic modulus is highly influential on pavement deflections and stresses. There is no internal stress built up when the concrete is fresh and in a plastic state. After the concrete starts to set, larger stresses develop in a concrete with greater stiffness, provided the same temperature change and restraint conditions. The modulus of elasticity represents the stiffness of the concrete and is significantly influenced by time after initial mixing and mixture design parameters such as w/c ratio and proportion of paste to aggregate, as well as the aggregate type [7].

Strength

The strength and fracture properties control when the concrete cracks [16]. In terms of the distress in PCC shoulders analyzed for US 22, Indiana County, strength development is very important. Early strength gain can be achieved by curing at higher temperatures; however, this will lower the ultimate strength of the concrete. In the first week after paving, when the concrete has yet to gain sufficient strength, shoulders that are tied on to the mainline have a tendency to be dragged/pushed when the mainline is expanding/contracting. In the case of the transverse cracking in the 2-ft shoulders at US 22, Indiana County, it is reasonable to suspect that the shoulder had not achieved sufficient strength when it was being dragged by the mainline.

Drying Shrinkage

Originally, differential drying shrinkage occurring as a result of the relatively higher shrinkage of the shoulder relative to the mainline during the first few days after construction was postulated as a potential cause of the cracking. However, it was determined that since the cracking was noticed at an early age, differential drying shrinkage most likely did not have a significant influence on the development of cracking.

7.10.3 Construction

Restraints to the thermal deformation of the shoulder do not only come from the base but also from the mainline through the tie bars when they are not thermally compatible due to the separate construction times. The following paragraphs will discuss the sources and influences of stress transferred between the mainline and shoulder through the tie bars.

Temperature

Temperature is the main environmental cause of the stress transferred between the mainline and shoulder through the tie bars. The temperature profile across the depth of a PCC slab is often nonlinear and can be characterized by a uniform temperature that is the depth weighted average of the temperature profile and a temperature gradient that describes the change of the temperature profile across the depth. A positive temperature gradient is defined when the top of a slab is warmer than the bottom and vice versa. Accordingly, the deformation of a slab (for either mainline or shoulder) can be broken down into two components, namely the expansion/contraction and the curling (upward or downward). The first component is dominated by the uniform temperature. When the concrete temperature is higher than the temperature when zero stress occurs, the PCC slabs expand and vice versa. The second component of the deformation in the slab is the curling of the PCC slabs that is a result of the existence of temperature gradients. A slab would tend to curl downward when subjected to a positive temperature gradient and upward with a negative temperature gradient. The restraint of either deformation component results in stress development in a concrete slab.

Since the uniform temperatures and the temperature gradients in the shoulder and mainline are the same due to the fact that they are exposed to the same environment, the only difference that would lead to the thermal incompatibility between the two lies in the difference between their zero-stress uniform temperatures and temperature gradients.

7.10.4 Zero Stress Temperature

The zero stress temperature is the temperature of the concrete shortly after final set time and before this time no stress develops in the slab when there is a change in temperature. After the zero stress temperature occurs, it then becomes the base temperature of the concrete throughout its life, with temperatures above the zero stress temperature causing expansion and temperatures below the zero stress temperature causing contraction of the slab. The zero stress temperature is primarily a function of the ambient conditions at the time the concrete is placed but is also a

function of the heat of hydration generated as the concrete sets. The relationship that the MEPDG uses to estimate the zero stress temperature can be found in Equation 5 [7].

Equation 5

where,

T_z = Temperature at Which the PCC Layer Exhibits Zero Thermal Stress, °F

CC = Cementitious Content, lb/yd^3

H = -0.0787+0.007*MMT-0.00003*MMT^2

MMT = Mean Monthly Temperature for the Month of Construction, °F.

According to PennDOT specifications, paving operations are only performed when the ambient temperature is between 50°F and 90°F. This corresponds to a zero-stress temperature range of 70°F to 130°F, given the cementitious materials content used in this project.

Built-In Temperature Gradient

A built-in temperature gradient is defined as the gradient present in the slab at the time of concrete sets [17]. As previously described, the concrete set time indicates the time when the concrete start to transition from a plastic material to a solid one [16]. In general, the set time is coupled with the time when stresses begin to develop and volume changes occur due to changes in temperature and moisture. The zero-stress temperature gradient of the slab, also referred to as the built-in temperature gradient, is defined as the temperature gradient in the slab for which the slab will be flat and experience no stress [18]. When the temperature gradient present in the slab is larger than the zero-stress gradient, the slab will curl downwards. Accordingly, the slab will curl upwards when the temperature gradient is lower than the zero-stress gradient.

7.10.5 Construction Sequence

For US 22, Indiana County, thermal incompatibility between the mainline and the shoulder is believed to be a significant factor in transverse cracking in the shoulder. In this project, the mainline was paved in the fall and the shoulders were paved the following summer. Based on Equation 5, it can be determined that the zero-stress temperature of the mainline was more than 20° F lower than that of the shoulder. When thermal incompatibility exists between the mainline and the shoulder, the rates at which volume changes occur relative to each other could induce stress in both the mainline and the shoulder. It is therefore believed that the construction

sequence adopted in this project must have introduced excessive tensile stress in the shoulder, which resulted in the formation of transverse cracks in the shoulder. In order to investigate this hypothesis more rigorously, a finite element model was developed to represent the conditions that were present when the shoulders cracked at US 22, Indiana County.

7.11 Finite Element Model Set-Up: US 22, Indiana County

In order to assess the potential causes of distress listed in Section 7.10, a finite element model was developed with the goal of providing insight into the potential exact cause of the cracking in the shoulder and an explanation for the variation in performance observed in the field between the sections listed in Table 55. As a result of this modeling, the critical combinations of parameters that resulted in the shoulder transverse cracking were identified. Assessing the critical parameters obtained from the model and the conditions in the field allowed a comparison between the different sections with 2-ft shoulders to be compared. The results from the model using the field data to compare the sections are presented in Section 7.14.2

ABAQUS Version 6.9 [19] was used to establish the model. ABAQUS is a general purpose finite element software and is widely used in areas such as structural, geotechnical, materials, mechanical, and biomedical engineering. An overall view of the model developed as part of this project in ABAQUS can be seen in Figure 157. It contains approximately 6,500, 20-node, reduced integration, 3-D, quadratic, brick elements. The adequate mesh fineness for the model was determined by reducing the fineness until the nodal stresses at the outside edge converged.

7.11.1 Parts

The model shown in Figure *157* consists of several sections, namely the shoulder, the mainline, and the tie bars. Within each section, there are several parts. In ABAQUS, defining the geometry, by creating parts, is the basis for which the mesh is created. The various parts used to create the model can be seen in Figure 158. For the 2-ft shoulder, the overall dimensions of the shoulder section are 24 in x 180 in x 12 in. The overall dimensions of the mainline section are 144 in x 180 in x 12 in. The steel section is made up of tie bars. The tie bars are 30-in long with a diameter of 0.625 in.

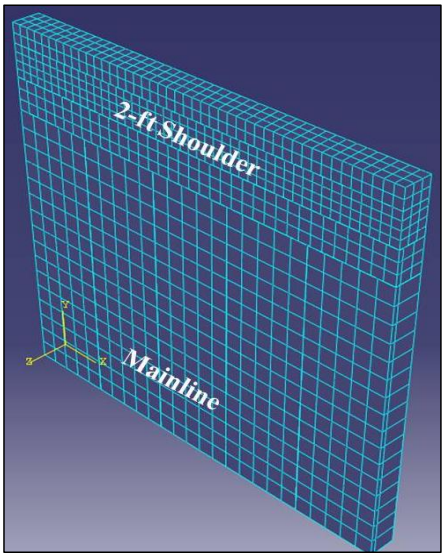

Figure 157: Overall View of Shoulder Transverse Cracking Model for US 22, Indiana County.

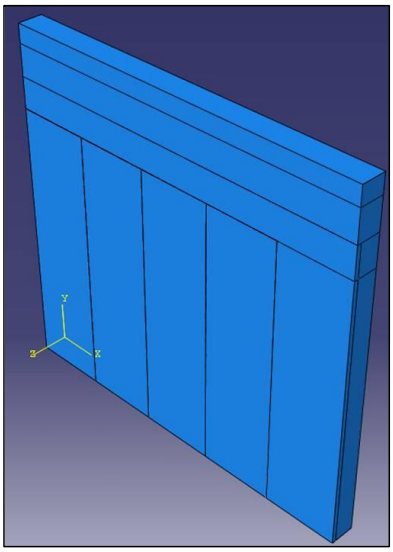

Figure 158: Overall View of Parts in the Shoulder Transverse Cracking Model for US 22, Indiana County.

7.11.2 Contact Interactions

Two contact interactions were used in this model. The first is between the slab and the supporting foundation and the second is between the mainline and the shoulder.

Elastic Foundation

A Winkler foundation was used to model the granular material beneath the PCC slab. With a Winkler foundation, the slab rests on a bed of springs as shown in Figure 159. These springs release when the slab deforms upward to avoid tension in the springs. The interaction is defined in the initial step and is carried out through the entire analysis. The stiffness of the foundation is defined by setting the stiffness of the spring equal to the modulus of subgrade reaction (k-value) representing the composite stiffness of all layers beneath the slab.

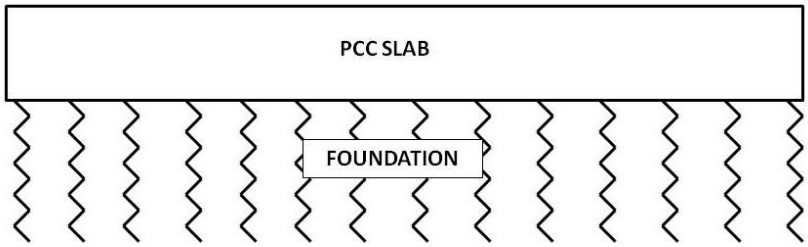

Figure 159: Model of a Slab Resting on a Winkler Foundation.

Mainline to Shoulder Contact

Contact between the mainline and the shoulder is defined by a surface-to-surface contact. In ABAQUS, surface-to-surface contacts are necessary to model interactions between two deformable bodies. A discretization method and sliding formulation must be chosen.

Choosing the proper discretization method is important so that the interaction between the surfaces is accurately modeled. The user can either choose surface-to-surface or node-to-surface. In general, the surface-to-surface discretization is more accurate than node-to-surface in terms of pressure and stress results. The surface-to-surface discretization was chosen despite additional required computation time.

With respect to choosing a sliding formulation in ABAQUS, there are two approaches for defining the relative motion between two surfaces, finite-sliding and small-sliding. The most general approach, finite-sliding, allows the contact surfaces to undergo separation, sliding, and rotation. In the small sliding approach, it is assumed that there will be little to no sliding

between the surfaces. Slave nodes (defined in the next paragraph) should slide less than an element length from their corresponding anchor point and still be contacting their local tangent plane. A definition of the anchor point and local tangent plane from the ABAQUS User Manual [19] can be seen in Figure 160. Small sliding was used since the amount of sliding (e.g. less than 1-in) expected is less than an element length (i.e. 2-in).

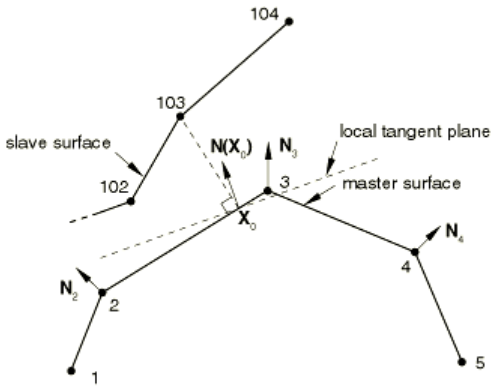

Figure 160: Anchor Point and Local Tangent Plane for Small Sliding[20].

Furthermore, when selecting the surfaces of the interaction, one surface must be defined as the master surface and the other must be defined as the slave surface. There are a few general guidelines provided by ABAQUS for selecting the master and slave surfaces. For a surface-to-surface discretization with small sliding, the choice of the master and slave surfaces is not very sensitive. For this contact interaction, the mainline was chosen as the master surface and the shoulder was chosen as the slave surface.

Once the contact interaction is defined, a contact interaction property must be defined. In the case of the mainline and shoulder interactions, "hard" contact, no separation, and no friction was chosen. This hard contact minimizes the penetration of the slave surface into the master surface at the constraint locations and provides limitless contact pressure once the nodes of the slave surface contacts the master surface. However, it allows no transfer of tensile stress across the interface. Regarding the tangential behavior, the contact between the lane and shoulder joint was initially modeled with coulomb friction. This assumption, however, led to an extreme build-up of pressure at the interface. By modeling the surfaces to be frictionless, more reasonable results

were obtained. From a practical sense this is also more reasonable as well since the interaction is modeling a cold joint.

7.11.3 Loading

ABAQUS allows users to define a sequence of one or more analysis steps. By dividing the analysis into steps, it provides a convenient way to capture changes in the loading and boundary conditions of the model, changes in the way parts of the model interact with each other, and any other changes that may occur in the model during the course of the analysis.

In this model, loading was applied in two steps. In the first step, a gravity load was applied. In the second step, a temperature was applied throughout the entire model.

Gravity Load

In ABAQUS, a gravity load can be applied if the density of the material is defined. The density for the concrete is defined as 0.084 lb/in^3 and the density for the steel is 0.28 lb/in^3. The acceleration, which has a magnitude of 386.4 in/s^2, is applied in the z-direction that generates the gravity load for all the parts based on their densities.

Temperature Load

Nodal temperatures can be applied as an initial condition or in any analysis step. Temperatures can be applied via direct specification or through the use of an analytical field. Applying a temperature via direct specification allows the user to assign a uniform temperature to any part. An analytical field is a mathematical function that defines spatially varying parameters, like temperature. If the temperature distribution throughout a slab is known (i.e. both the uniform temperature and the temperature gradient), a linear or quadratic function can be used to define the distribution and apply it to the model through an analytical field. Using an analytical field to define a temperature distribution requires significantly more computational time in comparison to using direct specification to apply a uniform temperature.

In this project, uniform temperatures were applied to the parts in order to study the stress developed due to the restraint of the contraction/expansion of the slabs. As the second step, temperature gradients were applied and would be used to study the stress developed due to the restraint of the curling of the slabs. When applying a uniform temperature, the temperature data came from mean monthly temperatures typical for the Blairsville area of Pennsylvania. Temperature gradients were predicted using the EICM [3]. In order for expansion or contraction to occur due to a change in temperature, a coefficient of thermal expansion must also be defined.

Surface Traction

The restraint provided by the base was modeled by a surface traction force. Since the traction force is applied over a surface, the units are in psi. By modeling the base this way, the computational time was significantly decreased since a separate base did not have to be meshed. If the slab is expanding, the surface traction force is applied radially inward and if the slab is contracting, the surface traction force is applied radially outward. This is conceptually illustrated in Figure 161.

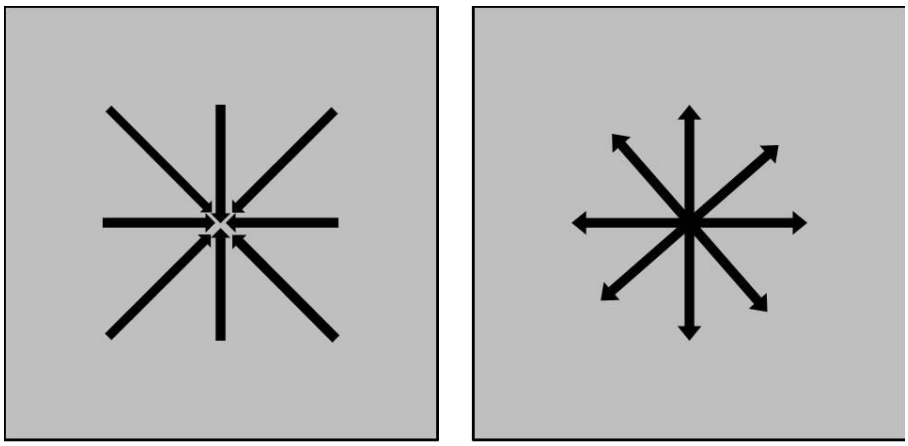

Expansion Contraction

Figure 161: Surface Traction Applied to Bottom of Slab to Represent the Base Constraints.

The surface traction force was calculated by determining the force required to drag the slab across a base and then dividing that force by the surface area of the bottom of the slab. Equation *6* was used to determine the surface traction force.

Equation 6

The force required to drag a slab across a base can be calculated using Equation *7*.

Equation 7

where:

F=Force required to drag slab across base, lbs

L=Length of slab, in

W=Width of slab, in

H=Slab thickness, in

UW=Unit weight of slab, pci

μ=Coefficient of friction

A study was performed at the Indian Institute of Technology that established coefficients of friction between the concrete slab and the underlying base as a function of the base type. The study determined that once the initial bond between the concrete slab and base was broken, the coefficient of friction significantly decreased [21]. In this study, the surface traction force was found to be 1.8 psi and 1.5 psi for a stabilized base and an unstabilized base, respectively.

7.11.4 Boundary Conditions

The boundary conditions in the shoulder transverse cracking model are defined as shown in Figure 162. In the model, the adjacent lane is tied to the mainline. To simulate this in ABAQUS, the outer edge of the mainline is restricted in the y direction. A symmetry boundary condition is applied relative to the y-axis, which makes the effective length of the model 90-in. With this type of boundary condition, the computational time is decreased by one half with no loss in accuracy. The entire model is free in the z-direction.

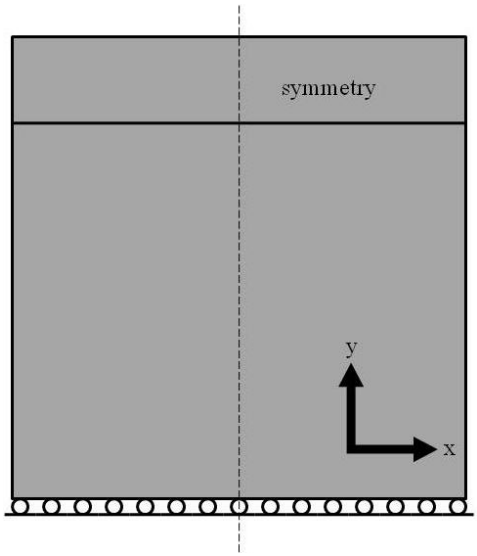

Figure 162: Shoulder Transverse Cracking Boundary Conditions.

7.11.5 Mesh

As mentioned in the introduction to Section 7.1. 20-node quadratic, reduced integration brick elements were used to mesh. Because there are several geometric discontinuities throughout the model, i.e. tie bars and dowel bars, difficulties can arise during meshing resulting in elements of large aspect ratios and interior angles that are less than 60° or greater than 120°. By creating partitions in the model, the majority of the problems in meshing can be eliminated. The shoulder is where the cracking was observed, which is why the mesh in the shoulder is much finer than the rest of the model. The optimum mesh fineness was determined by starting with very fine mesh and gradually reducing the fineness until the nodal stresses in the shoulder converged to a single value.

7.12 Finite Element Model Verification and Validation: US 22, Indiana County

7.12.1 Verification of the FEM Using Westergaard's Equations

Westergaard developed closed-form solutions of critical stresses for slab-on-grade pavements under three different loading conditions, namely interior, edge and corner loading [22]. The

solutions are an industry standard and are often used to verify numerical models. Several studies have been previously performed using different elements and mesh finenesses and then comparing them to the Westergaard equations. These studies have shown that an 8-node linear element, which is an 8-node brick, does not predict acceptable results in comparison to Westergaard's solution, even with a very fine mesh [23]. The 20-and 27-node quadratic brick elements were also evaluated. With a fine mesh, both elements do a good job in predicting stresses that are similar to those calculated using Westergaard's equations. There is a limitation in using this type of element however, namely the execution time of the 27-node element is 60 percent more than the execution time of the 20-node element [24]. The reduced integration 20-node quadratic brick element was chosen to be used for modeling, even for tie bars and dowel bars. The established model with the reduced integration 20-node quadratic brick element yielded the same predictions as the Westergaard's solution for all three loading conditions.

7.12.2 Validation of the FEM Using Field Measurements

The finite element model was also validated using field strain measurements and temperature data. Strains at three different depths were collected from vibrating wire strain gages installed in a smart pavement at US-22 in Murrysville, Pennsylvania [18]. Strains measured in the field due to changes in temperatures are compared to the strains predicted using the finite element model The temperature profile that was established using the temperature readings from the same smart pavement was introduced into the model to represent a point in time after paving. Temperature data was collected from the smart pavement project for over five years and the data is an excellent representation of typical temperature distributions encountered in Pennsylvania. Twenty-two different temperature profiles were chosen to validate the model. Using the method by Janssen and Snyder [25], the equivalent linear temperature gradients for the 22 profiles were calculated and ranged from -0.8 °F/in to 1.86 °F/in. The zero-stress temperature profile for the pavement in the field, which was established using [18], was used to define the initial condition in the model. The equivalent linear zero-stress temperature gradient was 0.32 °F/in. The predicted strain is plotted against the measured strain for all 22 temperature profiles. The results are presented in Figure 163, Figure 164 and Figure 165, for the top, middle and bottom of the slab, respectively. The correlation coefficient (R^2) between the predicted and measured is equal to 0.92, 0.99, and 0.89 for the top middle and bottom of the slab, respectively. This indicates that the models accurately reflect the response of the pavement measured in the

field for 22 different temperature loading conditions.

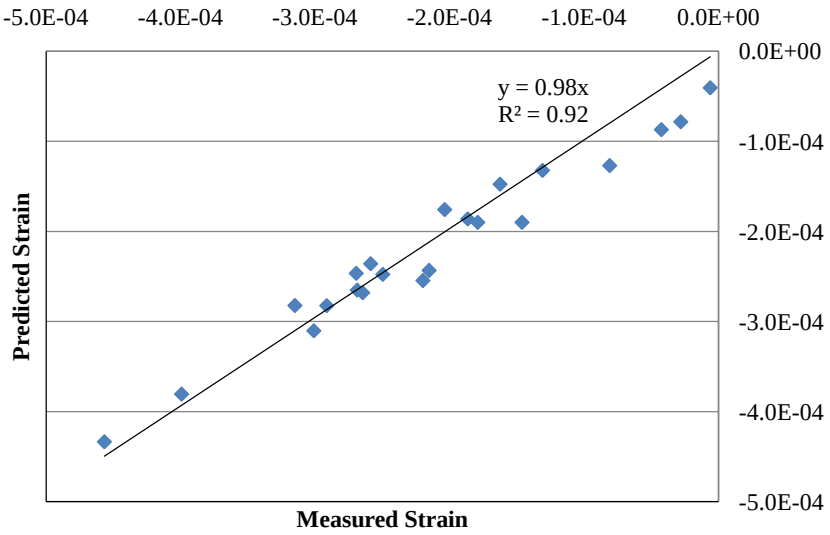

Figure 163: Predicted vs. Measured Strains for the Top of the Slab.

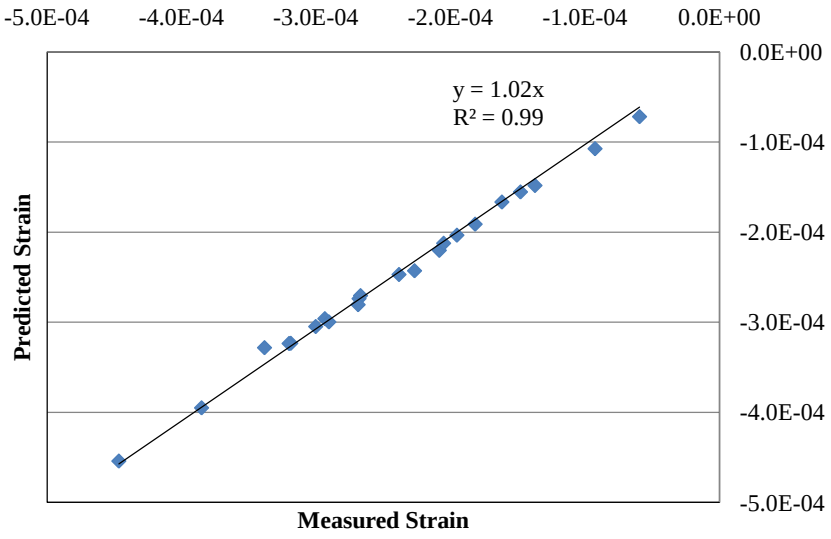

Figure 164: Predicted vs. Measured Strains for the Middle of the Slab.

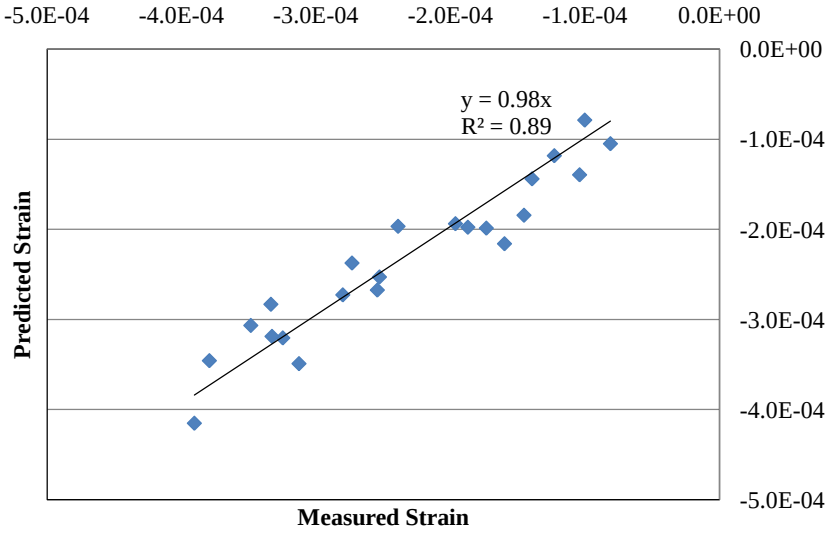

Figure 165: Predicted vs. Measured Strains for the Bottom of the Slab.

7.13 Finite Element Model Parametric Studies: US 22, Indiana County

As mentioned in section 7.10, the parameters that were hypothesized to be responsible for the shoulder transverse cracking consist of CTE, stiffness/strength of the shoulder, shoulder width, and construction sequence. The values of these parameters used in the finite element model except the construction sequence can be found in Table 64. The elastic modulus and Poisson's ratio of the mainline represent the values of the concrete cores tested in the laboratory. The elastic modulus of the shoulder was varied between 2.8 and 3.3 million psi as 1-day and 7-day stiffness, respectively. It is understood that the stress development is a function of the stiffness of the concrete. This indicates that the stress developed at 1 day would be lower than that at 7 days. However, as the hydration proceeds, the concrete is also stronger at 7 days than 1 day. Therefore, it is reasonable to assume that a crack would develop wherever the principal stress due to the change of uniform temperatures is greater than the tensile strength of the concrete or the principle stress due to temperature gradients is greater than the flexural strength. A two-step procedure was employed to consistently estimate the flexural strength and the elastic modulus at any age of the concrete based on the 28-day compressive strength, since the 28-day compressive strengths can usually be more readily obtained. The first step is to use the compressive strength to estimate the modulus of rupture according to Equation 8.

Equation 8

where,

MR = modulus of rupture, psi

f'c = compressive strength at 28 days, psi

The next step is to determine the ratio of the tensile and flexural strength at a given age to the corresponding values at 28 days using Equation 9.

Equation 9

where,

F_STRRATIO_3 = ratio of tensile and flexural strength at a given age to tensile and flexural strength at 28 days

AGE = specimen age, years

Once the strength ratio for a particular age is established, the tensile/flexural strength can be determined by multiplying the ratio for a given day by the tensile/flexural strength at 28 days. Using Equation 8 and Equation 9, together with Equation 10 below, the elastic modulus can be estimated for a given compressive strength at any age of the concrete.

Equation 10

where,

E_c= PCC elastic modulus, psi

ρ = unit weight of concrete, lb/ft^3

f'c = PCC compressive strength at 28 days, psi

Using the procedure outlined above, the strength of the concrete was established for each analysis based on the tensile/flexural strength. Using this method, a modulus of rupture of 400 psi and a f't of 360 psi was established for a stiffness of 2.8 million psi and a modulus of rupture of 450 psi and f't of 405 psi was established for a stiffness of 3.3 million psi.

The values of 4.5, 5.5 and 7.5 x 10-6 /°F were chosen for the CTE because they represent the low, medium, and high values typical for paving mixes. Shoulder widths of 2 ft, 5 ft and 10 ft were chosen to be included in the study with a 2-ft shoulder representing the shoulder that cracked at US 22, Indiana County. While the 2-ft shoulder was used on this project, it is thought that one of the factors contributing to the cracking is the width of the shoulder. Therefore, two additional shoulder widths of 5-ft and 10-ft were also considered to investigate the effects of the shoulder width. The unit weight of the concrete is 0.084 pci, which corresponds to a typical value of 145 pcf.

Table 64: Material Properties for Shoulder Transverse Cracking Model.

	Elastic Modulus,10^6psi	Poisson's ratio	Modulus of Rupture, psi	CTE, 10^{-6}/°F	Unit Weight, pci	Width, in
Mainline	4.5	0.17	650	4.5, 5.5, 7.5	0.084	144
Shoulder	2.8 and 3.3	0.17	400 and 450	4.5, 5.5, 7.5	0.084	24, 60, 120
Tie Bar	29	0.3	n/a	n/a	0.28	n/a

The following variables were defined in this model to study how the difference in zero-stress temperatures affects the shoulder transverse cracking.

T_S= Zero-stress temperature of the shoulder, °F

T_M= Zero-stress temperature of the mainline, °F

T_A= Pavement temperature at a point in time after paving of the shoulder is completed, °F

T_D=T_M-T_S, °F

T_C=T_M-T_A, °F

The mainline was paved in October corresponding to a zero-stress temperature of approximately 80°F using Equation 5. The 2-ft shoulder was paved in the following July, which corresponds to a zero-stress temperature ranging from 90°F to 110°F. The cracking was identified within the first week after paving the shoulder. Using the ambient temperatures recorded during this week, the pavement temperatures were calculated using the EICM [3], which ranged from 50°F to 80°F. The construction sequences in terms of the temperatures are presented in Table 65.

Table 65: Potential Construction Sequences Critical to Shoulder Transverse Cracking.

T_M, °F	T_S, °F	T_C, °F
80	90, 100, 110	30, 20, 10, 0

7.13.1 Parametric Analysis of Shoulder Transverse Cracking Model

The following sections will discuss each parameter and the influence it has on the development of transverse cracking in the shoulder. Figure 166 shows a summary of the results for the stiffness of 3.3 million psi (corresponding to the seventh day). As shown in Figure 166, a crack is likely to occur for any stress larger than 405 psi.

From Figure 166 it seems that whether or not a crack will occur depends on the values of T_D and T_C. Assuming a CTE of $5.5x10^{-6}$/°F and 7-day strength/stiffness, a T_D of -10°F will not result in cracking unless the value of T_C is 20°F or higher. A T_D of -20°F will not produce cracking if T_C is lower than 10°F. A T_D of -30°F will result in cracking even if T_C is 0°F. The potential for a shoulder to develop transverse cracking based on the construction sequence and CTE can also be expressed as shown in Table 66.

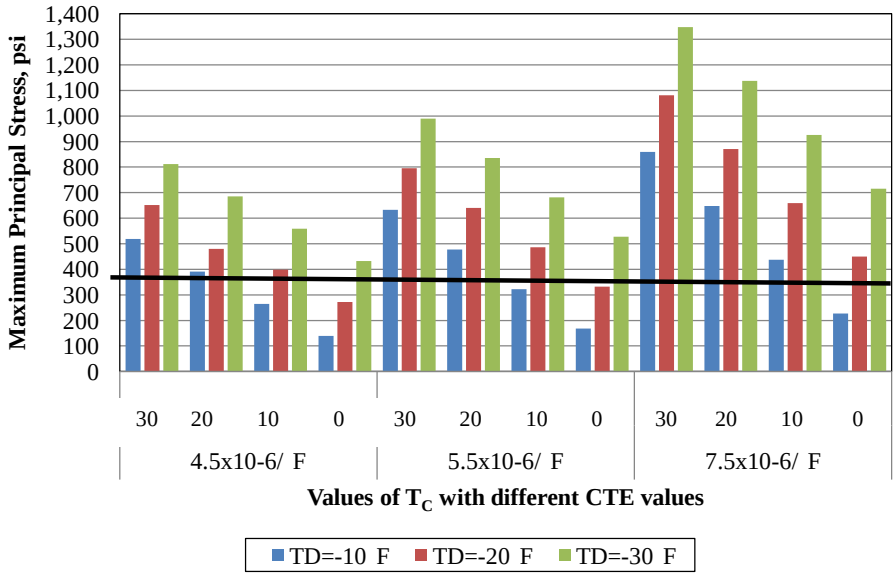

Figure 166: Critical Value of T_C for Different CTE Values with a Tensile Strength of 405 psi.

Table 66: Crack Potential Based on Construction Sequence and CTE.

	CTE 4.5 x10^{-6} /°F			
	T_C, °F			
T_D, °F	30	20	10	0
-30				
-20				
-10				
	CTE 5.5 x10^{-6} /°F			
	T_C, °F			
T_D, °F	30	20	10	0
-30				
-20				
-10				
	CTE 7.5 x10^{-6} /°F			
	T_C, °F			
T_D, °F	30	20	10	0
-30				
-20				
-10				

Note: Highlighted Cell Indicates Risk a Crack May Develop

Based on this result, the best way to avoid the shoulder transverse cracking seems to be constructing the shoulder and the mainline at similar temperatures. If it is unavoidable to construct the mainline and shoulder during the same season, Equation 5 can be used to determine the difference in zero-stress temperatures for the mainline and shoulder. The best months to construct pavements are the months when the pavement temperatures night are not too low. In Pennsylvania, these months seem to be from May to September. It is also possible to pave in April and October as long as the ambient temperature is relatively high.

Coefficient of Thermal Expansion

Figure 166 shows the effect that CTE has on transverse cracking in the shoulder. As expected, a larger CTE results in a higher chance for crack to develop. A lower CTE reduces the chance for cracking. According to the LTPP database, the national average for CTE is approximately 5 to 5.5 x10^{-6} /°F.

Shoulder Width

Figure 167, Figure 168 and Figure 169 show screen shots from three models that are identical except for the shoulder width. In Figure 167, the three models have a CTE of 4.5x10^{-6}/°F and

stiffness of 2.8 million psi. There is no crack present and at first glance, it would appear as if there is no difference between the three different shoulder widths with respect to the maximum stress magnitude. Despite seeing a lack of variation in the magnitude of the stress, the distribution of stress in the shoulder is different among the three models in Figure 167. In the 2-ft shoulder, there is an area of higher stress that is located in the center of the shoulder and extends across almost the entire width. In the 5-ft shoulder, that same area of higher stress still extends across almost the entire width of the shoulder but the area of higher stress begins to taper as it reaches the outside edge of the shoulder. In the 10-ft shoulder, the area of higher stress extends across a noticeably smaller width of the shoulder. It can be noticed from Figure 167 that the tie bars have a major influence on the area of higher stress. Although not completely apparent, the area of higher stress begins where the first tie bar is located and ends where the last tie bar is located. Figure 170 is more effective in illustrating this point.

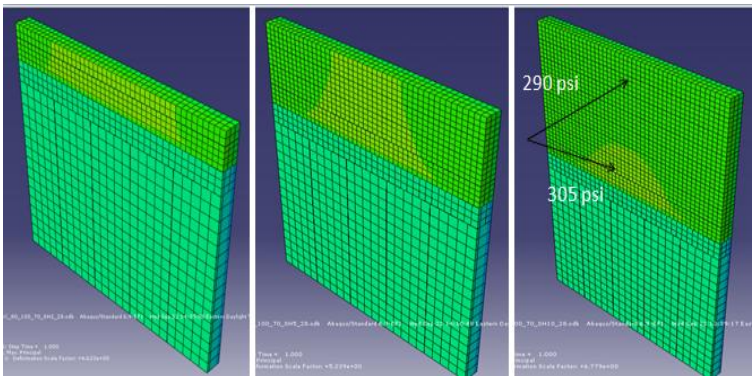

Figure 167: Influence of Shoulder Width When T_D=-20°F and T_C=70°F for the Shoulder Transverse Cracking Model.

In Figure 168, the three models have a CTE of 5.5×10^{-6}/°F and a stiffness of 2.8 million psi. The calculated stress in this figure is less than the strength of the concrete. It should be noted that for the color schemes within the same figure, areas represented by the same color share the same magnitude of stress. These same comparisons cannot be made between different figures because colors represent different magnitudes of stress for different figures. Similar to Figure 167, there is an area of higher stress in the 2-ft shoulder that is located in the center of the shoulder and extends across the entire width. However, compared to Figure 167, the area of higher stresses in Figure 168 diminished significantly quicker and extends only a 1-ft across the

shoulder. This might be due to the fact that the thermal incompatibility (T_D=-10°F) for models in Figure 168 is smaller than that for models in Figure 167 (T_D=-20°F).

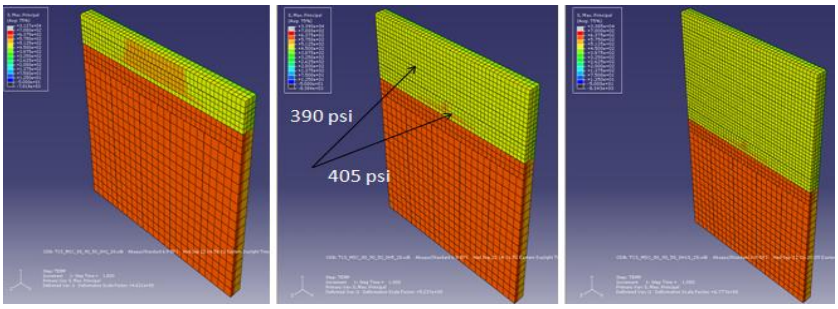

Figure 168: Influence of Shoulder Width When T_D=-10°F and T_C=50°F for the Shoulder Transverse Cracking Model.

In Figure 169, the three models have a CTE of 7.5x10^{-6}/°F and stiffness of 2.8 million psi. In all three of the models, the predicted stresses exceed the defined strength of the concrete indicating a crack occurring for all three models. In the 2-ft shoulder, there is an area of higher stress that is located in the center of the shoulder and extends across the entire shoulder width. In the 5-ft shoulder, the same area of higher stress still extends across the entire width of the shoulder; however, it begins to thin out as it reaches the outside edge. In the model with the 10-ft shoulder, the area of higher stress extends only a few feet across the shoulder. In all three of the models, the area of the shoulder that has a high stress concentration is the area around the tie bars.

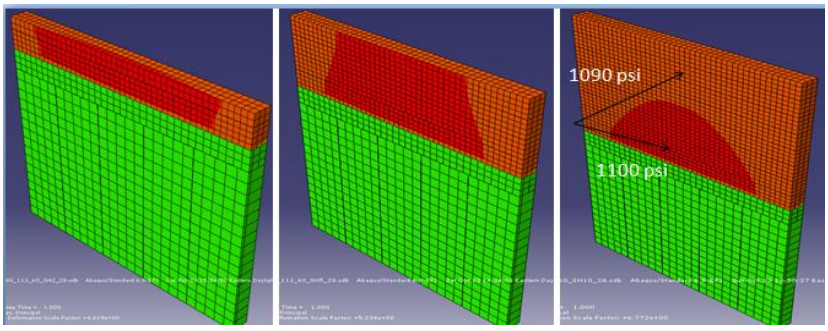

Figure 169: Influence of Shoulder Width When T_D=-30°F and T_C=70°F for the Shoulder Transverse Cracking Model.

Figure 170 illustrates the concentration of stress surrounding the tie bars. This is a model

that is sliced in the z-direction so that the tie bars are visible. The larger stresses clearly begin to form around the tie bars. This holds true for all of the cases in the parametric study.

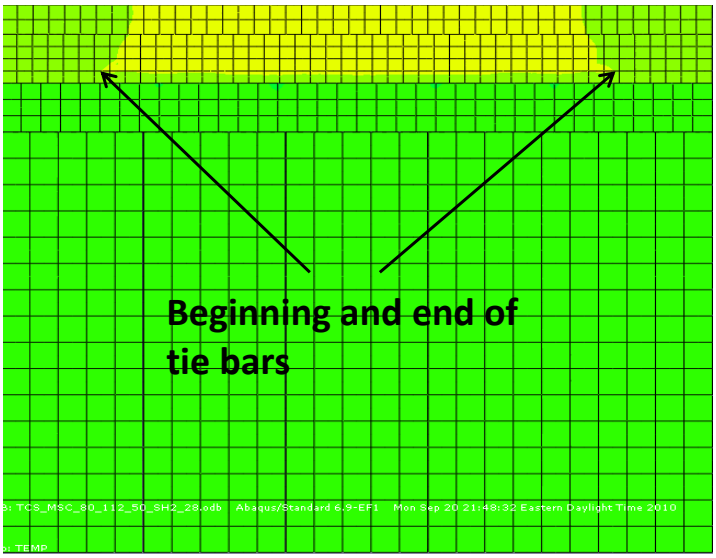

Figure 170: Illustration of the Stress Concentration Surrounding the Tie Bars in the Shoulder Transverse Cracking Model.

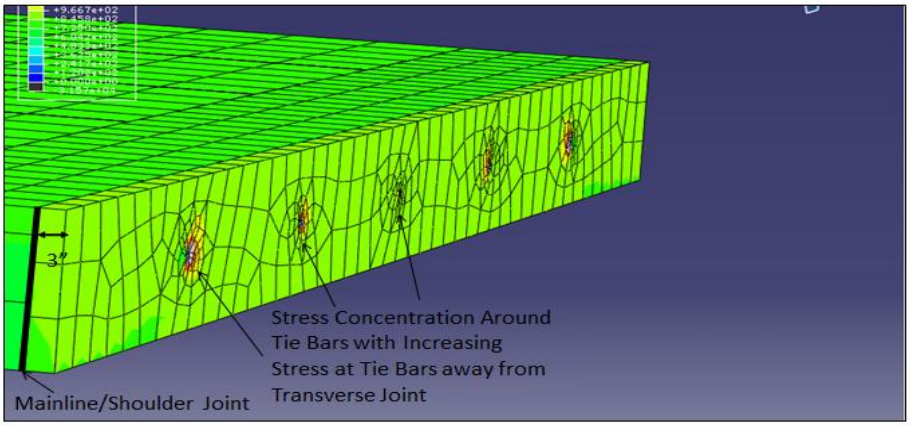

(a)

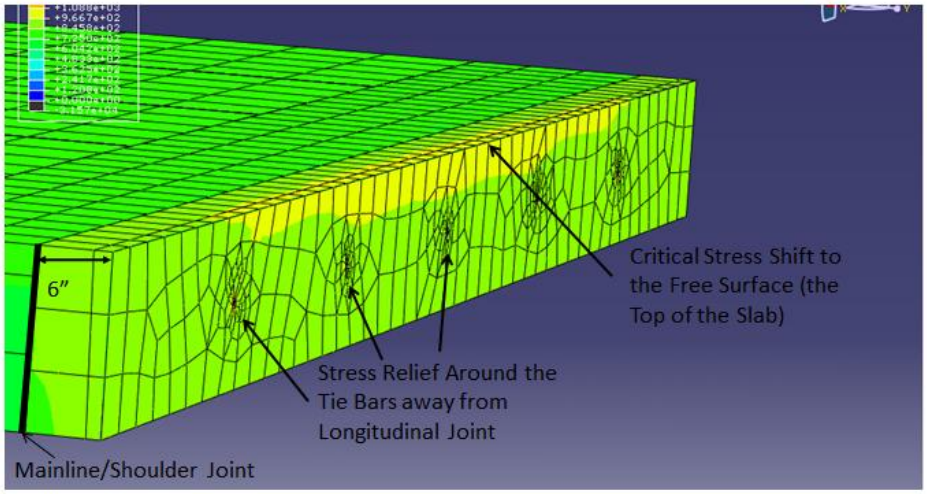

(b)

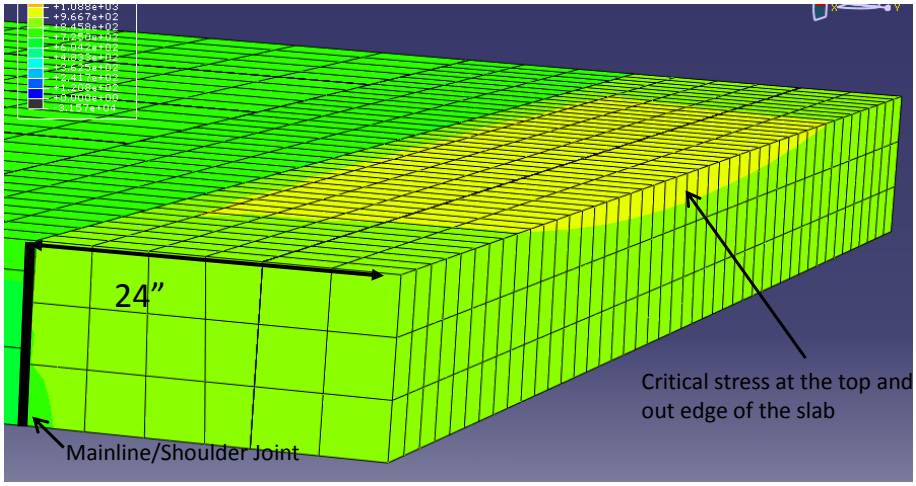

(c)

Figure 171: Illustration of the Shift of Stress Concentration from the Tie Bars to the Free Surfaces in the Shoulder Transverse Cracking Model.

Cross sections were cut as shown in Figure 146 to examine the details in the stress concentration around the tie bars. In Figure 171, three such cross sections that are 3 in, 6 in and

24 in away from the mainline/shoulder joint are shown. From Figure 171 (a), it is easy to observe that the stress concentration is more severe at the tie bars that are closer to the transverse joints. This observation results from the symmetry of the problem resulting in less constraint to relative displacement between the mainline and the shoulder at the transverse joint than at the mid-slab. More importantly, it is found through examination of Figure 171 (a, b, and c) that the stress concentration shifts away from the tie bars towards the free surfaces. Comparing Figure 171 (a, b, and c) it can be seen that trend becomes more pronounced as the cross section moves further away from the mainline/shoulder joint and starting with the cross section that is at 2 to 3-in from the mainline/shoulder joint.

This shift of stress concentration is highly oriented, as shown in Figure 171 (b) towards the free surfaces where the least constraint for displacements exists. Furthermore, in Figure 171 (b), it can be seen that the stress concentration zone reaches the top of the slab after 6-in from the mainline/shoulder joint. After a distance of 6 in from the mainline/shoulder joint, this zone remains constant and within the top 2 to 3 in of the shoulder as indicated by Figure 171 (c) that shows a cross section 24 in away from the lane-shoulder joint.

An additional conclusion based on Figure 171 (a) through (c) seems to be that the stress concentration occurs in the concrete surrounding the tie bars caused by the load transfer through the tie bars and the critical stress most likely lies at a zone that is around the top and outer edge of the shoulder. Although in Figure 171 (c), it appears that such a zone might cross the majority of the width of the shoulder, in actuality the zone will get narrower when the microcracks start to occur in the concrete around the tie bars due to the dramatic stress generated at these locations. Microcracking around the tie bars, starting with the tie bars towards the transverse joints will release some of stresses there and the stresses will be redistributed resulting in more stress at the middle of the shoulder. A cascading effect would likely result in this instance with each occurrence of microcracking at a tie bar resulting in the stress zone moving closer to the top and outer edge of the shoulder.

Based on the numerical modeling, the cracks might have initiated at the top and outer edge of the shoulder. This agrees with the field observation as mentioned in Section 7.7. It is unknown if there are any cases where this distress occurs in a shoulder that has a width greater than 2 ft. It is believed that if this distress commonly occurred in larger shoulders, it would have already been studied and documented since 5 and 10-ft shoulders are much more common than 2-ft shoulders.

Since there is no known documentation of this distress that is specific to shoulders with larger widths, it might be unique to 2-ft shoulders. Because the area of high stress concentration does not extend all the way across the 10-ft shoulder, it is believed that micro cracks will form around the tie bars relieving the stress in the area and causing the stresses to redistribute.

Stiffness and Strength

The stiffness of the concrete was only defined using the elastic modulus and Poisson's ratio. However, by increasing the stiffness, the trigger value for flexural strength also increases. Figure 172 shows 12 different scenarios with two different stiffnesses. The stiffness of 2.8 million psi corresponds to the 1-day strength and 3.3 million psi corresponds to the 7-day strength. The stresses seen with 3.3 million psi stiffness are larger than the stresses seen with 2.8 million psi stiffness; however, the strength for the stiffer concrete is also greater. Based on the results from Figure 172, it can be concluded that the transverse cracks in the shoulder could occur at any of the first few days.

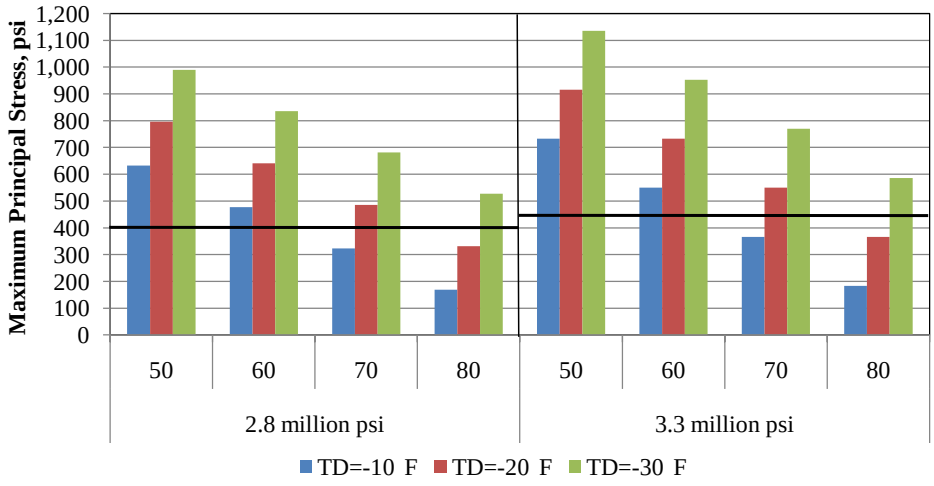

Figure 172: Influence of Concrete Stiffness and Strength on the Shoulder Transverse Cracking.

Gradients

The parametric study was carried out assuming that the temperature throughout the slab was uniform. By doing this, only the stress due to uniform temperature change alone was examined. By introducing a gradient, the stress due to restraining the curling of slabs is highlighted in addition to the stress due to uniform temperature change. Six different linear temperature gradients were used with two different values of T_S in order to evaluate the effect that gradients have on stresses in the shoulder. All six of the gradients have the same average temperature of 60°F and their temperature distributions throughout the slab are presented in Table 67.

Table 67: Temperature Gradients Used in the Shoulder Transverse Cracking Model

	Depth, in					
Gradient °F/in	0	2.5	5	7.5	10	12
-0.38	56	57	58	59	60	61
-0.75	54	56	58	60	62	64
-1.5	50	54	58	62	66	69
0.38	61	60	59	58	57	56
0.75	64	62	60	58	56	54
1.5	66	62	58	54	50	47

Figure 173 shows the effect of positive and negative gradients in comparison to a uniform temperature for a TD of -10°F and -30°F. In general, the critical tensile stress occurs at the bottom of the slab when a positive gradient is present and it occurs at the top of the slab when a negative gradient is present. Therefore, in Figure 173, the stresses with the negative gradients were recorded at the bottom of the slab and the stresses with the positive gradients were recorded at the top of the slab. When there is no gradient present, the critical stress location is at the top of the slab.

As shown in Figure 173, a positive gradient does not have an effect on the magnitude of stress when compared to a situation with no gradient. If there is a negative gradient present in the slab, the stresses at the top of the slab are magnified, even for the smallest gradient of -0.38 °F/in.

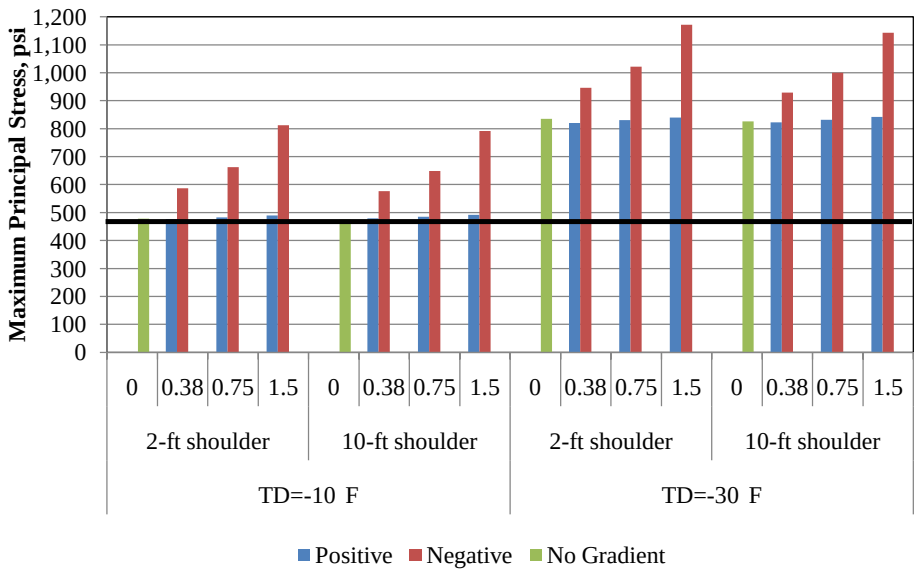

Figure 173: Effect of Gradients When T_S = 110 °F in the Shoulder Transverse Cracking Model

7.14 Finite Element Model Conclusions: US 22, Indiana County

7.14.1 General Finite Element Model Conclusions

The following general conclusions were made based on the results of the parametric study undertaken as part of the investigation into the cracks in the 2-ft shoulder of US 22, Indiana County:

- Casting the mainline and the shoulder in different month results in different zero-stress temperatures and gradients. The difference in zero-stress temperatures T_D and the transient pavement temperature T_C are found to be the most significant factor in the occurrence of the shoulder transverse cracking. The critical combinations of T_D and T_C for the cracks to occur are presented in Table 66.
- This cracking in the shoulders could have developed the first day after paving.
- The cracks initiate at the top of the slab, close to the tie bar.

- A large CTE increases the probability that a crack will develop.
- A 2-ft shoulder increases the probability that a crack will develop because the tie bars extend over half the width of the slab. With a 2-ft shoulder there is less concrete beyond the tie-bar in the direction of the free edge and less concrete through which the stress concentration around the tie bar can dissipate.
- The presence of a negative gradient magnifies the effect of a uniform temperature change and increases the probability that a crack will develop.

7.14.2 Finite Element Model Conclusions With Respect to US 22, Indiana County

The finite element model developed as part of addressing the distress found at US 22, Indiana County identifies the critical factors that generally influence the initiation of a crack in a shoulder. Based on the results of this model, criteria were established for limiting shoulder cracking.

Of the parameters investigated as part of the parametric study, the concrete properties such as the CTE, strength, and stiffness, as well as other necessary parameters such as the range of ambient temperatures in the week after paving and the shoulder thickness are well known. The parameters that are known with less certainty are the temperature gradients in both the shoulder and mainline and the zero stress temperatures of both the shoulder and the mainline. In Section 7.4 it was stated that the zero stress temperature for the mainline, $T_{M,}$ can be assumed to be 80^{o}F, based on the mean monthly average temperatures. However, this does not explain the discrepancy in the observations of the percentage of cracked panels as shown in Table 61.

The fact that the lab determined parameters did not vary much between the sections might be due to the fact that they were paved with the same concrete mix, from the same concrete plant and over a relatively short period of time. It is believed that the variation shown in Table 61, is due to the variation in the parameters that are known with less certainty, such as the zero stress temperatures for both the mainline and the shoulder. These parameters were also stated to be one of the most important parameters influencing the probability for cracking in Section 7.14.2.

In order to get a better estimate of the zero stress temperatures of the mainline and the shoulder, T_M and T_S respectively, the available construction records were reviewed to obtain

ambient temperatures and concrete temperatures corresponding with the paving of both the 2-ft shoulders and the mainline. Table 69, together with Figure 174, presents the available information for this project with regards to determining the construction sequencing and also the zero stress time.

The available information regarding the paving of the shoulders was that the paving of the 2-ft shoulders took place during the week of July 6th, 2009 (sometime in the week before the cracks were noticed) and that the range of temperatures during that week was 50-73^{o}F. These temperatures correspond to a range of zero stress temperatures of 71-105 ^{o}F as determined by using these ambient conditions as the mean monthly temperature in Equation 5.

For the 7 mainline sections corresponding to the 2-ft shoulder sections, information regarding the exact construction data was available for only the three westbound sections, namely Sections 1, 3, and 6. Using the ambient temperatures recorded in the construction records for these sections and Equation 5, a range of zero stress temperatures was predicted for each section. This range can be found in Table 69. Using the range of values shown in Table 69, Table 68 was generated and shows that the range of potential differences in the zero stress time between the mainline and the shoulder encompasses the entire range of the value T_D investigated as part of the parametric study in Section 7.13.1. An examination of the temperatures during the week after paving shows that the entire range of T_C investigated as part of the parametric study was also encompassed.

Because of the limitations in establishing the inputs to be used by the model in this instance, a more general approach was taken to comment on the results of the finite element modeling effort with respect to what actually happened in the field at US 22, Indiana County. From Table 68, it can be observed that the most negative value of T_D corresponds with Section 1, and a nearly zero value of T_D corresponds with Section 6. Looking at the cracking that developed in the field, it can be seen that the largest amount of cracking occurred in Section 1 and that no cracking occurred in Section 6 with the cracking in Section 4 being between the cracking observed in Sections 1 and 6. This observation reflects field conditions quite well and bolsters the conclusions drawn from the model as presented in Table 66, where for concrete with a CTE of 5.5 °F/in, slabs with T_D of 0 will not crack and slabs with T_D of -25 will crack the most.

Table 68: Range of Possible Differences in T_D for US 22, Indiana County

Section	T_D(min), °F	T_D(max), °F	T_D(mean), °F
1	-63	6	-25
4	-38	6	-16
6	-20	17	4

7.14.3 Example of Determining the Potential for Cracking in Multi-phase Paving

An example calculation has been provided below to provide further clarification of the steps in the analysis process. This example is based on the data collected for Section 1 of this project.

Step 1. Determine the Zero-Stress Temperature for the Mainline, T_M

Equation 5 [7]is used to determine T_M. The inputs needed for this equation include the ambient temperature during construction (MMT) and the cement content for the concrete mixture (CC). The average ambient temperature is 46 °F, as provided in Table 69, and the cement content is 500 lbs/yd^3, as provided in Table 57. Using these inputs and Equation 5, the T_M is calculated as 64 °F.

Step 2. Determine Zero-Stress Temperature of the Shoulder, T_S

The average ambient temperature and cement content for the shoulder are 67 °F and 500 lbs/yd^3 from Table 69 and

Table 57, respectively. Equation 5 is again used to determine T_S, which is 89 °F.

Step 3. Determine Difference in Zero-stress Temperatures, T_D

The difference in zero-stress temperatures between the mainline and the shoulder is calculated as $T_D=T_M-T_S=64-89=-25°F$.

Step 4. Determine the Ambient Temperature at a Point in Time after Paving of the Shoulder, T_C

Table 60 summarizes the climatic conditions for the first week after the 2-ft shoulders were paved. The lowest temperature encountered during this time period is 52°F. Therefore, T_C was found to be between 12°F and -18°F.

Step 5. Determine the Cracking Potential

Table 66 can now be used to determine the cracking potential. Since the CTE for Section 1 is 5.8×10^{-6} /°F from Table 63, the second table in Table 66 would be appropriate. With T_D= 25°F and T_C being between 12°F and -18°F, Table 67 indicates that there is a potential for cracks to develop in the 2-ft shoulders of Section 1. This prediction agrees with what has been observed, as shown in Table 69.

Table 69: Available Sequencing Information for the Construction of US 22, Indiana County

Section	Structure	Direction	Date Paved	Concrete Temps °F	Ambient Temps °F	Zero Stress Temps*	Percent Shoulders Cracked	Remarks
	Mainline	WB	10/20/08	55-68	31-61	42-85		No Midbay Sawing
1	Shoulder		7/15/09**	Unknown	52-82	71-105	84	
	Mainline	EB	Unknown	Unknown	Unknown	Unknown		No Midbay Sawing
2	Shoulder		7/15/09**	Unknown	52-82	71-105	25	
	Mainline	EB	Unknown	Unknown	Unknown	Unknown		No Midbay Sawing
3	Shoulder		7/15/09**	Unknown	52-82	71-105	11	
	Mainline	WB	10/17/08	62-67	48-55	67-77		Sawed/Sealed at Midbay
4	Shoulder		7/15/09**	Unknown	52-82	71-105	57	
	Mainline	EB	Unknown	Unknown	Unknown	Unknown		Sawed/Sealed at Midbay
5	Shoulder		10/20/08	Unknown	52-82	71-105	0	
	Mainline	WB	10/15/08	62-67	61-75	85-98		Sawed/Sealed at Midbay
6	Shoulder		10/20/08	Unknown	52-82	71-105	0	
	Mainline	EB	Unknown	Unknown	Unknown	Unknown		No Midbay Sawing
7	Shoulder		10/20/08	Unknown	52-82	71-105	0	

* Predicted Using Equation 4 ** Only Week, Not Exact Day of Paving Known

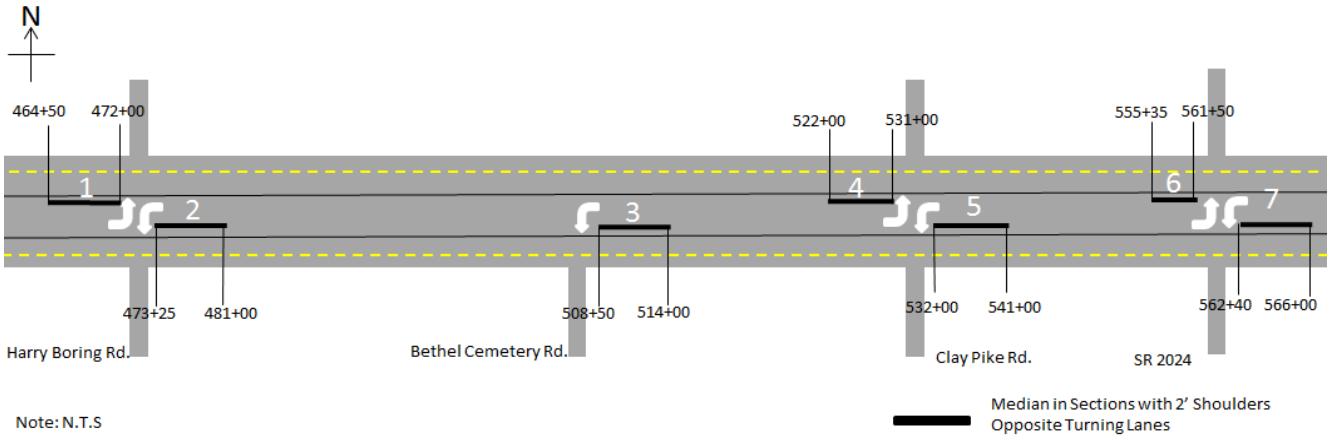

Figure 174: Relative Location and Stationing of 2-ft Shoulder Sections of US 22, Indiana County

7.15 Rehabilitation Recommendations: US 22, Indiana County

For addressing the main distress, the mid-slab shoulder cracks that developed in the 2-ft shoulders, the best solution is likely to simply monitor the 2-ft shoulders to see if more cracks develop or how the existing cracks respond to either extreme temperature conditions and vehicle loads. It does not seem necessary to seal the cracks at this point due to the fact that cracks are tight and most likely prevent infiltration of water on their own. While both the mainline and shoulder concrete has gained strength and will continue to gain additional strength with time, the additional stress induced by wheel loads and more extreme environmental conditions has not been evaluated. It seems likely that additional cracks will not in the 2-ft shoulders. If these cracks do deteriorate, then either full-depth repairs, or possibly cross stitching if the deterioration was of low severity, would be acceptable.

7.16 Future Projects: US 22, Indiana County

For US 22, Indiana County this research has provided a better understanding of distresses that develop due to delayed shoulder construction for PCC pavements through a validated finite element model. The model revealed the mechanism of the distress for US 22, Indiana County and the factors that influence it. The following recommendations can be made for preventing such distress in future practice.

- If paving in a region where large daily swings in temperature are common, it is recommended that the mainline and shoulder be paved during the same season to reduce the value of T_D below 20°F. The values of T_D and T_C should follow the guidelines proposed in Table 66. When at all possible, both values should be kept to a minimum.
- Shoulders with widths less than 5-ft are more likely to crack than shoulders larger than 5-ft because of the depth of tie bar embedment. Based on this observation it is recommended that to prevent cracking, shoulders less than 5-ft wide should be avoided when possible if paving of the adjacent lances will not be performed in the same season. Specifications should address stricter placement conditions when shoulders less than 5-ft wide are placed such as requiring that these shoulders be placed monolithically. In general, placing shoulders with the mainline monolithically will significantly reduce the potential for this type of cracking to occur.
- Based on this study, the best months to construct the mainline and shoulder separately in

Pennsylvania are from May to September. If the mainline is constructed outside of this time window, the contractor should wait to tie on the shoulder until the value of TD meets the criteria in Table 66. It is possible to pave the shoulder in April is the mainline is paved in October as long as the ambient temperature is higher than normal. To estimate the best times for paving in other climatic regions, Equation 2.1 can be used to determine the difference in zero-stress temperatures for each month. For this study, it is also important to consider the value of T_A, use Table 66 for guidance

- Using a concrete with lower CTE will help to reduce the potential for a crack to develop if mainline and the shoulder are to be paved during different seasons.

8 Conclusions and Options to Consider

A summary of the conclusions obtained from the analysis performed on the six projects is provided below along with recommendations for future prevention and options to consider in the future.

8.1 Conclusions

1. OGS

This section discusses the performance of the pavement sections with OGS. As presented in Sections 2.2, 5.2, and 6.2, three of the projects, SR-60 (Distressed section), I-79 (Distressed and Control sections), and I-80 (Distressed and Control sections) were placed with an OGS layer. For both the SR-60 and I-79 projects, the increase in performance observed in the Control sections was the result of an increase in the flexural capacity of the slab. For the SR 60 project, the use of a stabilized base increased the structural capacity of the pavement and the number of fatigue cracks was reduced when compared with the section with the OGS base. On I-79, both the Control and Distressed sections had an OGS but the fatigue cracking was less in the Control section since the slab thickness was 1 in thicker in the Control section. There also appeared to be drainage issues that contributed to the increase in cracking observed in the I-79 Distressed section.

As presented in Section 6.2, I-80 had an OGS in two different layers. The first OGS layer is under the rubblized PCC layer and the other is under the PCC slab. Both sections exhibited less cracking than was predicted using the MEPDG. This indicates that a good performance can be achieved with this type of base material. An analysis of the fatigue cracking for the pavements having an OGS has shown that a reduction in the structural capacity of a pavement with an OGS, as compared to a pavement with a bonded stabilized base, should be accounted for when establishing the slab thickness.

Loss of support underneath joints and cracks was found for all of the sections with OGS. Since no evidence of pumping was observed in the field, this loss of support is attributed to the consolidation or degradation of the OGS over time. It should be noted that the majority of the loss of support issues were at cracks and not near the doweled joints. The effect of this loss of support depends on the structural characteristics of the pavement, as well as the soundness of the aggregate used to construct the OGS. It was observed that for thicker slabs with relatively small

loss of support due only to consolidation, there is no effect on the pavement performance. In other cases, when in addition to the loss of support due to consolidation there is erosion or the migration of fines from the lower layers, additional distress will develop.

The site visit for I-79 revealed that additional loss of support occurred in the Distressed section. This observation was supported by the FWD data analysis. This loss of support was observed in areas where the evidence of drainage deficiencies was noticed. Consequently, the transverse cracking observed in the Distressed section of I-79 can be attributed to the higher critical stresses present in the slab due to unsupported areas created by the consolidation and erosion of the OGS. In the case of the Control section for I-79, the loss of support due to consolidation of the OGS was not sufficiently large to affect the performance of the section.

Granular bases are used quite successfully by many states and can be a viable base layer option for JPCP. Most of the difficulties with the OGS used by PennDOT can be attributed to the fact that the permeability is so high that the stability of the layer is greatly sacrificed. The OGS gradation specification was most likely developed based on the old FHWA recommendations of a permeability of 2,000 ft/day. Since this time, it has been found that this large permeability is unnecessary and that it can actually be detrimental to the performance of the pavement if a layer with this permeability is not stabilized. It is recommended that the gradation be adjusted so that the permeability is closer to 750 ft/day. This would be helpful in maintaining a sufficient amount of permeability while still providing some stability. If a granular base is used the reduction in the flexural capacity of the pavement should also be considered when establishing the thickness of the slab to account for the reduction in flexural capacity as compared to when a stabilized base is used. Designing the pavement using the MEPDG will more accurately account for this as compared to using the AASHTO 1993 Design Guide.

2. Placement, Finishing and Curing

Drying shrinkage cracking was observed on the majority of these projects. These cracks typically propagate to a depth of about 0.75 in. They typically are a greater concern in contributing to material-related distress than fatigue cracking since, although the cracks do not propagate to a significant depth, they make the surface of the pavement more porous. This was observed in projects like 202 where a combination of factors contributed to the degradation of the concrete, including increased surface porosity as a result of drying shrinkage cracking.

Although not common, it appears drying shrinkage cracks that developed on I-80 appeared to eventually contribute to the development of full depth fatigue cracks.

These cracks can be prevented through the adoption of proper curing and finishing practices. The soaked burlap drag commonly drug behind the paver as shown in Figure 77 should be eliminated. This practice creates a high water to cement ratio at the surface and thereby increases the potential for drying shrinkage cracking and reducing the overall durability of the surface by increasing the porosity. Several of the projects also exhibited paste worn away at the surface, as seen in Figure 65. Eliminating this activity would help reduce the surface wear observed as well.

Proper curing should include not only avoiding adding water to the pavement surface to aid in finishing but also a uniform application of curing compound at an appropriate application rate. It is also critical that the curing compound used have sufficient water retention characteristics. The Minnesota Department of Transportation has found that the use of 100% poly-alpha-methystyrene resin is effective in retaining water in the concrete. It is also important that a sufficient amount of resin be present and therefore it is suggested that the curing compound consist of a minimum of 42 percent solids. It is suggested that the following curing compound requirements be considered for adoption:

Table 70: Recommended Curing Compound Requirements

Properties	**Minimum**	**Maximum**
Total Solids, % by Weight of Compound	42	
% Reflectance in 72 Hours (ASTM E1347)	65	
Loss of Water, kg/m^2 in 12 Hours (ASTM C156)		0.15
Loss of Water, kg/m^2 in 24 Hours (ASTM C156)		0.40
Settling Test, ml/100 ml in 72 Hours		2
V.O.C. Content, g/L		350
Infrared Spectrum Vehicle	100 % Alpha Methylstyrene	

These recommended values are based on those provided by the Minnesota Department of Transportation Specifications. Additional information regarding the study that led to the development of these specifications can be found at the following web address, http://www.mrr.dot.state.mn.us/research/pdf/200106p.pdf, March 2011.

In the case of I-80, it appears that additional precautions might have been necessary in the vicinity of the Distressed section where wind protection might not have been sufficient due to a

lack of trees adjacent to the roadway. Inspection should include monitoring the ambient relative humidity, wind speed and temperature as well as the temperature of the concrete. Figure 175 should be used to insure adequate curing conditions are available.

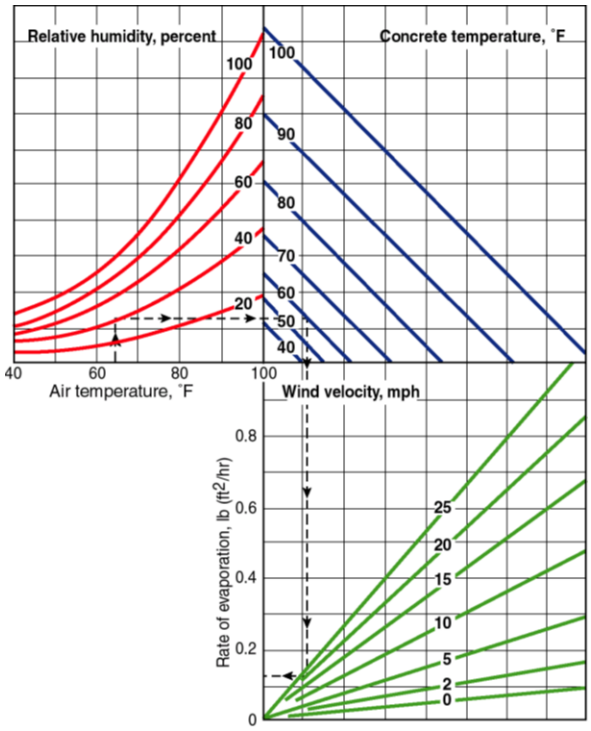

Figure 175: Effects of Concrete Temperature and Ambient Conditions on the Rate of Evaporation During Curing (PCA Design and Control of Concrete Mixtures, 2002).

Consolidation is a component of the placement process that can have an effect on the durability of the concrete. Over-consolidation can be another possible cause of the reduction in entrained air between the time the fresh concrete was tested and the entrained air was measured in the hardened concrete. Over-consolidation can also contribute to segregation. The recommendation for future projects is therefore to be more vigilant with respect to adhering to construction specifications. Special attention should be paid to insuring proper workability of the concrete and also preventing over consolidation by ensuring the vibration settings on the

paver are correct. The Minnesota Department of Transportation (MnDOT) requires the paving vibrators run between 60 and 100 hertz. Refinement of the concrete mixture design would also be beneficial in reducing the potential for segregation. Using a more uniformly graded coarse aggregate along with using a lower water/cementicious ratio will help reduce the potential for segregation as well as drying shrinkage cracking at the pavement surface.

3. Mixture Design Refinement

A refinement of the concrete mixture design specification should also be performed. This will help reduce the potential for segregation and make the concrete more durable. Using a more uniformly graded coarse aggregate along with using a lower water/cementitious ratio will help reduce the potential for segregation as well as drying shrinkage cracking at the pavement surface. Reducing the allowable water to cementitious ratio would also reduce the porosity of the paste and therefore increase the durability but increase the importance of proper curing. The durability can also be increased by decreasing the paste to aggregate ratio. Using a more densely graded aggregate would be helpful in reducing the paste content since a smaller volume of voids will be present between the aggregate particles.

4. Alkali Silica Reaction

ASR was identified in three of the projects, I-80, SR-22, Westmoreland County and SR-202. Of the three projects, it was only detrimental to the performance of sections of SR-22 . The petrographic analysis indicated that the GGBFS present in portions of this project was successful in mitigating the ASR. The approved mixture design for this project did contain GGBFS. The sections without sufficient quantities of GGBFS developed ASR predominately in the coarse aggregate, although very slight amounts of ASR was detected in some chert fine aggregate particles, as well. These projects do not indicate that ASR is a reoccurring problem and was only observed when the approved mixture design was not used.

5. Multi-lane paving

Care should be taken when paving adjacent lanes during drastically different climate conditions, especially if the lane being added is narrow, to reduce the potential for the development of transverse cracks in the shoulder. The SR-22 project near Blairsville in Indiana County analyzed for this study had a 2-ft shoulder being attached to the mainline. An estimate of the temperature of the slab at the zero stress time can be determined for the mainline, T_M, and

shoulder, T_S, using Equation 5. The maximum temperature within the first five days after the shoulder lane is placed, T_C, can be established based on the daily temperatures anticipated after paving the additional lane. T_C and the change in temperature, T_D, ($T_M - T_S = T_D$) can be used along with Table 66 to determine if the potential for transverse cracking in the shoulder exists. An example calculation is provided in Section 7.14.3.

6. Dowel Bar Lock-up

Dowel bar lock-up was found on the SR-22 project in Westmorland County. PennDOT Publication 408 Section 705.3 specifies the following bond breaking requirements:

3.a Type A. Coating material develops sufficiently low bond strength with concrete so that a bondbreaker is not necessary.
3.b Type B. Coating material develops bond strength with concrete so that a bondbreaker is necessary. Shop-applied bondbreakers are to conform to the pull-out load requirements of AASHTO M 254.

It was noticed on other projects throughout the region that although dowels are originally coated with a bond breaker material, this material can become dirty while being stored on-site and that some of these dirty bars were installed at the time of paving. This could contribute to dowel lockup as well and should be avoided on future projects. To avoid dowel bar lock-up, modifications can be made to this specification by changing statement 3.b to the following:

"*3.b Type B. Coating material develops bond strength with concrete so that a bondbreaker is necessary. Shop-applied bondbreakers are to conform to the pull-out load requirements of AASHTO M 254. If the dowel bar assemblies are pre-coated with Tectyl 506 at the fabrication site, a thorough inspection of the dowel bar assemblies is warranted prior to paving. This material is tacky, and it will pick up dirt if it is not protected from the environment.*"

8.2 Options to Consider

- The automated distressed data collected did not generally match well with the manual distress data collected. The adoption of the MEPDG will require local calibration as indicated by the lack of agreement between the predicted and observed performance. To perform a local calibration, the difference between the manual and automated distress data must be rectified.
- Develop repair techniques for repairing the distress exhibited on SR-202. These should include evaluating a variety of surface preparation techniques (small jack hammers, hydro demolition, etc.) as well as bonding agents.
- It is apparent that refinements of the concrete mixture design could be made to help

reduce the potential for material related distress as well as increasing the ease in which the concrete could be placed, finished and cured. These refinements should be established based on preliminary laboratory mixes and trial field projects. Other states have already taken steps in revising their concrete paving mixture design specifications to optimizing the performance of their pavements. It is recommended that these specifications be referred to as an initial step in evaluating how PennDOT specifications can be improved. The relevant mixture design and aggregate gradation specifications for these states, most of which are in wet-freeze climates, are provided in Appendix A.

Appendix A: Mixture Design and Aggregate Specifications of Select State DOTs

Illinois DOT

Aggregate Gradation Specifications

1003.02 Fine Aggregate for Portland Cement Concrete and Mortar.

The aggregate shall be according to Article 1003.01 and the following.

(a) Description. The fine aggregate shall consist of washed sand, washed stone sand, or a blend of washed sand and washed stone sand approved by the Engineer. Stone sand produced through an air separation system approved by the Engineer may be used in place of washed stone sand.

(b) Quality. The fine aggregate for portland cement concrete shall meet Class A Quality, except that the minus No. 200 (75 μm) sieve Illinois Modified AASHTO T 11 requirement in the Fine Aggregate Quality Table shall not apply to washed stone sand or any blend of washed stone sand and washed sand approved by the Engineer. The fine aggregate for masonry mortar shall meet Class A Quality.

(c) Gradation. The washed sand for portland cement concrete shall be Gradation FA 1 or FA 2. Washed stone sand for portland cement concrete, which includes any blend with washed sand, shall be Gradation FA 1, FA 2, or FA 20. Fine aggregate for masonry mortar shall be Gradation FA 9.

(d) Use of Fine Aggregates. The blending, alternate use, and/or substitution of fine aggregates from different sources for use in portland cement concrete will not be permitted without the approval of the Engineer. Any blending shall be by interlocked mechanical feeders at the aggregate source or concrete plant. The blending shall be uniform, and

the equipment shall be approved by the Engineer.

FINE AGGREGATE GRADATIONS											
Grad No.	Sieve Size and Percent Passing										
	3/8	No. 4	No. 8 [4/]	No. 10	No. 16	No. 30 [5/]	No. 40	No. 50	No. 80	No. 100	No. 200 [1/]
FA 1	100	97±3			65±20			16±13		5±5	
FA 2	100	97±3			65±20			20±10		5±5	
FA 3	100	97±3		80±15			50±20		25±15		3±3
FA 4	100				5±5						
FA 5	100	92±8								20±20	15±15
FA 6		92±8 [2/]								20±20	6±6
FA 7		100		97±3			75±15		35±10		3±3
FA 8			100				60±20			3±3	2±2
FA 9			100					30±15		5±5	
FA 10				100			90±10		60±30		7±7
FA 20	100	97±3	80±20		50±15			19±11		10±7	4±4
FA 21 [3/]	100	97±3	80±20		57±18			30±10		20±10	9±9

1004.02 Coarse Aggregate for Portland Cement Concrete.

The aggregate shall be according to Article 1004.01 and the following.

(a) Description. The coarse aggregate shall be gravel, crushed gravel, crushed stone, crushed concrete, crushed slag, or crushed sandstone.

(b) Quality. The coarse aggregate shall be Class A quality.

(c) Gradation. The gradations of coarse aggregate used in the production of portland cement concrete for pavements and structures shall be according to Table 1 of Article 1020.04. Washing equipment will be required where producing conditions warrant.

COARSE AGGREGATE GRADATIONS												
Grad No.	Sieve Size and Percent Passing											
	3 in.	2 1/2 in.	2 in.	1 1/2 in.	1 in.	3/4 in.	1/2 in.	3/8 in.	No. 4	No. 16	No. 50	No. 200 [1/]
CA 1	100	95±5	60±15	15±15	3±3							
CA 2		100	95±5		75±15		50±15		30±10	20±15		8±4
CA 3		100	93±7	55±20	8±8		3±3					
CA 4			100	95±5	85±10		60±15		40±10	20±15		8±4
CA 5				97±3 [2/]	40±25		5±5		3±3			
CA 6				100	95±5		75±15		43±13	25±15		8±4
CA 7				100	95±5		45±15 [3/8/]		5±5			
CA 8				100	97±3	85±10	55±10		10±5	3±3 [4/]		
CA 9				100	97±3		60±15		30±15	10±10		6±6
CA 10					100	95±5	80±15		50±10	30±15		9±4
CA 11					100	92±8	45±15 [5/8/]		6±6	3±3 [4/ 6/]		
CA 12						100	95±5	85±10	60±10	35±10		
CA 13						100	97±3	80±10	30±15	3±3 [4/]		
CA 14							90±10 [7/]	45±20	3±3			
CA 15							100	75±15	7±7	2±2		
CA 16							100	97±3	30±15	2±2 [4/]		
CA 17	100								65±20	45±20	20±10	10±5
CA 18	100				95±5				75±25	55±25	10±10	2±2
CA 19	100				95±5				60±15	40±15	20±10	10±5

Mix Design Requirements

1020.04 Concrete Classes and General Mix Design Criteria.

The classes of concrete shown in Table 1 identify the various mixtures by the general uses and mix design criteria. If the class of concrete for a specific item of construction is not specified, Class SI concrete shall be used. Special classifications may be made for the purpose of including the concrete for a particular use or location as a separate pay item in the contract. The concrete used in such cases shall conform to this section.

TABLE 1. CLASSES OF PORTLAND CEMENT CONCRETE AND MIX DESIGN CRITERIA

Class of Conc.	Use	Specification Section Reference	Cement Factor cwt/cu yd (3) Min.	Cement Factor cwt/cu yd (3) Max	Water / Cement Ratio lb/lb	Slump in. (4)	Mix Design Compressive Strength (Flexural Strength) psi, minimum Days 3	14	28	Air Content %	Coarse Aggregate Gradations
PV	PCC Pavement PCC Base Course PCC Base Course Widening PCC Driveway Pavement PCC Shoulders Shoulder Curb	420 or 421 353 354 423 483 662	5.65 (1) 6.05 (2)	7.05	0.32 - 0.42	2 - 4 (5)	Ty III 3500 (650)	3500 (650)		5.0 - 8.0	CA 5 & CA 7, CA 5 & CA 11, CA 7, CA 11, or CA 14

Table 1 of Section 1020.04

(9) At the Contractor's option, a water-reducing admixture or a retarding admixture may be used for Class PV, MS, SC, and SI concrete. When a water-reducing admixture is added, a cement factor reduction of up to 0.30

hundredweight/cu yd (18 kg/cu m), from the concrete designed for a specific slump without the admixture, will be permitted. When an approved high range water-reducing admixture is used, a cement factor reduction of up to 0.60 hundredweight/cu yd (36 kg/cu m),from a specific water cement/ratio without the admixture, will be permitted based on a 14 percent minimum water reduction. A cement factor below 5.35 hundredweight/cu yd (320 kg/cu m) will not be permitted. A cement factor reduction will not be allowed for concrete placed underwater. Cement factor reductions shall not be cumulative when using multiple admixtures.(10) For Class PV, MS, and SI, a retarding admixture shall be added to the concrete mixture when the concrete temperature is 85 ºF (30 ºC) or higher. This requirement may be waived by the Engineer when fly ash compensated mixtures are used.

Finely Divided Minerals.

Use of finely divided minerals shall be according to the following.

(1) Fly Ash. At the Contractor's option, fly ash from approved sources may partially replace portland cement in concrete mixtures, for Class PV, PP-1, RR, BS, PC, PS, MS, DS, SC, and SI, except when blended cements are used. A mix design consisting of cement, fly ash, and ground granulated blast-furnace slag may be used only when specified by the Department.

Fly ash and all other materials proposed for portland cement concrete mix designs shall be furnished to the Engineer at least 60 days prior to the initiation of work. The Engineer may elect to waive the required mix designs if the proposed materials combination has been previously approved and has demonstrated satisfactory field performance.The use of fly ash shall be according to the following.

a. Measurements of fly ash and cement will be rounded up to the nearest 5 lb (2.5 kg).

b. When Class F fly ash is used in Class PV, MS, SC, and SI concrete, the amount of cement replaced shall not exceed 15 percent by weight (mass) and the replacement ratio (fly ash:cement replaced) shall be a minimum of 1.5:1.

c. When Class C fly ash is used in Class PV, MS, SC, and SI concrete, the amount of cement replaced shall not exceed 20 percent by weight (mass), at a minimum replacement ratio of 1.25:1. For Class C fly ash, the minimum replacement ratio may be reduced to 1:1, if the fly ash calcium oxide is 18 percent or greater,the fly ash loss on ignition is less than 2.0 percent, and a water reducing or high range water-reducing admixture is used. Ground Granulated Blast-Furnace (GGBF) Slag. At the Contractor’s option, GGBF slag may partially replace portland cement in concrete mixtures, for Class PV, PP-1, PP-2, RR, BS, PC, PS, MS, DS, SC, and SI, except when blended cements are used. For Class PP-3 concrete, GGBF slag shall be used according to Article 1020.04. A mix design consisting of cement, GGBF slag, and fly ash may be used only when specified by the Department. GGBF slag and all other materials proposed for portland cement concrete mix designs shall be furnished to the Engineer at least 60 days prior to the initiation of work. The Engineer may elect to waive the required mix designs if the proposed materials combination has been previously approved and has demonstrated satisfactory field performance.

The use of GGBF slag shall be according to the following. a. Measurements of GGBF slag and cement shall be rounded up to the nearest 5 lb (2.5 kg).b. When GGBF slag is used in Class BS, PV, MS, SI, DS, and SC concrete, the amount of cement replaced shall not exceed 25 percent by weight (mass). The replacement ratio (GGBF slag:cement replaced) shall be a minimum of 1:1 for Grade 100 and 120.

Minnesota DOT

Aggregate Gradation Specifications

3126 Fine Aggregate for Portland Cement Concrete

F Gradation Requirements

Fine aggregate shall be well graded from coarse to fine; and when tested by means of laboratory sieves, shall conform to the following requirements:

Sieve Size Percent Passing

9.50 mm (**⅜ inch**).....100
4.75 mm (**# 4**) 95-100
2.36 mm (**# 8**) *(A)* 80-100
1.18 mm (**# 16**).....55-85
600 µm (**# 30**).....30-60
300 µm (**# 50**) *(B)*..... 5-30
150 µm (**# 100**) 0-10
75 µm (**# 200**) 0-2.5

(A) If the fine aggregate is used with a coarse aggregate that meets the requirements for coarse aggregate designation CA-15, the quantity passing the 2.36 mm (**# 8**) sieve may be decreased to 75 percent.
(B) Fine aggregate of which less than 5 percent passes a 300 µm (**# 50**) sieve may be used provided an approved inorganic material is added, by separate measurement, to correct the deficiency in gradation.

G Requirements for Uniformity of Grading

The gradation requirements specified above represent the extreme limits that will determine acceptability for use of fine aggregate from all sources of supply. However, the gradation from any one source shall be reasonably uniform and free from wide variation within the gradation limits.
For the purpose of controlling the uniformity of the materials from each individual source, an initial Fineness Modulus will be determined when the work begins. Thereafter, additional determinations will be made as additional material is delivered to the work and any material that shows a deviation from the initially determined Fineness Modulus of more than 0.20 tolerance shall be rejected or, at the discretion of the Engineer, it may be used subject to such adjustments in the mix composition as the Engineer deems necessary to compensate for the variation in gradation.

3127.1

The Fineness Modulus of fine aggregate is determined by subtracting the total of the cumulative percentages, by mass, passing the following standard sieves having square openings, from 7 and dividing by 100. Standard sieves are 9.50 mm (**⅜ inch**), 4.75 mm (**# 4**), 2.36 mm (**# 8**), 1.18 mm (**# 16**), 600 µm (**# 30**), 300 µm (**# 50**), and 150 µm (**# 100**).

3137 Coarse Aggregate for Portland Cement Concrete

B Classification

The aggregate shall conform to one of the following classifications. The class of aggregate to be used shall be optional with the Contractor unless otherwise specified in the Contract.
B1 Class A
Class A aggregate shall consist of crushed quarry or mine trap rock
(basalt, diabase, gabbro or other related igneous rock types), quartzite, gneiss or granite. Other igneous or metamorphic quarry or mine rock

may be used only with specific approval of the Engineer. Crushed aggregate produced from igneous or quartzite stones retained on a 100 mm (**4 inch**) screen will also be permitted by approval of the Engineer.

B2 Class B

Class B aggregate shall consist of all other crushed quarry or mine rock; i.e., carbonates, rhyolite, schist.

B3 Class C

Class C aggregate shall consist of natural or partly crushed natural gravel obtained from a natural gravel deposit. It may contain a quantity of material obtained from crushing the oversize stone in a deposit, provided such crushed material is uniformly mixed with the natural, uncrushed particles.

B4 Class D

Class D aggregate shall consist of a mixture of any two or more classes of approved aggregate (A, B, C, and R). The use of Class D aggregate, as well as the relative proportions of the different constituent aggregates, shall be subject to the approval of the Engineer. The relative proportions of the constituent aggregates shall be accurately controlled either by the use of a blending belt approved by the Engineer prior to production or by separately weighing each aggregate during the batching operations.

B5 Class R

Class R aggregate shall consist of aggregate obtained from
recycling concrete, which shall be crushed to the specified gradation. It
shall be handled and stockpiled in such a manner that it will not become contaminated with foreign matter.

Concrete removal and crushing operations must take into account any special problems associated with the presence of reinforcing steel. The fine fraction (passing the 4.75 mm (**# 4**) sieve) obtained in crushing the old concrete shall be removed to the extent possible and be wasted.

The original source of the aggregate must be known so the Engineer can determine its suitability for the intended use. Quality requirements of 3137.2D shall not apply specifically; however, the Engineer may consider any of those requirements in determining suitability of the aggregate.

E Gradation Requirements

Coarse aggregate shall be the uniform product of the plant producing it, unless it is necessary to remove some of the sizes in order to meet the following gradation requirements. Unless otherwise specified, coarse aggregate shall contain all of the sizes included within the specified limits. Broken or noncontinuous gradations will not be permitted.

The gradations required, or which will be permitted at the Contractor's option, will be specified in the concrete mix number.

The requirements of these gradations are listed in Table 3137-2. Whenever the size of coarse aggregate selected for use has less than 100 percent passing the 25.0 mm (**1 inch**) sieve, the coarse aggregate shall be produced, furnished, and proportioned for the work in at least two fractions. The Contractor shall maintain a uniform gradation in each size of coarse aggregate used during the handling and batching operations

TABLE 3137-1
COARSE AGGREGATE FRACTION SIZE FOR CONCRETE
Percent by mass (weight) passing square opening sieves *(A)*

Size Numbers Fraction size	50 mm (2 in)	37.5 mm (1 ½in)	31.5 mm (1 ¼in)	25.0 mm (1in)	19.0 mm (¾in)	16.0 mm (⅝in)	12.5 mm (½in)	9.5 mm (⅜in)	4.75 mm (# 4)
CA-0				100	95-100				0-10
CA-1	100	80-100			5-30				0-5
CA-2	100	90-100			5-35				0-5
CA-2M	100	90-100			20-50			0-10	0-5
CA-3		100	85-100		5-35				0-5
CA-3M		100	85-100		20-55			0-10	0-5
CA-4			100	85-100	25-60			0-10	0-5
CA-4M			100	85-100	40-75			0-15	0-5
CA-5				100	85-100			30-60	0-10
CA-6					100	85-100		40-70	0-10
CA-7						100	85-100	50-100	0-25
CA-8 *(A)*								100	55-95

TABLE 3137-2
COARSE AGGREGATE DESIGNATION FOR CONCRETE
Percent by mass (weight) passing square opening sieves *(A)*

Aggregate Designation	50 mm (2 in.)	37.5 mm (1 ½ in.)	31.5 mm (1 ¼ in.)	25.0 mm (1 in.)	19.0 mm (¾ in.)	16.0 mm (⅝ in.)	12.5 mm (½ in.)	9.5 mm (⅜ in.)	4.75 mm (# 4)
CA-00				100	95-100				0-10
CA-15	100	90-100			35-65			5-25	0-7
CA-25 or 2M6	100	95-100			50-80			20-40	0-7
CA-35 or 3M6		100	95-100		55-85			20-45	0-7
CA-45 or 4M6			100	95-100	65-95			25-55	0-7
CA-50				100	85-100			30-60	0-12
CA-60					100	85-100		40-70	0-12
CA-70						100	85-100	50-100	0-25
CA-80 *(A)*								100	55-95

Optional Incentive for Well-Graded Aggregate

An optional incentive of $2.60 per m3 (**$2.00 per cubic yard**) of concrete is available to the Contractor provided a concrete mixture is designed and produced with a combined aggregate gradation that meets the following requirements.

Sieve Sizes	% Retained
50 mm (**2 inch**)	0%
37.5 mm (**1 ½ inch**)	≤ 8%
25 mm (**1 inch**)	8% to 18%
19 mm (**3/4 inch**)	8% to 18%
12.5 mm (**1/2 inch**)	8% to 18%
9.5 mm (**3/8 inch**)	8% to 18%
4.75 mm (**# 4**)	8% to 18%
2.36 mm (**# 8**)	8% to 18%
1.18 mm (**# 16**)	8% to 18%
600 µm (**# 30**)	8% to 18%
300 µm (**# 50**)	≤ 18%
150 µm (**# 100**)	≤ 8%
75 µm (**# 200**)	≤ 1.6%

If the previous gradation is not met an optional incentive of $0.65/m3 (**$0.50 per cubic yard**) of concrete is available to the Contractor provided a concrete mixture is designed and produced with a combined aggregate gradation that meets the following requirements:

Sieve Sizes	% Retained
50 mm (**2 inch**)	0%
37.5 mm (**1 ½ inch**)	≤ 7%
25 mm (**1 inch**)	7% to 18%
19 mm (**3/4 inch**)	7% to 18%
12.5 mm (**1/2 inch**)	7% to 18%
9.5 mm (**3/8 inch**)	7% to 18%
4.75 mm (**# 4**)	7% to 18%
2.36 mm (**# 8**)	7% to 18%
1.18 mm (**# 16**)	7% to 18%
600 µm (**# 30**)	7% to 18%
300 µm (**# 50**)	≤ 18%
150 µm (**# 100**)	≤ 7%
75 µm (**# 200**)	≤ 1.6%

Compliance is determined based on the Contractor's composite aggregate gradation test results as verified by Agency testing. The Agency's statistical analysis of samples for well-graded aggregate control incentive will be based on a lot basis representing one days paving. The incentive payment shall be calculated on a lot basis. The lot represents the cumulative average of the sublot values on each sieve.

Mix Design Requirements and Incentives

A6 Cementitious Materials – General

The minimum cementitious material requirements shall be (315 kg/m3 (**530 pounds per cubic yard**). Of the cementitious fraction, the minimum portland cement content shall be 237 kg/m3 (**400 pounds per cubic yard**) whether using fly ash or ground granulated blast furnace slag as a portland cement replacement (See below for Special Requirements for Quartzite and Gneiss) . Any additional cementitious material necessary to meet any requirement described herein shall be the responsibility of the Contractor with no additional compensation from the Agency. Total cementitious shall not exceed 356 kg/m3 (**600 pounds per cubic yard**) except for high-early mixes.

Mn/DOT 2461.3D is modified to allow up to 30 percent replacement with fly ash. Portland cement may be replaced with up to 35 percent ground granulated blast furnace slag (GGBFS), however, ternary mixes (Portland cement, GGBFS, fly ash or other cementitious materials) are not allowed

Specification 3101 is hereby modified such that the total alkalis in the portland cement (Na2O + 0.658 K2O) shall not exceed 0.60 percent. The total alkalis in the cementitious material shall not exceed 3.0 kg/m3 (**5.0 pounds per cubic yard**).

A6a Special Cementitious Requirements for Quartzite and Gneiss

If the Contractor selects to use coarse aggregate from sources identified by Mn/DOT as quartzite or gneiss and the aggregate does not comply with the 0.04 percent expansion limits of ASTM C-1293, the other cementitious material shall be:

(1) 30% of an approved fly ash meeting the following requirements:
Mn/DOT 3115 is modified such that fly ash used as cementitious material in the concrete mixture shall have a minimum Si02 + Fe2O3 +Al2O3 of 66.0% on a dry weight basis. In addition, it shall have a minimum Si02 content of 38.0%.

-or-

(2) 35% of an approved ground granulated blast furnace slag.

A7 Concrete Mix Design

Grade A paving concrete shall be designed and placed at a water cementitious ratio not greater than 0.40. The Mn/DOT Concrete Engineering Unit shall provide the mix design. In lieu of a mix design provided by the Mn/DOT Concrete Engineering Unit, the Contractor has the option to supply the mix design.

A7a(2) Optional Contractor Mix Design

The Contractor shall design the concrete paving mixture based on a volume of 1.000 m3 (**cubic yard**) according to industry standard practice.
The concrete pavement placement may commence 15 days after preliminary approval of the Contractor's concrete pavement mix design by the Concrete Engineer. Final approval of the mixture is based on satisfactory field placement.
A7a(3) Coarse Aggregate Gradation
All coarse aggregate for concrete pavement that does not contain 100% recycled concrete shall meet the following gradation:

Sieve	Percent Passing
50 mm (**2 inch**)	100
37.5 mm (**1 1/2 inch**)	95-100
19 mm (**3/4 inch**)	35-70
9.5 mm (**3/8 inch**)	10-30
4.75 mm (**#4**)	0-7

A7a(4) Admixtures (Other than Mineral Admixtures)

An approved Type A water reducing admixture shall be used. (Approved list on file at the Departments' Concrete Engineering Unit Website) The use of any admixtures other than air entraining agents and Type A water reducers require the approval of the Concrete Engineer.

A7b Large Concrete Paving Projects > 3825 m3 (**5000 cubic yards**)

Unless modified in the Special Provisions of the Contract, the following shall apply:
A7b(1) General
The concrete pavement placement may commence 15 days after preliminary approval of the Contractor's concrete pavement mix design and job mix formula (JMF) by the Concrete Engineer. Final approval of the mixture is based on satisfactory field placement.

A7b(2) Contractor Concrete Mix Design

The Contractor shall design the concrete paving mixture based on a volume of 1.000 m3 (**cubic yard**) according to industry standard practice. Grade A paving concrete shall be designed and placed at a water cementitious ratio not greater than 0.40.
High early mixes may have up to 100 % portland cement. High-early mixes are not eligible for incentive payments for water/cementitious ratio.

For the minor work such as fill-ins or other work not provided by the Contractor's primary concrete plant, the Contractor may choose to use a 3A41HE mix designed by Mn/DOT in lieu of the Contractor mix design requirement.

A7b(3) Job Mix Formula

A Formula (JMF) containing proportions of materials and individual gradations of each material plus a composite gradation. All admixtures shall also be included. The JMF shall be based on the combination of coarse and fine aggregate for the following sieves:
50 mm (**2 inch**), 37.5 mm (**1-1/2 inch**), 25 mm (**1 inch**), 19 mm (**3/4 inch**), 12.5 mm (**1/2 inch**), 9.5 mm (**3/8 inch**), 4.75 mm (**# 4**), 2.36 mm (**# 8**), 1.18 mm (**# 16**), 600 µm (**# 30**), 300 µm (**# 50**), 150 µm (**# 100**) and 75 µm (**# 200**). During the testing process, additional fill-in sieves may need to be added to prevent overloading. Table 3137-1 and Table 3137-2 and the gradation requirements of Mn/DOT 3126 are hereby deleted. The percent passing the 50 mm (**2 inch**) sieve shall be 100 percent; the percent passing the 75 µm (**# 200**) sieve shall not exceed 1.6 percent.*
*(Note: See Mn/DOT 3137.2D1i for additional requirements for coarse aggregate cleanliness.) The JMF submittal shall include working ranges based on the composite gradation of the above sieves The working range limits of the composite gradation are based on a moving average of 4-tests (N=4). The working ranges are:

Sieve Size	Working Range
4.75 mm (**# 4**) sieve or greater	+/- 5 %
2.36 mm (**# 8**) to 600 µm (**# 30**) sieve	+/- 4 %
300 µm (**# 50**) sieve	+/- 3 %
150 µm (**# 100**) sieve	+/- 2 %

A new concrete mix design and JMF shall be submitted if the moving average falls outside of the JMF working range or any proportions of the mix design are adjusted.

A7b(4) Admixtures (Other than Mineral Admixtures)

An approved Type A water reducing admixture may be used at the discretion of the Contractor. (Approved list on file at the Departments' Concrete Engineering Unit Website). The use of any admixtures other than air entraining agents and Type A water reducers require the approval of the Concrete Engineer.

A7b(5) Water/Cementitious Ratio

The water/cementitious ratio shall conform to the requirements of Table WC-1.
Concrete mix not meeting the 0.40 water/cementitious requirement shall not knowingly be placed in the work. Should any non-conforming material be inadvertently placed in the work, it will be accepted for payment according to Table WC-1.

Table WC-1

QI Value	Payment incentive/disincentive per m^3 (cubic yard)
0.35 or less	+$5.20 (**$4.00**)
0.36	+$3.90 (**$3.00**)
0.37	+$2.60 (**$2.00**)
0.38	+$1.62 (**$1.25**)
0.39	+$0.65 (**$0.50**)
0.40	0.00
0.41	-$0.65 (**$0.50**)
0.42	-$1.62 (**$1.25**)
0.43	-$2.60 (**$2.00**)
0.44	-$3.90 (**$3.00**)
0.45+	Determined by the Concrete Engineer

Washington DOT

Aggregate Gradation Specifications 9-03.1 Aggregates for Portland Cement Concrete

9-03.1(1) General Requirements

Portland cement concrete aggregates shall be manufactured from ledge rock, talus, or sand and gravel in accordance with the provisions of Section 3-01. The material from which concrete aggregate is manufactured shall meet the following test requirements:

Los Angeles Wear, 500 Rev. 35 max.
Degradation Factor (Structural and Paving Concrete) 30 min.
Degradation Factor (Other as defined in 6-02.3(2)B 20 min.

Aggregates tested in accordance with AASHTO T 303 with expansion greater than 0.20 percent are Alkali Silica Reactive (ASR) and will require mitigating measures. Aggregates tested in accordance with ASTM C 1293 with expansion greater than 0.04 percent are Alkali Silica Reactive (ASR) and will require mitigating measures. Aggregates for use in Commercial Concrete as defined in 6-02.3(2)B shall not require mitigation.
Mitigating measures for aggregates with expansions from 0.21 to 0.45 percent, when tested in accordance with AASHTO T 303, may be accomplished by using low alkali cement as per 9-01.2(3) or by using 25% Class F fly ash by total weight of the cementitious materials. The Contractor may submit an alternative mitigating measure through the Project Engineer to the State Materials Laboratory for approval along with evidence in the form of test results from ASTM C 1567 that demonstrate the mitigation when used with the proposed aggregate controls expansion to 0.20 percent or less. The agency may test the proposed ASR mitigation measure to verify its effectiveness. In the event of a dispute, the agency's results will prevail. Mitigating measures for aggregates with expansions greater than 0.45 percent when tested in accordance with AASHTO T-303 shall include the use of low alkali cement per 9-1.2(3) and may include the use of fly ash, lithium compound admixtures, ground granulated blast furnace slag or other material as approved by the Engineer. The Contractor shall submit evidence in the form of test results from ASTM C 1567 through the Project Engineer to the State Materials Laboratory that demonstrate the proposed mitigation when used with the aggregates proposed will control the potential expansion to 0.20 percent or less before the aggregate source may be used in concrete. The agency may test the proposed ASR mitigation measure to verify its effectiveness. In the event of a dispute, the agency's results will prevail.

The use of fly ash that does not meet the requirements of Table 2 of AASHTO M 295 may be approved for use. The Contractor shall submit test results according to ASTM C 1567 through the Project Engineer to the State Materials Laboratory that demonstrate that the proposed fly ash when used with the proposed aggregates and Portland cement will control the potential expansion to 0.20-percent or less before the fly ash and aggregate sources may be used in concrete. The Contracting Agency may test the proposed ASR mitigation measure to verify its effectiveness. In the event of a dispute, the Contracting Agency's results will prevail. Passing petrographic analysis (ASTM C 295) accepted by WSDOT prior to August 1, 2005, is acceptable as proof of mitigation until the aggregate source is reevaluated. ASTM C 1293 sampling and testing must be coordinated through the WSDOT State Materials Laboratory, Documentation Section utilizing the ASA (Aggregate Source Approval) process. Cost of sampling, testing, and processing will be borne by the source owner.

9-03.1(2) Fine Aggregate for Portland Cement Concrete
Fine aggregate shall consist of sand or other inert materials, or combinations thereof, approved by the Engineer, having hard, strong, durable particles free from adherent coating. Fine aggregate shall be washed thoroughly to remove clay, loam, alkali, organic matter, or other deleterious matter.

9-03.1(2)B Grading
Fine aggregate shall be graded to conform to the following requirements expressed as percentages by weight:

	Class 1		Class 2	
	Percent Passing		Percent Passing	
Sieve Size	**Min**	**Max**	**Min**	**Max**
3/8"	100		100	
No. 4	95	100	95	100
No. 8	68	86		
No. 16	47	65	45	80
No. 30	27	42		
No. 50	9	20	10	30
No. 100	0	7	2	10
No. 200	0	2.5	0	2.5

9-03.1(2)C Use of Substandard Gradings
Fine aggregate with more than the maximum percentage passing any sieve may be accepted provided the cement content of the finished concrete is increased at the Contractor's expense, ⅓ percent for each 1 percent the fine aggregate passing each sieve is in excess of the maximum. Under no circumstances shall fine aggregate Class 1 be used which has a grading finer than the following:

Sieve Size	Percent Passing
No 8	95
No 16	80
No 30	60
No 50	25
No 200	2.5

9-03.1(4) Coarse Aggregate for Portland Cement Concrete
Coarse aggregate for concrete shall consist of gravel, crushed stone, or other inert material or combinations thereof having hard, strong, durable pieces free from adherent coatings. Coarse aggregate shall be washed to remove clay, silt, bark, sticks, alkali, organic matter, or other deleterious material.

Passing	AASHTO GradingNo. 467		AASHTO Grading No. 4		AASHTO GradingNo. 57		AASHTO GradingNo. 67		AASHTO Grading No. 7		AASHTO Grading No. 8	
Sieve Size	Min.	Max.	Min.	Max.	Min.	Max.	Min.	Max.	Min.	Max.	Min.	Max.
2"	100	.	100	--	.	.	.	.	.	.	.	.
1.5"	95	100	90	100	100	.	.	.	.	.	.	.
1"	.	.	20	55	95	100	100	.	.	.	.	.
.75"	35	70	0	15	.	.	90	100	100	.	.	.
.5"	.	.	--	--	25	60	.	.	90	100	100	.
.375"	10	30	0	5	.	.	20	55	40	70	85	100
No. 4	0	5	--	--	0	10	0	10	0	15	10	30
No. 8	.	.	--	--	0	5	0	5	0	5	0	10
No. 16	.	.	--	--	.	.	.	.	.	.	0	5

9-03.1(5) Combined Aggregate Gradation for Portland Cement Concrete
As an option to using Coarse and Fine graded aggregates for Portland Cement Concrete, aggregate gradation may consist of a combined gradation. Aggregates shall consist of sand, gravel, crushed stone, or other inert material or combinations thereof, having hard, strong durable particles free from adherent coatings. Aggregates shall be washed to remove clay, loam, alkali, organic matter, silt, bark, sticks, or other deleterious matter.

Mix Design Requirements

5-01.3(1)A2 Portland Cement Concrete
Portland cement concrete shall meet the requirements of Sections 5-05.3(1) and 5-05.3(2) and be air entrained with a design air content of 5.5-percent.

5-05.3(1) Concrete Mix Design for Paving
The Contractor shall provide a concrete mix design for each design of concrete specified in the Contract. The Contractor shall use ACI 211.1 as a guide to determine proportions. Concrete strength, placement, and workability shall be the responsibility of the Contractor. Following approval of the Contractor's proposal, all other requirements of Section 5-05 shall apply.

1. **Materials.** Materials shall conform to Section 5-05.2. Fine aggregate shall conform to Section 9-03.1(2), Class 1. Coarse aggregate shall conform to Section 9-03.1(4), AASHTO grading No. 467. An alternate combined gradation conforming to Section 9-03.1(5) may be proposed, that has a nominal maximum aggregate size equal to or greater than a 1½-inch sieve. Fly ash, if used, shall not exceed 35-percent by weight of the total cementitious material, shall conform to Section 9-23.9 and shall be limited to Class F with a maximum CaO content of 15-percent by weight. Ground granulated blast furnace slag, if used, shall not exceed 25-percent by weight of the total cementitious material and shall conform to Section 9-23.10. When both ground granulated blast furnace slag and fly ash are included in the concrete mix, the total weight of both these materials is limited to 35-percent by weight of the total cementitious material. As an alternative to the use of fly ash, ground granulated blast furnace slag and cement as separate components, a blended hydraulic cement that meets the requirements of Section 9-01.2(4) Blended Hydraulic Cements may be used. The water/cement ratio shall be calculated on the total weight of cementitious material. The following are considered cementitious materials: Portland cement, fly ash, ground granulated blast furnace slag and microsilica. The minimum cementitious material for any mix design shall be 564-pounds per cubic yard.

REFERENCES

1. Miller, J.S. and W.Y. Bellinger, *Distress Identification Manual for the Long-Term Pavement Performance Program*. 2003, Office of Infrastructure Research and Development: McLean, Va. p. 164.
2. Wells, S.A., B.M. Phillips, and J.M. Vandenbossche, *Quantifying Built-In Construction Gradients and Early-Age Slab Deformation Caused by Environmental Loads in a Jointed Plain Concrete Pavement.* International Journal of Pavement Engineering, 2006. **7**(4).
3. Larson, G.E. and B.J. Dempsey, *Integrated Climatic Modle Version 3.2 BETA*. 2006.
4. Raja, Z.I. and M.B. Snyder, *Factors Affecting Deterioration of Transverse Cracks in Jointed Reinforce Concrete Pavements.* Transportation Research Record, 1991(1307): p. 7.
5. Transportation, P.D.o., *Publication 408 - Specifications*. 2011, Pennsylvania Department of Transportation: Harrisburg, PA.
6. Tanesi, J.K., A.R. Abbas, and R.C. Meininger. *Effect of Coefficient of Thermal Expansion Variability on Concrete PAvement Performance as Predicted Using The Mechanistic-Empirical Pavement Design Guide*. in *Transportation Research Board Annual Meeting*. 2007. Washington, D.C.
7. ARA Inc., E.C.D., *Guide for Mechanistic-Empirical Design of New and Rehabilitated Pavement Structures. NCHRP Project 1-37A, Final Report*. 2004, Transportation Research Board of the National Academies: Washington, D.C.
8. Officials, A.A.o.S.H.a.T., *Guide for Design of Pavement Structures*. 1993, American Association of State Highway and Transportation Officials: Washington, D.C.
9. Lukanen, E.O., R.N. Stubstad, and M.L. Clevenson, *Study of LTPP Pavement Temperatures*. 2005, Office of Infrastructure R&D, Federal Highway Administration: McLean, Va. p. 36.
10. Ioannides, A.M. and L. Khazonovich. *Analytical and Numerical Methods for Multi-Layered Concrete Pavements*. in *Third International Workshop on the Design and Rehabilitation of Concrete Pavements*. 1994. Krumbach, Austria.
11. Khazonovich, L., S.D. Tayabji, and M.I. Darter, *Backcalculation of Layer Parameters for LTPP Test Sections, Volume I: Slab on Elastic Solid and Slab on Dense Liquid Foundation Analysis of Rigid Pavements*. 2001, Federal Highway Administration: Washington, D.C.
12. Yu, H.T. and L. Khazonovich, *Use of Magnetic Tomography Technology to Evaluate Dowel Placement - Final Report*. 2005, Federal Highway Administration: Washington, D.C.
13. Khazonovich, L., K. Hoegh, and M.B. Snyder, *Guidelines for Dowel Alignment in Concrete Pavements*. 2009, NCHRP. p. 59.

14. Survey, N.C.S., *National Cooperative Soil Characterization Database*. 2011.
15. Huang, Y.H., *Pavement Analysis and Design*. 2nd ed. 2004, Englewood Cliffs, NJ: Prentice-Hall, Inc. 805.
16. Ruiz, J.M., et al., *Computer Based Guidelines for Concrete Pavements Volume II - Design and Construction Guidelines and HIPERPAV II User's Manual*. 2005, FHWA: McLean, VA.
17. Wells, S.A., *Early Age Response of Jointed Plain concrete Pavements to Environmental Loads*, in *Civil and Environmental Engineering*. 2005, University of Pittsburgh: Pittsburgh, PA. p. 188.
18. Asbahan, R., *Effects of the Built-In Construction Gradient and Environmental Conditions of Jointed Plain Concrete Pavements*, in *Civil Engineering*. 2009, University of Pittsburgh: Pittsburgh, PA. p. 586.
19. ABAQUS/CAE, *ABAQUS Version 6.7*. 2007, Dassault Systems: Providince, RI.
20. *ABAQUS/CAE*. 2007, Dassault Systems: Providence, Rhode Island.
21. Maitra, S.R., K.S. Reddy, and L.S. Ramachandra, *Experimental Evaluation of Interface Friction and Study of Its Influence on concrete Pavement Response.* Journal of Transportation Engineering, 2009. **135**(8): p. 9.
22. Westergaard, H.M. *Analysis of Stresses in Concrete Pavements Due to Variations of Temperature*. in *Highway Research Board Conference*. 1927.
23. Kuo, C.M., *Three-Dimensional Finite Element Analysis of Concrete Pavement*, in *Civil Engineering*. 1994, University of Illinois: Urbana, Illinois.
24. Lee, Y.H., H.T. Wu, and S.T. Yen, *Parameter Studies and Verifications on Three Dimensional Finite Element Analysis of Rigid Pavements.* Canadian Journal of Civil Engineering, 2004. **31**(5): p. 15.
25. Janssen, D.J. and M.B. Snyder, *The Temperature-Moment Concept for Evaluating Pavement Temperature Data.* Journal of Infrastructure Engineering, 2000. **6**(2): p. 81-83.